Metal-Free Transfer Hydrogenation of Polar Unsaturated Compounds with Polar Hydrogen Donors—Scope, Limitations and Reaction Mechanism

DISSERTATION

zur

Erlangung der naturwissenschaftlichen Doktorwürde

(Dr. sc. nat.)

vorgelegt der

Mathematisch-naturwissenschaftlichen Fakultät

der

Universität Zürich

von

XIANGHUA YANG

aus der

V. R. China

Promotionskomitee

Prof. Dr. Heinz Berke (Vorsitz und Leitung)

Prof. Dr. Roger Alberto

Zürich, 2011

CONTENTS

Acknowledgments

Four years have passed since I started my PhD studies in the University of Zurich in October 2007. Looking back, I am very glad that I made the right decision to pursue my PhD here and I feel so lucky that I met so many kind and supportive people along the way. Without them, this PhD thesis would not have been accomplished.

First of all, I would like to express my sincerest gratitude to my supervisor, Prof. Dr. Heinz Berke, for offering me the opportunity to study in his group and letting me work on this interesting and frontier topic. Throughout my PhD study - especially during the revisions of manuscripts and this dissertation, he provided patient guidance, generous support, sustained encouragement and inspirable suggestions that I really need.

I am indebted to Prof. Dr. Roger Alberto for being a committee member of my doctorate study and as co-referee of this dissertation, to Prof. Dr. Roland Sigel for leading the Graduate School of Chemical and Molecular Science Zurich (CMSZH) which provide us with useful training courses as well as opportunities to visit various companies.

Thank Prof. Dr. Zhixiang Wang and Lili Zhao from the Chinese Academy of Sciences for collaboration on computational studies and Prof. Dr. R. Tom Baker (CCRI, Ottawa) for fruitful discussions.

I am grateful to Dr. Koushik Venkatesan for his kind suggestions and helping with submitting papers, to Dr. Christian Frech for GC-TCD measurements, and to Dr. Ferdinand Wild for his generous help with MS, DTA/DSC measurement and other technical problems. I also wish to thank Dr. Thomas Fox for his kind introductions and discussions in NMR measurements, Dr. Olivier Blacque for helping with crystal structure determinations and some calculations, and Heinz Spring for elemental analyses.

Many thanks go to Beatrice Spichtig, Susanna Sprokkereef, Linda Wehrle, Nathalie Fichter, Sabine Stockhause and Dr. Jae Kyoung Pak for their great help with administrative tasks and to Manfred Jöhri for his support concerning electronics and hardwares.

My special thanks go to all the members of our group, in special: Dr. Balz Dudle, Rajesh Kunjanpillai and Dr. Rajkumar Jana for the friendly work atmosphere in the glovebox and in the lab; Gabrielle Grieco and Jeanne Bolliger for GC-MS and Carolina Egler for MS measurements; Anne Landwehr for the glasswares and helpful discussions; Narayana Rao Jay

Anand for helping with the pump oil relating stuffs; Pascal Pluess for kindly helping me with the translation work; Dr. Yan Li, Dr. Chunfang Jiang and Dr. Yanfeng Jiang for a lot of helpful instructions in the lab and out of the lab's life in Zurich.

I would like to thank my Chinese friends Dr. Ying Zhou, Min Sheng, Xia Meng, Xiaoxian Yuan, Tingting Zhong, Mei Xue, Yuzheng Zhang, Dr. Xinjun Luan, Lubin Ni, Dr. Hailin Dong, Kai Zhou, Yunjun Shen, Dr. Xiaoqiong Wan, Dr. Yu Liu, and so on, for the precious and enjoyable leisure activities. I thank Xiaolin Qin for leading me to realize and enjoy the magic power of photograph and table-tennis.

I owe my heartfelt gratitude to Prof. Dr. Chanjuan Xi (Tsinghua University, Beijing), the advisor of my master thesis, for introducing me to experimental chemistry and more importantly, for sharing me with her hearty opinions about life. I'm also indebted to Prof. Dr. Wenhua Sun (Chinese Academy of Science) for his suggestions on how to be a real scientist and kindly recommending me to Prof. Berke.

It is impossible to end without expressing my appreciation to my family. Thank my mother Birong Xie and my father Jian'an Yang for illegally giving birth to me and for their endless love and support that I can always rely on. Thank my elder brother Lianghua Yang, my elder sister Lingling Yang and their families for their willingness to take care of me, either I'm a small kid or a grown-up.

Last but not least, I wish to express the most special thanks to my beloved husband, Hongning Zhang. It's his love, tolerant, encouragement and accompany that enables me to get through the most difficult times. To him I dedicate this dissertation.

This work was financially supported by the Swiss National Science Foundation, the Swiss-German joint project 'Unconventional approaches to the activation of dihydrogen', the CMSZH Graduate School and the University of Zurich, which are gratefully acknowledged.

Xianghua Yang

2011, Zurich

Abbreviations

AB	ammonia borane
ATR	attenuated total fef raction
Bu	butyl
BZ	borazine
Bz	benzyl
CTB	cyclotriborazane
Cy	cyclohexyl
d	day
DFT	density functional theory
DMAB	*N*,*N*-dimethyl amine borane
DMF	dimethylformamide
DMSO	dimethyl sulfoxide
DSC	differential scanning calorimetry
DTA	differential thermal analysis
Et	ethyl
Eq./eq.	Equation/equivelent
EWG	electron withdrawing group
FT	Fourier transform
GC/MS	gas-chromatography/mass-spectrometry
h	hours
Hz	hertz
IR	infrared
kJ	kilo Joule
KIE	kinetic isotope effect
MAB	*N*-methyl amine borane
Me	methyl
min	minutes
PBZ	polyborazine
Ph	phenyl
ppm	part per million
py	pyridine
RDS	rate determining step
r.t.	room temperature
s	seconds
STP	standard temperature and pressure

tBAB	*N-tert*-butyl amine borane
THF	tetrahedronfuran
TS	transition state
m-	*meta-*
o-	*ortho-*
p-	*para-*
σ	substituent constant
ρ	reaction constant
δ	chemical shift
ν	frequency
NMR	nuclear magnetic resonance
br	broad (NMR)
d	doublet (NMR)
t	triplet (NMR)
s	singlet (NMR)
q	quadralet (NMR)
COSY	correlation spectroscopy
DEPT	distortionless enhancement by polarization transfer
HETCOR	heteronuclear correlation spectroscopy
MAS	magic angle spinning
ROSEY	rotating-frame Overhauser effect spectroscopy
NOE	nuclear Overhauser effect
2D	two dimentional

Introduction (I): Ammonia Borane for Chemical Hydrogen Storage

Energy is one of the most fundamental parts of the universe and the most indispensable element for the development of our modern society. Everything happening around us is connected to energy in one form or another. Generally, energy is stored in four different forms:[1] mechanical energy (wind, waterfalls, etc.), electric and magnetic field energy (capacitors, coils, etc.), nuclear energy (uranium, deuterium, etc.) and chemical energy (batteries, fossil fuels, hydrogen, etc.). The 'energy' chemists often refers to as energy stored in chemicals, which can be defined as non-renewable (oil, coal and natural gas) in contrast to renewable (solar, wind, tides, hydro and biomass) sources referring to the reproducibility of the energy resources. Chemical energy is based on the energy of unpaired outer electrons (valence electrons) eager to be stabilized by electrons from other atoms. The hydrogen atom is most attractive because its electron is accompanied by only one proton. Hydrogen thus has the best ratio of valence electrons to protons (and neutrons) of all elements in the periodic table, and the energy gain per electron is very high.

1.1 Fossil fuels

Coal, oil and natural gas are called 'fossil fuels' because they have been formed from the organic remains of prehistoric plants and animals. Fossil fuels actually represent stored solar energy from hundreds of millions of years ago before the time of dinosaurs.[2] Nowadays, fossil fuels provided around 60% of the world's electrical power and more than 80% of the world's total energy demands (including heating, transportation, electricity generation and so on).[3] Since fossil fuels take millions of years to form, it's impossible to be produced even with the newest technologies. In another word, they are not renewable energy and their supplies are finite. Although there is no shortage of fossil fuels currently, they will be one day used off. It's better not to be too dependent on fossil fuels, on the one hand we need to improve the efficiency of energy usage and conserve energy in all circumstances, on the other hand we have to look for sustainable substitutions.

Besides the supply limitation, there is another problem along with using of fossil fuels: generation of carbon dioxide and other environmentally harmful carbon particulates, sulphur and nitrogen oxides. Carbon dioxide is a well-known greenhouse gas, since it traps heat (infrared absorption) in the atmosphere. Since about 1850, global use of fossil fuels has increased to dominate energy supply, both replacing many traditional uses of bioenergy and providing new services. The rapid rise in fossil fuel combustion (including gas flaring) has produced a corresponding rapid growth in CO_2 emissions (Figure 1.1),[4] which *very likely* enhanced the natural greenhouse effect and lead to an increase in global average temperature and related climate changes. Concentrations of CO_2 have continued to grow to about 390 ppm CO_2 or 39% above pre-industrial levels by the end of 2010. The global average temperature has increased by 0.76 °C (0.57 °C to 0.95 °C) between 1850 to 1899 and 2001 to 2005, and the warming trend has increased significantly over the last 50 years.

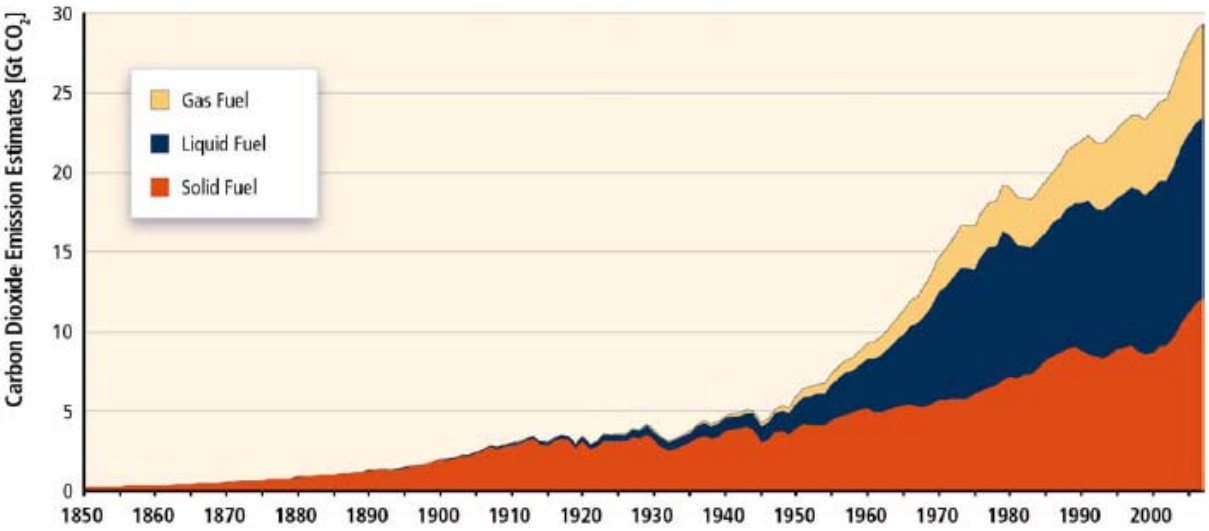

Figure 1.1 Global CO_2 emissions from fossil fuel burning, 1850 to 2007. Gas fuel includes flaring of natural gas. All emission estimates are expressed in Gt CO_2.[5]

Moreover, fossil fuels such as coal contain radioactive materials, mainly uranium and thorium, which are exposed to human beings while using. The process of transporting and storing of oil has a big impact on the environment whenever something goes wrong. An oil spill on the sea, pipeline explosion or well fire would be huge disasters. Altogether, it is essential to discover renewable and clean energy sources to gradually replace fossil fuels.

1.2 Renewable energy sources

Renewable energy is derived from natural processes that are replenished constantly. In its various forms, it derives directly from the sun, or from heat generated deep within the earth. Included in the definition is electricity and heat generated from solar, wind, ocean, hydropower, biomass, geothermal resources, biofuels and hydrogen derived from renewable resources, as the international energy agency explains. Renewable energy sources play a role in providing energy services in a sustainable manner and, in particular, in mitigating climate change. They are effective in lowering CO_2 emissions because they have low carbon intensity with emissions per unit of energy output typically 1 to 10% that of fossil fuels.

The international exploration on renewable energy sources began with the fuel crises of the 1970s. In 2008, about 12.9% of global primary energy supply was provided by renewable energy sources (Figure 1.2). The largest renewable energy contributor was biomass (10.2%), with the majority (roughly 60%) of the biomass fuel used in traditional cooking and heating applications in developing countries but with rapidly increasing use of modern biomass as well.[6] Hydropower represented 2.3%, whereas other renewable energy sources accounted for 0.4%.

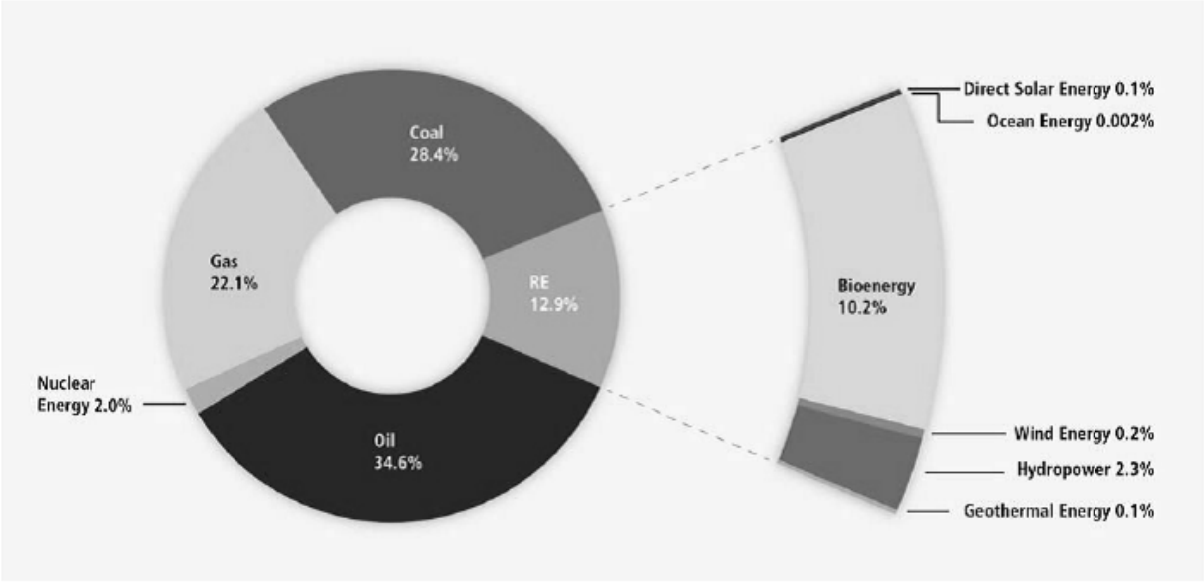

Figure 1.2 Shares of energy sources in total global primary energy supply in 2008. [4]

1.3 Hydrogen economy

The idea of taking hydrogen as a kind of energy carrier initially appeared in the fiction *The Mysterious Island* by Jules Verne in 1874. In the book, he wrote: "I believe that one day water can be used as fuel, and the hydrogen and oxygen which compose the water can be used separately or together. This practice will furnish endless resource for heat and light which coal can't compete with. So I believe once coal is used up, water can be used for heating. Water will be the future coal."

Being considered to be the bridge that connects the era of fossil energy and the future of renewable energy or nuclear energy, hydrogen energy is becoming the vital part of energy strategy and technology competition. There are multiple steps whereby primary energy is converted into an energy carrier (usually heat, electricity, mechanical work, etc.), and then into an energy service. Hydrogen is an ideal choice as an energy carrier - although it is the most abundant element in the universe, it does not naturally exist in its elemental form on Earth. Pure hydrogen must be produced from other hydrogen-containing compounds, and a source of energy is always required during the production. It tends to consume more energy for hydrogen production and storage. Therefore, some people are still suspecting and hesitating to develop hydrogen energy technology.

Hydrogen has been touted as a future transportation fuel due to its versatility, pollutant-free end use and storage capability. It has the potential to tap vast new energy resources to provide transport with zero or near zero emissions. Hydrogen gas can be produced from renewable energy sources by several routes including biomass gasification, the reformation of biomethane, or electrolysis of water. The potential renewable energy resource base for hydrogen is therefore greater than for biogas or syngas. Future production of hydrogen from variable renewable energy resources, such as wind or solar power by electrolysis, will depend significantly on the interaction with existing electricity systems and the degree of surplus capacity.[7] In the short term, blending of hydrogen with natural gas (up to 20% by volume) and transporting it long distances in existing gas grids could be an option. In the longer term, the construction of pipelines for carrying pure hydrogen is possible,

constructed from special steels to avoid embrittlement.

The United States is the first country which came up with the strategic vision of hydrogen energy and hydrogen economy, setting off a new upsurge of R&D of hydrogen globally. A U.S. MARKAL model's results show that hydrogen fuel cell vehicles compete well against conventional and hybrid vehicles in the near future (Figure 1.3). Their market penetration is the highest among the competing technologies due to a high efficiency that more than offsets a higher capital cost. This is the main reason for the overall energy efficiency improvements observed in a hydrogen economy.[8]

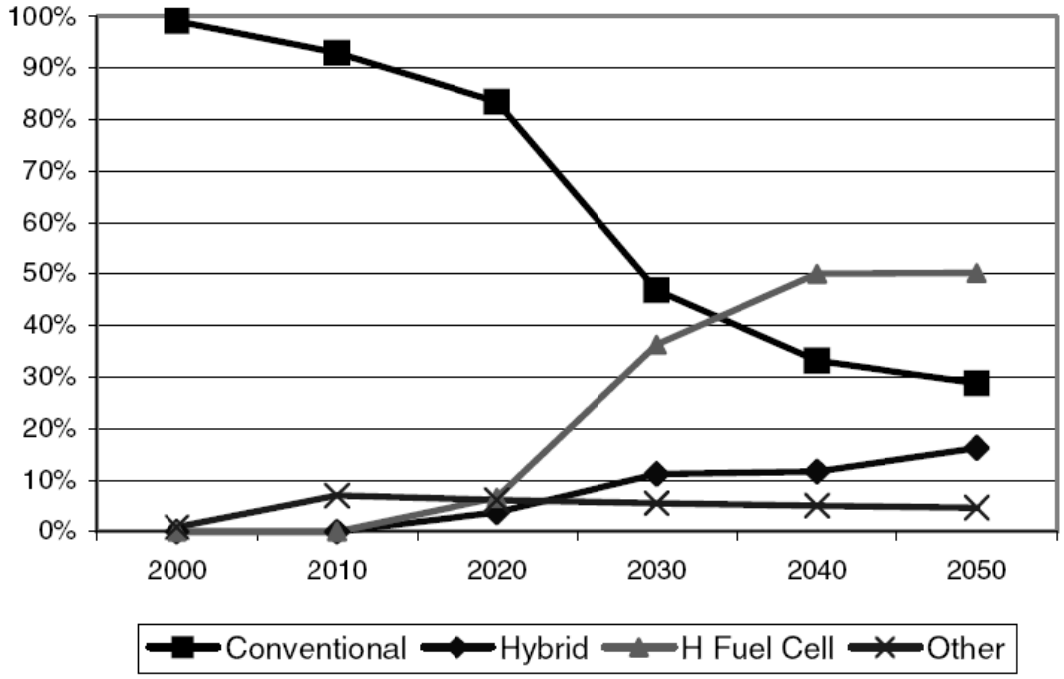

Figure 1.3 Passenger travel market share by vehicle type.

The significance of hydrogen energy as a future energy is also highlighted in China's policy, embodied in their *Energy science and technology in China, A roadmap to 2050* as follows: to replace oil as a transportation fuel; to improve the energy use efficiency as an efficient energy carrier; to reduce emission as a low pollution fuel; to develop distributed energy to improve the security and efficiency of energy system; and to reduce CO_2 emission. According to the roadmap, fuel cell vehicles will take up 1/3 of the whole number on road by the year 2050.[9] Policies on developing hydrogen economy can also be found in other countries such as Canada, New Zealand, Japan and some European countries.

The current technology to produce hydrogen with large-scale fossil fuel has been quite mature, but not efficient enough with 50% to 60% production rate. Calculated with the life cycle method of "from mine to wheel", the hydrogen production rate needs to reach 70%, in order to make the overall use efficiency of fuel cell vehicles reach 40% or beyond (15% to 30% of petrol vehicle). Thus, it is needed to focus on improving the hydrogen production efficiency, lowering cost, optimizing system integration technology, and reducing CO_2. Hydrogen technologies can reduce carbon emissions if hydrogen is produced from renewable technologies or nuclear energy. Hydrogen from fossil fuel with carbon sequestration can also help in reducing carbon emissions. One advantage of hydrogen production through reforming or gasification processes is that the carbon dioxide produced can be readily extracted for storage. Recent studies showed that capturing CO_2 adds about 25-30% to the cost of producing hydrogen.[10]

In addition, it is needed to develop the research of distributed field hydrogen production technology, take advantage of the current energy transportation infrastructure (e.g. electric power, natural gas pipeline network, vehicles) to transport raw material for hydrogen production and energy to the final use spot, and to produce hydrogen on the spot. This technology process has been regarded as the best way to establish hydrogen refueling station and to offer distributed hydrogen resource for fuel cells at present because field hydrogen production can avoid high cost transportation process and doesn't need rebuilt huge transportation infrastructures. Moreover, supporting all kinds of "renewable energy hydrogen production technology" including solar power, nuclear power and biomass should be emphasized. It's also essential to increase the proportion of hydrogen produced with renewable energy and nuclear power.

Fuel cell is an essential component in the development of hydrogen economy.[11] When hydrogen or hydrocarbon is burnt with air in a traditional internal combustion engine, the efficiency of the transformation from chemical to mechanical is limited by the Carnot efficiency (about 25%). While hydrogen is burnt electrochemically with oxygen in a fuel cell which produces electricity and drives electric engine, the efficiency can reach 50-60%, twice as much as the thermal process. Though fuel cell has many commercial demonstrations in

aspects of mobile power source, dispersed power station and micro power supply, some key technology problems haven't been appropriately resolved and commercial promotion proceeds slowly. The main problems are: 1) the cost of the key material and components (electrolyte membrane, bipolar plate and catalyst) for fuel cell is too high; 2) the circulation system of fuel and oxidant, the management system and management control system of water and heat need further optimization; 3) the long-running cell performance especially stability, reliability and environment adaptability need further improvement; 4) the cell construction and preparation technology need further optimization.[9]

In a hydrogen economy, key economic determinant is the cost and safety of the fuel distribution system from the site of manufacture of the hydrogen to the end user. This is true of any fuel, but hydrogen presents unique challenges due to its high diffusivity, extremely low density as a gas and liquid and very broad flammability range relative to hydrocarbons and low-molecular-weight alcohols. These unique properties present special cost and safety obstacles at every step of distribution, from manufacture to, ultimately, on-board vehicle storage. On-board vehicle storage is discussed separately because its requirements are potentially quite different, even though some of the same technologies may be modified for vehicle use, such as high-pressure cylinders or liquid hydrogen containers. The US Department of Energy (DOE) has established a series of targets for hydrogen storage materials to make sure that a vehicle can travel more than 500 km on a single hydrogen fill. Included are stringent systems volumetric (9.72 MJ L^{-1} 2015) and gravimetric target (9 wt% 2015).

Also critical is the form of hydrogen being shipped and stored for subsequent use. Hydrogen can be stored (and transported) as a pressurized gas, a cryogenic liquid or absorbed by nanoporous materials through physisorption in terms of physical hydrogen storage. However, high-pressure and cryogenic hydrogen storage systems are impractical for vehicular applications due to safety concerns and/or volumetric constraints. But with a chemical hydrogen carrier, molecular hydrogen may not be needed, and the manufacture, transportation, distribution and storage systems would be quite different.

1.4 Chemical hydrogen storage

In terms of chemical hydrogen storage, hydrogen is up-taken in a chemical compound via formation of chemical bond with other element and can be released through certain chemical reactions. Materials for chemical hydrogen storage can be divided into two classes: metal hydride and chemical hydride.

1.4.1 Metal hydrides

For hydrogen storage, one of the critical issues is the hydrogen gravimetric density of the material. Therefore, only the hydride complexes of some light elements in the periodic table, are considered for hydrogen storage. Normally metal hydride is termed as a group of materials which are combination of hydrogen and group 1, 2, 3 light metals, e.g. Li, Na, B and Al. Typical complex hydrides include alanates, borohydrides, amides, imides, alane etc.[12] Table 1.1 shows the primary hydrolysis equation and associated hydrogen storage properties of some well-known metal hydride materials, including lithium hydride, LiH; sodium hydride, NaH; calcium hydride, CaH_2; lithium aluminum hydride, $LiAlH_4$; lithium borohydride, $LiBH_4$ and sodium borohydride, $NaBH_4$.[13]

Table 1.1 Candidate hydride hydrolysises and hydrogen storage properties.

Hydride and reactions	Fraction H[a]	H_2 specific mass (kg H_2/kg)[b]	H_2 density (kg H_2/liter)[c]
$LiH + H_2O \rightarrow LiOH + H_2$	0.126	0.252	0.122
$NaH + H_2O \rightarrow NaOH + H_2$	0.042	0.083	0.106
$CaH_2 + 2\ H_2O \rightarrow Ca(OH)_2 + 2\ H_2$	0.048	0.095	0.121
$LiAlH_4 + H_2O \rightarrow LiOH + Al + 2.5\ H_2$	0.105	0.132	0.121
$LiBH_4 + H_2O \rightarrow LiOH + HBO_2 + 2\ H_2$	0.184	0.367	0.235
$NaBH_4 + 2\ H_2O \rightarrow NaBO_2 + 4\ H_2$	0.105	0.211	0.226
Millenium Cell 35% Solution $NaBH_4 + 4\ H_2O \rightarrow NaBO_2 + 4\ H_2 + 2\ H_2O$	-	0.077	0.077

[a] The number of hydrogen atoms in the hydride divided by its molecular weight; [b] Defined as the mass (kg) of H_2 produced per mass of original hydride material or solid product; [c] Determined from the mass of hydrogen produced per volume of hydride or solid product.

These hydrides have relatively high hydrogen densities and are, in most cases, commercially available. The lithium-containing hydrides of LiH, $LiAlH_4$, and $LiBH_4$ rate especially well and represent a class of materials that can exceed the 2015 DOE storage targets (9 wt%) based on reaction chemistry. Since the energy convertor will supply reactant water, almost all of the storage property listings in Table 1.1 (specific mass and density) exclude the volume of water. The only exception is the last reaction, which describes the commercialized Millennium Cell's Hydrogen on Demand System™, using an aqueous solution containing 35 wt% $NaBH_4$ and liberates hydrogen when it comes into contact with a catalyst.[14]

Typically, hydrogen can be generated from metal hydrides via two mechanisms: through a direct reaction with water or through thermal decomposition. The thermal decomposition of metal hydrides usually requires very high temperatures up to 600 ^oC. In fact, many of these "complex hydrides" have been utilized in "one-pass" hydrogen storage systems in which hydrogen is evolved from the hydride upon contact with water. However, the hydrolysis reactions are highly irreversible and could not serve as the basis for rechargeable hydrogen storage systems. The thermodynamics of the direct, reversible dehydrogenation of some complex hydrides lie within the limits that are required for a practical, onboard hydrogen carrier. However, most of these materials are, plagued by high kinetics barriers to dehydrogenation and/or rehydrogenation in the solid state.[15]

1.4.2 Chemical hydrides

Chemical hydrides are chemicals with hydrogen atoms bonded to non-metal elements via covalent bonds. Hydrogen containing chemicals which are useful for hydrogen storage include methanol, ammonia and cycloalkanes. At STP most of them are in liquid phase and therefore provide possibility of using existing infrastructure for gasoline. The hydrogen storage capacities of these chemical hydrides may range in the scale of 6-8 wt%. The supply of hydrogen through liquid organic hydrides (LOH) using catalytic reaction pair of dehydrogenation and hydrogenation is a useful process for supply of hydrogen. This is one of the most promising methods to store, transport and supply with *in situ* generation of hydrogen

due to several advantages associated with this system, including: CO_x-free hydrogen refueling at fuelling stations, reversible catalytic reactions, recyclable reactants and products and relatively high hydrogen contents (6-8% on weight basis and about 60-62 kg H_2/m^3 on volume basis).[16]

Several cycloalkanes may be used as hydrogen carrier as LOH include cyclohexane, methylcyclohexane, tetraline, decaline, cyclohexylbenzene, bicyclohexyl, 1-methyldecaline, etc. A few reactions of dehydrogenation of cycloalkanes are depicted in Table 1.2. One mole of cycloalkane has potential to transport 3-6 mol of hydrogen. The endothermic energy requirement for these reactions is in the range of 64-69 kJ per mole of H_2, which is much lower than the energy for oxidation of H_2 (248 kJ/mol). Due to high boiling points of cycloalkanes, the present infrastructures such as oil tankers and tank lorries can be used for the long-term storage and long-distance transportation of hydrogen in the form of LOH.

Table 1.2 Various potential cycloalkanes with hydrogen storage capacity and endothermic energy requirement.[16]

Reactions	n H_2	H content[a]		kJ/mol	kJ/mol per H_2
		wt%	mol/L		
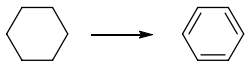	+ 3 H_2	7.2	27.77	+ 205.9	+ 68.6
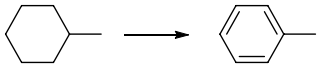	+ 3 H_2	6.2	23.29	+ 204.8	+ 68.3
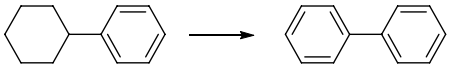	+ 3 H_2	3.8	17.63	+ 197.8	+ 65.9
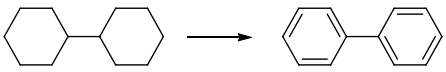	+ 6 H_2	7.3	32.0	+ 399.5	+ 66.6
	+ 5 H_2	7.3 7.3	32.44 31.46	(*cis*-) + 320.1 (*trams*-) + 333.4	+ 64.0 + 66.7

[a] The H contents of the starting materials at STP.

Chemical hydrides are definitely potential candidate for hydrogen storage. However, highly selective and efficient dehydrogenation and hydrogenation catalysts still need to be pursued. Catalyst development also required to target catalytic-reactor configuration to overcome heat transfer limitations for this strongly endothermic reaction. Recycling of chemical hydrides as in case of aromatic–cycloalkane pairs would be advantageous for reuse

of materials, yet the economics has to be worked out for transportation cost in both ways and the weight penalty. A noteworthy example is *N*-ethylcarbazole (Scheme 1.1), which can be hydrogenated over Ru/Al_2O_3 with 70 bar of hydrogen at 130 ^oC.[17] The reverse dehydrogenation takes place over Pd/SiO_2 at170 ^oC to give 5.8 wt% of hydrogen gas.[18]

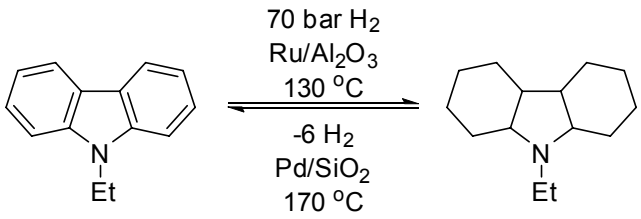

Scheme 1.1 Reversible hydrogenation and dehydrogenation of *N*-ethylcarbazole.

When hetero-atoms are involved, more chemical hydride systems that can up-take and release hydrogen are discovered. One important principle is the *Frustrated Lewis Pair*,[19] meaning a compound or mixture containing a Lewis acid and a Lewis base that cannot combine to form an adduct due to steric hindrance. In 2006, Stephan and co-workers reported the first case of reversible and metal-free hydrogen activation over a phosphino-borane compound $[(C_6H_2Me_3)P(C_6F_4)B(C_6F_5)_2]$ to make a phosphonium-borate compounds $[(C_6H_2Me_3)PH(C_6F_4)BH(C_6F_5)_2]$, as shown in Scheme 1.2.[20] The hydrogenated compound cleanly loses H_2 at temperatures above 100 ^oC.

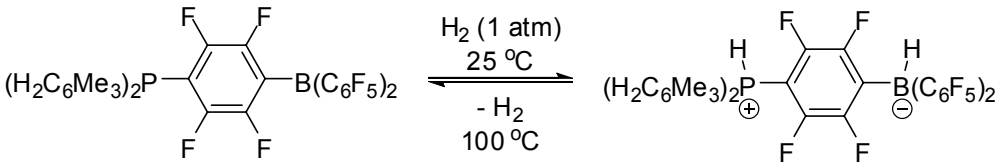

Scheme 1.2 Metal-free, reversible hydrogen activation.

This kind of hydrogen activation processes represented a new concept for catalysis and could be applied for catalytic hydrogenation reactions of unsaturated compounds such as imines,[21] enamines[21c, 22] and silyl enol ethers.[23] All these systems have very low gravimetric capacities which make them unsuitable for hydrogen storage, but studying such basic reactions of hydrogen addition to non-metal systems can garner insight into the design of reversible systems with higher storage capacities.

Hydrogen can also be released from organic compounds through hydrolysis, as in the case of benzimidazolines. The C-H bond in the 2-position is hydridic enough to react with water forming H_2 in the presence of a Pd catalyst (Scheme 1.3).[24]

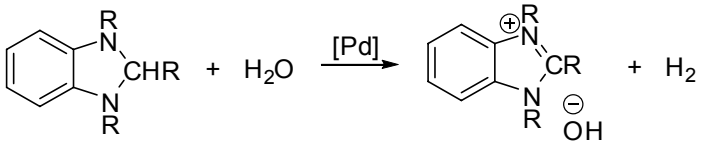

Scheme 1.3 Hydrogen evolution through hydrolysis of chemical hydride.

A remarkable chemical hydride is ammonia borane, which is most studied and proved to be the most promising candidate for on-board chemical hydrogen storage and transportation. It will be thoroughly discussed in the next section.

1.5 Ammonia borane

Ammonia borane (**AB**, H_3NBH_3) is a nonflammable, nonexplosive and air-stable white solid at STP and soluble in relatively polar solvents such as NH_3, water, THF, acetonitrile, etc. The melting point of **AB** is in the range 110-114 ^oC, while ultra-pure material melts at *ca.* 125 ^oC. It is the simplest molecular boron-nitrogen- hydride compound containing hydridic H_B, protic H_N and a strong enough B-N bond that under most conditions hydrogen loss is favored over dissociation to ammonia and borane. Its combination of low molecular weight (30.7 g/mol), high gravimetric hydrogen capacity (19.6 wt%) and volumetric density (0.10-0.14 kg/l) has attracted a flurry of recent investigations into its hydrogen release and rehydrogenation activities, comparing favorably with many other hydrogen storage materials (Figure 1.4).[25] However, one has to keep in mind that if all 3 equivalents of hydrogen were to be released, it would yield boron nitride which is a chemically very stable compound. Therefore, in effect only a maximum of two-thirds of the theoretical hydrogen content of **AB** (13.06 wt%) can be used. A significant effort is being directed toward controlling the kinetics of its decomposition (see section **1.5.1**), with respect to onset temperatures, rapid release, and avoidance of side products such as ammonia or borazine, which can damage a fuel cell.

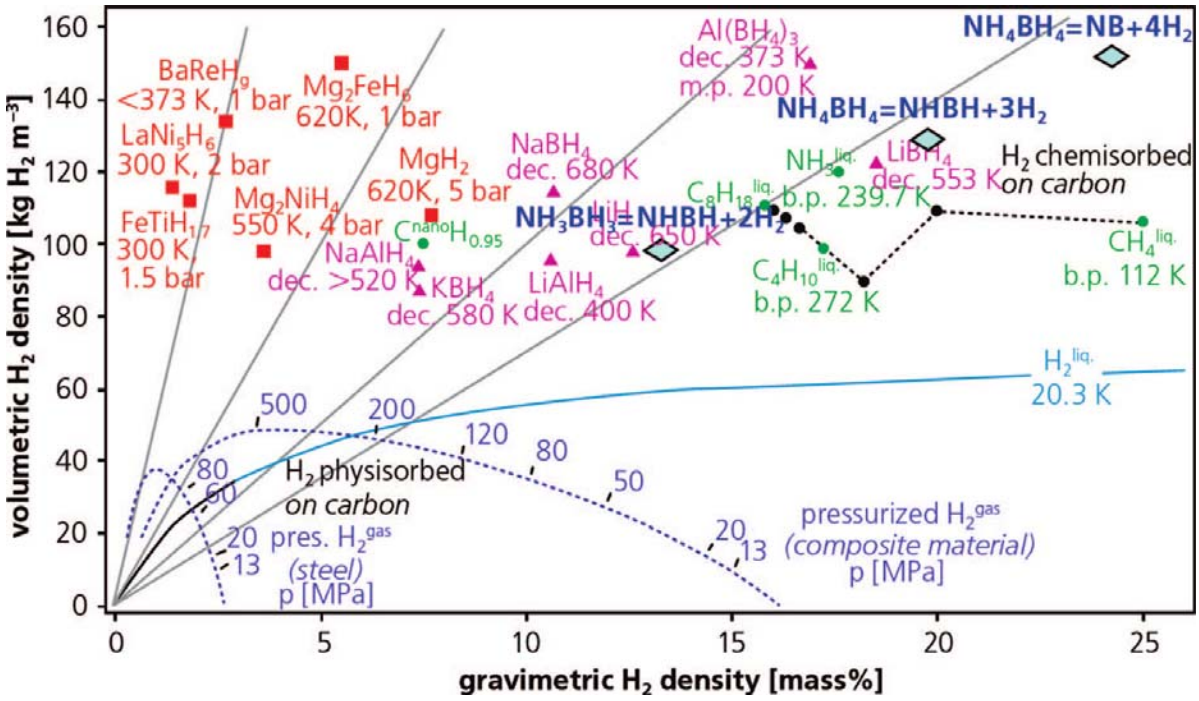

Figure 1.4 Volumetric and gravimetric hydrogen storage densities in various materials and **AB** and its formal thermal decomposition products.[26]

AB was first prepared by Shore and Parry in 1955 using NH_4Cl and $LiBH_4$ in THF.[27] After that, numerous methods for syntheses and/or purification of **AB** were discovered, all of which fall within three types of reaction. Generally, these methods can be classified as salt-metathesis followed by H_2 release (Table 1.3, entries 1-4), Lewis acid-Lewis base exchange (Table 1.3, entries 5-7), or isomerization of the diammonate of diborane (DADB) (Table 1.3, entry 8). These routes are well established in literature and thus will not be discussed in detail.

Table 1.3 Various methods for synthesis of **AB**.

entry	reaction	solvent	yield %
1[27]	$NH_4Cl + LiBH_4 \rightarrow H_3NBH_3 + LiCl + H_2$	THF with trace	45
	$(NH_4)_2SO_4 + 2\ LiBH_4 \rightarrow 2\ H_3NBH_3 + Li_2SO_4 + 2\ H_2$	NH_3	45
2[28]	$NH_4HCO_2 + NaBH_4 \rightarrow H_3NBH_3 + NaHCO_2 + H_2$	THE or dioxane	95
	$(NH_4)_2SO_4 + 2\ NaBH_4 \rightarrow 2\ H_3NBH_3 + Na_2SO_4 + 2\ H_2$	Et_2O	96
3[29]	$NH_4Cl + NaBH_4 \rightarrow H_4NBH_4 + LiCl$ $\rightarrow H_3NBH_3 + NaCl + H_2$	Anhydrous NH_3/THF	99
	$NH_4F + LiBH_4 \rightarrow H_3NBH_3 + LiF + H_2$	NH_3/THF	99
4[30]	$(NH_4)_2CO_3 + 2\ NaBH_4 \rightarrow 2\ H_3NBH_3 + Na_2CO_3 + 2\ H_2$	THF	60-80
5[31]	$BH_3\ THF + NH_3 \rightarrow H_3NBH_3$	THF, excess NH_3	50
6[32]	$B_2H_6 + 2\ NH_3 \rightarrow 2\ H_3NBH_3$	Et_2O	45
7[33]	$BH_3\ SMe_2 + NH_3 \rightarrow H_3NBH_3 + SMe_2$	Et_2O	86
8[34]	$[H_2B(NH_3)_2]BH_4 \rightarrow 2\ H_3NBH_3$	diglyme, small amount of B_2H_6	80-91

Although **AB** is isoelectronic with ethane, the structures, bonding and reactivity of the two compounds are very different. Whereas ethane contains a covalent C-C bond, the polar B-N bond of **AB** (Pauling electronegativities for B and N are 2.04 and 3.04; dipole moment is 5.216(17) D)[35] is dative with the lone pair of ammonia interacting with the empty p-orbital of borane. This difference in bonding modes is also reflected in the bond dissociation enthalpies: ethane, $\Delta H^o_{dis} = 376 \pm 2$ kJ/mol; **AB**, $\Delta H^o_{dis} = 108.4$ kJ/mol (calculated).[36]

Reactions to dehydrogenate **AB** have been investigated theoretically. Dehydrogenation reaction energies have been calculated for successive losses of hydrogen from **AB** in the gas phase. Dixon and Gutowski used *ab initio* molecular orbital theory to show that the enthalpies

of reaction modes as shown in entry 2 and 3 (Table 1.4) vary significantly from the dehydrogenation of ethane and ethylene, respectively.[35] Himmel and Schnoeckel used Gaussian98 (B3LYP method) to calculate the gas phase reaction enthalpies at 298.2 K of various main group hydrogenation reactions, indicating that dehydrogenation reactions of **AB** are exothermic (-26.6 kJ/mol for reaction mode of entry 2) and endothermic (133.3 kJ/mol for reaction mode of entry 3).[37] Dixon and Gutowski further extended the reaction series to include dehydrogenation of iminoborane HNBH (Table 1.4, entry 4, 562.3 kJ/mol) and ammonium borohydride $[NH_4][BH_4]$ (Table 1.4, entry 1, -70.3 kJ/mol at 0 K). Ammonium borohydride is not stable above *ca.* -40 ^oC, limiting its usefulness as a chemical hydrogen storage medium.[35]

Table 1.4 Reaction enthalpies (ΔH in kJ/mol) calculated at 298 K.

entry	reactions	H_3NBH_3	H_3CCH_3
1	$[H_4X][YH_4] \rightarrow H_3XYH_3 + H_2$	-70.3[a]	64.96[b]
2	$H_3XYH_3 \rightarrow H_2XYH_2 + H_2$	-21.3	136.4
3	$H_2XYH_2 \rightarrow HXYH + H_2$	131.4	175.8
4	$HXYH \rightarrow XY + H_2$	562.1	609.9

[a] This value id calculated at 0 K; [b] Value calculated from the heats of formation supplied in the *NIST Thermochemical Tables*[38] for the equation: $2\ CH_4 \rightarrow H_3CCH_3 + H_2$.

The structures and abbreviations of the dehydrocoupling products of **AB** that will be referred to later on are described in Figure 1.5. Removing one equivalent of H_2 from AB yields aminoborane (NH_2BH_2) as an analogue of ethylene,[39] which is highly reactive and only stable at low temperatures.[40] Aminoborane readily oligomerizes to form products of the type $(NH_2BH_2)_n$. Cyclotriborazane (**CTB**, $(NH_2BH_2)_3$) is an analogue of cyclohexane as a crystalline solid which is stable below 100 ^oC. Pentamer (cyclopentaborazane, $(NH_2BH_2)_5$) has been characterized by IR spectroscopy, powder X-ray diffraction and solution molecular weight experiments.[41] The nature of polyaminoborane (**PAB**) is more nebulous as there are a variety of routes by which polymerization may occur, and as a result there are likely structures that are linear, branched, or cyclic.[25a]

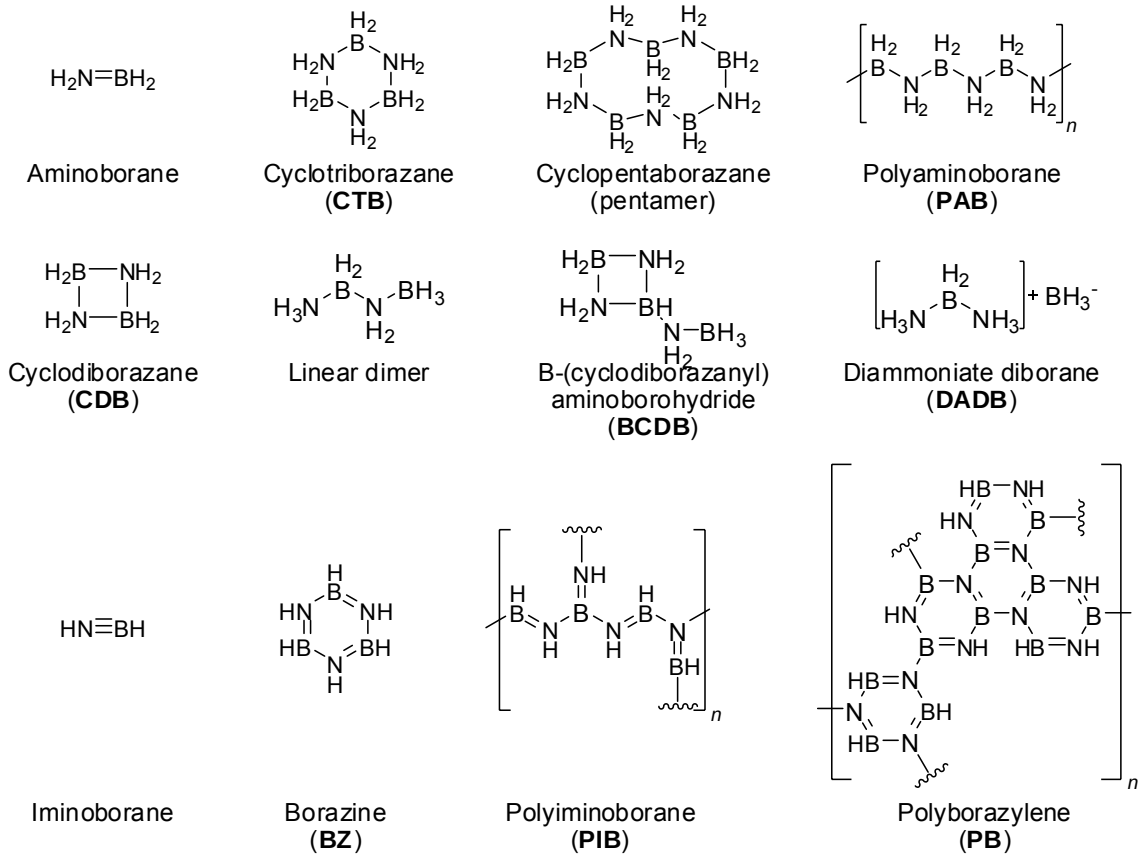

Figure 1.5 Dehydrogenation products of **AB**.

Iminoborane (NHBH) is an analogue of acetylene, and is the result of removing two equivalents of H_2 from **AB**. Like aminoborane, it is only observable at low temperatures as it readily oligomerizes as temperature and concentration increase. Borazine ($(NHBH)_3$, **BZ**) is a well-defined iminoborane oligomer. Both polyiminoborane (**PIB**) and polyborazylene (**PB**, cyclic polyiminoborane) have ill-defined amounts of cross-linking and branching that are likely dependent on the synthetic conditions employed.

1.5.1 H_2 release from AB

1.5.1.1 Thermal decomposition of AB in the solid state

As a thermally unstable molecule, **AB** has been found to decompose in three distinct steps (Scheme 1.4), which was studied for the first time in 1978 by Hu and co-workers applying thermogravimetric analysis (TGA), differential thermal analysis (DTA) and thermomanometry with relatively large heating rates (5-10 ^{o}C/min).[42] Chemical analysis of the decomposition steps was attempted by pyrolysis/trapping experiments, where the products

were analyzed by IR spectroscopy and deduced by the calculation of the mass balance, which did not allow a detailed understanding of the process.

$$H_3N\text{-}BH_3 \longrightarrow 1/x\ (H_2N\text{-}BH_2)_x + H_2 \quad (1)$$

$$(H_2N\text{-}BH_2)_x \longrightarrow (HN\text{-}BH)_x + H_2 \quad (2)$$

$$(HN\text{-}BH)_x \longrightarrow x\ BN + H_2 \quad (3)$$

Scheme 1.4 Generalized thermolysis of **AB**.

A later study was done by Sit and co-workers in 1987, attempted to resolve the thermo-gravimetric and DTA signals during the decomposition of **AB** at a heating rate of 2 ^{o}C/min.[43] The melt endotherm was found at 114 ^{o}C, preceded by a slow hydrogen loss. This was followed by an exotherm at 125 ^{o}C, which was ascribed to hydrogen loss to give [NH_2=BH_2] and H_2. [NH_2=BH_2] had been tentatively identified in the gas phase by mass spectrometry[44] but is highly unstable and forms polyaminoboranes (**PAB**). At 155 ^{o}C, the mixture of **PAB** became unstable and released another equivalent of H_2 to give borazine and other related dehydrocoupling products.

In 2000, Wolf and co-workers analyzed the influence of the heating rate on the calorimetrically obtained data (DSC) and also performed detailed isothermal studies.[45] The results revealed that, at 1 ^{o}C/min, an exothermic reaction at 95 ^{o}C preceded the endothermic melt, which in turn was followed by a large exothermic peak with a maximum at 113 ^{o}C, overlapped by a further peak starting at 125 ^{o}C. When the heating rate was reduced to 0.05 ^{o}C, the first exothermic peak could be completely separated beginning at 82 ^{o}C with no melt endotherm apparent. This meant that, given enough time at lower temperatures, the decomposition process is complete *before* the melt. Melt endotherms at higher rates only exist because there may be still some residual **AB**. Melting points tend to be strongly influenced by the impurities present, and therefore, the observed melting temperature may be highly variable with the heating rate.

Two years later, a more detailed study was published, which confirmed these findings and included also FT-IR and mass spectrometric analyses.[46] In this context the thermal stability

of **AB** at constant 50-60 °C was also studied, which represented the extreme temperatures that may be found in a fuel cell.[47] The estimated half-life of **AB** was found to be on the order of months at 50 °C, but only weeks at 60 °C.

A nonvolatile white residue was observed after the first decomposition step of **AB**, which is often described as polyaminoborane (**PAB**) of the composition BNH_4, but is likely to contain borazinyl residues with cyclic and cross-linked structures. This intermediate product was also investigated by TGA and DSC.[44] The following decomposition steps were assigned to the loss of 1 equivalent of H_2 to give polyiminoboranes (**PIB**) and related compounds (eq 2, Scheme 1.4)[48] and gradual loss of formally half an equivalent to give a material of the composition NBH and finally boron nitride (eq 3, Scheme 1.4).

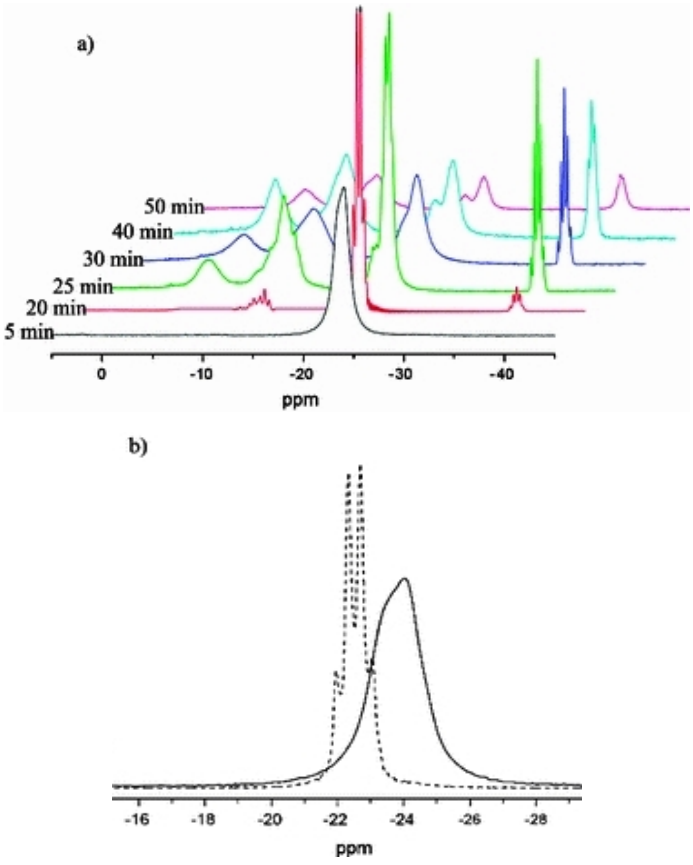

Figure 1.6 (a) The 18.8 T ^{11}B MAS-NMR of ND_3BH_3 is shown as a function of time heated at 88 °C (t = 5, 20, 25, 30, 40 and 50 min). At high magnetic fields, the **AB** resonance collapses to a single line and **PAB** products are more readily observed. (b) Overlay of times 5 (solid) and 20 min (dashed). The downfield chemical shift and line narrowing demonstrates the formation of a new product, while the quartet and the J^1(B-H) coupling of 94 Hz confirm a -BH_3, thus a new phase of **AB**.[49]

A much more detailed mechanism of the decomposition of **AB** was provided by Shaw and Autrey and co-workers, who used solid state ^{11}B and $^{11}B\{^1H\}$ MAS NMR spectroscopy to follow the reaction *in situ* under isothermal conditions of 88 ^oC.[49] The peak shape in solid state NMR is highly dependent on the external magnetic field and while spectra at 7.1 T showed a broad peak with second order quadripolar interactions, this effect was much reduced at 18.8 T, where only a single peak was visible for **AB** at δ -24.0 ppm (Figure 1.6).

Shortly after heating, a new species containing a BH_3 group formed, which showed quartet splitting in the proton coupled ^{11}B NMR spectrum (Figure 1.6, (b)). It was proposed that this represented a new, "mobile" phase of **AB**, because there was no visible melting at this temperature, which is below the reported melting point of 112-114 ^oC. After this induction period, hydrogen started to evolve, and three further species were observed: the diammoniate of diborane (**DADB**), $[(NH_3)_2BH_2]^+[BH_4]^-$, and two BH_2NH_2 species which were possibly the linear ($NH_3BH_2NH_2BH_3$) and the cyclic dimer $(NH_2BH_2)_2$ of aminoborane. After longer decomposition times, broad and relatively poorly defined peaks of thermally produced **PAB** started to emerge (for the chemical shifts of the features discussed, see Table 1.5).

Table 1.5 Chemical shifts and coupling constants of products observed at low conversion during the *in situ* heating of **AB** at 18.8 T. [49]

Chemical shift/ppm	Identity	^{11}B–^1H *J*-coupling/Hz
−38.2	BH_4 (**DADB**)	77
−24.0	**AB**	-
−22.5	New phase **AB**	94
−21.1	BH_3 (linear dimer)	84
−13.2	BH_2 (**DADB**)	116
−12.1	BH_2 (linear dimer)	104
−10.9	BH_2 (??)	103
−10.7	BH_2 (??)	102

Based on these observations discussed before, a mechanistic model was presented which was comprised of three distinct steps: induction, nucleation and growth (Scheme 1.5). In the induction period, a mobile phase of **AB** is generated, in which the dihydrogen bonding

network is perturbed. **DADB** is generated in the subsequent nucleation process, which can then react with **AB** to form dimeric, oligomeric and eventually polymeric products or isomerize to form the cyclic dimer. This mechanism further supported by a study using TGA/DSC, optical microscopy and high temperature X-ray powder diffraction.[50]

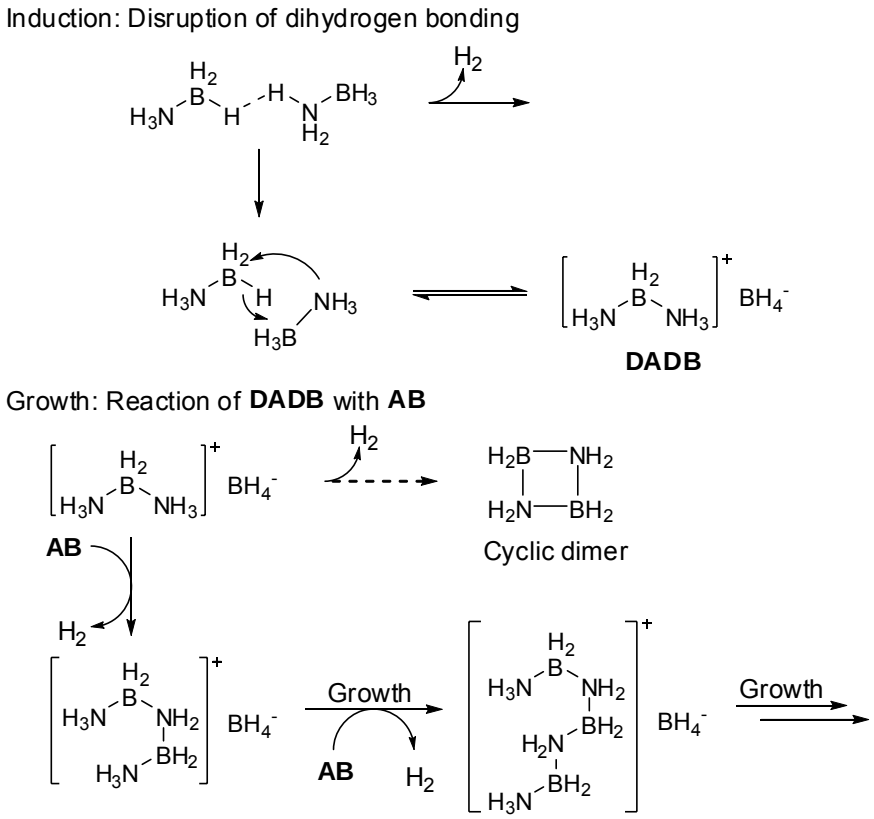

Scheme 1.5 Proposed thermal dehydrogenation mechanism of **AB** showing discrete induction, nucleation and growth steps leading to hydrogen release.

The thermal decomposition of **AB** was also analyzed at high pressures up to 600 bar.[51] H_2 was used as a pressurizing gas (using mercury as a pressure transmitter) because there was a particular interest in the question of whether any reversibility of the dehydrogenation could be observed. However, no evidence for a reversible process was found. The DSC trace at 600 bar with a heating rate of 0.15 ^oC/min showed a first exothermic mass loss at 87 ^oC and a second at approximately 132 ^oC, which were not fully resolved. Both events led to a loss of approximately 1 equivalent of H_2 each. With this low heating rate, no melting transition was observed, as **AB** would have fully decomposed before the melting temperature of 114 ^oC. Lowering the pressure to 250 bar did not significantly alter the results. It could be argued that all the observed effects were simply due to a low heating rate, with the pressure effect almost

negligible, because the crystallographic form of **AB** is reported to change from tetragonal to orthorhombic only at higher pressures than the 600 bar used for this study.

Lowering the pressure below ambient pressure was also shown to have a dramatic effect on the thermal decomposition of **AB**, using TGA, DTA and mass spectrometry.[52] The samples were held at 90 ^{o}C under various pressures between 50 and 1040 mbar, where at ambient pressure, hydrogen was released after approximately 6 h, dropping to around 3.5 h at 50 mbar. Other impurities such as diborane, aminoborane (NH_2=BH_2), or borazine were also observed with higher intensity at lower pressures.

The thermal decomposition of **AB** was also done in the presence of oxygen using another analytical technique, emission thermophotometry (ETP).[53] It was observed that when **AB** was heated in the presence of oxygen at a heating rate of 20 ^{o}C/min, there was a light emission starting at 180 ^{o}C and continuing up to 350 ^{o}C (the highest temperature at which measurements were obtained). The high onset temperature suggested that it was not **AB** itself that ignited (light emission) but rather a decomposition product. Since pentaborane was known to ignite with a white luminescence in oxygen mixtures below the explosion limit,[54] it was surmised that a similar B-H oxidation may have occurred, although this phenomenon was never further investigated.

Nevertheless, the dehydrogenation of **AB** at 85 ^{o}C under carbon dioxide atmosphere was proved to be significantly accelerated as confirmed by ATR-FTIR, Raman, and ^{11}B and ^{13}C solid-state MAS NMR measurements.[55] Not only the presence of CO_2 enhances the thermolysis kinetics, the hydrogen release also becomes faster as the CO_2 pressure increases from 1.70 to 3.67 bar (Figure 1.7). Around 4 bar of CO_2, 1.33 equiv of H_2 is released from **AB** in 1 h. The accelerated **AB** thermolysis could be due to CO_2 reacting with **AB** (Figure 1.8), intermediates like **DADB**, or primary thermolysis products including linear dimers of aminoborane (**LDAB**).

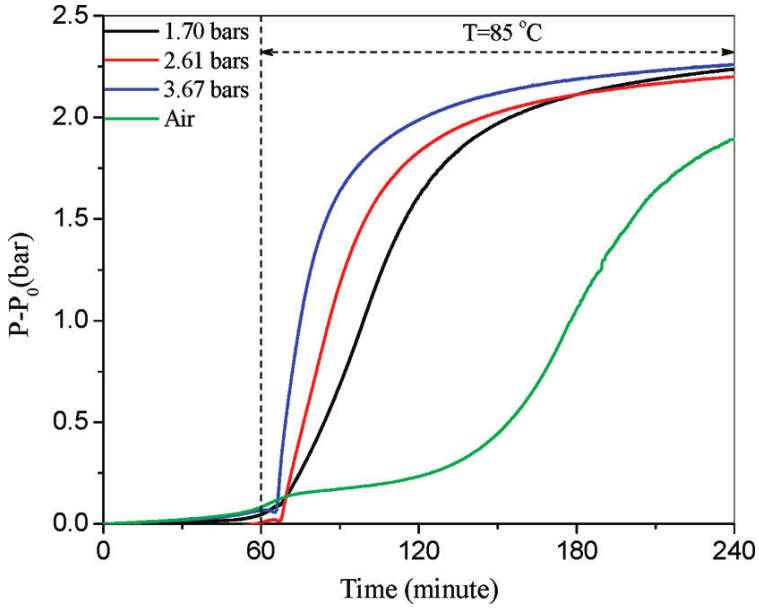

Figure 1.7 Pressure profiles of **AB** thermolysis for 3.32 bar of air and CO_2 pressures of 1.70, 2.61, and 3.67 bar.[55]

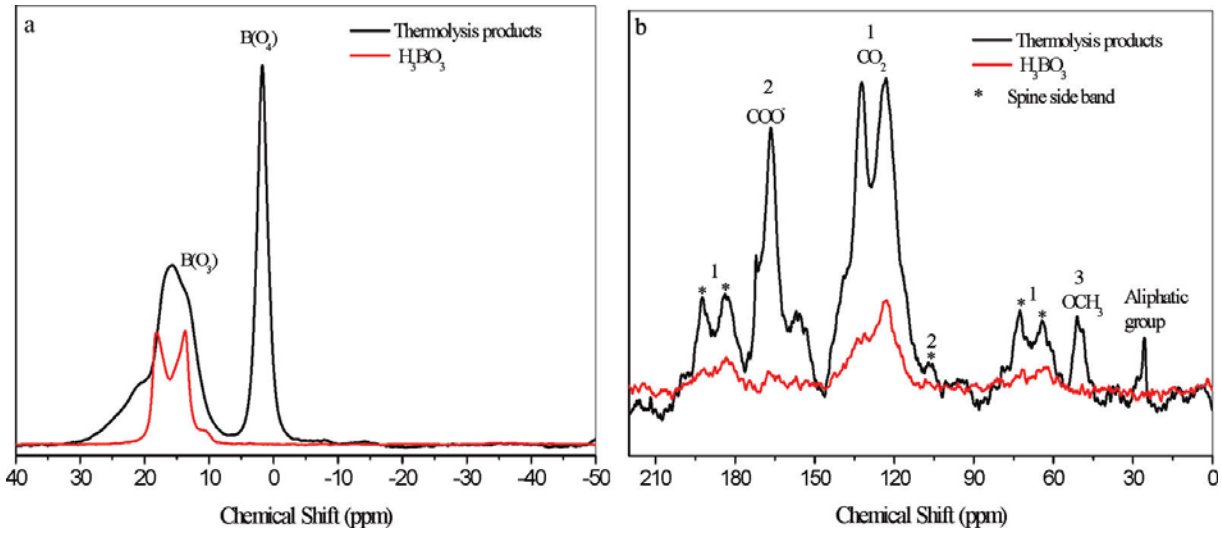

Figure 1.8 ^{11}B (a) and ^{13}C (b) MAS NMR of solid thermolysis products of **AB** for 21.7 bar (at 85 °C) of CO_2.[55]

1.5.1.2 Thermal decomposition of AB in solution

The first studies on the thermal decomposition process of **AB** in solution aimed to spectroscopically identify the elusive, postulated [$H_2N{=}BH_2$] species.[56] For this purpose, thermal reactions of 0.15 M **AB** in acetonitrile, diglyme, glyme, 2-methyl tetrahydrofuran, pyridine, and THF were analyzed by *ex situ* ^{11}B NMR spectroscopy. While acetonitrile and pyridine showed a reaction with the substrate, the ethereal solvents showed mainly products

associated with hydrogen loss. In all of the above reactions, a peak at around δ -11 ppm occurred in varying amounts, which was assigned to cyclotriborazane (**CTB**) by comparison with an authentic sample, but it was conceded that small cyclic oligomers of different ring sizes were undistinguishable. Borazine (**BZ**, δ 30.2 ppm) and μ-aminodiborane (δ -28.9 ppm) were also identified.

Two decades later, the solution decomposition of **AB** was reinvestigated by Baker and co-workers, fueled by renewed interest in this molecule as a hydrogen storage material.[57] A 500 MHz spectrometer with a high pressure spinning NMR cell (produced from polyether ether ketone (PEEK)) made it possible to follow the reaction of **AB** in glyme (1 M) at various temperatures *in situ* with a much higher resolution of the peaks. The first significant finding was that the reaction followed second order kinetics in **AB**, as a consequence of which the stability of an **AB** solution is extremely concentration dependent. Because of this observation, the authors also ruled out the unimolecular formation of [$H_2N{=}BH_2$] followed by a [2+2] cycloaddition. For the latter process to conform to second order kinetics, the [2+2] cyclization would need to be rate determining, leading to a buildup of [$H_2N{=}BH_2$], which was not observed experimentally. By ^{11}B NMR spectroscopy performed at 80 ^{o}C, the initial products appeared between δ -10.8 and -15 ppm (Figure 1.9, Left).

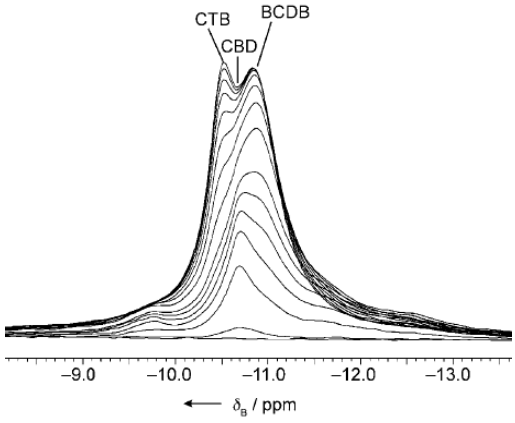

Species	^{11}B [ppm][a] (80 °C)	$^{1}J_{B,H}$ [Hz]	^{15}N [ppm][b] (20 °C)	$^{1}J_{N,H}$ [Hz]
NH_3BH_3	−21.6 (BH_3)	96 (q)	−384.5 (NH_3)	70 (q)
CDB	−10.8 (BH_2)	104 (t)	−376.7 (NH_2)	65 (t)
BCDB	−23.4 (BH_3)	93 (q)	−375.9 (NH_2)	65 (t)
	−10.9 (BH_2)	104 (t)	−370.9 (NH_2)[c]	66 (t)
	−5.0 (BH)	114 (d)		
CTB	−10.6 (BH_2)	102 (t)	−370.0 (NH_2)	66 (t)
borazine	31.1 (BH)	133 (d)	−281.7 (NH)	102 (d)
polyborazylene	27.2 (B)	–	−324.4 (NH)	75 (d)

[a] ^{11}B chemical shifts relative to the IUPAC standard $BF_3{\cdot}OEt_2$ (δ=0 ppm) at 20 °C (Ξ=32.083974). [b] ^{15}N chemical shifts referenced to NH_4Cl (δ=−360.2 ppm) relative to the IUPAC standard CH_3NO_2 (δ=0 ppm; Ξ=10.136767). [c] Signal for the NH_2 group outside the ring.

Figure 1.9 Left: Time-dependent $^{11}B\{^{1}H\}$ NMR spectra for the first 3.5 h (0, 10, 20, 30, 40, 50, 60, 80, 100, 120, 140, 160, 180, 200, 220 min, from bottom to top) of the thermolysis of **AB** (1 M) at 80 °C; **CBD** was the first species to appear. Right: **AB**-dehydrogenation products identified by ^{11}B and ^{15}N NMR spectroscopy, in order of appearance.[57]

The initial peak at δ -10.8 ppm was tentatively assigned to be cyclodiborazane (**CDB**), followed by three peaks growing at the same rate (δ -10.9 ppm (BH_2), -5.0 ppm (BH), and -23.4 ppm (BH_3), possibly *B*-(cyclodiborazanyl)aminoborohydride (**BCDB**)). Cyclotriborazane (**CTB**, δ -10.6 ppm), assigned by comparison to an authentic sample, was the last peak to grow in. In order to further corroborate these results, the authors also measured ^{15}N NMR spectra (Figure 1.9, right).

Based on these results, a novel mechanism for dehydrogenation of **AB** in solution was postulated (Scheme 1.6). It is proposed that **AB** reacts initially in a bimolecular reaction to give the instable **DADB**. This may then undergo hydrogen loss with concomitant ring closure to give **CDB**, which may react with another equivalent of **AB** under hydrogen loss to give **BCDB**. Both **CDB** and **BCDB** may convert into **CTB**, although there was no direct evidence for this. This reaction mechanism is largely based on the NMR data but seems slightly at odds with a second order fit for the kinetics, since firstly the initial step was assumed to be reversible (which is not an assumption for the simple second order fit used), and secondly, **AB** is also postulated to be consumed in a subsequent step. Depending on the actual rate constants for the steps involved, it may be difficult to differentiate between different kinetic models, and additional studies such as kinetic isotope effects may be required.

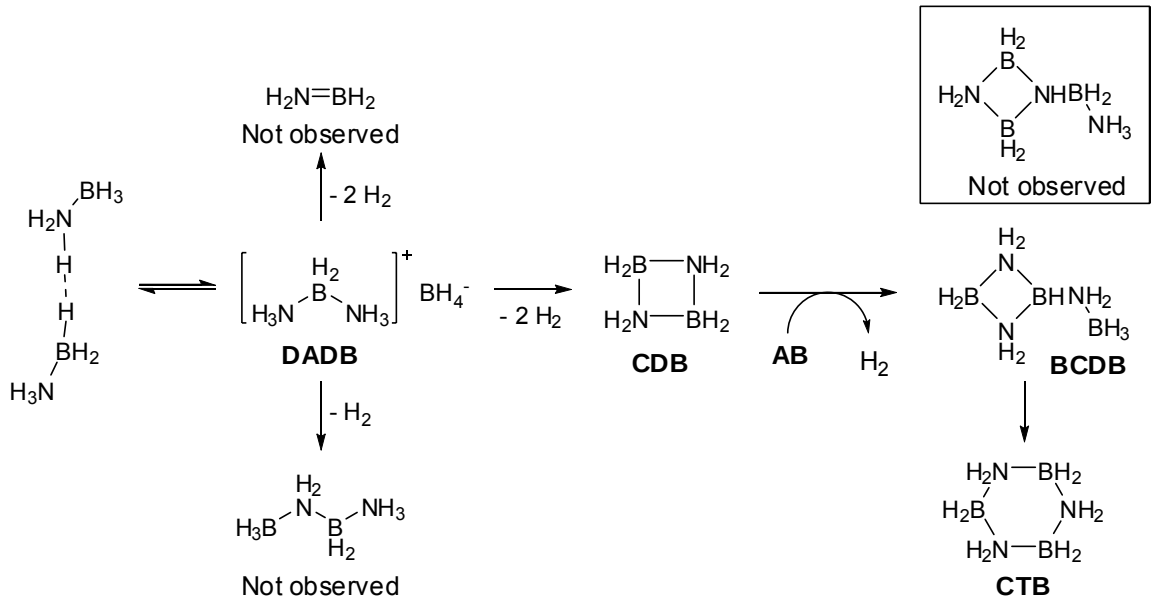

Scheme 1.6 Proposed thermal dehydrogenation mechanism of **AB** showing discrete induction, nucleation and growth steps leading to hydrogen release.[57]

Interestingly, the formation of borazine (**BZ**, δ 31.1 ppm) was also observed, concurring with the formation of **CTB**, which seemed inconsistent with **BZ** formation by simple dehydrogenation of **CTB**. This result seemed also not to be in accordance with an earlier report that substantial **BZ** formation from **CTB** required temperatures above 100 ^{o}C.[58] However, it has to be considered that an isothermal experiment and a temperature gradient experiment cannot be directly compared, as the onset of decomposition is highly heating rate dependent. The earlier work also described an intermediate species at (δ -22.0 ppm, -BH_3), which similarly is evidence against a simple dehydrogenation process from **CTB** to **BZ**. A catalytic effect of BH_3 as a Lewis acid derived from dissociated **AB** was not considered.

In a contribution from 2008, it was shown that noncatalytic hydrothermolysis may be a viable option for a process that releases H_2 from **AB** and water.[59] A mixture of **AB** in gelled water with nanoscale aluminum powder in a ratio of **AB**/Al/H_2O) 2:3:3 was prepared, which was subsequently ignited. The fuel burnt in a self-sustained combustion, because the release of hydrogen is exothermic, to release 7.7 wt% of dihydrogen, which is significantly more than the theoretical yield for Al/H_2O mixtures alone: 5.6 wt%. Another way to realize catalyst free hydrothermolysis was to use Ar pressure to increase the boiling point of water, so hydrolysis temperatures of up to 170 ^{o}C could be reached. At temperatures as low as 135 ^{o}C at an initial pressure of 14.6 atm, 3 equivalents of H_2/**AB** molecule were released. Isotope studies showed that approximately 2 equivalents originated from **AB** and one from water. Crucially, the reaction was very selective so that by ^{11}B NMR and MS no **BZ** formation could be detected. This type of reaction was further developed by combining the exothermic reaction of a nano aluminium/water combustion with **AB** dehydrogenation in a spatially separated reaction space.[60]

Lately in 2011, the first thermolysis of **AB** in water without additives was approached by the same group over a wide range of **AB** concentrations (6-88 wt%), at pressure 14.7 and 200 psi, and temperatures 85-135 ^{o}C.[61] It is shown that with increasing **AB** concentration up to 77 wt%, the H_2 yield increases, and that the role of thermolysis, when compared with hydrolysis, increases. The maximum hydrogen storage capacity was 11.6 and 14.3 wt% at pressure 14.7 and 200 psi, respectively, which was obtained at 77 wt% **AB** and $T_{reactor}$ ~ 85 ^{o}C

along with rapid kinetics. The material-based H_2 yield (~14.3 wt%) is sufficiently higher than the DOE target value (9 wt%, 2015), suggesting that the noncatalytic **AB** hydrothermolysis method could be promising for hydrogen storage in fuel cell-based vehicle applications.

A different approach to lowering the temperature of the thermal decomposition of **AB** was attempted by Sneddon and co-workers, who carried out the thermolysis in an ionic liquid (bmimCl: 1-butyl-3-methylimidazolium chloride).[62] While heating pure **AB** at 85 ^{o}C gave a negligible amount of H_2 after 3 h, heating in bmimCl showed immediate release of H_2 and gave 0.95 equivalent after 3 h at 85 ^{o}C and even 1.5 equivalents after 3 h at 95 ^{o}C (0.8 equivalent at 95 ^{o}C after 3 h for **AB**). The nonvolatile products were analyzed by ^{11}B NMR spectroscopy, and the chemical shifts compared to calculated shifts. It was inferred from this that primarily acylic linear and branched products had been obtained. Initially, considerable amounts of the ions BH_4^- and BH_2^+ were formed, likely to be stabilized by the ionic liquid, which then disappeared over time. This observation is similar to Autrey's and Shaw's when they followed the thermal decomposition of **AB** by *in situ* ^{11}B NMR spectroscopy, where **DADB** was observed as an initial product.[57] The mechanistic role of the ionic liquid has not been determined, but the authors speculated that it may help reduce the energy of polar transition states during the dehydrogenation process. In another temperature dependent study, a significant increase in the H_2 yield was observed at temperatures over 107 ^{o}C in the bmimCl aided **AB** thermolysis.[63]

The use of a hexagonal boron nitride (h-BN) framework was also attempted for the facilitated dehydrogenation of **AB**.[64] It was argued that the potential advantage of such an approach is the fact that no other elements are being introduced into the system, thus potentially facilitating a regeneration process. Mixtures of these materials were prepared in different ratios via ball milling, which increased the surface area of the h-BN particles from 12 m^2/g to 251 m^2/g and the thermolysis was analyzed by TGA, DSC, MS, PXRD, and MAS-^{11}B-NMR spectroscopy. Indeed, with increased h-BN content, the onset of the decomposition decreased substantially to approximately 70 ^{o}C for a ratio of 4/1 h-BN/AB, probably due to the disruption of hydrogen bonding of **AB** by h-BN. However, the concomitant formation of **BZ** increased dramatically, rendering this system unsuitable for fuel

cell applications.

1.5.1.3 Metal catalyzed dehydrocoupling of AB

The first report on catalytic dehydrocoupling of **AB** in the open literature was done by Manners and coworkers in 2001, focused on the use of Rh(I)- or Rh(III)- based precatalysts at, or close to, ambient temperature.[65] The initial and subsequent report included a description of the effective first use of **AB** itself as a substrate to give **BZ** and an insoluble material with a complex and presumably oligomeric structure.[33]

In 2006, an extremely effective catalyst was reported, demonstrating that Brookhart's iridium pincer complex, (POCOP)IrH_2(POCOP)[μ3-1,3-(OP*t*$Bu_2C_6H_3$)]),[66] was able to dehydrogenate **AB** in a dilute THF solution with a catalyst loading of 0.5 mol% within 14 minutes.[67] The product of the reaction was poorly soluble and was characterized by IR, powder X-ray diffraction and solid state ^{11}B MAS NMR spectroscopy. The authors proposed that this product is cyclopentaborazane $[NH_2\text{-}BH_2]_5$, based on the PXRD pattern, which is close to the data set reported by Shore.[40a] However, it cannot be concluded that the product was not linear and oligomeric or polymeric in nature. It is significant that only 1 equivalent of hydrogen was released. There is too little evidence at present to fully understand this selectivity, but it is possible that the main reason may be the sterically crowded catalytic center, which hinders the reaction of secondary amine-boranes. Initial recycling studies showed that the catalyst was converted over time to a resting state; addition of hydrogen was then shown to regenerate the active catalyst. The dormant species was initially assumed to be (POCOP)$IrH_2(BH_3)$. It was possible to prepare this complex by two other independent routes and to characterize its structure by neutron diffraction.[68] The first route involved the treatment of the precursor of (POCOP)IrHCl with sodium borohydride, whereas in the second route Brookhart's catalyst was employed directly and BH_3·THF added (Scheme 1.7). Although the signal to parameter ratio was not high, it was possible to determine that in the dormant borohydride complex two H atoms on Ir are bound like hydrides, whereas BH_3 assumes the role of a B-H-σ-donating ligand.

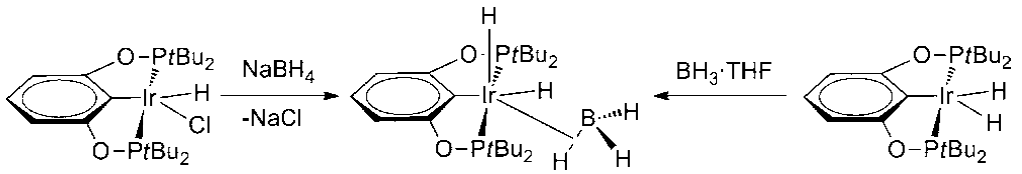

Scheme 1.7 Two independent routes for the formation of the dormant borohydride complex.

A possible mechanism for the dehydrogenation of **AB** by (POCOP)IrH_2 was described by Paul and Musgrave, who used a slightly simplified model.[69] They analyzed two different pathways, one via a 14-electron iridium species, which they concluded could not take place at room temperature, and another via a 16-electron species. Here, the catalyst was initially electrostatically stabilized by binding the substrate via the hydridic hydrogen H_B. In a concerted transition state (TS), the protic hydrogen H_N was transferred to the iridium, followed by dissociation of the dehydrogenated **AB**. In the second TS, the H_2 was formed and left the complex. Both barriers for the TSs were similar, so it is possible that there are two rate limiting steps in this reaction. Experimentally, the tetrahydride appeared as the major detectable intermediate, which is in accordance with the mechanism presented.

Another catalytic system for dehydrogenation of **AB** is based on nickel carbene complexes (Figure 1.10).[70] On mixing a $Ni(cod)_2$ solution in C_6D_6 with various *N*-heterocyclic carbine (NHC) ligands, and adding this mixture to a solution of **AB** in diglyme in a 1:10 ratio at 60 ^oC, immediate hydrogen evolution was observed. After 4 h, up to 2.8 equivalents of hydrogen had evolved, which makes this one of the most effective (presumably) homogeneous systems for the dehydrogenation of **AB** to date. The major products showed peaks from 40 to 18 ppm by ^{11}B NMR spectroscopy and were attributed to cross-linked borazine-type species. Importantly, this was one of the first studies to report kinetic isotope effects for NH_3BD_3 (1.7), ND_3BH_3 (2.3), and ND_3BD_3 (3.0), which combined with computational studies[71] provided useful mechanistic insights.

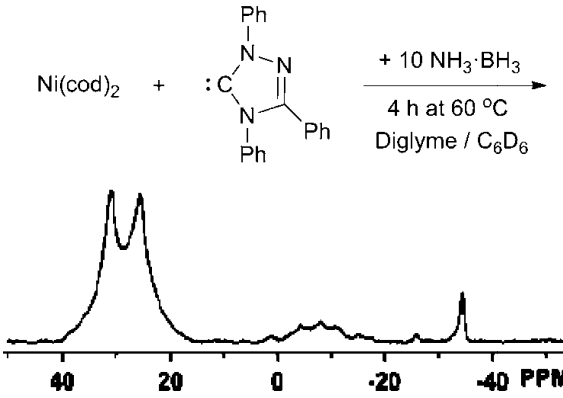

Figure 1.10 $^{11}B\{^{1}H\}$ NMR spectrum in C_6D_6/diglyme from the reaction of 10 equiv of **AB** with 1 and 2 equiv, respectively, of $Ni(cod)_2$ and Enders' NHC after 4 h at 60 °C. The signal at -36 ppm is attributable to the NHC-BH_3 adduct (ca. 2% of total B).

Afterwards in 2008 and 2009, two highly active ruthenium catalysts were reported independently.[72] In the first report, *t*BuOK activated Ru-catalysts were screened for the dehydrogenation of **AB**,[72a] which had already been successfully used for alcohol redox processes.[73] Thereby, it introduced a further concept for the hypothesis driven catalyst discovery besides the isoelectronic relationship with ethane and the similarity of the process to other E-H/E-H dehydrocoupling processes. These catalysts released up to 1 equivalent of H_2 within 5 minutes, with catalyst loadings as low as 0.03 mol%. Interestingly, up to 2 equivalents of H_2 were released from *N*-methylamineborane (**MAB**) and the overall hydrogen yield from **AB** could be increased via co-dehydrogenation it with **MAB**.

The other catalyst was a bifunctional Ru(II) complex bearing a PNP amido chelate ligand, which could undergo reversible hydrogenation reactions at both the amine functionality and the ethylene backbone (Scheme 1.8).[72b]

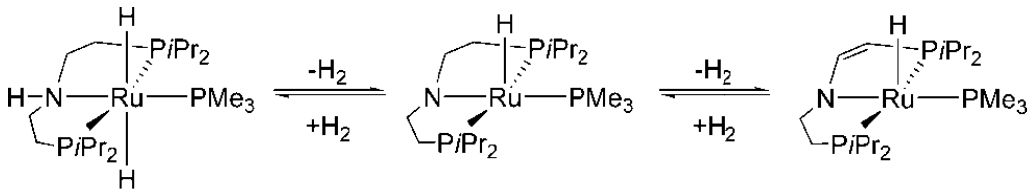

Scheme 1.8 Hydrogenation/dehydrogenation equilibria between the amino (left), amido (middle), and enamido (right) complexes.

This complex proved to be a very active catalyst for the dehydrogenation of **AB**. Catalyst loadings of 0.1 mol% led to the evolution of slightly more than 1 equivalent of H_2 within 10

min (pseudo-first-order rate constant = 0.0013 s^{-1}). Even catalyst loadings as low as 0.01 mol% were effective (0.83 equivalent of H_2, pseudo-first-order rate constant = 0.0021 s^{-1}). However, the mechanism for this reaction has not been fully studied. Kinetic isotope effects (KIEs) suggest a concerted mechanism, with KIEs of 2.1 ($D_3B{\cdot}NH_3$), 5.2 ($H_3B{\cdot}ND_3$), and 8.1 ($D_3B{\cdot}ND_3$) found relative to **AB** dehydrogenation.

1.5.1.4 Metal catalyzed solvolysis of AB

Metal-assisted solvolysis is a chemically different approach to catalytic dehydrocoupling reactions for the utilization of **AB** for hydrogen production/storage. Since tertiary amine-boranes may be used as hydrogen source,[74] it is the borane moiety of the complex which reacts, providing hydridic hydrogen atoms, whereas the protons to form hydrogen are obtained from the protic solvent. The idea of using such a process with the explicit aim of generation of hydrogen was introduced in 2006.[75] While **AB** is stable in water under STP, addition of catalytic amounts of Pt black, Pd black, or a Rh precatalyst ($\{Rh(1,5\text{-cod})(\mu\text{-Cl})\}_2$) led to the rapid release of up to 2 equivalents of H_2. In terms of weight, this is equivalent to 8.9 wt% of the system $NH_3{\cdot}BH_3/H_2O$. At the time, a number of different metal catalysts were evaluated, with the Pt black catalyst shown to be the most efficient: reaction was complete within 10 min using 1.8 mol% of Pt black. It was immediately recognized as a promising way of generating hydrogen for use in fuel cells,[76] a large volume of reports were published on this field subsequently (Table 1.6). Thus, only some special examples will be discussed herein.

Table 1.6 Reported metal matalyzed solvolysis of **AB** for the production of dihydrogen.

entry	Concentr-ation (**AB**)	catalyst	solvent	T/ °C	t/min	equiv. H_2
1[75]	1 M	Pt (20% on C) (2 mol%)	H_2O	r.t.	2	~ 3
		PtO_2 (2 mol%)			8	~ 3
		Pt black (2 mol%)			12	~ 3
		K_2PtCl_4 (2 mol%)			19	~ 3
		$[Rh(1,5\text{-COD})(\mu\text{-Cl})]_2$ (2 mol%)			15	~ 2.6
		Pd (2 mol%)			250	~2.6
2[77]	Solid	Dowex (12 wt%) CO_2	H_2O	r.t.	8	~2.8

3[78]	Solid	Co (10% on C) (2 mol%) Ni (10% on γ-Al_2O_3) (2 mol%)	H_2O	r.t.	60	~ 2.9 ~2.9
4[79]	Solid	$Ni_{0.88}Pt_{0.12}$ hollow sphere (2 mol%)	H_2O	r.t.	30	~3
5[80]	Solid	Rh colloids (1 mol%) Ir colloids (1 mol%) Co colloids (1 mol%)	H_2O	r.t.	40 s 105 60	~ 2.8 ~ 3 ~3
6[28]	2 M	$RuCl_3$ (0.5 mol%) $NiCl_2$ (2 mol%) $CoCl_2$ (2 mol%) Pd/C (2 mol%) Raney Ni (2 mol%) $PdCl_2$ (2 mol%) $RhCl_3$ (2 mol%)	MeOH	25	5 60 40 90 50 110 < 10	~3
7[81]	0.16 M	amorphous Fe nanoparticles (0.1 mol%)	H_2O	r.t.	8	~3
8[82]	16 M	K_2PtCl_6 (0.1 mol%)	H_2O	25	330	~3
9[83]	0.32 M	nanoclusters of Ru, Rh, Pt, Pd, Au, supported on γ-Al_2O_3, C, SiO_2; 2 wt% (Pd, Au also reported but less effective)	H_2O	r.t.	< 3	~3
10[84]	0.02 M	PtM/C (M: Ir, Ru, Co, Cu, Sn, Au, Ni. metal content: 20 wt%) (NiM/C; M: Au, Ag, Cu, Sn, Co. metal content: 20 wt%)	H_2O	r.t.	10-140 25-400	2.5-2.9 2.6-2.9
11[85]	0.025 M	$NiCl_2 \cdot 6H_2O$ (7 mol%) $CoCl_2 \cdot 6H_2O$ (7 mol%) $CuCl_2 \cdot 6H_2O$ (7 mol%)	H_2O		125 45 250	2.7
12[86]	0.03 M	amorphous Cu, Ag, Au nanoparticles Cu nanoparticles (15 mol%) $Cu@Cu_2O$ core shell nanoparticles (15 mol%) Cu_2O nanoparticles (15 mol%)	H_2O MeOH MeOH	r.t.	40-60 93-100	1.1 1.7 2.1
13[87]	0.12 M	Rh (0.05 mol%) on different supports, best on TiO_2 (1 wt%)	H_2O	40	7	2.7
14[88]	1 M	$Ni_{60}Co_{20}Cu_{20}$/active carbon fiber 10 wt%, and others tested in high throughput screening	H_2O	25	40	~3
15[89]	0.75 M	Co-Co_2B nanocomposite (20 mol%) Ni-Ni_3B nanocomposite (20 mol%)	MeOH	25	2.5 4.2	3

16[90]	300 mM	starch stabilized Ni nanoparticles (0.1 mol%)	H_2O	r.t.	6	~3
17[91]	100 mM	zeolite framework stabilized rhodium(0) nanoclusters; 0.8 mol% Rh	H_2O	25	5	~3
18[92]	160 mM	nickel clusters contained within silica nanospheres (20-30 nm); 1-5 mol%	H_2O	r.t.	22-75	~3
19[93]	260 mM	Ru/C; 0.2 mol%	H_2O	25	17	~3
20[94]	160 mM	nickel catalyst stabilized by poly(*N*-vinyl-2-pyrrolidone); $NaBH_4$ as coreductant; 10 mol% Ni	H_2O	25	9	2.7
21[95]	100 mM	laureate stabilized Ru(0) nanoclusters, 2 mol%	H_2O	25	5	~3
22[96]	100 mM	zeolite confined Cu(0) nanoclusters; 2 mol%	H_2O	25	130	~3
23[97]	330 mM	3 wt% Ru on carbon, various particle sizes; 0.2 mol% Ru	H_2O	26	10	3
24[98]	200 mM	monodisperse Ni nanoparticles, 4 mol% Ni	H_2O	25	10	3
25[99]	100 mM	2 mM intrazeolite cobalt(0) nanoclusters with 0.85 wt% of Co, corresponding to 2 mol%, and various other loadings	H_2O	25	33.3 h	2.3
26[100]	152 mM	bimetallic Au-Ni nanoparticles embedded in SiO_2 nanospheres, Au/**AB** = 0.019, Ni/**AB** = 0.065	H_2O	18	14	2.9
27[101]	170 mM	magnetically recyclable hollow Co-B nanospindles from poly(styrene-*co*-methacrylic acid) and $Co(OAc)_2$ with KBH_4, 5 mg of catalyst to 8.3 mmol of **AB**, metal loading not presented.	H_2O	25	30	3
28[102]	260 mM	magnetically recyclable Au@Co core-shell nanoparticles, 2 mol%	H_2O	25	11	3
29[103]	25 mM	nanoparticle-assembled Co-B thin film, 10 mg for 3.75 mmol of **AB**	H_2O	25	11	2.9
30[104]	100 mM	zeolite confined Pd(0) nanoclusters 3 mol%	H_2O	25	15	3

31[105]	50 mM	Pd-activated TiO_2-supported Co-Ni-P ternary alloy	H_2O	25 55	60 mL/min g 400 mL/min g
32[106]	0.5 wt%	Cobalt-tungsten-boron-phosphorus porous particles supported on Ni foam	H_2O	30	4.0 L/min g
33[107]	0.5 wt%	carbon supported Ni core-Pt shell $Ni_{1-x}@Pt_x/C$ (x = 0.32, 0.43, 0.60, 0.67, and 0.80) nanoparticles	H_2O	25	5.5 L/min g
34[108]	120 mM	cobalt boride catalyst formed *in situ* from Co_3O_4	H_2O	40	10 3
35[109]	140 mM	ruthenium (Ru) nanoparticles immobilized in montmorillonite	MeOH	25	29 L/min g

One of the most important characteristics of a good catalyst is the accessibility of the catalytic sites and high internal surface area,[110] for example, this was shown by using a templated synthesis to produce catalytically active Ni-Pt hollow nanospheres as catalysts.[79] Nickel(II) chloride was adsorbed onto a poly(styrene *co*-methacrylic acid) (**PSA**) template, reduced by $NaBH_4$, and reductively doped with varying amounts of platinum, before dissolving the polymeric core to form a hollow sphere. Commercial nickel powders showed essentially no catalytic activity, but pure nickel hollow spheres showed already substantial catalysis. By increasing the amount of Pt doping, the catalytic activity could be increased to release of approximately 3 equivalents of H_2 (2 equivalents from **AB**, 1 equivalent from water) within 20-30 min for a Ni/Pt ratio of 88/12. This structural catalyst design of the hollow spheres led to a very high surface area with concomitant low density and avoided aggregation. Most importantly, only small amounts of precious metal had to be used. If the results are compared to those using pure Pt black,[75] the use of the nanospheres allows the reduction of the Pt loading to 0.2 mol% instead of 2 mol%, despite the concentrations (0.5 wt% and 0.33 wt%, respectively) and reaction times (20-30 and 10 min, respectively) being similar.

The stored hydrogen in **AB** can be released either by thermolysis or catalyzed hydrolysis, and both routes having advantages and issues. There is only one report envisaged the combination of thermolysis and hydrolysis: **AB** was firstly thermolyzed and then the solid by-product believed to be polyaminoborane $[NH_2BH_2]_n$ (**PAB**) was catalytically

hydrolyzed.[111] After the primary thermolysis process, **PAB** was hydrolyzed in the presence of a metal catalyst (Ru) at 40 ^{o}C, a total of 3 equiv. H_2 is released from **AB** and **PAB**-H_2O. Relatively high hydrogen generation rate was obtained through hydrolysis of **PAB**, and the by-products stemming from the **PAB** hydrolysis are ammonium borates.

The importance of the physical structure of the catalyst was even more elegantly demonstrated when it was shown that even a nonprecious metal such as iron can show remarkable reaction kinetics, provided the suitable morphology of the catalyst is ensured.[81] In an attempt to utilize iron nanoparticles, $FeSO_4$ was reduced with $NaBH_4$ and **AB** was added immediately afterward (**AB**/$FeSO_4$/$NaBH_4$ = 1/0.12/0.16), recording the reaction progress by MS and volumetrically. The reaction took more than 160 min to complete. However, when the nanoparticles were formed *in situ*, i.e. **AB** was added immediately, the reaction proceeded to completion within 8 min. Careful analysis by PXRD, TEM, and SAED (selective area electron diffraction) revealed that while R-Fe crystallites had formed, the *in situ* reduction led to amorphous nanoparticles. These formed suspensions in water were also similarly effective in air. Furthermore, these amorphous nanoparticles could be recycled without loss of activity. This was the first time that a nonprecious metal catalyst achieved similar efficiencies to platinum based materials for **AB** hydrolysis.

In a word, these processes have plenty of advantages such as high efficiency, chemical robustness and the fact that inexpensive metal catalysts have been developed, which make them economically interesting.

1.5.1.5 Acid-catalyzed dehydrocoupling of AB

In 2007, the successful use of Lewis and Brønsted acids to release hydrogen from **AB** under nonhydrolytic conditions at 60 ^{o}C was reported by Baker and Dixon (Table 1.7).[112]

They postulated that the acid initially abstracts a hydride from **AB** to form an amine-borenium ion (**1**), which then reacts with another **AB** molecule with loss of dihydrogen to eventually form compound **3**. Compound **3** itself could then abstract a hydride from **AB** or other neutral oligomers to give a linear dimer, which would consume a borenium cation to

give **4** and the cationic part of **DADB** without release of dihydrogen (Scheme 1.9).

Table 1.7 Reactivities of **AB** with Acids at 60 °C.

acid	loading (mol%)	conc. **AB** (M)	time (h)	H_2 (equiv.)
$B(C_6F_5)_3$	25	0.14[a]	24	0.6
$B(C_6F_5)_3$	0.5	2.6[b]	20	1.1
$HOSO_2CF_3$	25	0.13[a]	18	0.8
$HOSO_2CF_3$	0.5	6.2[c]	18	1.3
HCl	0.5	2.9[c]	20	1.2

[a] Reaction in glyme; [b] Reaction in tetraglyme; [c] Reaction in diglyme.

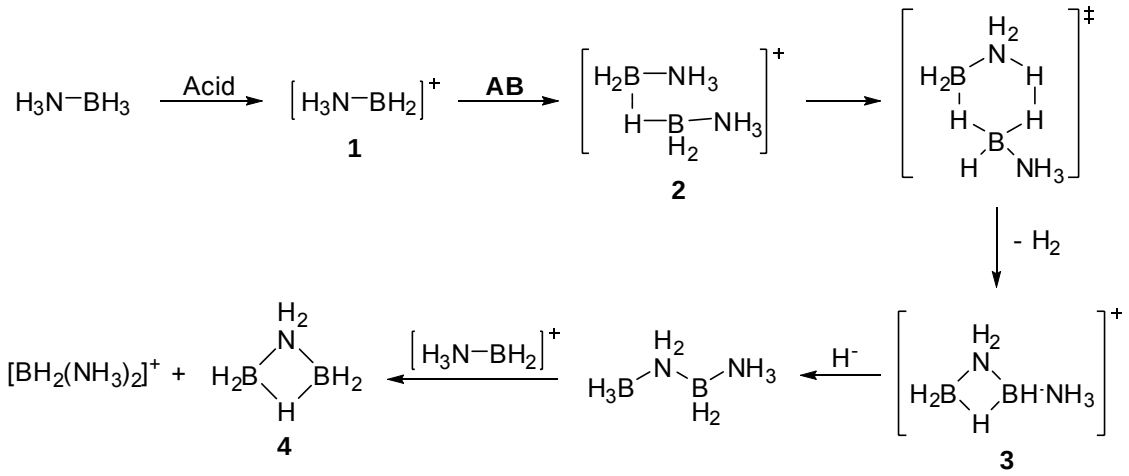

Scheme 1.9 Postulated mechanism for the reaction of **AB** with acids, the counter anion was either $HB(C_6F_5)_3$ or OTf.

It was reasoned that, therefore, if the amount of acid was reduced, the formation of **4** should be repressed and more **AB** (or its oligomers) present for actual loss of H_2. Indeed, when less acid was used, the overall yield of H_2 increased, although it has to be pointed out that the concentration of **AB** was also increased at the same time, so that a concentration effect seems equally likely. The proposed mechanism was further reinforced by computational studies and ^{11}B NMR measurements and similarities to the dehydrogenation of **AB** in ionic liquids and in glyme without additional reagents.

In this context, it is necessary to mention that the dehydrocoupling of **AB** has been achieved using a frustrated Lewis acid Lewis base pair.[113] The reactivity of Lewis acids and

bases which are too sterically hindered to react directly, or may only form metastable complexes, has been used extensively to activate small molecules and recently been reviewed.[19b-d] In addition, a computational study has appeared explaining the molecular mechanism of the reaction.[114]

1.5.2 Regeneration of AB

A key component of a practical scheme for the use of H_2 as a transportation fuel is the ability to regenerate the hydrogen carrier in a cost efficient and sustainable manner. More so than with the release of H_2 from a carrier, the challenge of regeneration is intimately entwined with the engineering costs of large scale industrial processes. Even though it may be possible to regenerate a particular form of spent fuel with good yields and rates, the reagents used can be too expensive, overly hazardous, or too difficult to utilize on the scale required for mass fuel production. The potential costs of regeneration have previously prompted the DOE to make "no go" decisions on materials such as $NaBH_4$. Therefore for **AB** to remain a viable candidate as a H_2 carrier, the issue of regeneration must be addressed, and it may impose restrictions on what sort of dehydrogenation schemes are reasonable. Due to the thermodynamics of **AB** dehydrogenation,[115] off-board regeneration of the spent fuel is likely to be required, where off-board regeneration is removal of the spent fuel from a vehicle and regeneration occurring at a processing plant. It is also evident that ceramic BN (fully dehydrogenated **AB**) is energetically undesirable as it represents a thermodynamic sink. This limits the usable H_2 density of **AB**, but the 18 wt% of H_2 release reported by Baker demonstrates that metal-catalyzed dehydrogenation is capable of H_2 release well above the DOE target while still generating "spent fuel" that is energetically feasible to regenerate. Despite the large amount of research into the release of dihydrogen from **AB**, there have been only a few reports on strategies to tackle the need for spent fuel to be regenerated apart from conference papers and patents.

The first system for regeneration of **AB** was reported in 2007 by Ramachandran and co-workers, discussed a system in which the transition metal catalyzed solvolysis product of **AB**, $[NH_4][B(OMe)_4]$, could be converted back to **AB** at ambient temperature using NH_4Cl

and $LiAlH_4$, releasing another equivalent of hydrogen (Scheme 1.10).[28] However, this process results in the loss of H_2 and NH_3 which must be trapped and recycled and the formation of $Al(OMe)_3$ which must be converted back to $LiAlH_4$.

$$NH_4B(OMe)_4 + LiAlH_4 + NH_4Cl \rightarrow Al(OM3)_3 + \mathbf{AB} + MeOH + H_2 + LiCl + NH_3$$

Scheme 1.10 Regeneration of **AB** from $NH_4B(OMe)_4$.

We already discussed that both thermolysis (at temperatures below ca. 500 °C, above which, evidence for boron nitride is seen[116]) and metal-catalyzed dehydrogenation lead to products of the type **PAB** $(H_2NBH_2)_n$ and/or **PB** $(HNBH)_n$. Strategies for regenerating **AB** from mixtures of **PAB**/**PB** have been proposed by Sneddon[117][118] and Mertens[119] that do not depend on the nature of **PAB**/**PB** by using an acid (HX) to form B–X bonds and then conversion of those B– X bonds into B–H bonds.

A better approach to the regeneration problem was put forward using a DFT approach to determine a reagent that might convert the spent fuel, which mainly consists of **PB**, to a more useful and clearly defined compound.[120] As a model for **PB**, **BZ** was used and it was found that a reaction with 1,2-benzenedithiol had an exothermic reaction enthalpy of -20.4 kcal/mol in the condensed phase. Indeed, when 1,2-benzenedithiol was reacted with **PB** under reflux conditions in THF, the formation of $(C_6H_4S_2)BH\cdot(NH_3)$ (^{11}B NMR: δ = -5.6, *d*, $^1J^{B\text{-}H}$ = 128 Hz) and $[NH_4][B(C_6H_4S_2)_2]$ (δ = 10.5 ppm, s) was observed. While the structure of the former compound could be proven by independent analysis, for the second one, this was not possible and chemical shift calculations by DFT and a comparison with $Li[B(C_6H_4S_2)_2]$ had to suffice. Using excess Bu_3SnH at 60 ^oC in THF, this salt could then be transformed into $(C_6H_4S_2)BH\cdot(NH_3)$ as well, which could be transformed back into **AB** and $C_6H_4S_2Sn(nBu)_2$ using nBu_2SnH_2 (Scheme 1.11).

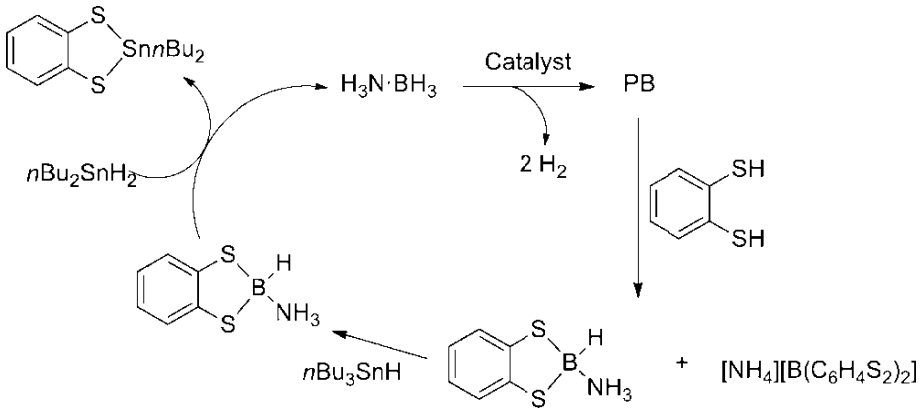

Scheme 1.11 Possible regeneration pathway for spent **AB** fuel.[120]

Using the approximation of efficiency, this process is estimated to be 65% efficient with regard to the energy input required which compares quite favorably with the estimated 46% efficiency in recovering **AB** from $NH_4B(OMe)_4$. In the analysis of an optimized version of this regeneration Scheme, it has been calculated that such a process could be up to 80% thermodynamically efficient.[121] Analysis also indicates that the generation of formic acid and the cost of mass transport of tin are a significant portion of the fuel regeneration cost, leaving room for improvement for a process that is estimated to have a cost equivalent of ca. $7–8 per kg of H_2.

The newest and probably also the best regeneration method up to now was published in 2011 by Sutton and co-workers,[122] demonstrating that the spent fuel type derived from the removal of greater than two equivalents of H_2 per molecule of **AB** (i.e., polyborazylene, **PB**) can be converted back to **AB** nearly quantitatively by 24-hour treatment with hydrazine (N_2H_4) in liquid ammonia (NH_3) at 40°C in a sealed pressure vessel. Considering that the presence of residual catalyst in **PB** mixtures could complicate the **AB** regeneration process, a purer form of **PB** that is derived from dehydrogenation of **BZ** was used. An important consideration here is that both catalytic and thermal (i.e., noncatalytic) routes to **PB** from **AB** (based on the volume of H_2 evolved) yield a hydrogen-depleted material in which greater than two equivalents of hydrogen are released from **AB**. The **PB** generated in either methodology to this point appears to be indistinguishable from the other. This leads to the general acceptance of the formulation of **PB** as "BNH_x" where x is greater than zero, less than two, but typically one.[123] This material thus corresponds to a spent fuel derived from the loss of greater than

two equivalents of H_2 per molecule of **AB**, but still allows for the preservation of some of the energetic B–H bonds. This latter property confers both solubility for subsequent recycle chemistry as well as reduction of the overall energy required to regenerate the desired BH_3 fragments. Although synthetically prepared **PB** derived from **BZ** is a surrogate for real spent fuel, it represents a scenario in which as much H_2 has been liberated downstream of **AB** before ceramic BN is formed. This makes it an ideal material with which to demonstrate the conversion of this spent fuel form to **AB**.

The overall reaction cycle, including the production of hydrazine, is summarized in Scheme 1.12. In this scheme, the N_2 released from the N_2H_4 can be rehydrogenated to NH_3 and subsequently converted to N_2H_4. Although synthetic procedures such as the Olin-Raschig process produce hydrazine in high yields and great efficiency, we can begin to look to the future and think about a new route to hydrazine production. In conjunction with an **AB**-regeneration plant, in situ N_2H_4 production from NH_3 does not require high conversion rates to produce a N_2H_4/NH_3 feed for **AB** regeneration. In this scheme, the only material consumed is hydrogen, the production of which is widely recognized as the second major technical challenge for the hydrogen economy.

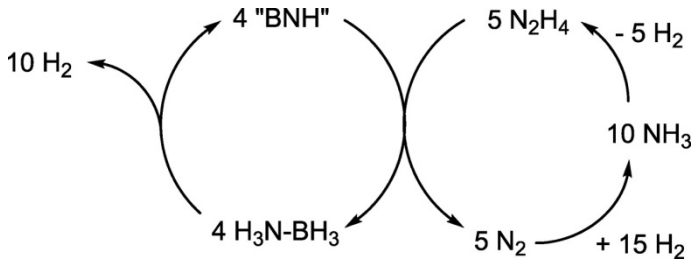

Scheme 1.12 Ideal overall reaction scheme for **AB** regeneration from **PB** ("BNH") with hydrazine (N_2H_4).

1.6 Final remarks

The global warming problem and the global energy crisis triggered on a global interest on renewable and clean energy sources to back up conventional fossil fuels. As an extremely clean energy carrier which could be produced from either fossil fuels or any renewable energy sources, hydrogen has attracted great attention. Thereafter, the 19.6 wt% H_2 in **AB** made it an attractive molecule for chemical hydrogen storage, and it is made more so by its stability and non-toxicity.

Research on **AB** as a potential hydrogen storage material has intensified since 2005 and is a highly active and exciting area. While much progress has been made in understanding the metal-catalyzed dehydrogenation of **AB** and the issues that affect the resultant end products, there are still areas that require further investigation. Most catalysts are still based on precious metals, which is not feasible from both cost and material availability perspectives on a global scale. Thus, more effort needs to be put forth toward developing non-precious metal catalysts which are less expensive and more abundant or even metal free catalysts. Considering the existence of both protic H_N and hydridic H_B in **AB**, it seems quite reasonable that it could be dehydrogenated and/or rehydrogenated by a similarly bi-functioned organic molecule, either catalytically or stoichiometrically.

1.7 References

[1] L. Schlapbach and A. Zuttel, *Nature* **2001**, *414*, 353-358.

[2] http://energyquest.ca.gov/index.html

[3] P. M. Grant, *Nature* **2003**, *424*, 129-130.

[4] Moomaw, W., F. Yamba, M. Kamimoto, L. Maurice, J. Nyboer, K. Urama, T. Weir, 2011: Introduction. In IPCC Special Report on Renewable Energy Sources and Climate Change Mitigation [O. Edenhofer, R. Pichs‐Madruga, Y. Sokona, K. Seyboth, P. Matschoss, S. Kadner, T. Zwickel, P. Eickemeier, G. Hansen, S. Schlömer, C. von Stechow (eds)], Cambridge University Press, Cambridge, United Kingdom and New York, NY, USA.

[5] Boden, T.A., G. Marland, and R.J. Andres (2009). Global, Regional, and National Fossil-Fuel CO2 Emissions. Carbon Dioxide Information Analysis Center, Oak Ridge National Laboratory, US Department of Energy, Oak Ridge, TN, USA. Available at: cdiac.ornl.gov/trends/emis/overview_2007.html.

[6] In addition, biomass use estimated to amount to 20 to 40% is not reported in official databases, such as dung, unaccounted production of charcoal, illegal logging, fuelwood gathering, and agricultural residue use.

[7] Sims, R., P. Mercado, W. Krewitt, G. Bhuyan, D. Flynn, H. Holttinen, G. Jannuzzi, S. Khennas, Y. Liu, M. O'Malley, L. J. Nilsson, J. Ogden, K. Ogimoto, H. Outhred, Ø. Ulleberg, F. van Hulle, 2011: Integration of Renewable Energy into Present and Future Energy Systems. In IPCC Special Report on Renewable Energy Sources and Climate Change Mitigation [O. Edenhofer, R. Pichs‐Madruga, Y. Sokona, K. Seyboth, P. Matschoss, S. Kadner, T. Zwickel, P. Eickemeier, G. Hansen, S. Schlömer, C. von Stechow (eds)], Cambridge University Press, Cambridge, United Kingdom and New York, NY, USA.

[8] P. Tseng, J. Lee and P. Friley in Hydrogen Economy: Opportunities and Challenges. http://www.iiasa.ac.at/Research/ECS/IEW2003/Papers/2003P_tseng.pdf

[9] Y. Chen, Y. Lu, C. Bai, E. Shi, X. Fang, Z. Li, X. Cao and J. Pan in *Energy Science & Technology in China: A Roadmap to 2050 Vol.* Science Press Beijing and Springer-Verlag Berlin Heidelberg, **2010**.

[10] D. Hart, P. Freund, and A. Smith, Using Hydrogen – Today and Tomorrow, IEA Greenhouse Gas R&D Programme, Cheltenham, UK, 1999.

[11] J. Larminie, Fuel cell systems explained, second edition 2003.

[12] I. P. Jain, P. Jain and A. Jain, *Journal of Alloys and Compounds* **2010**, *503*, 303-339.

[13] M. Klanchar, T. G. Hughes and P. Gruber, Attaining DOE Hydrogen Storage Goals with Chemical Hydrides, http://www.engr.psu.edu/h2e/Professors/Dr._Klanchar,_Martin/Attaining%20DOE%20Hydrogen%20Storage%20Goals%20With%20Chemical%20Hydrides-%20Dr.%20Klanchar.pdf

[14] Millennium Cell, Inc., "Hydrogen on Demand™ Fact Sheet," http://www.millenniumcell.com/news/hod.html.

[15] S.-i. Orimo, Y. Nakamori, J. R. Eliseo, A. Züttel and C. M. Jensen, *Chemical Reviews* **2007**, *107*, 4111-4132.

[16] R. B. Biniwale, S. Rayalu, S. Devotta and M. Ichikawa, *International Journal of Hydrogen Energy* **2008**, *33*, 360-365.

[17] K. Morawa Eblagon, K. Tam, K. M. K. Yu, S.-L. Zhao, X.-Q. Gong, H. He, L. Ye, L.-C. Wang, A. J. Ramirez-Cuesta and S. C. Tsang, *The Journal of Physical Chemistry C* **2010**, *114*, 9720-9730.

[18] a) F. Sotoodeh and K. J. Smith, *Journal of Catalysis* **2011**, *279*, 36-47; b) F. Sotoodeh, L. Zhao and K. J. Smith, *Applied Catalysis A: General* **2009**, *362*, 155-162.

[19] a) D. W. Stephan, J. S. J. McCahill and G. C. Welch, *Angewandte Chemie-International Edition* **2007**, *46*, 4968-4971; b) D. W. Stephan, *Organic & Biomolecular Chemistry* **2008**, *6*, 1535-1539; c) D. Stephan and G. Erker, *Angew. Chem. Int. Ed.* **2010**, *49*, 46-76; d) D. W. Stephan, *Dalton Transactions* **2009**, 3129-3136.

[20] G. C. Welch, R. R. S. Juan, J. D. Masuda and D. W. Stephan, *Science* **2006**, *314*, 1124-1126.

[21] a) Z. M. Heiden and D. W. Stephan, *Chemical Communications* **2011**, *47*, 5729-5731; b) T. Privalov, *Eur. J.*

Inorg. Chem. **2009**, 2229-2237; c) P. Spies, S. Schwendemann, S. Lange, G. Kehr, R. Frohlich and G. Erker, *Angew. Chem. Int. Ed.* **2008**, *47*, 7543-7546; d) J. Klankermayer and D. J. Chen, *Chemical Communications* **2008**, 2130-2131.

[22] G. Erker, S. Schwendemann, T. A. Tumay, K. V. Axenov, I. Peuser, G. Kehr and R. Frohlich, *Organometallics* **2010**, *29*, 1067-1069.

[23] a) H. D. Wang, R. Frohlich, G. Kehr and G. Erker, *Chem. Commun.* **2008**, 5966-5968; b) K. V. Axenov, G. Kehr, R. Frohlich and G. Erker, *Organometallics* **2009**, *28*, 5148-5158.

[24] D. E. Schwarz, T. M. Cameron, P. J. Hay, B. L. Scott, W. Tumas and D. L. Thorn, *Chemical Communications* **2005**, 5919-5921.

[25] a) F. H. Stephens, V. Pons and R. T. Baker, *Dalton Transactions* **2007**, 2613-2626; b) N. C. Smythe and J. C. Gordon, *European Journal of Inorganic Chemistry* **2010**, 509-521; c) A. Staubitz, A. P. M. Robertson and I. Manners, *Chemical Reviews* **2010**, *110*, 4079-4124; d) C. W. Hamilton, R. T. Baker, A. Staubitz and I. Manners, *Chemical Society Reviews* **2009**, *38*, 279-293.

[26] Karkamkar, A.; Aardahl, C.; Autrey, T. Mater. Matters 2007, 2, 6; available at http://www.sigmaaldrich.com/materialsscience/learningcenter/material-matters.html.

[27] S. G. Shore and R. W. Parry, *Journal of the American Chemical Society* **1955**, *77*, 6084-6085.

[28] P. V. Ramachandran and P. D. Gagare, *Inorganic Chemistry* **2007**, *46*, 7810-7817.

[29] D. J. Heldebrant, A. Karkamkar, J. C. Linehan and T. Autrey, *Energy & Environmental Science* **2008**, *1*, 156-160.

[30] M. G. Hu, J. M. Vanpaasschen and R. A. Geanangel, *J. Inorg. Nuclear Chem.* **1977**, *39*, 2147-2150.

[31] S. G. Shore and K. W. Boddeker, *Inorganic Chemistry* **1964**, *3*, 914-915.

[32] E. Mayer, *Inorganic Chemistry* **1972**, *11*, 866-869.

[33] C. A. Jaska, K. Temple, A. J. Lough and I. Manners, *Journal of the American Chemical Society* **2003**, *125*, 9424-9434.

[34] E. Mayer, *Inorganic Chemistry* **1973**, *12*, 1954-1955.

[35] a) R. D. Suenram and L. R. Thorne, *Chem. Phys. Lett.* **1981**, *78*, 157-160; b) L. R. Thorne, R. D. Suenram and F. J. Lovas, *J. Chem. Phys.* **1983**, *78*, 167-171.

[36] D. A. Dixon and M. Gutowski, *J. Phys. Chem. A* **2005**, *109*, 5129-5135.

[37] H.-J. Himmel and H. Schnöckel, *Chemistry – A European Journal* **2002**, *8*, 2397-2405.

[38] M. W. Chase, Jr., J. Phys. Chem. Ref. Data Monogr., 1998, 9, 1–1951.

[39] D. J. Grant and D. A. Dixon, *J. Phys. Chem. A* **2006**, *110*, 12955-12962.

[40] a) K. W. Böddeker, S. G. Shore and R. K. Bunting, *Journal of the American Chemical Society* **1966**, *88*, 4396-4401; b) H. A. McGee and C. T. Kwon, *Inorganic Chemistry* **1970**, *9*, 2458-2461.

[41] P. M. Zimmerman, A. Paul, Z. Y. Zhang and C. B. Musgrave, *Inorganic Chemistry* **2009**, *48*, 1069-1081.

[42] M. G. Hu, R. A. Geanangel and W. W. Wendlandt, *Thermochim. Acta* **1978**, *23*, 249-255.

[43] V. Sit, R. A. Geanangel and W. W. Wendlandt, *Thermochim. Acta* **1987**, *113*, 379-382.

[44] R. A. Geanangel and W. W. Wendlandt, *Thermochim. Acta* **1985**, *86*, 375-378.

[45] G. Wolf, J. Baumann, F. Baitalow and F. P. Hoffmann, *Thermochim. Acta* **2000**, *343*, 19-25.

[46] F. Baitalow, J. Baumann, G. Wolf, K. Jaenicke-Rossler and G. Leitner, *Thermochim. Acta* **2002**, *391*, 159-168.

[47] S. D. Rassat, C. L. Aardahl, T. Autrey and R. S. Smith, *Energy & Fuels* **2010**, *24*, 2596-2606.

[48] D. P. Kim, K. T. Moon, J. G. Kho, J. Economy, C. Gervais and F. Babonneau, *Polymers for Advanced Technologies* **1999**, *10*, 702-712.

[49] A. C. Stowe, W. J. Shaw, J. C. Linehan, B. Schmid and T. Autrey, *Phys. Chem. Chem. Phys.* **2007**, *9*, 1831-1836.

[50] M. Bowden, T. Autrey, I. Brown and M. Ryan, *Current Applied Physics* **2008**, *8*, 498-500.

[51] F. Baitalow, G. Wolf, J. P. E. Grolier, F. Dan and S. L. Randzio, *Thermochim. Acta* **2006**, *445*, 121-125.

[52] O. Palumbo, A. Paolone, P. Rispoli, R. Cantelli and T. Autrey, *Journal of Power Sources* **2010**, *195*, 1615-1618.

[53] R. A. Geanangel and W. W. Wendlandt, *Thermochimica Acta* **1987**, *113*, 383-385.

[54] F. P. Price, *Journal of the American Chemical Society* **1951**, *73*, 2141-2144.

[55] J. S. Zhang, Y. Zhao, D. L. Akins and J. W. Lee, *Journal of Physical Chemistry C* **2011**, *115*, 8386-8392.

[56] J. S. Wang and R. A. Geanangel, *Inorganica Chimica Acta* **1988**, *148*, 185-190.

[57] W. J. Shaw, J. C. Linehan, N. K. Szymczak, D. J. Heldebrant, C. Yonker, D. M. Camaioni, R. T. Baker and T. Autrey, *Angewandte Chemie-International Edition* **2008**, *47*, 7493-7496.

[58] R. Schellenberg, J. Kriehme and G. Wolf, *Thermochim. Acta* **2007**, *457*, 103-108.

[59] M. Diwan, V. Diakov, E. Shafirovich and A. Varma, *International Journal of Hydrogen Energy* **2008**, *33*, 1135-1141.

[60] M. Diwan, D. Hanna and A. Varma, *International Journal of Hydrogen Energy* **2010**, *35*, 577-584.

[61] M. Diwan, H. T. Hwang, A. Al-Kukhun and A. Varma, *Aiche Journal* **2011**, *57*, 259-264.

[62] a) M. E. Bluhm, M. G. Bradley, R. Butterick, U. Kusari and L. G. Sneddon, *Journal of the American Chemical Society* **2006**, *128*, 7748-7749; b) D. W. Himmelberger, L. R. Alden, M. E. Bluhm and L. G. Sneddon, *Inorganic Chemistry* **2009**, *48*, 9883-9889.

[63] S. Basu, Y. Zheng and J. P. Gore, *Journal of Power Sources* **2011**, *196*, 734-740.

[64] D. Neiner, A. Karkamkar, J. C. Linehan, B. Arey, T. Autrey and S. M. Kauzlarich, *Journal of Physical Chemistry C* **2009**, *113*, 1098-1103.

[65] C. A. Jaska, K. Temple, A. J. Lough and I. Manners, *Chem. Commun.* **2001**, 962-963.

[66] I. Gottker-Schnetmann and M. Brookhart, *Journal of the American Chemical Society* **2004**, *126*, 9330-9338.

[67] M. C. Denney, V. Pons, T. J. Hebden, D. M. Heinekey and K. I. Goldberg, *Journal of the American Chemical Society* **2006**, *128*, 12048-12049.

[68] T. J. Hebden, M. C. Denney, V. Pons, P. M. B. Piccoli, T. F. Koetzle, A. J. Schultz, W. Kaminsky, K. I. Goldberg and D. M. Heinekey, *Journal of the American Chemical Society* **2008**, *130*, 10812-10820.

[69] A. Paul and C. B. Musgrave, *Angewandte Chemie International Edition* **2007**, *46*, 8153-8156.

[70] R. J. Keaton, J. M. Blacquiere and R. T. Baker, *Journal of the American Chemical Society* **2007**, *129*, 1844-+.

[71] a) X. Z. Yang and M. B. Hall, *Journal of the American Chemical Society* **2008**, *130*, 1798-+; b) P. M. Zimmerman, A. Paul, Z. Y. Zhang and C. B. Musgrave, *Angewandte Chemie-International Edition* **2009**, *48*, 2201-2205; c) P. M. Zimmerman, A. Paul and C. B. Musgrave, *Inorganic Chemistry* **2009**, *48*, 5418-5433.

[72] a) N. Blaquiere, S. Diallo-Garcia, S. I. Gorelsky, D. A. Black and K. Fagnou, *Journal of the American Chemical Society* **2008**, *130*, 14034-+; b) M. Kass, A. Friedrich, M. Drees and S. Schneider, *Angewandte Chemie-International Edition* **2009**, *48*, 905-907.

[73] a) T. Li, R. Churlaud, A. J. Lough, K. Abdur-Rashid and R. H. Morris, *Organometallics* **2004**, *23*, 6239-6247; b) S. E. Clapham, A. Hadzovic and R. H. Morris, *Coordination Chemistry Reviews* **2004**, *248*, 2201-2237; c) K. Abdur-Rashid, S. E. Clapham, A. Hadzovic, J. N. Harvey, A. J. Lough and R. H. Morris, *Journal of the American Chemical Society* **2002**, *124*, 15104-15118.

[74] M. Couturier, J. L. Tucker, B. M. Andresen, E. Dube, S. J. Brenek and J. T. Negri, *Tetrahedron Lett.* **2001**, *42*, 2285-2288.

[75] M. Chandra and Q. Xu, *Journal of Power Sources* **2006**, *156*, 190-194.

[76] a) Q. Xu and M. Chandra, *Journal of Alloys and Compounds* **2007**, *446*, 729-732; b) P. Wang and X. D. Kang, *Dalton Transactions* **2008**, 5400-5413; c) T. Umegaki, J. M. Yan, X. B. Zhang, H. Shioyama, N.

Kuriyama and Q. Xu, *International Journal of Hydrogen Energy* **2009**, *34*, 2303-2311.
[77] M. Chandra and Q. Xu, *Journal of Power Sources* **2006**, *159*, 855-860.
[78] Q. Xu and M. Chandra, *Journal of Power Sources* **2006**, *163*, 364-370.
[79] F. Y. Cheng, H. Ma, Y. M. Li and J. Chen, *Inorganic Chemistry* **2007**, *46*, 788-794.
[80] T. J. Clark, G. R. Whittell and I. Manners, *Inorganic Chemistry* **2007**, *46*, 7522-7527.
[81] J. M. Yan, X. B. Zhang, S. Han, H. Shioyama and Q. Xu, *Angewandte Chemie-International Edition* **2008**, *47*, 2287-2289.
[82] N. Mohajeri, A. T-Raissi and O. Adebiyi, *J. Power Sources* **2007**, *167*, 482-485.
[83] M. Chandra and Q. Xu, *J. Power Sources* **2007**, *168*, 135-142.
[84] C. F. Yao, L. Zhuang, Y. L. Cao, X. P. Ai and H. X. Yang, *International Journal of Hydrogen Energy* **2008**, *33*, 2462-2467.
[85] S. B. Kalidindi, M. Indirani and B. R. Jagirdar, *Inorganic Chemistry* **2008**, *47*, 7424-7429.
[86] S. B. Kalidindi, U. Sanyal and B. R. Jagirdar, *Physical Chemistry Chemical Physics* **2008**, *10*, 5870.
[87] V. I. Simagina, P. A. Storozhenko, O. V. Netskina, O. V. Komova, G. V. Odegova, Y. V. Larichev, A. V. Ishchenko and A. M. Ozerova, *Catalysis Today* **2008**, *138*, 253-259.
[88] J. H. Park, H. S. Kim, H. J. Kim, M. K. Han and Y. G. Shul, *Research on Chemical Intermediates* **2008**, *34*, 709-715.
[89] S. B. Kalidindi, A. A. Vernekar and B. R. Jagirdar, *Physical Chemistry Chemical Physics* **2009**, *11*, 770-775.
[90] J. M. Yan, X. B. Zhang, S. Han, H. Shioyama and Q. Xu, *Inorganic Chemistry* **2009**, *48*, 7389-7393.
[91] M. Zahmakiran and S. Ozkar, *Applied Catalysis B-Environmental* **2009**, *89*, 104-110.
[92] T. Umegaki, J. M. Yan, X. B. Zhang, H. Shioyama, N. Kuriyama and Q. Xu, *Journal of Power Sources* **2009**, *191*, 209-216.
[93] S. Basu, A. Brockman, P. Gagare, Y. Zheng, P. V. Ramachandran, W. N. Delgass and J. P. Gore, *Journal of Power Sources* **2009**, *188*, 238-243.
[94] T. Umegaki, J. M. Yan, X. B. Zhang, H. Shioyama, N. Kuriyama and Q. Xu, *International Journal of Hydrogen Energy* **2009**, *34*, 3816-3822.
[95] F. Durap, M. Zahmakiran and S. Ozkar, *International Journal of Hydrogen Energy* **2009**, *34*, 7223-7230.
[96] M. Zahmakiran, F. Durap and S. Ozkar, *International Journal of Hydrogen Energy* **2010**, *35*, 187-197.
[97] S. Basu, Y. Zheng, A. Varma, W. N. Delgass and J. P. Gore, *Journal of Power Sources* **2010**, *195*, 1957-1963.
[98] O. Metin, V. Mazumder, S. Ozkar and S. S. Sun, *Journal of the American Chemical Society* **2010**, *132*, 1468-+.
[99] M. Rakap and S. Ozkar, *International Journal of Hydrogen Energy* **2010**, *35*, 3341-3346.
[100] H. L. Jiang, T. Umegaki, T. Akita, X. B. Zhang, M. Haruta and Q. Xu, *Chemistry-a European Journal* **2010**, *16*, 3132-3137.
[101] D. G. Tong, X. L. Zeng, W. Chu, D. Wang and P. Wu, *Journal of Materials Science* **2010**, *45*, 2862-2867.
[102] J. M. Yan, X. B. Zhang, T. Akita, M. Haruta and Q. Xu, *Journal of the American Chemical Society* **2010**, *132*, 5326-+.
[103] N. Patel, R. Fernandes, G. Guella and A. Miotello, *Applied Catalysis B-Environmental* **2010**, *95*, 137-143.
[104] M. Rakap and S. Ozkar, *International Journal of Hydrogen Energy* **2010**, *35*, 1305-1312.
[105] M. Rakap, E. E. Kalu and S. Ozkar, *International Journal of Hydrogen Energy* **2011**, *36*, 254-261.
[106] J. G. Yang, F. Y. Cheng, J. Liang and J. Chen, *International Journal of Hydrogen Energy* **2011**, *36*, 1411-1417.
[107] X. J. Yang, F. Y. Cheng, J. Liang, Z. L. Tao and J. Chen, *International Journal of Hydrogen Energy* **2011**, *36*, 1984-1990.

[108] V. I. Simagina, O. V. Komova, A. M. Ozerova, O. V. Netskina, G. V. Odegova, D. G. Kellerman, O. A. Bulavchenko and A. V. Ishchenko, *Applied Catalysis a-General* **2011**, *394*, 86-92.

[109] H. B. Dai, X. D. Kang and P. Wang, *International Journal of Hydrogen Energy* **2010**, *35*, 10317-10323.

[110] S. Ozkar, *Applied Surface Science* **2009**, *256*, 1272-1277.

[111] U. B. Demirci, S. Bernard, R. Chiriac, F. Toche and P. Miele, *Journal of Power Sources* **2011**, *196*, 279-286.

[112] F. H. Stephens, R. T. Baker, M. H. Matus, D. J. Grant and D. A. Dixon, *Angewandte Chemie-International Edition* **2007**, *46*, 746-749.

[113] A. J. M. Miller and J. E. Bercaw, *Chemical Communications* **2010**, *46*, 1709-1711.

[114] Y. Guo, X. He, Z. S. Li and Z. G. Zou, *Inorganic Chemistry* **2010**, *49*, 3419-3423.

[115] C. R. Miranda and G. Ceder, *The Journal of Chemical Physics* **2007**, *126*, 184703.

[116] M. G. Hu, R. A. Geanangel and W. W. Wendlandt, *Thermochimica Acta* **1978**, *23*, 249-255.

[117] L. G. Sneddon, Amineborane Hydrogen Storage – New Methods for Promoting Amineborane Dehydrogenation/Regeneration Reactions,DoE Hydrogen Annual Progress Report, 2007 http://www.hydrogen.energy.gov/pdfs/progress07/iv_b_5e_sneddon.pdf).

[118] L. G. Sneddon, Amineborane based Chemical Hydrogen Storage,DoE Hydrogen Annual Merit Review, 2007 (http://www.hydrogen.energy.gov/pdfs/review07/st_27_sneddon.pdf).

[119] S. Hausdorf, F. Baitalow, G. Wolf and F. O. R. L. Mertens, I*nternational Journal of Hydrogen Energy 2***008,** 3*3,* 608-614.

[120] B. L. Davis, D. A. Dixon, E. B. Garner, J. C. Gordon, M. H. Matus, B. Scott and F. H. Stephens, A*ngewandte Chemie-International Edition 2***009,** 4*8,* 6812-6816.

[121] K. C. Ott, R. T. Baker, A. K. Burrell, B. L. Davis, H. V. Diyabalanage, J. C. Gordon, C. W. Hamilton, N. Henson, M. Inbody, K. D. John, T. A. Semelsberger, R. Shrestha, F. H. Stephens, Chemical Hydrogen Storage R&D at Los Alamos National Laboratory, DOE Hydrogen Annual Progress Report, 2008 (http://hydrogen.energy.gov/pdfs/progress08/iv_b_1f_ott.pdf).

[122] A. D. Sutton, A. K. Burrell, D. A. Dixon, E. B. Garner, J. C. Gordon, T. Nakagawa, K. C. Ott, J. P. Robinson and M. Vasiliu, S*cience 2***011,** 3*31,* 1426-1429.

[123] P. J. Fazen, E. E. Remsen, J. S. Beck, P. J. Carroll, A. R. McGhie and L. G. Sneddon, C*hemistry of Materials 1***995,** 7*,* 1942-1956.

Introduction (II): Transfer Hydrogenation Reactions

2.1 Hydrogenation

Hydrogenation is the addition of molecular hydrogen (H_2) to an unsaturated compound or element, usually in the presence of a catalyst. Non-catalytic hydrogenation takes place only at very high temperatures (usually > 450 ^oC), thus catalysts are required for this reaction to be usable.[1] Hydrogenation differs from protonation or hydride addition, since the products have the same charge as the reactants.

The utility of catalytic hydrogenation has a very long history. The earliest hydrogenation reaction is the platinum catalyzed addition of H_2 to oxygen in the Döbereiner's lighter, a device commercialized as early as 1823.[2] Nevertheless, the French chemist Paul Sabatier is considered the father of the hydrogenation process, who discovered in 1897 that the introduction of a trace of nickel as a catalyst facilitated the addition of hydrogen to molecules of gaseous hydrocarbons in what is now known as the Sabatier process. For this work Sabatier shared the 1912 Nobel Prize in Chemistry.[3] The hydrogenation of liquid oils, which is now a world-wide industry, was patented as early as 1902 by a German chemist Wilhelm Normann.[4] The Haber-Bosch process for hydrogenation of nitrogen to produce ammonia, which has often been called 'the most important invention of the 20th century',[5] was first described in 1905. Another widely used industrial process, the Fischer-Tropsch process that converts a mixture of carbon monoxide and hydrogen into liquid hydrocarbons, was first reported in 1922.[6]

In 1924 Murray Raney developed a nickel fine powder catalyst named after him which is still widely used in hydrogenation reactions such as conversion of nitriles to amines or the production of margarine.[7] In 1938, Otto Roelen described the oxo process which involves the addition of both hydrogen and carbon monoxide to alkenes, giving aldehydes. Since this process entails C-C coupling, it and its many

variations remains highly topical into the new decade.[8] The 1960s witnessed the development of homogeneous catalysts, e.g., Wilkinson's catalyst.[9] In the 1980s, the Noyori asymmetric hydrogenation represented one of the first applications of hydrogenation in asymmetric synthesis, a growing application in the production of fine chemicals.[10]

Based on the phase of the catalyst in the hydrogenation process, two types of techniques are being applied: homogeneous catalysis with the catalyst dissolved in the solution that contains the substrate, and heterogeneous catalysis with the catalyst in solid form suspended in the solution with the substrate or treated with gaseous substrate - which is more common in industry. Based on the chemical content of the catalyst, it can be divided into metal catalyzed hydrogenation and metal free hydrogenation. However, there are only few examples on metal free catalyst for hydrogenations, such as the Frustrated Lewis Pairs.[11]

Although most hydrogenation processes use gaseous hydrogen, which is commercially available within the storage medium of a pressurized cylinder. The hydrogenation process often uses greater than 1 atmosphere of H_2, usually conveyed from the cylinders and sometimes augmented by "booster pumps". Gaseous H_2 is produced industrially from hydrocarbons by the process known as steam reforming, as discussed already in the previous chapter. Nevertheless, some hydrogenation processes involve alternative hydrogen donors instead of H_2, which are called transfer hydrogenations as will be discussed in the next session.

2.2 Transfer hydrogenation

Transfer hydrogenation is the addition of two hydrogen atoms to an unsaturated molecule from a hydrogen source other than gaseous H_2. Hydrogen donors for transfer hydrogenation which usually also serve as solvents include hydrazine, dihydronaphthalene, dihydroanthracene, alcohols, formic acid and ammonia salts.[12] Comparing to hydrogenations with gaseous H_2, transfer hydrogenation can be done under ambient pressure and relatively lower temperatures. For example, the aluminum complex catalyzed Meerwein-Ponndorf-Verley[13] (MPV) transfer hydrogenation of carbonyl substrates to alcohols with alcohols as the hydrogen sources, can be carried out conveniently at room temperature with high chemoselectivity[14] and/or stereoselectivity.[15] Based on the type of catalyst applied in the process, it can be divided into two categories: metallocatalytic transfer hydrogenation and organocatalytic transfer hydrogenation.

2.2.1 Metallocatalytic transfer hydrogenations

In the area of organic synthesis, a useful family of hydrogen transfer catalysts has been developed based on ruthenium and rhodium complexes with diamine and phosphine ligands.[16] This kind of catalyst that containing both Lewis acid and Lewis base ligand is also called bifunctional catalyst.[17] A representative catalyst precursor is derived from (cymene)ruthenium dichloride dimer and the tosylated diphenylethylenediamine. These catalysts are mainly employed for the reduction of ketones and imines to alcohols and amines, respectively. The hydrogen-donor is typically isopropanol, which is converted to acetone upon donation of hydrogen.

Transfer hydrogenations can proceed with high enantioselectivities when the starting material is prochiral, as shown in equation (1), where RR'C*H-OH is a chiral product. A typical catalyst is the cymene(R,R-HNCHPhCHPhNTs), where Ts = $SO_2C_6H_4Me$ and R,R refers to the absolute configuration of the two chiral carbon centers. This work was recognized with the 2001 Nobel Prize in Chemistry to Ryōji

Noyori.[18]

$$RR'C{=}O + Me_2CHOH \rightarrow RR'C^*H\text{-}OH + Me_2C{=}O \quad (1)$$

Besides the broadly investigated ruthenium and rhodium catalysts, other transition metal based catalysts such as iridium,[19] palladium,[20] chromium[21] and nickel[22] complexes also displayed good catalytic activities, especially on asymmetric transfer hydrogenations.[23]

Another family of hydrogen-transfer agents is those based on main group metals, such as aluminium alkoxides for the MPV transfer hydrogenations[14, 24] and magnesium for the synthesis of asenapine.[25]

2.2.2 Organocatalytic transfer hydrogenations

Organocatalytic transfer hydrogenation is also well-known as metal free transfer hydrogenation, since the functionalized organic catalyst is usually metal free. Although the history of organocatalysis is apparently long,[26] the first organocatalytic transfer hydrogenation was described only recently in 2004 by the group of List, with a Hantzsch ester as the hydrogen donor and an iminium salt as the catalyst (Scheme 2.1).[27]

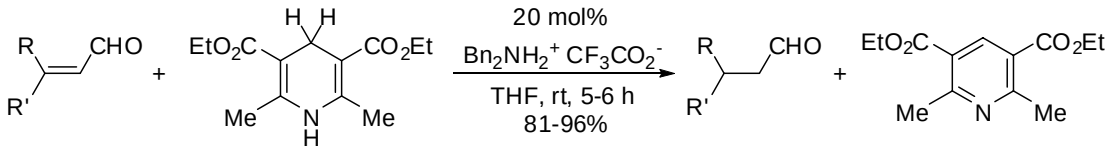

Scheme 2.1 Organocatalytic transfer hydrogenation of α,β-unsaturated aldehyde catalyzed by an iminium salt.[27]

In this particular reaction the substrate is an α,β-unsaturated carbonyl compound. The proton donor is oxidized to the pyridine form and resembles the biochemically relevant coenzyme nicotinamide adenine dinucleotide (NADH, Scheme 2.2). In the catalytic cycle for this reaction the amine and the aldehyde first form an iminium ion, then proton transfer is followed by hydrolysis of the iminium bond regenerating the catalyst (Scheme 2.3).

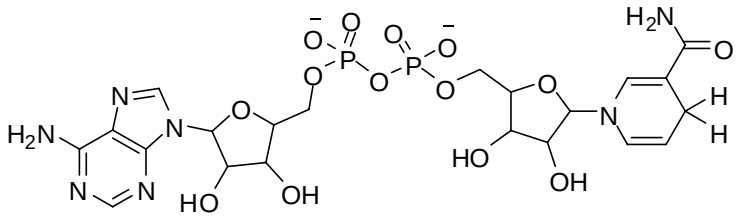

Scheme 2.2 NADH for naturally hydrogenation.[28]

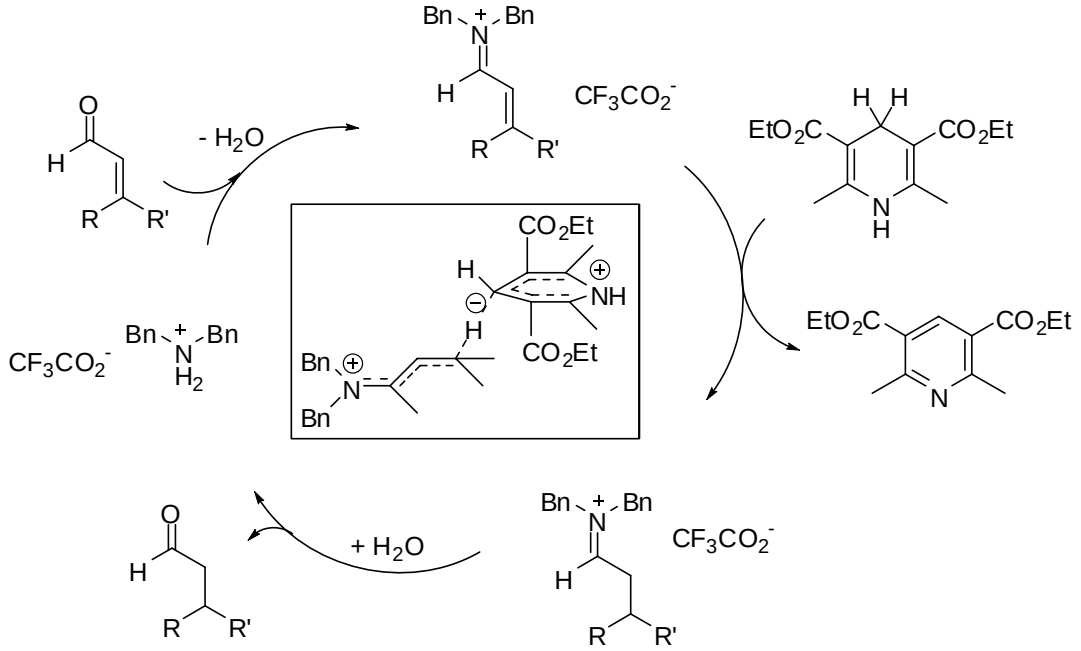

Scheme 2.3 Proposed mechanism of the iminium catalysis. [27]

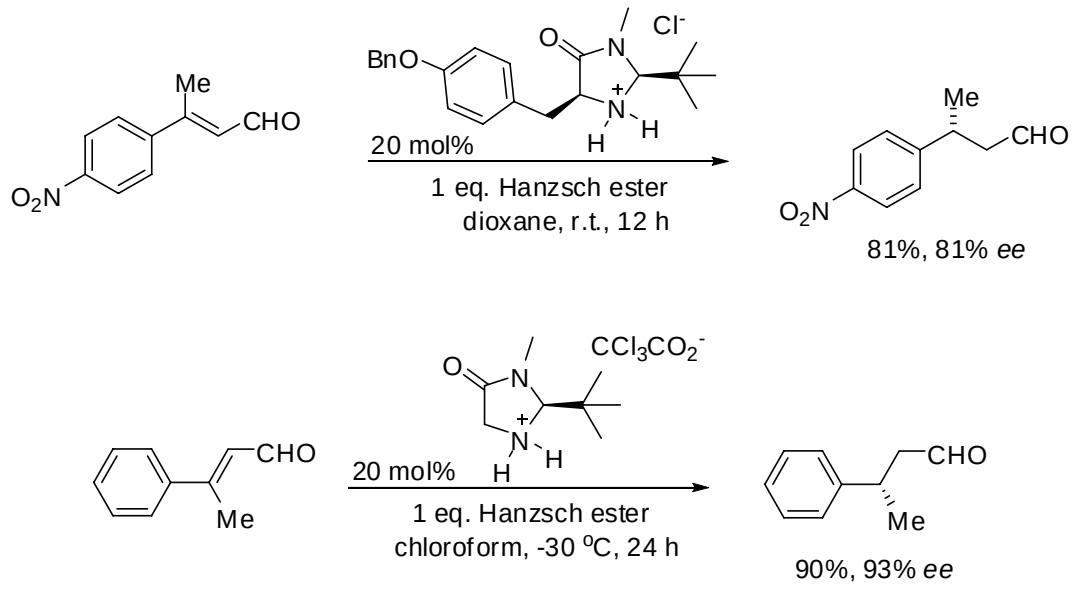

Scheme 2.4 Asymmetric transfer hydrogenation of α,β-unsaturated aldehyde catalyzed by a chiral imidazolidinone catalyst.[27] [29]

By adopting a chiral imidazolidinone MacMillan organocatalyst an enantioselectivity of 81% ee was obtained (Scheme 2.4, top). The group of MacMillan reported a similar asymmetric organocatalytic transfer hydrogenation independently also in 2004 (Scheme 2.4, bottom).[29]

The transfer hydrogenation of quinolines with Hantzsch esters as hydrogen source was achieved with Brønsted acids such as Diphenyl phosphate (DPP) or TFA and 1,2,3,4-tetrahydroquinolines were obtained in excellent yields under mild reaction conditions.[30] When chiral Brønsted acids were applied as catalysts, asymmetric transfer hydrogenation would take place, resulted in a variety of 2-aryl- and 2-alkyl-substituted tetrahydroquinolines with excellent enantioselectivities and good yields (Scheme 2.5).[31] More examples on asymmetric transfer hydrogenation of imine derivatives using Hantzsch esters as hydrogen donors were reviewed recently.[32] The reductions of C=O containing compounds can also be obtained with Hantzsch esters as the hydrogen sources, however, a metal catalyst is required.[33][34]

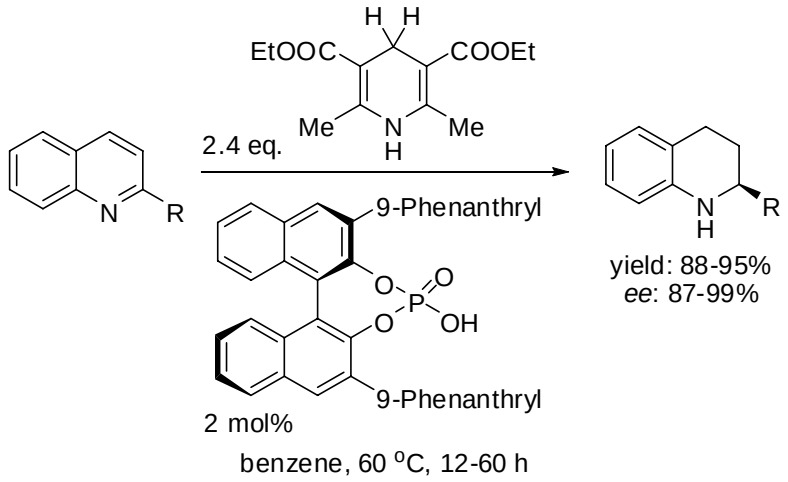

Scheme 2.5 Asymmetric transfer hydrogenation of α,β-unsaturated aldehyde catalyzed by a chiral imidazolidinone catalyst.

Comparing with the traditional metal catalyzed hydrogenation or transfer hydrogenation, Hantzsch ester mediated organocatalytic transfer hydrogenation processes have the following advantages: 1) mild reaction conditions, as most of the reactions can be carried out at room temperature (or with slight heating and cooling)

in conventional solvents; 2) operational simplicity, as there is no requirement either for special high-pressure apparatus, commonly needed for the hydrogen-gas process, or for air-free conditions, which is mostly necessary for the process involving metal hydrides; 3) ready availability of Hantzsch esters; 4) safe handling; 5) compatibility with organocatalysts; 6) suitability for hydrocascade catalysis. All these points make this biomimetic reductive process very attractive in organic synthesis.

On the other hand, problems remain with the current approach, such as: 1) poor atom economy, as only two protons are used per molecule and stoichiometric amounts of Hantzsch esters are needed; 2) problematic removal of the pyridine by-product for industrial-scale synthesis; 3) low efficiency for some of the current catalytic systems. Thus, efforts towards the easy separation and recycling of Hantzsch esters will be highly desirable and likely to address some of these remaining issues.

2.3 Goals and strategies

Transfer hydrogenation is one of the potential methods for chemical hydrogen storage. It contains dehydrogenation of one compound and hydrogenation of another compound, while the final hydrogenation product could be easier to release hydrogen than the starting material.[35] Recently, transfer hydrogenation using amine-borane compounds as hydrogen donors catalyzed by organometallic complexes has been reported.[36] Our goal is to carry out metal free transfer hydrogenations with amine borane complexes (especially ammonia borane) as hydrogen sources, aim at finding certain organic molecules which can first uptake hydrogen from ammonia borane and in the end be able to release hydrogen again. Thus, two separated steps are included as shown in Scheme 2.6.

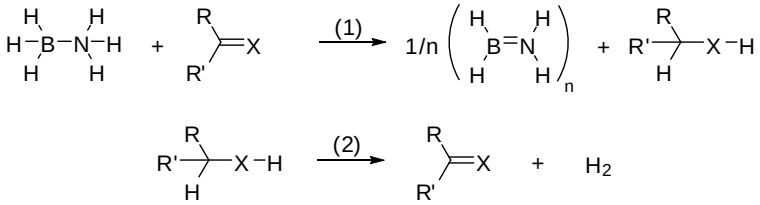

Scheme 2.6 The goal of this thesis: Metal free transfer hydrogenation using ammonia borane as hydrogen source. X = O, NR or CRR'.

Strategy for step (1): Noticing the significantly polarized H_B and H_N atoms in ammonia borane, unsaturated compounds with similarly polarized double bonds such as imines (C=N), carbonyl compounds (C=O) and the so-called push-pull olefins (C=C) could be considered as the hydrogen acceptors. It seems reasonable that in a polarity-match mode (Scheme 2.7), direct transfer hydrogenation might happen even without a catalyst.

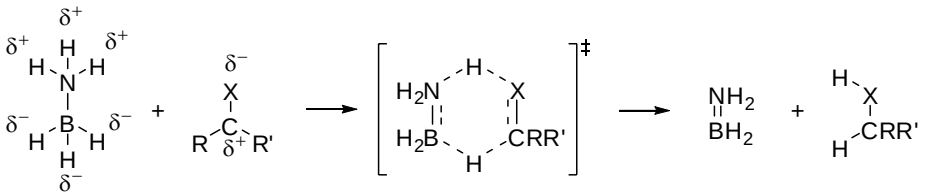

Scheme 2.7 Possible 'polarity match' uncatalyzed double H transfer process. X = O, NR or CRR'.

Strategy for step (2): Since a broad variety of polar unsaturated compounds will

be tested in the transfer hydrogenation processes and some of them might not be easily dehydrogenated, only a selected group of compounds will be employed for re-dehydrogenation. An easy and eco-friendly way to judge the dehydrogenation reactivity is to theoretically calculate the energy barrier between the substrate and its dehydrogenated form. The compound will be used only if it is thermodynamically feasible for dehydrogenation.

2.4 References

[1] a) F. S. Sinnatt, J. G. King and A. MacFarlane, *Industrial & Engineering Chemistry* **1937**, *29*, 133-140; b) B. Bosnich and K. Roberts Nicholas in *Asymmetric Catalytic Hydrogenation*, *Vol. 196* AMERICAN CHEMICAL SOCIETY, **1982**, pp. 337-354; c) W. S. Knowles, *Accounts of Chemical Research* **1983**, *16*, 106-112.

[2] G. B. Kauffman, *Platinum Metals Review* **1999**, *43*, 122-128.

[3] a) E. K. Rideal, *Journal of the Chemical Society (Resumed)* **1951**, 1640-1647; b) Morachevskii, *Russian Journal of Applied Chemistry* **2004**, *77*, 1909-1912.

[4] http://en.wikipedia.org/wiki/Wilhelm_Normann

[5] V. Smil, *Nature* **1999**, *400*, 415-415.

[6] Fischer, F.; Tropsch, H., German Patent 484337 1925.

[7] Raney, M. "Method of Preparing Catalytic Material". U.S. Patent 1,563,587, issued 1925; "Method of producing Finely Divided Nickel". U.S. Patent 1,628,190, issued 1927.

[8] M.-Y. Ngai, J.-R. Kong and M. J. Krische, *The Journal of Organic Chemistry* **2006**, *72*, 1063-1072.

[9] J. A. Osborn, F. H. Jardine, J. F. Young and G. Wilkinson, *Journal of the Chemical Society A: Inorganic, Physical, Theoretical* **1966**, 1711-1732.

[10] R. Noyori, T. Ohkuma, M. Kitamura, H. Takaya, Noboru Sayo, H. Kumobayashi and S. Akutagawa, *J. Am. Chem. Soc.* **1987**, *109*, 5856-5858.

[11] a) D. W. Stephan, G. C. Welch, L. Cabrera, P. A. Chase, E. Hollink, J. D. Masuda and P. R. Wei, *Dalton Transactions* **2007**, 3407-3414; b) D. W. Stephan, J. S. J. McCahill and G. C. Welch, *Angewandte Chemie-International Edition* **2007**, *46*, 4968-4971; c) D. W. Stephan, *Organic & Biomolecular Chemistry* **2008**, *6*, 1535-1539; d) D. W. Stephan, *Dalton Transactions* **2009**, 3129-3136.

[12] a) T. van Es and B. Staskun, *Org. Syn.* **1988**, *6*, 631; b) G. Brieger and T. J. Nestrick, *Chemical Reviews* **1974**, *74*, 567-580; c) R. A. W. Johnstone, A. H. Wilby and I. D. Entwistle, *Chemical Reviews* **1985**, *85*, 129-170; d) B. C. Ranu, A. Sarkar, S. K. Guchhait and K. Ghosh, *Journal of the Indian Chemical Society* **1998**, *75*, 690-694.

[13] a) H. Meerwein and R. Schmidt, *Justus Liebigs Ann. Chem.* **1925**, *444*, 221-238; b) W. Ponndorf, *Angew. Chem.* **1926**, *39*, 138-143; c) A. Verley, *Bull. Soc. Chim. Fr.* **1925**, *37*, 871-874.

[14] C. F. d. Graauw, J. A. Peters, H. v. Bekkum and J. Huskens, *Synthesis* **1994**, 1007-1017.

[15] T. Ooi, T. Miura and K. Marouka, *Angew. Chem. Int. Ed.* **1998**, *37*, 2347-2349.

[16] R. Noyori, *J. Syn. Org. Chem. Jpn.* **1992**, *50*, 1131-1139.

[17] R. Noyori, M. Yamakawa and S. Hashiguchi, *J. Org. Chem.* **2001**, *66*, 7931-7944.

[18] R. Noyori, *Adv. Syn. Cata.* **2003**, *345*, 15-32.

[19] a) A. Benyei and F. Joo, *Journal of Molecular Catalysis* **1990**, *58*, 151-163; b) T. Abura, S. Ogo, Y. Watanabe and S. Fukuzumi, *Journal of the American Chemical Society* **2003**, *125*, 4149-4154; c) J. R.

Miecznikowski and R. H. Crabtree, *Polyhedron* **2004**, *23*, 2857-2872; d) X. F. Wu, J. K. Liu, X. H. Li, A. Zanotti-Gerosa, F. Hancock, D. Vinci, J. W. Ruan and J. L. Xiao, *Angewandte Chemie-International Edition* **2006**, *45*, 6718-6722.

[20] a) J. B. Arterburn, M. Pannala, A. M. Gonzalez and R. M. Chamberlin, *Tetrahedron Letters* **2000**, *41*, 7847-7849; b) J. F. Bower and M. J. Krische, *Iridium Catalysis* **2011**, *34*, 107-138; c) H. Wiener, J. Blum and Y. Sasson, *Journal of Organic Chemistry* **1991**, *56*, 4481-4486.

[21] K. Micskei, C. Hajdu, L. A. Wessjohann, L. Mercs, A. Kiss-Szikszai and T. Patonay, *Tetrahedron-Asymmetry* **2004**, *15*, 1735-1744.

[22] R. Barrios-Francisco and J. J. Garcia, *Inorganic Chemistry* **2009**, *48*, 386-393.

[23] a) S. Hashiguchi, N. Uematsu and R. Noyori, *Journal of Synthetic Organic Chemistry Japan* **1997**, *55*, 99-109; b) S. Gladiali and E. Alberico, *Chemical Society Reviews* **2006**, *35*, 226-236; c) X. F. Wu, C. Wang and J. L. Xiao, *Platinum Metals Review* **2010**, *54*, 3-19.

[24] a) Y. Z. Zhu, S. Jaenicke and G. K. Chuah, *Journal of Catalysis* **2003**, *218*, 396-404; b) G. K. Chuah, S. Jaenicke, Y. Z. Zhu and S. H. Liu, *Current Organic Chemistry* **2006**, *10*, 1639-1654; c) Y. Z. Zhu, G. K. Chuah and S. Jaenicke, *Journal of Catalysis* **2006**, *241*, 25-33.

[25] M. v. d. Linden, T. Roeters, R. Harting, E. Stokkingreef, A. S. Gelpke and G. Kemperman, *Organic Process Research & Development* **2008**, *12*, 196-201.

[26] a) P. R. Schreiner, *Chemical Society Reviews* **2003**, *32*, 289-296; b) P. I. Dalko and L. Moisan, *Angewandte Chemie International Edition* **2001**, *40*, 3726-3748; c) P. I. Dalko and L. Moisan, *Angewandte Chemie International Edition* **2004**, *43*, 5138-5175.

[27] J. W. Yang, M. T. Hechavarria Fonseca and B. List, *Angewandte Chemie International Edition* **2004**, *43*, 6660-6662.

[28] a) B. Alberts, D. Bray, J. Lewis, M. Raff, K. Roberts, J. D. Watson, Molecular Biology of the Cell, 3rd ed., Garland, New York, 2002; b) J. M. Berg, J. L. Tymoczko, L. Stryer, Biochemistry, 5th ed., W.H. Freeman & Company, New York, 2002.

[29] S. G. Ouellet, J. B. Tuttle and D. W. C. MacMillan, *Journal of the American Chemical Society* **2004**, *127*, 32-33.

[30] a) M. Rueping, C. Azap, E. Sugiono and T. Theissmann, *Synlett* **2005**, 2367-2369; b) M. Rueping, T. Theissmann and A. P. Antonchick, *Synlett* **2006**, 1071-1074.

[31] a) M. Rueping, A. P. Antonchick and T. Theissmann, *Angewandte Chemie International Edition* **2006**, *45*, 3683-3686; b) M. Rueping, E. Sugiono, C. Azap, T. Theissmann and M. Bolte, *Organic Letters* **2005**, *7*, 3781-3783.

[32] Z. Y. Wang and Z. J. Jiang, *Asian Journal of Chemistry* **2010**, *22*, 4141-4149.

[33] S. L. You, *Chemistry-an Asian Journal* **2007**, *2*, 820-827.

[34] a) S. Zehani, G. Gelbard, J. Chem. Soc. Chem. Commun. 1985, 1162 – 1163; b) S. Zehani, J. Lin, G. Gelbard, Tetrahedron 1989, 45,733 – 740.

[35] H. Berke, *Chemphyschem* **2010**, *11*, 1837-1849.

[36] a) Y. Jiang and H. Berke, *Chem. Commun.* **2007**, 3571-3573; b) C. A. Jaska and I. Manners, *J. Am. Chem. Soc.* **2004**, *126*, 2698-2699; c) T. J. Clark, K. Lee and I. Manners, *Chemistry-a European Journal* **2006**, *12*, 8634-8648.

Transfer Hydrogenation of Imines with Ammonia Borane: A Concerted Double-H Transfer Reaction?

3.1 Introduction

Ammonia-borane (H_3N-BH_3, **AB**) is considered a feasible material for chemical hydrogen storage due to its ideally very high storage capacity (19.6 weight % H) and thus has attracted much attention.[1] Dehydrogenations of **AB** were accomplished either thermally or by transition metal catalysis.[2] Considering **AB** as a significantly polarized molecule, we reckoned that it could be dehydrogenated by direct reaction with a similarly polarized unsaturated compound via the rarely explored reaction mode of double H transfer (Scheme 3.1).

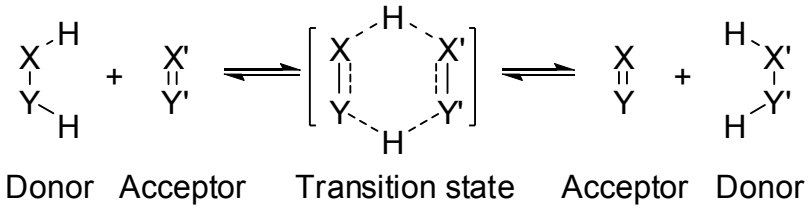

Scheme 3.1 Double H transfer as an elementary process. X, Y, X' and Y': main group element or transition metal fragments.

In certain cases double H transfers are the crucial step of multi-step transition metal catalyzed transfer hydrogenations[3,4] with separate processes for hydrogenation and dehydrogenation. In contrast to these catalyses the "true" double H transfer reaction is an all-in-one transfer hydrogenation with concerted hydrogenation and dehydrogenation reactions merged into one unique elementary step.

Such elementary processes of double H transfer are as yet rare. DFT calculations suggest that the prototypical homopolar reaction course of H_2 exchange between ethane and ethylene could principally proceed along the lines of Scheme 3.1.[3,5] Despite its principal character of a 4+2 symmetry-allowed concerted process, it was calculated to possess a very high barrier making it difficult to put this reaction into

reality. However, polar such reaction variants are expected to possess much lower barriers. For example, the aluminum complex catalyzed Meerwein-Ponndorf-Verley reduction[6] of carbonyl substrates to alcohols is thought to proceed along such a reaction path, and can be carried out at room temperature.[7] The mechanistically related reductions of olefins and acetylenes with diimine proceed even below room temperature.[8] The Ru or Ir catalyzed multi-step transfer hydrogenation reactions provide a powerful basis for the preparation of primary or secondary amines.[9] Furthermore, Noyori- and Shvo-type transfer hydrogenations are widely applied in organic chemistry.[10] All these catalytic reactions are thought to proceed in their essential H_2 transfer step as "bifunctional activation" processes with double H transfers. It was also demonstrated in recent studies that rhenium catalysts can promote multi-step transfer hydrogenations of olefins using **AB** and dimethylamine borane as a polar hydrogen donor.[11] Herein, we want to probe the direct reaction between imines and **AB** reaching eventually the conclusion of concerted polar double H transfers.

3.2 Results and discussions

N-benzylidene aniline (**1a**), as the simplest aromatic Schiff-base derivative, was selected as the reference compound for the reaction with **AB**. In order to avoid decomposition of the Lewis pair **AB**, only temperatures below 60 ^{o}C and concentrations lower than 0.2 M were applied.[12] For the reaction of **1a** with **AB**, very practical rates were obtained at 60 ^{o}C (Table 3.1, entries 1, 5 and 6). The transfer hydrogenation was found to proceed even at room temperature, naturally then at a much slower pace (Table 3.1, entry 4). Since the thermal dehydrogenation of **AB** was nearly invisible at room temperature, we can exclude the possible reaction pathway via thermal dehydrogenation of **AB** followed by imine hydrogenation. With the progressing of the transfer-hydrogenation, trace amount of H_2 was always obtained. This side reaction can be considered as a proof for the generation of [BH_2NH_2], which was supposed to be able to catalyze the dehydrogenation of **AB**.[13,14] But it was only a minor competition reaction here, because 1 eq. of **AB** can hydrogenate 2 eq. of **1a**

nearly quantitatively if given enough time (Table 3.1, entry 6). A scrambling experiment with **AB** and its doubly deuterated derivative **A(D)B(D)** was also carried out to see whether **AB** would decompose at such conditions. No reaction was noticed over several hours at 60 ^{o}C and several days at room temperature, thus it can be excluded that the transfer hydrogenation could proceed via Lewis acid (BH_3) or base (NH_3) mediation.

Table 3.1 Reactions of **AB** with various imines in THF.[a]

Entry	R/R' of Imine or amine		Temp./^{o}C	Time	Yield/%[b]
1	R = R' = Ph	**1a/b**	60	7 h	99 (>99[c])
2	R = R' = Ph	**1a/b**	50	14 h	(>99)
3	R = R' = Ph	**1a/b**	40	2 d	(>99)
4	R = R' = Ph	**1a/b**	rt	5 d	(84[d])
5[e]	R = R' = Ph	**1a/b**	60	3 h	(>99)
6[f]	R = R' = Ph	**1a/b**	60	24 h	(93[g])
7	Ph/Bn	**2a/b**	60	3 d	99 (>99)
8	Ph/*t*Bu	**3a/b**	60	4 d	45 (46)
9	Cy/*t*Bu	**4a/b**	60	3 d	97 (99)
10	Ph/$CHPh_2$	**5a/b**	60	1 d	99 (>99)
11	Ph_2/H	**6a/b**	60	14 h	98 (>99)
12	p-$MeOC_6H_4$/Ph	**7a/b**	60	8 h	99 (>99)
13	p-ClC_6H_4/Ph	**8a/b**	60	5 h	99 (>99)
14	p-O_2N/Ph	**9a/b**	60	3 h	99 (>99)
15	Ph/p-C_6H_4OMe	**10a/b**	60	1 d	99 (>99)
16	Ph/p-C_6H_4Cl	**11a/b**	60	4 h	99 (>99)
17	Ph/ p-$C_6H_4NO_2$	**12a/b**	60	0.5 h	99 (>99)
18	p-ClC_6H_4/p-C_6H_4OMe	**13a/b**	60	20 h	98 (>99)
19	R = R' = p-ClC_6H_4	**14a/b**	60	4 h	99 (>99)
20	p-$MeOC_6H_4$/p-C_6H_4Cl	**15a/b**	60	5 h	99 (>99)
21	R = R' = p-C_6H_4OMe	**16a/b**	60	20 h	99 (>99)

[a] 0.1 mmol **AB** react with 0.1 mmol imine, unless mentioned; [b] GC-MS yield and in brackets NMR yields based on the initial amount of imine; [c] Isolated yield 92%; [d] 100 % could be obtained if given a longer reaction time; [e] The amount of **AB** was 0.2 mmol; [f] The amount of **1a** was 0.2 mmol; [g] Better result can be obtained given longer reaction time.

After this initial test on the double H transfer to benzylidene aniline, an extended selection of imines was probed with a 1 : 1 ratio of imine to **AB** applying various conditions given in Table 3.1 (entries 7-21). The reaction times for various *p*-substituted *N*-benzylidene anilines were found to vary between 0.5 h and several days. Alkyl imines turned out to be much slower (Table 3.1, entries 7-10), in particular *N*-*t*-butyl benzyl imine (Table 3.1, entry 8). Later we will see that this is more due to the electron-donating than to the stereochemical property of the *t*-Bu group.

Although the imines are all uniquely transformed to amines, the dehydrogenation products of **AB** were manifold. According to the ^{11}B NMR spectra (see supplementary material), **AB** was converted to B-(cyclodiborazanyl)amino-borohydride (**BCDB**), borazine (**BZ**), polyborazylene (**PBZ**) and cyclotriborazane (**CTB**). After long reaction times (2 days at 60 ^{o}C with 0.1 mmol **AB** and 0.5 mmol **1a**), both **BCDB** and **CTB** had disappeared completely, indicating they are intermediates on the way from **AB** to **BZ** and **PBZ**. Other possible products, like $[NH_3BH_2NH_3]^+[BH_4]^-$ and cyclo-diborazane, were not observed even at room temperature.

The reaction course of **AB** and **1a** was further studied tracing the boron containing products. Firstly, **BZ** and **CTB** were employed to react with **1a**. While **BZ** turned out to be stable towards **1a**, **CTB** was found to hydrogenate **1a** much faster than **AB** and the dehydrogenation product was almost exclusively **BZ**. Although clearly identified in the ^{11}B NMR spectrum, we were not able to separate these B-containing products. In accordance with earlier conclusions on other **AB** dehydrogenations, the appearance of **CTB** and **BCDB** witnesses the primary intermediacy of the very reactive $[H_2B{=}NH_2]$ molecule, which decayed in fast subsequent reaction steps. It remains an open question whether **CTB** was formed by directly cyclization of $[H_2B{=}NH_2]$ (path **A**, Scheme 3.2) or via isomerization of **BCDB** (path **B**, Scheme 3.2).[12,14]

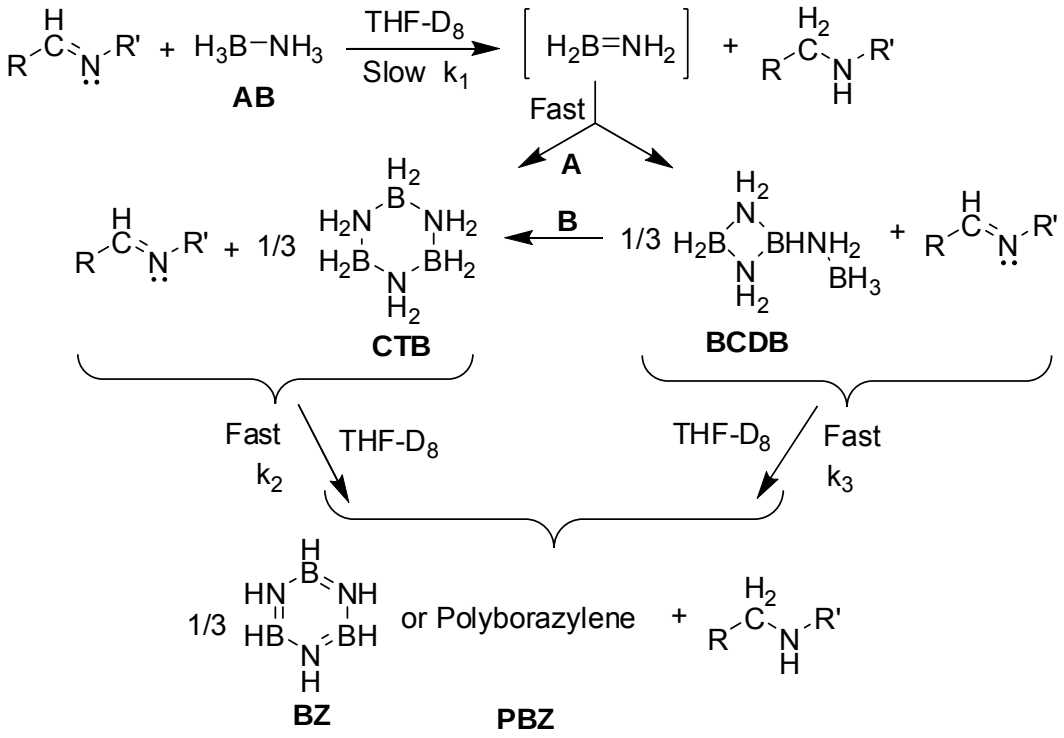

Scheme 3.2 Proposed overall reaction route.

As illustrated in Scheme 3.2, the overall reaction rate from **AB** to **BZ** and **PBZ** may be described by k_1, k_2 and k_3, potentially the double H transfer steps. Under pseudo-first order conditions with excess of **1a** k_1 and k_2 were determined in reactions with **AB** and **CTB,** respectively. Since **BCDB** could not be prepared in pure form, k_3 could not be determined. **BCDB** was anticipated to be a hydrogen donor comparable to **CTB** and therefore its reaction rate with **1a** was assumed to be close to k_2. In separate experiments under comparable conditions k_2 was found 6 times faster than k_1, therefore k_1 of the **AB** dehydrogenation is rate determining. In conjunction with the kinetically "silent" consumption of **1a** via the reactions with **CTB** and **BCDB**, the order of the reaction is one half in **1a** and one in **AB** as established by curve fitting in appropriate kinetic experiments (see Suppl. Material S4).

These facts would be in agreement with a mechanistic picture featuring the k_1, k_2 and k_3 steps as double H transfers. This poses the important question whether these polar transfers are proceeding in a concerted or stepwise pathway.[3,4] We tried to gain insights by DFT calculations using Gaussian 03 program. [15](see Suppl. Material S5).

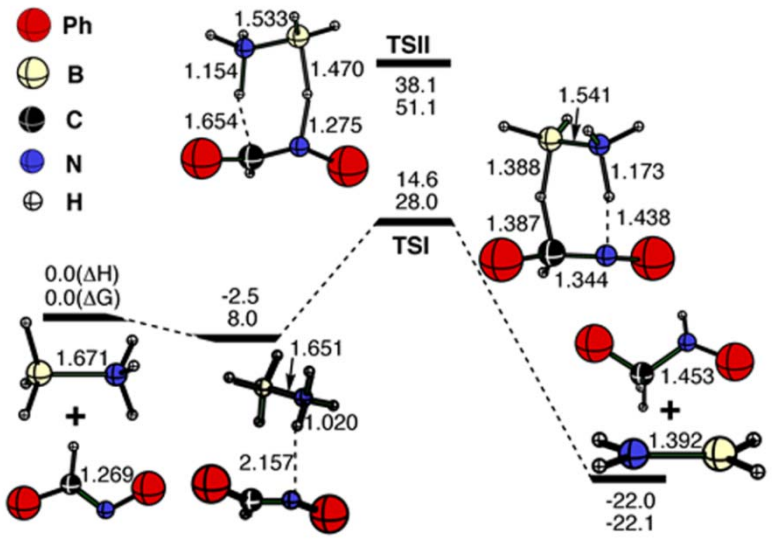

Scheme 3.3 DFT calculations for the reaction of **AB** with benzylidene aniline **1a** leading to aminoborane and *N*-benzylaniline **1b**. The bond lengths (in Å) were obtained at the M05-2X/6-311++G**level. The ΔH and ΔG (in kcal mol^{-1}) in THF solvent at the condition of 298 K and 1 *atm* were corrected with the M05-2X/6-311++G** gas phase harmonic frequencies.

The quantum mechanics calculations carried out at the M05-2X/6-311++G** level indicate the double H transfer pathway for the reaction of **AB** with **1a**.[16] A thermodynamically and kinetically feasible concerted reaction path resulted (Scheme 3.3). Two 6-membered cyclic double H transfer transition states (**TSI** and **TSII**) were approached with different **AB** orientation with respect to the imine C=N bond. As expected, the reaction path via **TSI** with B-H···C and N-H···N transfers is energetically highly favoured over the alternative **TSII** with N-H···C and B-H···N transfers (by *ca.* 23 kcal mol^{-1}). In **TSI** the transferred H atoms on the B and N sides of **AB** have opposite polarization with respect to the attacked C and N atoms, respectively. From the charge point of view this naturally copes with the low energy pathway, while the opposite orientation in **TSII** would have the transferred hydrogen atoms attacked at evenly charged centers disfavouring the pathway. Moreover, an initial N-H···N hydrogen bonding in the reaction path via **TSI** would help to pre-organize **TSI** in the right orientation but not **TSII**. Stepwise reaction paths were also considered with the assumption that the relative energies of the first H transfer is the energetically decisive step.[17] All such possible reaction channels are predicted to

be endergonic. The most energetically favoured was 44.9 kcal mol^{-1} higher in free energy than the reactants (see Suppl. Material S5), which is 16.9 kcal mol^{-1} higher than the transition state (**TSI**). This undoubtedly verifies the favourable concerted double-H transfer mechanism. Note that the concerted reaction path for the hydrogen transfer between ethane and ethylene has computationally been spotted to be more favourable than the stepwise pathway.[3] The concerted pathway was reconfirmed by the MP2/6-311++G** calculations, which gave similar geometric and energetic results (see Suppl. Material S5).

To further support the understanding of the regioselectivity of this reaction suggested by the calculations, deuterium labelling studies were carried out. Deuterated **AB**'s (BD_3NH_3 (**AB(D)**), BH_3ND_3 (**A(D)B**)and BD_3ND_3 (**A(D)B(D)**)) were employed to react with *N*-benzylidene aniline **1a**. The *in situ* ^1H and ^{13}C NMR spectra proved stereo-controlled reaction courses. A product deuterated at the C-end of the C=N bond was obtained from an experiment with **AB(D)** and **1b** showing a triplet (J(CD) = 20 Hz) for the CHD group in the ^{13}C NMR spectrum appearing at the same chemical shift as the CH_2 group of the benzyl phenyl amine **1b**. A doublet at 4.23 ppm in the ^2H NMR spectrum further confirmed the presence of the CHD unit. In the related experiment taking **A(D)B** and the imine, absence of the N-H signal in the ^1H NMR spectrum and appearance of a N-D resonance in the ^2H NMR spectrum indicated the exclusive formation of a N-D bond. Both of these results are supportive of the **TSI** geometry of Scheme 3.3. In the case of **A(D)B(D)**, both the CH and N positions of the amine were fully deuterated as verified by ^2H NMR spectroscopy.

In addition to these D labelling studies, primary Deuterium Kinetic Isotope Effects (DKIE) were investigated. Considering the manifold dehydrogenation products of **AB**, all the reactions were carried out with *in situ* NMR measurements under approximate "pseudo-first order" conditions for **AB** with the imines in excess (0.5 mmol of **1a** reacting with 0.1 mmol **AB**). According to the kinetic conversion chart based on ^{11}B NMR (Figure 3.1), the rate constants (k) were simulated and the DKIE values obtained.

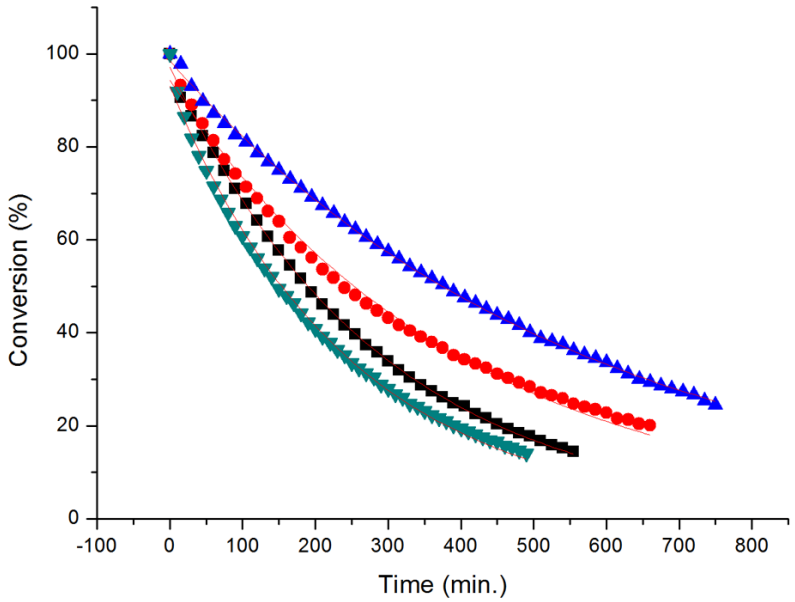

Figure 3.1 Conversion chart of the reaction of 0.5 mmol benzylidene aniline **1a** with 0.1 mmol **AB**, **AB(D), A(D)B** or **A(D)B(D)** pursued by ^{11}B NMR in THF-D_8 at 60 ^{o}C, determined by intensities of **AB** on the ^{11}B NMR spectra with 15 min interval. The black squares stand for reactions with **AB**, red circles for **A(D)B(D)**, green triangles for **AB(D)** and blue triangles for **A(D)B**. Simulated reaction constants were: $k_{AB} = 0.00350$, $k_{AB(D)} = 0.00404$, $k_{A(D)B} = 0.00181$, $k_{A(D)B(D)} = 0.00251$.

$$k_{\mathbf{AB}}/k_{\mathbf{AB(D)}} = 0.87, \qquad k_{\mathbf{AB}}/k_{\mathbf{A(D)B}} = 1.93, \qquad k_{\mathbf{AB}}/k_{\mathbf{A(D)B(D)}} = 1.39 \qquad \text{(Eq. 1)}$$

For the reaction of **1a** with **AB(D)**, an inverse DKIE (Eq. 1, DKIE = 0.87) was obtained, which speaks for the formation of a stronger bond with a steeper potential energy curve in the presumably late transition state.[18] Together with the given size of the isotope effect, this could be rationalized on the basis of the transfer of the hydridic H_B atom possessing a flatter ground state potential curve. The H-C bond developed in the late transition state is expected to cause a steeper potential energy curve.

In the case of the reaction with **A(D)B**, a normal DKIE (Eq. 1, DKIE = 1.93) was observed. This indicates that breakage of the N-H bond participates in the rate determining step and that both the broken and the installed bonds have approximately the same strengths.[18] For the double DKIE reaction of **A(D)B(D)** with the imine, a DKIE smaller than **A(D)B** was observed (Eq. 1, DKIE = 1.39). This value would constitute a sort of average with approximate cancellation of the kinetic effects of the two mono-deuterated cases. The "averaging" of the double DKIE's of double H

transfers is however presently not fully understood on a quantum mechanical basis of the single DKIE ones.[19] According to the sizes of the single DKIE's, we may conclude that both H transfers participate in the rate determining step. This makes a concerted mechanism quite plausible, because if it proceeds via a stepwise mechanism, the reaction rate should at least not be affected by one of the D-labelling reactions.

The Hammett correlation was then also checked for the reactions of **AB** with the *p*-H, -OMe, -Cl or -NO_2 substituted *N*-benzylidene anilines: **1a**, **7a**, **8a**, **9a**, **10a**, **11a** and **12a**. The initial rate constants (k) were calculated from the conversion charts. Hammett correlations (Figure 3.2) plotting log k vs substitutents constants σ [20] gave different slopes for substrates substituted on the C- or N-side phenyls of the imine. The slope of the Hammett plot (ρ) represents the sensitivity constant, indicating the susceptibility of the reaction to substituents. From Figure 3.2, a ρ of 1.61 was obtained for the reactions with imines substituted at the *para*-position of the N-side, and a ρ of 0.69 for those substituents at the C-side.

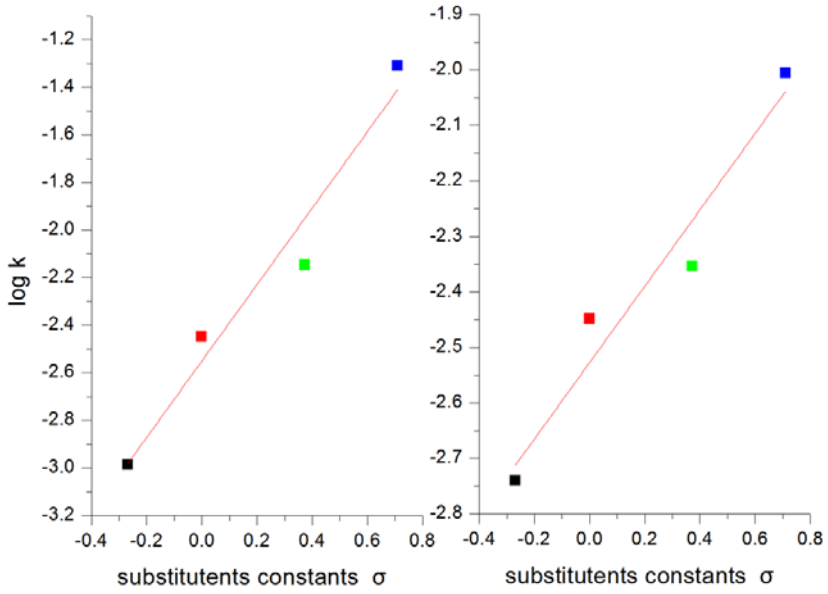

Figure 3.2 Hammett plots for the reactions of 0.1 mmol **AB** with 0.5 mmol *p*-substituted diaryl imines extracted from kinetic ^{11}B NMR spectra in THF-D_8 at 60 ^{o}C. The left chart with a ρ = 1.61 stands for the reactions with *p*-substitutent at the aniline side, and the right one with a ρ = 0.69 for *p*-substitution at the benzylidene side. From left to right (or from bottom to top), the squares represented for –OMe, –H, –Cl and –NO_2 groups, respectively.

A positive ρ means that negative charge is built up during the transition state, and a $\rho > 1$ says that the reaction is very sensitive to substituents.[18,20] Negative charge build-up during the reaction means increased electron density in the transition state, which seems realistic for a concerted mechanism and thus supportive for a simultaneous double H transfer. If the two H were transferred one-after-another, the charges generated on the B-H^--C side and that of the N-H^+-N side should be of different signs, which would result in one ρ positive and the other one negative.

3.3 Conclusions

In conclusion, "metal-free" transfer hydrogenations of imines with ammonia borane were observed to proceed under mild conditions. Based on DKIE determinations, Hammett correlations and DFT calculations, the reaction courses are proposed to follow the profile of concerted double H transfers. The adaptability and generality of this type of reaction applying to other unsaturated compounds with the goal of the development of respective catalytic reactions is currently under investigation in our group.

This work is financially supported by the Swiss National Science Foundation and the University of Zurich. The computational study is supported by the Chinese Academy of Sciences. We thank Prof. Dr. R. Tom Baker (CCRI, Ottawa) for fruitful discussions.

3.4 References

1. a) C. W. Hamilton, R. T. Baker, A. Staubitz, I. Manners, *Chem. Soc. Rev*. **2009**, *38*, 279-293; b) F. H. Stephens, V. Pons, R. T. Baker, *Dalton Trans.* **2007**, *25*, 2613-2626; c) T. B. Marder, *Angew. Chem., Int. Ed.* **2007**, *46*, 8116-8118; d) A. Gutowska, L. Li, Y. Shin, M. Wang, X. S. Li, J. C. Linehan, R. S. Smith, B. D. Kay, B. Schmid, W. Shaw, M. Gutowski, T. Autrey, *Angew. Chem., Int. Ed.* **2005**, *44*, 3578-3582; d) E. Fakioglu, Y. Yurum, T. Nejat Veziroglu, *Int. J. Hydrogen Energy* **2004**, *29*, 1371-1376; e) W. Grochala, P. P. Edwards, *Chem. Rev.* **2004**, *104*, 1283-1315.
2. a) T. He, Z. Xiong, G. Wu, H. Chu, C. Wu, T. Zhang, P. Chen, *Chem. Mater.*, **2009**, *21*, 2315-2318; b) M. E. Sloan, T. J. Clark, I. Manners, *Inorg. Chem*., **2009**, *48*, 2429-2435; c) D. Neiner, A. Karkamkar, J. C. Linehan, B. Arey, T. Autrey, S. M. Kauzlarich, *J. Phys. Chem. C*, **2009**, *113*, 1098-1103; d) S. Basu, A. Brockman, P. Gagare, Y. Zheng, P. V. Ramachandran, W. N. Delgass, J. P. Gore, *J. Power Sources,* **2009**, *188*, 238-243; e) P. M. Zimmerman, A. Paul, C. B. Musgrave, *Inorg. Chem*., **2009**, *48*, 5418-5433; f) V. Pons, R. T. Baker, *Angew. Chem., Int. Ed.* **2008**, *47*, 9600-9602; g) P. Wang, X.-D. Kang, *Dalton Trans.*, **2008**, 5400-5413; h) F. H. Stephens, R. T. Baker, M. H. Matus, D. J. Grant, D. A. Dixon, *Angew. Chem., Int. Ed.,* **2007**, *46*, 746-749; i) R. J. Keaton, J. M. Blacquiere, R. T. Baker, *J. Am. Chem. Soc*., **2007**, *129*, 1844-1845; j) T. Marder, *Angew. Chem., Int. Ed.,* **2007**, *46*, 8116-8118; k) D. Pun, E. Lobkovsky, P. J. Chirik, *Chem. Commun.*, **2007**, 3297-3299; l) M. C. Denney, V. Pons, T. J. Hebden, D. M. Heinekey, K. I. Goldberg, *J. Am. Chem. Soc.,* **2006**, *128*, 12048-12049.
3. D. J. Miller, D. M. Smith, B. Chan, M. Radom, *Molecular Physics*, **2006,** *104*, 777 – 794.
4. a) A. Comas-Vives, G. Ujaque, A. Lledós, *Organometallics*, **2007**, *26* , 4135-4144; b) C. Riichardt, M. Gerst, J. Ebenhoch, *Angew. Chem. Int. Ed.* **1997**, *36*, 1406-1430.
5. I. Fernández, M. A. Sierra, F. P. Cossío, *J. Org. Chem.* **2007**, *72*, 1488-1491.
6. a) H. Meerwein, R. Schmidt, *Justus Liebigs Ann. Chem.* **1925**, *444*, 221-238; b) W. Ponndorf, *Angew. Chem.* **1926**, *39*, 138-143; c) A. Verley, *Bull. Soc. Chim. Fr.* **1925**, *37*, 871-874.
7. E. J. Campbell, H. Zhou, S. T. Nguyen, *Org. Lett.* **2001**, *3*, 2391-2393.
8. S. Siegel, G. M. Foreman, D. Johnson, *J. Org. Chem.* **1975**, *40*, 3589-3593.
9. a) H. Matsunaga, K. Nakanishi, M. Nakajima, T. Kunieda, T. Ishizuka, *Heterocycles*, **2009**, *78*, 617-622; b) J. Canivet, G. Suess-Fink, *Green Chem.*, **2007**, *9*, 391-397; c) R. Kadyrov, T. H. Riermeier, *Angew. Chem., Int. Ed.* **2003**, *42*, 5472-5474; d) J. E. D. Martins, G. J. Clarkson, M. Wills, *Org. Lett.* **2009**, *11*, 847-850; e) D. Gnanamgari, A. Moores, E. Rajaseelan, R. H. Crabtree, *Organometallics*, **2007**, *26*, 1226-1230; f) P. Roszkowski, Z.Czarnocki, *Mini-Rev. Org. Chem.* **2007**, *4*, 190-200.
10. a) R. Noyori, T. Okhuma, M. Kitamura, H. Takaya, N. Sayo, H. Kumobayashi, S. Akuragawa, *J. Am. Chem. Soc.* **1987**, *109*, 5856-5858; b) R. Noyori, in *Asymmetric Catalysis In Organic Synthesis*. Wiley-Interscience. John Wiley & Sons, New York, **1994**, pp. 16-94 and references cited therein; c) Y. Blum, D. Czarkie, Y. Rahamim, Y. Shvo, *Organometallics* **1985**,

4, 1459-1461; d) Y. Shvo, D. Czarkie, Y. Rahamim, D. F. Chodosh, *J. Am. Chem. Soc.* **1986**, *108*, 7400-7402; e) C. P. Casey, N. A. Strotman, S. E. Beetner, J. B. Johnson, D. C. Priebe, T. E. Vos, B. Khodavandi, I. A. Guzei, *Organometallics*, **2006**, *25*, 1230-1235.

11. Y. Jiang, H. Berke, *Chem. Commun.* **2007**, 3571-3572.
12. a) W. J. Shaw, J. C. Linehan, N. K. Szymczak, D. J. Heldebrant, C. Yonker, D. M. Camaioni, R. T. Baker, T. Autrey, *Angew. Chem. Int. Ed.* **2008**, *47*, 7493-7496. b) M. G. Hu, R. A. Geanangel, W. W. Wendlandt, *Thermochim. Acta.* **1978**, *23*, 249-255.
13. P. M. Zimmerman, A. Paul, Z. Zhang, C. B. Musgrave, *Inorg. Chem*., **2009**, *48*, 1069-1081.
14. V. Pons, R. T. Baker, N. K. Szymczak, D. J. Heldebrant, J. C. Linehan, M. H. Matus, D. J. Grant, D. A. Dixon, *Chem. Commun.* **2008**, 6597- 6599.
15. M. J. Frisch, et al. Gaussian 03 Revision E.01, Gaussian Inc., Pittsburgh, PA, **2003**. See [S5] in the supporting information for complete form. For M05-2X functional, see a) Y. Zhao, N. E. Schultz, D. G. Truhlar, *J. Chem. Theory Comput.* **2006**, *2*, 364-382; b) Y. Zhao, D. G. Truhlar, D. G. *Acc. Chem. Res.* **2008**, *41*, 157-167. For IEFPCM, see a) Tomasi, B. Mennucci, E. Cances, *J. Mol. Struct. (THEOCHEM)* **1999**, *464*, 211-226. b) W. Sang-Aroon, V. Ruangpornvisuti, *Int. J. Quantum Chem.* **2008**, *108*, 1181-1188.
16. a) P. M. Zimmerman, A. Paul, Z. Zhang, C. B. Musgrave, Angew. *Chem. Int. Ed.,* **2009**, *48*, 2201-2205; b) A. Staubitz, M. Besora, J. N. Harvey, I. Manners, *Inorg. Chem.*, **2008**, *47*, 5910-5918; c) X. Yang, M. B. Hall, *J. Am. Chem. Soc.,* **2008**, *130*, 1798-1799; d) J. Li, S. M. Kathmann, G. K. Schenter, M. Gutowski, *J. Phys. Chem. C*, **2007**, *111*, 3294-3299; e) Y. Luo, K. Ohno, *Organometallics*, **2007**, *26*, 3597-3600; f) A. Paul, C. B. Musgrave, Angew. *Chem. Int. Ed.,* **2007**, *46*, 8153-8156; g) V. S. Nguyen, M. H. Matus, D. J. Grant, M. T. Nguyen, D. A. Dixon, *J. Phys. Chem. A*, **2007**, *111*, 8844-8856.
17. See calculation results in Table S1 and S2 from the supporting information, also the experimental details.
18. J. H. Espenson, in *Chemical kinetics and reaction mechanisms*, *2nd ed*. McGRAW-HILL, Inc. **1995**, pp. 214-220, 225-228.
19. H. H. Limbach, Single and multiple hydrogen/deuterium transfer reactions in liquids and solids. In *Hydrogen Transfer Reactions*. J. T. Hynes, J. Klinman, H. H. Limbach, R. L. Schowen, Eds.; Wiley-VCH: Weinheim, Germany, **2007**; Vols. 1 & 2, Chapter 6, pp. 135-221, and references cited therein.
20. a) L. P. Hammett, *J. Am. Chem. Soc*. **1937**, *59*, 96-103; b) L.P. Hammett, *Chem. Rev*. **1935**, *17*, 125-136.

3.5 Supporting information

S1. General remarks:

All operations were carried out under an inert atmosphere of N_2 using Young Schlenk or Young NMR-tubes in a glove-box (Model MB-150B-G). All solvents (including deuterated solvents) were dried and deoxygenated employing appropriate drying / deoxygenating agents and then were freshly distillated under nitrogen before use (THF, toluene, hexane, pentane, ether, sodium / benzophenone). NMR spectra were recorded on the following spectrometers: Varian Gemini-200 instrument (^{1}H at 199.98 MHz and ^{13}C at 50.29 MHz), Varian Gemini-300 instrument (^{1}H at 300.1 MHz, ^{13}C at 75.4 MHz and ^{11}B at 64.15 MHz), Bruker DRX-500 instrument (^{1}H at 500.2 MHz and ^{13}C at 125.8 MHz). δ (^{1}H) and δ (^{13}C) relative to $SiMe_4$ and δ (^{11}B) relative to $Et_2O{\cdot}BF_3$. IR spectra were obtained using ATR on a Bio-rad FTS-45 instrument. Mass spectra were run on a Finnigan-MAT-8400 mass spectrometer.

S2. Synthesis of starting materials

a) Ammonia borane (**AB**) and deuterated **AB**'s:[s1] BD_3NH_3 (**AB(D)**) was prepared as follows: $NaBD_4$ (126.6 mg), $(NH_4)_2CO_3$ (325.8 mg) and dry THF (5 mL) were added to a Young-Schlenk tube. The mixture was then heated with stirring at 40 °C for 24 h. The resulting mixture was diluted with additional THF and filtered. The filtrate was evaporated and the prepared crude residual BD_3NH_3 was sublimed at 60 °C under vacuum for purification. **AB** can be prepared from $NaBH_4$ in the same way. BH_3ND_3 (**A(D)B**) was prepared by dissolving **AB** in D_2O and stripping off the D_2O under vacuum at room temperature, this procedure was repeated three times. BD_3ND_3 (**A(D)B(D)**) was prepared from **AB(D)** using this method. Formation of deuterated **AB**'s was confirmed by IR, ^{1}H-, ^{2}H- and ^{11}B NMR spectra.

b) Imines: Some of the imines (**1a**, **2a**, **3a**, **5a** and **6a**) were ordered from Aldrich or Fluka and used as delivered. Other imines were prepared by following literature procedures:[s2] The aldehyde (10 mmol) and the amine (10 mmol) were mixed

together in a Schlenk tube and stirred without solvent for 10 min, and then 20 mL of CH_2Cl_2 or toluene and 2 g 4 Å molecular sieve were added. The mixture was set to react at room temperature and monitored by NMR. When the reaction finished, the mixture was filtered, the solvent evaporated under reduced pressure. The crude products were recrystallized from hexane. All of the imines were usually white or pale yellow solids and were moved into the glove box soon after purification. Almost quantitative yields of these imines were obtained.

c) Cyclotriborazane (CTB):[s3] A Young Schlenk tube was charged with 5 mL of dry diethyl ether and then chilled with liquid nitrogen, 5 mmol (0.497 mL) of pure borazine was condensed on the top of the ether. The mixture was warmed to -80 ^oC and with continuous stirring 20 mL of 1 M HCl in diethyl ether was added. The reaction was stirred over night, then ether and excess HCl were pumped off and the solid residue was heated to 65 ^oC with pumping to remove all volatile compounds, leaving a white solid ($B_3N_3H_6 \cdot 3HCl$). 20 mL of dry diglyme was condensed onto the solid and all of the solid dissolved when warmed to room temperature. The Schlenk tube was chilled with liquid nitrogen again and 0.75 g of sodium borohydride added onto the frozen solution under N_2. The Schlenk tube was evacuated again and connected with a glass bridge to another Young Schlenk tube containing 20 mL of triethylamine to absorb the diborane. Then the mixture was warmed to room temperature with continuous stirring until the reaction completed. Decantation of the liquid from the white solid and then removal of the diglyme from the liquid left a white solid. Upon slow warming with continuous pumping a white solid began to sublime between 90 and 100 ^oC at pressures below one micron (mercury diffusion pump).

S3. Typical transfer hydrogenation procedure:

All of these reactions were carried out in duplicate, and the results reported here are the averages. The reactions were monitored by ^{11}B NMR and/or ^1H NMR until completion.

a) In a glove-box, a 0.5 mm Young NMR tube was charged with imine (0.1 mmol, for Pseudo-first order conditions 0.5 mmol), **AB** (0.1 mmol) and dry THF-D_8 (0.6 mL). The tube was sealed with the screw cap and then put into an oil bath (for kinetics the NMR instrument) preheated to 60 ^{o}C. The reaction was monitored by ^{1}H NMR every 30 min. (for kinetics every 5, 10 or 15 min.). The typical resonance of the starting material (-CH=N: singlet, δ 8.51 ppm) decreased, and a new signal of the saturated amine (-CH_2-NH: doublet, δ 4.29 ppm) gradually appeared. The disappearance of starting material indicates that the transformation has completed, then the NMR tube was cooled to room temperature and ^{13}C and ^{11}B NMR spectra were then recorded. The dehydrogenated products of **AB** were borazine (**BZ**), B-(cyclodiborazanyl)amino-borohydride (**BCDB**), cyclotriborazane (**CTB**) and polyborazylene (**PBZ**), which were identified by their typical chemical shift on ^{11}B NMR.

b) In a glove-box, a 50 mL Young Schlenk tube was charged with a magnetic stirring-bar, imine (0.5 mmol), **AB** (0.5 mmol) and dry THF (5 mL). After sealing with a screw cap, the tube was taken out from the glove-box to an oil bath preheated to 60 ^{o}C and stirred until the reaction was complete. THF was then removed under vacuum (also the **BZ**), and dry hexane (10 mL, 3 times) was used to extract the hydrogenated product from the residue. The product was pure to the detection limit of ^{1}H- and ^{13}C NMR.

S4. Typical spectra and kinetic charts.

a) ^{11}B NMR

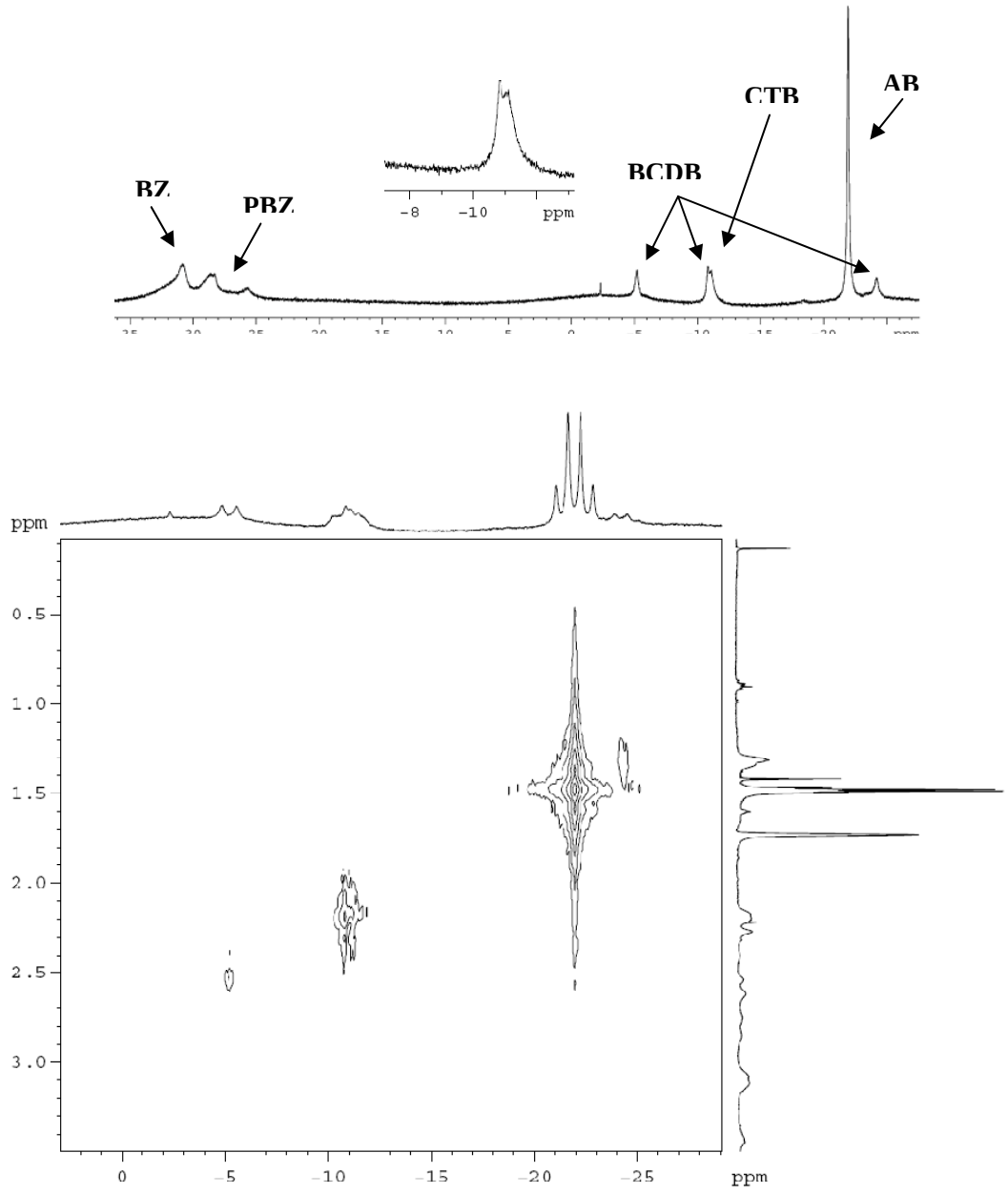

Figure S1. ^{11}B NMR of the reaction of 0.1 mmol **1a** with 0.1 mmol **AB** in THF-D_8 after 7 hours at 60 ^{o}C, recorded at room temperature; chemical shift relative to $Et_2O{\cdot}BF_3$. up: ^{1}H-decoupled ^{11}B NMR spectrum; down: ^{1}H-^{11}B HETCOR NMR spectrum, the horizontal spectrum is ^{11}B NMR with ^{1}H coupling and the vertical one is ^{1}H NMR with ^{11}B decoupled. The five boron compounds noted in the spectrum were assigned respectively in the analytic data (S6). (The given stoichiometry and reaction time did not allow the reaction to go to completion, when **1a** was in excess, signals for **AB**, **BCDB** and **CTB** completely disappeared from the spectrum after 2 days.)

b) Kinetics for reaction order

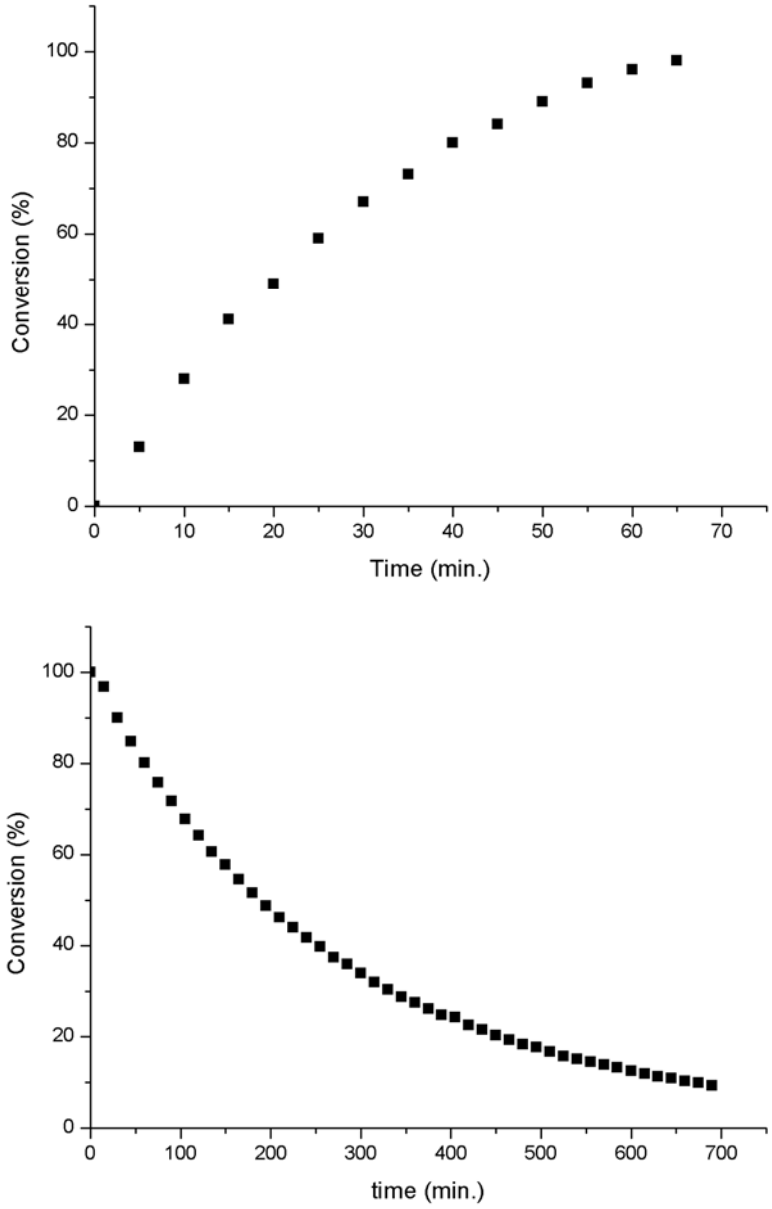

Figure S2. Kinetic conversion charts for reactions of the imine **1a** with **AB** in THF-D_8 at 60 ^{o}C. Top: 0.1 mmol **1a** with 0.5 mmol **AB**. The values were obtained by integration of **1b**/(**1a**+**1b**) in kinetic ^{1}H NMR experiments with 5 min intervals, $t_{3/4}$ / $t_{1/2}$ = 2188s / 1243s = 1.76 → reaction order = 1/2; Bottom: 0.5 mmol **1a** with 0.1 mmol **AB**, the values for **AB** were obtained from intensities of the ^{11}B NMR signals with 15 min intervals, $t_{3/4}$ / $t_{1/2}$ = 23044s / 11437s = 2.01 → reaction order = 1.

c) Compare of the reaction rate difference between **CTB** and **AB**

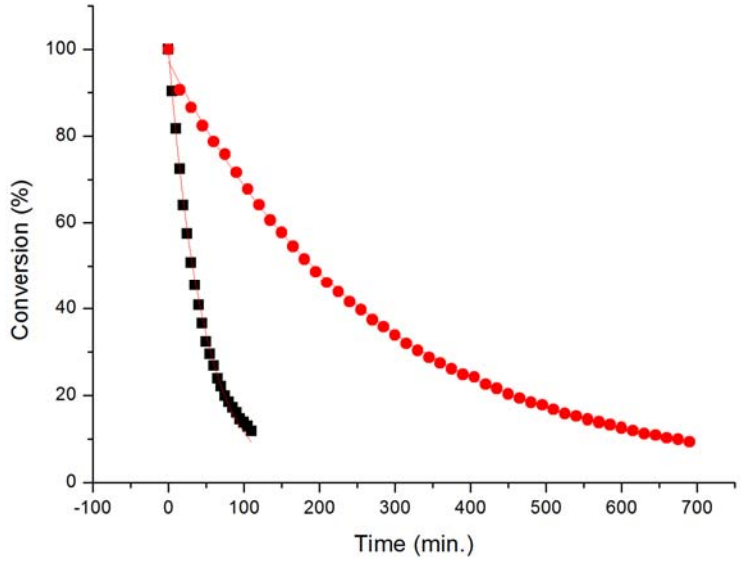

Figure S3. Kinetic conversion chart for reactions of 0.5 mmol **1a** with 0.1 mmol **CTB** (black squares, with 5 min interval) or **AB** (red circles, with 15 min interval) in THF-D_8 at 60 ^{o}C based on the intensities of the starting materials obtained from the ^{11}B NMR. The large excess of **1a** was taken to approach pseudo-first order conditions. After fitting with a 1st order curve, k_{CTB} / k_{AB} = 0.0215 / 0.0035 = 6.

d) Kinetics for the Hammett plot: ^{11}B NMR pursuits were carried out with 0.1 mmol of **AB** and 0.5 mmol of the imines in a Young NMR tube on a 300 MHz NMR machine, preheated to 60 ^{o}C. Conversion charts were formed based on the time-to-time intensity of **AB**, and all the curves were fitted to a 1st order reaction.

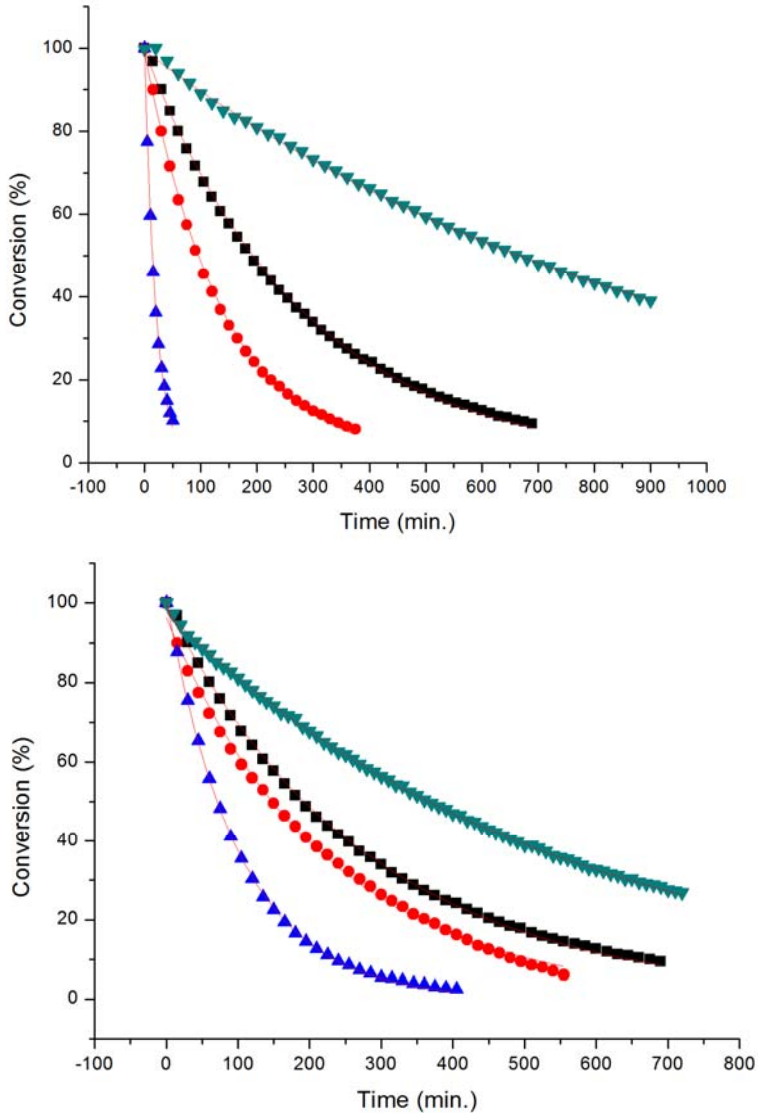

***Figure S4*:** Conversion charts for reactions of 0.1 mmol **AB** with 0.5 mmol *p*-substituted diaryl imines in THF-D_8 at 60 ^{o}C. The left chart stands for the reactions with the *p*-substitutent at the aniline side, and the right one for substitutions on the benzylidene side. Black squares for -H, red cycles for -Cl, green triangles for -OMe and blue ones for -NO_2 groups, respectively.

S5. Computational Details

Using Gaussian 03 package of program,[s4] the stationary points on the reaction paths were optimized and characterized to be minima or transition states by harmonic frequency analyses at the M05-2X/6-311++G** level. T. The M05-2X/6-311++G** harmonic frequencies were used to correct the enthalpies and free energies. Solvent

effects (THF was solvent in the experiment) were taken into account by the IEFPCM polarizable continuum solvent model. The IEFPCM calculations were carried out at the M05-2X/6-311++G** level with the M05-2X/6-311++G** gas phase geometries.

Table S1: Relative energies of the products for the stepwise reactions taking place via a PhCHNHPh intermediate.

PhCHNPh + BH_3NH_3 → PhCHNHPh$^+$ + $BH_3NH_2^-$	ΔH=45.2[a] (128.0)[b] kcal mol^{-1} ΔG=44.9 (126.2) kcal mol^{-1}
PhCHNPh + BH_3NH_3 → PhCHNHPH· + BH_3NH_2·	ΔH=63.4 (44.8) kcal mol^{-1} ΔG=62.0 (41.8) kcal mol^{-1}
PhCHNPh + BH_3NH_3 → PhCHNHPH$^-$ + $BH_2NH_3^+$	ΔH=67.6 (157.3) kcalmol^{-1} ΔG=65.9 (153.9) kcal mol^{-1}
PhCHNPh + BH_3NH_3 → PhCHNHPH$^+$ + $BH_2NH_3^-$	ΔH=119.4 (198.8) kcal mol^{-1} ΔG=119.0 (197.0) kcal mol^{-1}
PhCHNPh + BH^3NH_3 → PhCHNHPH· + BH_2NH_3·	ΔH=64.3 (54.0) kcal mol^{-1} ΔG=63.2 (51.5) kcal mol^{-1}
PhCHNPh + BH_3NH_3 → PhCHNHPH$^-$ + $BH_2NH_3^+$	ΔH=82.9 (157.4) kcal mol^{-1} ΔG=81.1 (154.0) kcal mol^{-1}

[a] At M05-2X(IEFPCM)/6-311++G**(IEFPCM) level. [b] The values in the parentheses are in the gas phase at M05-2X/6-311++G** level.

Table S2: Relative energies of the products for the stepwise reactions taking place via a PhCHNHPh intermediate.

PhCHNPh + BH_3NH_3 → PhCHHNPh$^+$ + $BH_3NH_2^-$	ΔH=159.9[a] (183.5)[b] kcal mol^{-1} ΔG=159.7 (181.7) kcal mol^{-1}
PhCHNPh + BH_3NH_3 →PhCHHNPh· + BH_3NH_2·	ΔH=65.7 (54.6) kcal mol^{-1} ΔG=65.8 (53.1) kcal mol^{-1}
PhCHNPh + BH_3NH_3 →PhCHHNPh$^-$ + $BH_3NH_2^+$	ΔH=117.3 (148.3) kcal mol^{-1} ΔG=116.3 (145.8) kcal mol^{-1}
PhCHNPh + BH_3NH_3 →PhCHHNPh$^+$ + $BH_2NH_3^-$	ΔH=230.7 (254.3) kcal mol^{-1} ΔG=230.4 (252.5) kcal mol^{-1}
PhCHNPh + BH_3NH_3 →PhCHHNPh· + BH_2NH_3·	ΔH=74.9 (63.8) kcal mol^{-1} ΔG=75.5 (62.8) kcal mol^{-1}
PhCHNPh + BH_3NH_3 →PhCHHNPh$^-$ + $BH_2NH_3^+$	ΔH=117.3 (148.3) kcal mol^{-1} ΔG=116.5 (145.9) kcal mol^{-1}

[a] At M05-2X(IEFPCM)/6-311++G** level. [b]The values in the parentheses are the energies in the gas phase at M05-2X/6-311++G** level.

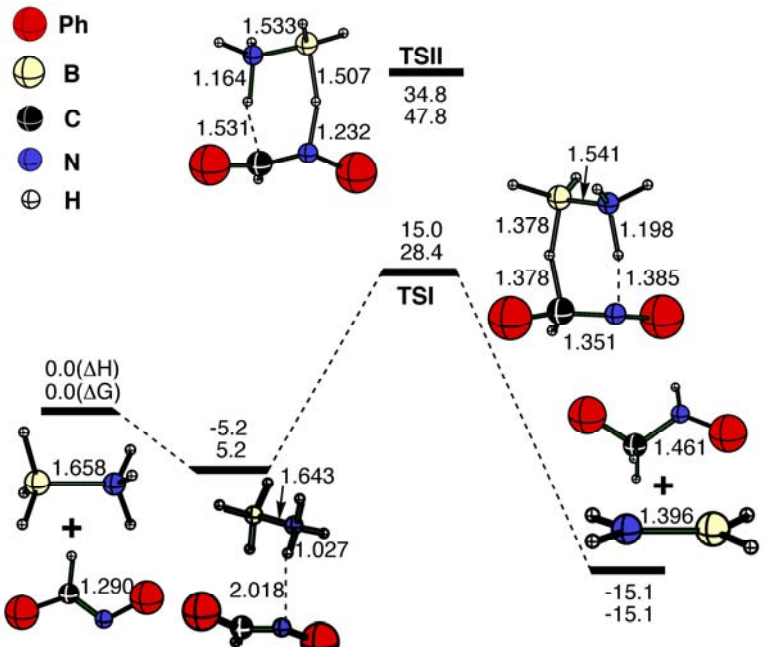

Scheme S1. MP2/6-311++G** geometric and energetic results for the concerted pathway of the reaction of **AB** with **1a** leading to **1b**. The ΔH and ΔG (in kcal mol^{-1}) values in THF solvent are corrected with the M05-2X/6-311++G** harmonic frequencies at 298 K and 1 atm condition.

S6. Analytical data:

N-benzylaniline (**1b**)[s5-9] 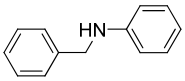

^{1}H NMR (THF-D_8): δ (ppm) 4.27-4.30 (d, *J* = 6 Hz, 2H), 5.32 (br, N-H), 6.50-6.59 (m, 3H), 6.99-7.38 (m, 7H); **^{13}C NMR** (THF-D_8): δ (ppm) 48.63, 113.36, 117.21, 127.58, 128.09, 129.18, 129.67, 141.45, 150.02.

N-benzylaniline(C-D) (**1b**) [s8] 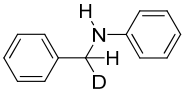

^{1}H NMR (THF-D_8): δ (ppm) 4.26-4.31 (t, *J* = 5 Hz, 1H), 5.28 (br, N-H), 6.49-6.57 (m, 3H), 6.99-7.36 (m, 7H); **^{2}H NMR** (THF-H_8): δ (ppm) 4.23 (d, *J* = 2 Hz, CHD); **^{13}C NMR** (THF-D_8): δ (ppm) 48.31 (t, *J* = 20 Hz), 113.34, 117.21, 127.59, 128.22, 129.18, 129.66, 141.42, 150.02; **MS** (m/z) = 184.

N-benzylaniline(N-D) (**1b**) [s8] 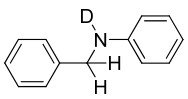

^{1}H NMR (THF-D_8): δ (ppm) 4.27 (s, 2H), 6.48-6.58 (m, 3H), 6.98-7.36 (m, 7H); **^{2}H NMR** (THF-H_8): δ (ppm) 5.29 (br, N-D); **^{13}C NMR** (THF-D_8): δ (ppm) 48.82, 113.67, 117.55, 127.65, 128.30, 129.20, 129.69, 141.23, 149.69; **MS** (m/z): 184.

N-benzylaniline(C-D,N-D) (**1b**) [s9] 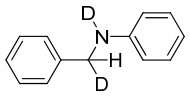

^{1}**H NMR** (THF-D_8): δ (ppm) 4.27 (s, 1H), 6.50-6.59 (m, 3H), 6.99-7.38 (m, 7H); ^{2}**H NMR** (THF-H_8): δ (ppm) 4.24 (d, *J* = 2 Hz, CHD), 5.28 (br, N-D); ^{13}**C NMR** (THF-D_8): δ (ppm) 48.47 (t, *J* = 20 Hz), 113.38, 117.24, 127.62, 128.25, 129.21, 129.69, 141.42, 150.04; **MS** (m/z): 185.

Dibenzylamine (**2b**)[s5-6,s10] 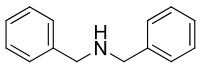

^{1}**H NMR** (THF-D_8): δ (ppm) 3.77 (s, 4H), 4.04 (br, N-H), 7.28-7.34 (m, 10H); ^{13}**C NMR** (THF-D_8): δ (ppm) 54.08, 127.45, 128.58, 128.96, 142.21; **MS** (m/z): 198.

N-benzyl-2-methylpropan-2-amine (**3b**)[s11-12] 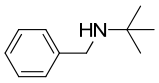

^{1}**H NMR** (THF-D_8): δ (ppm) 1.14 (s, 9H), 3.71-3.73 (d, *J* = 6 Hz, 2H), 7.10-7.36 (m, 5H); ^{13}**C NMR** (THF-D_8): δ (ppm) 29.60, 47.89, 51.01, 127.14, 128.78, 128.90, 143.49; **MS** (m/z): 164.

N-(cyclohexylmethyl)-2-methylpropan-2-amine (**4b**)[s13] 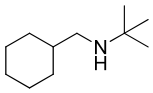

^{1}**H NMR** (THF-D_8): δ 1.03 (m, 9H), 1.19 (m, 5H), 1.69 (m, 1H), 2.37 (m, 2H), 4.56 (br, N-H); ^{13}**C NMR** (THF-D_8): δ 27.26, 27.89, 29.57, 32.60, 39.53, 40.60, 50.15, 50.45, 58.22; **MS** (m/z): 170.

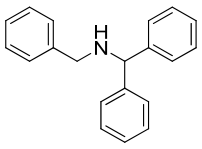

N-benzyl-1,1-diphenylmethanamine (**5b**)[s12]

^{1}**H NMR** (THF-D_8): δ 2.35 (br, N-H), 3.71 (d, *J* = 7 Hz, 2H), 4.87 (d, *J* = 4 Hz, 1H), 7.11-7.33 (m, 11H), 7.43-7.46 (m, 4H); ^{13}**C NMR** (THF-D_8): δ 50.84, 77.26, 125.71, 126.46, 126.63, 127.22, 127.44, 128.03, 129.68, 143.82, 159.71; **MS** (m/z): 272.

Diphenylmethanamine (**6b**)[s14] 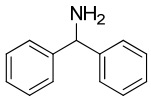

^{1}**H NMR** (THF-D_8): δ (ppm) 1.14 (s, 9H), 3.71-3.73 (d, *J* = 6 Hz, 2H), 7.10-7.36 (m, 5H); ^{13}**C NMR** (THF-D_8): δ (ppm) 60.94, 127.29, 127.87, 128.18, 147.32, 147.88; **MS** (m/z): 182.

N-(4-methoxybenzyl)aniline (**7b**)[s5-7] 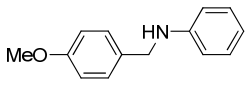

^{1}**H NMR** (THF-D_8): δ (ppm) 3.74 (s, 3H), 4.19-4.22 (d, *J* = 6 Hz, 2H), 5.19 (br, N-H), 6.49-6.59 (m, 3H), 6.82-6.86 (m, 2H), 6.99-7.06 (m, 2H), 7.24-7.29 (m, 2H); ^{13}**C NMR** (THF-D_8): δ (ppm) 48.12, 55.48, 113.37, 114.59, 117.13, 129.37, 129.64, 133.07, 150.06, 159.97; **MS** (m/z): 213.

N-(4-chlorobenzyl)aniline (**8b**)[s5-6,s15] 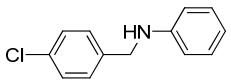

^{1}**H NMR** (THF-D_8): δ (ppm) 4.27-4.30 (d, *J* = 6 Hz, 2H), 5.41 (br, N-H), 6.50-6.57 (m, 3H), 6.98-7.07 (m, 2H), 7.24-7.37 (m, 4H); ^{13}**C NMR** (THF-D_8): δ (ppm) 47.81, 113.44, 117.44, 128.08, 129.67, 129.72, 133.10, 140.44, 149.71; **MS** (m/z): 217.

N-(4-nitrobenzyl)aniline (**9b**)[s5-7,s11,s15] 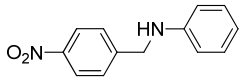

^{1}**H NMR** (THF-D_8): δ (ppm) 4.44-4.47 (d, *J* = 6 Hz, 2H), 5.62 (br, N-H), 6.52-6.57 (m, 3H), 7.00-7.08 (m, 2H), 7.57-7.61 (m, 2H), 8.14-8.19 (m, 2H); ^{13}**C NMR** (THF-D_8): δ (ppm) 47.87, 113.49, 117.76, 124.34, 128.78, 129.82, 148.15, 149.37, 149.79; **MS** (m/z): 228.

N-benzyl-4-methoxyaniline (**10b**)[s11] 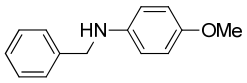

^{1}**H NMR** (THF-D_8): δ (ppm) 3.64 (s, 3H), 4.23-4.25 (d, *J* = 6 Hz, 2H), 4.92 (br, N-H), 6.50-6.55 (m, 2H), 6.65-6.69 (m, 2H), 7.17-7.37 (m, 4H); ^{13}**C NMR** (THF-D_8): δ (ppm) 49.52, 55.80, 114.39, 115.38, 127.50, 128.25, 129.13, 141.77, 144.22, 152.88; **MS** (m/z): 213.

N-benzyl-4-chloroaniline (**11b**)[s5] 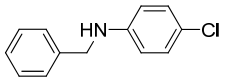

^{1}**H NMR** (THF-D_8): δ (ppm) 4.21-4.24 (d, *J* = 6 Hz, 2H), 5.06 (br, N-H), 6.45-6.50 (m, 2H), 6.96-7.00 (m, 2H), 7.16-7.36 (m, 4H); ^{13}**C NMR** (THF-D_8): δ (ppm) 48.56, 114.51, 121.53, 127.73, 128.18, 129.26, 129.54, 140.91, 148.75; **MS** (m/z): 217.

N-benzyl-4-nitroaniline (**12b**)[s5] 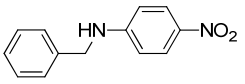

^{1}**H NMR** (THF-D_8): δ (ppm) 4.41-4.43 (d, *J* = 6 Hz, 2H), 6.61-6.65 (m, 2H), 6.75 (br, N-H), 7.20-7.34 (m, 5H), 7.97-8.02 (m, 2H); ^{13}**C NMR** (THF-D_8): δ (ppm) 46.83, 110.82, 125.65, 127.19, 128.38, 137.49, 138.50, 154.02; **MS** (m/z): 228.

N-(4-chlorobenzyl)-4-methoxyaniline (**13b**)[s16] 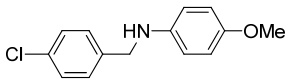

^{1}**H NMR** (THF-D_8): δ (ppm) 3.63 (s, 3H), 4.23 (d, *J* = 6 Hz, 2H), 5.00 (br, 1H), 6.47-6.50 (m, 2H), 6.64-6.67 (m, 2H), 7.22-7.35 (m, 4H); ^{13}**C NMR** (THF-D_8): δ (ppm) 48.72, 55.80, 114.61, 115.55, 129.40, 129.88, 133.21, 140.94, 144.06, 153.24; **MS** (m/z): 247.

4-chloro-N-(4-chlorobenzyl)aniline (**14b**)[s16-17] 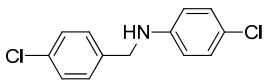

^{1}H NMR (THF-D_8): δ (ppm) 4.27-4.29 (d, *J* = 6 Hz, 2H), 5.62 (br, N-H), 6.50-6.55 (m, 2H), 7.00-7.04 (m, 2H), 7.26-7.36 (m, 4H); **^{13}C NMR** (THF-D_8): δ (ppm) 47.74, 114.46, 121.81, 129.37, 129.60, 133.29, 139.87, 148.46; **MS** (m/z): 251.

4-chloro-N-(4-methoxybenzyl)aniline (**15b**)[s17] 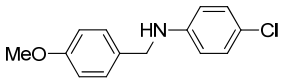

^{1}H NMR (THF-D_8): δ (ppm) 3.72 (s, 3H), 4.18 (d, *J* = 6 Hz, 2H), 5.42 (br, N-H), 6.51-6.54 (m, 2H), 6.82-6.85 (m, 2H), 6.99-7.02 (m, 2H), 7.22-7.25 (m, 2H); **^{13}C NMR** (THF-D_8): δ (ppm) 48.09, 55.49, 114.63, 114.79, 121.60, 129.53, 129.68, 132.71, 149.00, 160.29; **MS** (m/z): 247.

4-Methoxy-*N*-(4-methoxybenzyl)aniline (**16b**)[s7] 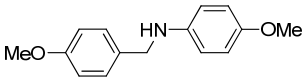

^{1}H NMR (THF-D_8): δ (ppm) 3.63 (s, 3H), 3.72 (s, 3H), 4.14-4.16 (d, *J* = 6 Hz, 2H), 4.77 (br, N-H), 6.50-6.54 (m, 2H), 6.64-6.67 (m, 2H), 6.81-6.85 (m, 2H), 7.23-7.26 (m, 2H); **^{13}C NMR** (THF-D_8): δ (ppm) 49.04, 55.47, 55.82, 114.53, 114.66, 115.49, 129.54, 133.58, 144.50, 153.05, 160.15; **MS** (m/z): 243.

BD_3NH_3 (**AB(D)**):[s1] **^{1}H NMR** (THF-D_8): δ (ppm) 3.84 (t, *J* = 48.5 Hz, NH_3); **^{2}H NMR** (THF-H_8): δ (ppm) 1.29 (br, B-D_3); **^{11}B NMR** (THF-D_8): δ (ppm) -22.5 (s, BD_3) ; **IR** (ATR): υ = 3307 (N-H), 2340 (B-H residue), 1741, 1657, 1376, 1292, 1095.

BH_3ND_3 (**A(D)B**):[s1] **^{1}H NMR** (THF-D_8): δ (ppm) 1.48 (q, *J* = 93Hz, BH_3); **^{2}H NMR** (THF-H_8): δ (ppm) 3.90 (s, N-D_3); **^{11}B NMR** (THF-D_8): δ (ppm) -22.5 (q, *J* = 95.1 Hz, BH_3); **IR** (ATR): υ = 3298 (N-H residue), 2474, 2304 (B-H), 2271, 2151, 1154, 1064.

BD_3ND_3 (**A(D)B(D)**):[s1] **^{2}H NMR** (THF-H_8): δ (ppm) 1.29 (br, B-D_3), 3.89 (s, N-D_3); **^{11}B NMR** (THF-D_8): δ (ppm) -22.5 (s, BD_3); **IR** (ATR): υ = 3289 (NH-residue), 2473, 2340 (BH-residue), 1714, 1165, 1064.

$(BH_2NH_2)_3$ (**CTB**):[s3,s18] **^{1}H NMR** (THF-D_8): δ (ppm) 2.27 (m, br, BH_2), 2.75 (t, *J* = 49Hz, NH_2); **^{11}B NMR** (THF-D_8): δ (ppm) -10.8 (t, *J* = 101 Hz, BH_2).

$BH_2(NH_2)_2BHNH_2BH_3$ (**BCDB**):[s18] **^{1}H NMR** (THF-D_8): δ (ppm) 1.31 (br, BH_3), 2.19 (br, BH_2), 2.55 (br, BH); **^{11}B NMR** (THF-D_8): δ (ppm) -24.2 (q, *J* = 95 Hz, BH_3), -11.3 (t, *J* = 100 Hz, BH_2), -5.4 (d, *J* = 115 Hz, BH).

$(BH{=}NH)_3$ (**BZ**):[s18] **^{1}H NMR** (THF-D_8): δ (ppm) 4.45 (br, q, *J* = 130Hz, BH), 6.37 (br, t, *J* = 53Hz, NH); **^{11}B NMR** (THF-D_8): δ (ppm) 30.1 (d, *J* = 133 Hz, BH).

Polyborazylene (**PBZ**):[s18] **^{11}B NMR** (THF-D_8): δ (ppm) 22~32 (br).

References:

[s1] a) M. G. Hu, J. M. Van Paasschen, R. A. Geanangel, *J. Inorg. Nucl. Chem.* **1977**, *39*, 2147-2150. b) G. H. Penner, Y. C. Phillis Chang, J. Hutzal, *Inorg. Chem.* **1999,** *38,* 2868-2873.

[s2] J. L. García Ruano, J. Alemán, I. Alonso, A. Parra, V. Marcos, J. Aguirre, *Chem. Eur. J.*, **2007**, *13*, 6179-6195.

[s3] a) G. H. Dah1, R. Schaeffer, *J. Am. Chem.* Soc., **1961**, *83*, 3032-3034; b) S. G. Shore, C. W. Hickam, *Inorg. Chem.,* **1963**, *2*, 638-640; c) K. W. Boddeker, S. G. Shore, R. K**.** Bunting, *J. Am. Chem.* Soc., **1966**, *88*, 4396-4401.

[s4] M. J. Frisch, G. W. Trucks, H. B. Schlegel, G. E. Scuseria, M. A. Robb, J. R. Cheeseman, J. A. Montgomery, Jr., T. Vreven, K. N. Kudin, J. C. Burant, J. M. Millam, S. S. Iyengar, J. Tomasi, V. Barone, B. Mennucci, M. Cossi, G. Scalmani, N. Rega, G. A. Petersson, H. Nakatsuji, M. Hada, M. Ehara, K. Toyota, R. Fukuda, J. Hasegawa, M. Ishida, T. Nakajima, Y. Honda, O. Kitao, H. Nakai, M. Klene, X. Li, J. E. Knox, H. P. Hratchian, J. B. Cross, C. Adamo, J. Jaramillo, R. Gomperts, R. E. Stratmann, O. Yazyev, A. J. Austin, R. Cammi, C. Pomelli, J. W. Ochterski, P. Y. Ayala, K. Morokuma, G. A. Voth, P. Salvador, J. J. Dannenberg, V. G. Zakrzewski, S. Dapprich, A. D. Daniels, M. C. Strain, O. Farkas, D. K. Malick, A. D. Rabuck, K. Raghavachari, J. B. Foresman, J. V. Ortiz, Q. Cui, A. G. Baboul, S. Clifford, J. Cioslowski, B. B. Stefanov, G. Liu, A. Liashenko, P. Piskorz, I. Komaromi, R. L. Martin, D. J. Fox, T. Keith, M. A. Al-Laham, C. Y. Peng, A. Nanayakkara, M. Challacombe, P. M. W. Gill, B. Johnson, W. Chen, M. W. Wong, C. Gonzalez, J. A. Pople, in *Gaussian 03 Revision E.01*, Gaussian Inc., Pittsburgh, PA, **2003**.

[s5] M. Tajbakhsh, M. M. Lakouraj, M. S. Mahalli, *Synth. Commun.* **2008**, *38*, 1976-1983.

[s6] K.-i. Fujita, Y. Enoki, R. Yamaguchi, *Tetrahedron* **2008**, *64*, 1943-1954.

[s7] R. Apodaca, W. Xiao, *Org. Lett.* **2001**, *3*, 1745-1748.

[s8] Y. Kayaki, H. Ikeda, J. Tsurumaki, I. Shimizu, A. Yamamoto, *Bull. Chem. Soc. Jpn*. **2008**, *81*, 1053–1061.

[s9] E. J. Roskamp, S. F. T. Pedersen, *J. Am. Chem. Soc.* **1987**, *109*, 6551-6553.

[s10] S. Cicchi, M. Bonanni, F. Cardona, J. Revuelta, A. Goti, *Org. Lett.* **2003**, *5*, 1773-1776.

[s11] B. T. Cho, S. K. Kang, *Tetrahedron*, **2005**, *61*, 5725-5734.

[s12] P. A. Chase, G.C. Welch, T. Jurca, D. W. Stephan, *Angew. Chem., Inter. Ed.*, **2007**, *46*, 8050-8053.

[s13] Z. Chen, Z. Chen, Y. Jiang, W. Hu, *Tetrahedron* **2005**, *61*, 1579-1586.

[s14] M. Ortega, M. A. Rodríguez, P. J. Campos, *Tetrahedron* **2005**, *61*, 11686-11691.

[s15] A. Heydari, S. Khaksar, M. Esfandyari, M. Tajbakhsh, *Tetrahedron* **2007**, *63*, 3363-3366.

[s16] K. Abiraj, B. Dinesh, G. R. Srinivasa, D. C. Gowda, *J. Chem. Research* **2006**, *8*, 534-535.

[s17] Y. Zhang, J. Jiang, *Huaxue Xuebao* **1987**, *45*, 103-106.

[s18] a) W. J. Shaw, J. C. Linehan, N. K. Szymczak, D. J. Heldebrant, C. Yonker, D. M. Camaioni, R. T. Baker, T. Autrey, *Angew. Chem. Int. Ed.* **2008**, *47*, 7493-7496; b) A. C. Stowe, W. J. Shaw, J. C. Linehan, B. Schmid, T. Autrey, *Phys. Chem. Chem. Phys.*, **2007**, *9*, 1831-1836.

S7. The Cartesian coordinates given by the M05-2X/6-311++G** optimizaitons and the energetic results, including the toal ZPE-corrected energies (E), enthaplies (H) and free energies (G). The gas phase harmonic frequencies were used for thermal and entropic corrections under the conditon of 298.15K and 1atm.

BH_3NH_3

E= -83.14244202 **H**= -83.13721502 **G**= -83.16551102 (in gas phase)
E= -83.15876042 **H**= -83.15398742 **G**= -83.18223842 (in THF)

B	0.000122	0.936616	0.000000
N	0.000122	-0.734180	0.000000
H	-1.168098	1.241149	0.000000
H	0.583677	1.242631	1.011517
H	0.583677	1.242631	-1.011517
H	-0.474311	-1.089510	-0.821185
H	0.947907	-1.091207	0.000000
H	-0.474311	-1.089510	0.821185

PhCH=NPh

E= -556.6179811 **H**= -556.6061271 **G**= -556.6566771 (in gas phase)
E= -556.6256778 **H**= -556.6138238 **G**= -556.6643738 (in THF)

C	0.381434	0.368298	-0.160004
H	0.050333	1.343670	-0.531960
N	-0.448886	-0.535673	0.160922
C	-1.823334	-0.238056	0.093635
C	-4.567539	0.243918	-0.066292
C	-2.678888	-1.207973	-0.430314
C	-2.356174	0.960736	0.572224
C	-3.722770	1.196496	0.489442
C	-4.039491	-0.959490	-0.524160
H	-2.253586	-2.142763	-0.767944
H	-1.703389	1.687289	1.037228
H	-4.128692	2.123532	0.871243
H	-4.692991	-1.710847	-0.945987
H	-5.630485	0.430280	-0.128113
C	1.835099	0.169062	-0.079149
C	4.595590	-0.160844	0.047801
C	2.375269	-1.031864	0.386238
C	2.685319	1.198867	-0.477670
C	4.063604	1.035628	-0.414477
C	3.749089	-1.193511	0.447345
H	1.700852	-1.819092	0.691776
H	2.264108	2.128692	-0.839687
H	4.718448	1.837539	-0.725530
H	4.166529	-2.123755	0.807575
H	5.667842	-0.292441	0.097235

BH_3NH_3_ PhCH=NPh_complex

E= -639.7732060 **H**= -639.7562080 **G**= -639.8183540 (in gas phase)
E= -639.7887912 **H**= -639.7717932 **G**= -639.8339392 (in THF)

C	0.338908	-0.507645	0.596820
H	0.015324	-0.367549	1.631580
N	-0.499950	-0.622786	-0.352941
C	-1.875346	-0.490683	-0.066491
C	-4.619391	-0.256864	0.376538
C	-2.366551	0.505152	0.781584
C	-2.767218	-1.346241	-0.714733
C	-4.129448	-1.238774	-0.479939
C	-3.735545	0.616245	0.997597
H	-1.678561	1.204328	1.239423
H	-2.370438	-2.094539	-1.386916
H	-4.812785	-1.916955	-0.972429
H	-4.109550	1.393526	1.649915
H	-5.682718	-0.167589	0.549356
C	1.786891	-0.544671	0.365308
C	4.536791	-0.520710	-0.041184
C	2.312162	-0.898735	-0.879126
C	2.645463	-0.190078	1.403336
C	4.018330	-0.173942	1.199933
C	3.682644	-0.886459	-1.079023
H	1.634491	-1.189121	-1.670009
H	2.232275	0.097940	2.361345
H	4.680573	0.115212	2.003690
H	4.090586	-1.163630	-2.041208
H	5.605947	-0.507602	-0.202649
B	0.722276	2.867700	-0.153825
N	-0.077544	2.166766	-1.416434
H	0.429362	4.039767	-0.197059
H	0.306591	2.322438	0.847306
H	1.894223	2.648827	-0.347094
H	-1.076827	2.326138	-1.345788
H	0.243086	2.555849	-2.294718
H	0.063364	1.157030	-1.433704

TSI

E= -639.7478717 **H**= -639.7329087 **G**= -639.7903357 (in gas phase)
E= -639.7595117 **H**= -639.7717932 **G**= -639.8339392 (in THF)

C	-0.393949	0.246966	-0.550904
H	-0.099420	0.601067	-1.539454
N	0.455756	-0.543914	0.126290

C	1.827747	-0.385208	-0.139511
C	4.605286	-0.183803	-0.502676
C	2.388857	0.745881	-0.745829
C	2.686599	-1.401186	0.300529
C	4.055293	-1.304141	0.117155
C	3.766005	0.835983	-0.927212
H	1.761689	1.568195	-1.060292
H	2.244577	-2.269571	0.770107
H	4.698545	-2.106178	0.453419
H	4.181598	1.716844	-1.397896
H	5.673743	-0.108662	-0.648459
C	-1.852624	-0.059861	-0.423788
C	-4.577709	-0.599974	-0.204515
C	-2.290495	-1.146202	0.325966
C	-2.785119	0.752930	-1.066101
C	-4.140773	0.484285	-0.960377
C	-3.651588	-1.412172	0.436529
H	-1.554459	-1.785272	0.792383
H	-2.442455	1.606920	-1.638270
H	-4.857667	1.119006	-1.462576
H	-3.986722	-2.261856	1.015837
H	-5.634961	-0.810767	-0.120701
B	-0.321534	2.174022	1.209640
N	0.157172	1.023341	2.116734
H	0.504940	3.015523	1.017261
H	-0.370266	1.527517	-0.017678
H	-1.469969	2.468615	1.354750
H	1.055073	1.191347	2.552869
H	-0.513771	0.753139	2.824253
H	0.301528	0.107046	1.399484

TSII

E= -639.7087984 **H**= -639.6935384 **G**= -639.7516314 (in gas phase)

E= -639.7223927 **H**= -639.7071327 **G**= -639.7652257 (in THF)

B	0.210772	2.803736	-0.170816
N	-0.769737	2.278658	-1.226131
C	-0.373478	-0.302804	-0.526743
H	-0.033929	-0.760612	-1.453283
N	0.518179	0.207964	0.332378
C	1.886397	-0.119410	0.188267
C	4.588649	-0.857828	0.090699
C	2.885071	0.793071	0.540632
C	2.257304	-1.408231	-0.205240

C	3.598941	-1.767398	-0.252762
C	4.218668	0.421927	0.493508
H	2.607385	1.793609	0.838284
H	1.492024	-2.135852	-0.432421
H	3.865670	-2.771492	-0.553817
H	4.976961	1.142650	0.767835
H	5.631351	-1.139551	0.049900
C	-1.765295	-0.459791	-0.122856
C	-4.480864	-0.620796	0.570278
C	-2.224798	0.064625	1.093729
C	-2.694152	-1.057628	-0.987962
C	-4.032539	-1.144001	-0.640509
C	-3.570188	-0.018144	1.430354
H	-1.511525	0.513038	1.771779
H	-2.352060	-1.463788	-1.932521
H	-4.731209	-1.621473	-1.314464
H	-3.907805	0.384816	2.376004
H	-5.525551	-0.688062	0.839724
H	-0.556711	2.557548	-2.175781
H	-0.705181	1.165361	-1.212591
H	-1.745343	2.472975	-1.025832
H	1.247546	3.176518	-0.628444
H	-0.308644	3.326464	0.767017
H	0.501774	1.481259	0.400597

BH_2NH_2

E= -81.99805464 **H**= -81.99388764 **G**= -82.02045264 (in gas phase)
E= -82.00134797 **H**= -81.99718097 **G**= -82.02374597 (in THF)

B	0.779389	0.000000	0.000003
N	-0.612573	0.000000	-0.000009
H	1.355246	-1.043003	-0.000004
H	1.355246	1.043003	0.000004
H	-1.159712	-0.842500	0.000026
H	-1.159710	0.842501	0.000017

$PhCH_2NHPh$

E= -557.8101088 **H**= -557.7976558 **G**= -557.8499738 (in gas phase)
E= -557.8281949 **H**= -557.8157419 **G**= -557.8680599 (in THF)

C	-0.438870	-0.785786	0.275108
N	0.433009	0.339700	-0.013123
C	1.812335	0.176928	-0.036460
C	4.614169	-0.044876	-0.049618
C	2.439904	-0.949134	0.505179
C	2.611361	1.187296	-0.591294
C	3.989638	1.073539	-0.597666
C	3.827882	-1.046796	0.498437
C	-1.881445	-0.370219	0.132081
C	-4.551230	0.411750	-0.115495
C	-2.364811	0.726900	0.845031
C	-2.745608	-1.067166	-0.705544
C	-4.076737	-0.681086	-0.827669
C	-3.691152	1.116187	0.721486
H	-0.258081	-1.110971	1.302735
H	1.855080	-1.750127	0.932347
H	2.135676	2.065492	-1.009613
H	4.583596	1.866261	-1.032338
H	4.292727	-1.925294	0.925361
H	5.691192	-0.130456	-0.054072
H	-1.691017	1.271996	1.493374
H	-2.375614	-1.915894	-1.266713
H	-4.738513	-1.231660	-1.482148
H	-4.056148	1.967466	1.279779
H	-5.584460	0.715487	-0.211312
H	-0.233623	-1.640254	-0.380838
H	0.075514	0.954830	-0.726170

Facile Metal Free Regioselective Transfer Hydrogenation of Polarized Olefins with Ammonia Borane

4.1 Introduction

Hydrogenation of double bonds is one of the most useful fundamental reactions in organic synthesis. Among the various methodologies developed, transfer hydrogenations have gained a prominent position in the field of homogenous hydrogenations.[1] Hydrogenations in form of 1,2-additions of H_2 to unsaturated compounds require a catalyst[2] and the use of H_2 gas needs special provisions for safety and proper reactivity due to low solubility of H_2 in many solvents. Transfer hydrogenations offer a viable alternative to hydrogenations with H_2. A number of compounds including alcohols and formic acid derivatives can be used as polar *in situ* hydrogen sources.[3]

Concerning the mechanism for transfer hydrogenations, they are commonly classified into two groups:[2] (a) direct hydrogen transfers from the hydrogen donor to the acceptor species, and (b) an indirect mechanism, by which the H atoms are transferred from the hydrogen donor to the acceptor through mediation by catalytic or non-catalytic centers.

A typical example for the first route is the aluminum complex catalyzed Meerwein-Ponndorf-Verley reduction of carbonyl substrates to alcohols, which was proposed to occur through a six-membered transition state including the Lewis acidic centers.[4] The second type, often also called bifunctional catalysis, is the preferred mechanism for metal catalyzed hydrogen transfers, where a metal hydride intermediate and a protic site are formed prior to the double H transfer to the hydrogen acceptor. The widely applied Noyori and Shvo type transfer hydrogenations are of this type.[5] However, double H transfers *via* the elementary process of direct transfer without the presence of a metal center are rare.[6]

We recently approached metal free transfer hydrogenation of imines with ammonia borane (BH_3NH_3, **AB**) as the hydrogen donor.[7] By various mechanistic studies it was proven to involve a concerted double H transfer. Herein, we will report another direct H transfer reaction with **AB** as hydrogen donor, applying polarized olefins as hydrogen acceptors and study the H transfer mechanism in detail.

4.2 Results and discussions

2-Cyclohexylidenemalononitrile (**1a**) was used first to test the reaction conditions. It was surprising to see that the 1:1 hydrogen transfer from **AB** to **1a** can be completed within 10 min in THF at room temperature and at 10 ^oC in less than 1 h, with **2a** as the only hydrogenated product and borazine ($(BHNH)_3$, **BZ**) as the by far predominant dehydrocoupling product (a small amount of polyborazine and cyclotriborazane were also observed).[8] When the solvent was changed to acetonitrile, 1 h was required to complete the hydrogenation at room temperature. Benzene and chloroform were also tried: in both cases, the reactions were slow presumably due to poor solubility of **AB** in these solvents, but the rate was much faster in the less polar solvent benzene (20 h) than in chloroform (more than 3 days). Considering that 10 min is too fast for proper pursuit of the reaction course at room temperature, acetonitrile was selected for the model studies.

To test the chemical scope of this reaction, a series of polarized olefins with two electron-withdrawing (EWD) groups on one side of the double bond and on the other side with H, alkyl or aryl substituents (**1a-1k**) were applied in the reaction with **AB** in acetonitrile at room temperature. High yields in the hydrogenated products were achieved (Table 4.1).

The required time for completion of the reactions varied from several minutes to several days. Comparing the reaction times of different olefins, it was found that alkyl groups accelerate the hydrogen transfers, since the required times for the olefins **1a-1e** were less than those for **1f-1h** (Table 4.1, entries 1-8). Comparing the effect of the

ester substituent with the stronger EWD group CN, the latter seemed to active the olefin more (entries 1 to 2 and 9 to 11). Hydrogen substituents also accelerated the reaction rates presumably imposing less steric hindrance on the reactants (entries 6, 7 and 9).

Table 4.1 Transfer hydrogenation reactions of various polarized olefins with **AB**.[a]

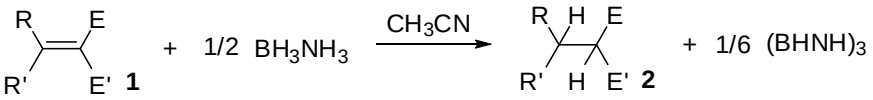

Entry	Olefin		Temperature	Time	Yield (%)[b]
1	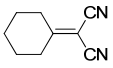	**1a**	r.t.	1 h	> 99 (86)
2	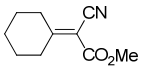	**1b**	r.t.	2 h	> 99
3	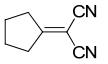	**1c**	r.t.	5 h	> 99
4	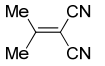	**1d**	r.t.	4 h	> 99
5	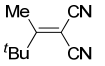	**1e**	r.t.	1 h	> 99
6	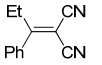	**1f**	r.t.	6 h	> 99
7	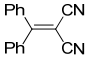	**1g**	r.t. 60 °C	5 d 6h	92 > 99
8	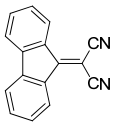	**1h**	r.t. 60 °C	2 d 0.5	98 > 99 (93)
9	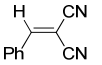	**1i**	r.t.	10 min	> 99 (90)
10	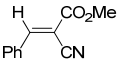	**1j**	r.t.	0.5 h	> 99
11	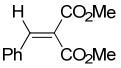	**1k**	r.t.	3d	98

[a] Reactions in acetonitrile with a 1:1 molar ratio of 0.1 mmol olefin to **AB**; [b] reactions pursued by ^{1}H NMR and the yields were established by GC-MS based on the amount of olefins, in brackets were the isolated yields with a 1 mmol scale, all reactions were carried out at least twice to ensure the results as reported.

To ensure the transfer hydrogenation to proceed with 'polarity-match' of the hydrogen donor and the acceptor, reactions of three different olefins (**1a, 1h** and **1i**)

with selectively deuterated **AB** adducts (BD_3NH_3 (**AB(D)**) and BH_3ND_3 (**A(D)B**)) were carried out. The reactions were pursued by *in situ* ^{1}H, ^{2}H and ^{13}C NMR spectroscopies, and only the expected regio-orientation of the deuterated products were observed for the given cases (Scheme 4.1). This confirmed regiospecificity in the hydrogen transfer processes. The possibility of radical involvement in the reaction course seemed less probable.

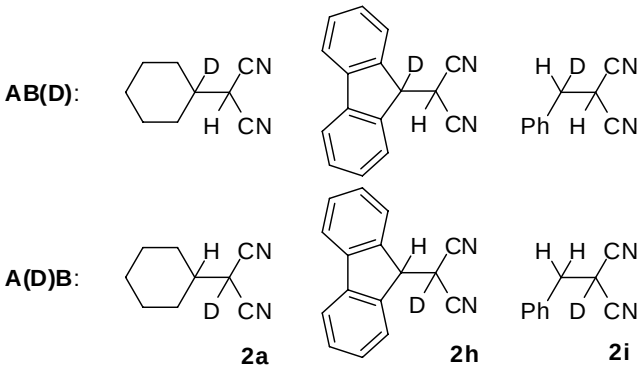

Scheme 4.1 Regio-specific hydrogenation products

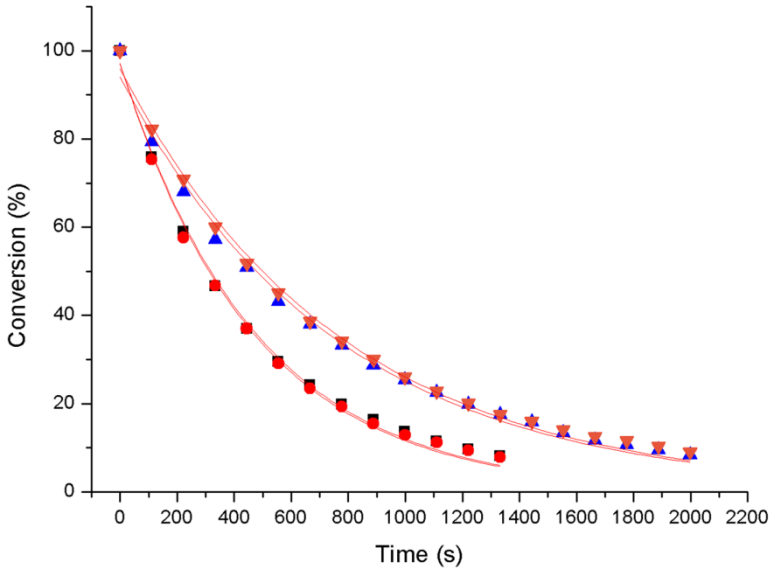

Figure 4.1 Conversion chart of the reaction of 0.5 mmol **1a** with 0.1 mmol **AB**, **AB(D)**, **A(D)B** or **A(D)B(D)** pursued by ^{11}B NMR in CH_3CN at r.t., derived from the intensities of **AB** of the ^{11}B NMR spectra with 2 min intervals. The black squares stand for reactions with **AB**, red circles for **AB(D)**, blue triangles for **A(D)B** and orange triangles for **A(D)B(D)**. Simulated reaction half-life times were: $t_{1/2}$(**AB**) = 309 s, $t_{1/2}$(**AB(D)**) = 308 s, $t_{1/2}$(**A(D)B**) = 480 s, $t_{1/2}$(**A(D)B(D)**) = 499 s. For first order reactions, the reaction constant $k = 0.693/t_{1/2}$,[9] thus: $k_{AB}/k_{AB(D)} = t_{1/2}(AB(D))/t_{1/2}(AB) = 1.00$, $k_{AB}/k_{A(D)B} = 1.55$, $k_{AB}/k_{A(D)B(D)} = 1.61$.

In addition to these dueterium labelling studies, the primary deuterium kinetic isotope effect (DKIE) was also investigated in reactions with **1a**. According to the kinetic conversion chart of Figure 4.1, which is based on ^{11}B NMR experiments, the rate constants (k) were simulated with a first order equation to obtain the DKIE values. In our former study on the hydrogen transfer from **AB** to imines, an inverse DKIE was observed with **AB(D)** and a normal DKIE with **A(D)B** indicating that in this case the cleavage of both H_B and H_N are involved in the rate determining step (RDS).[7] However, using the push-pull olefin **1a** as hydrogen-acceptor, a DKIE could not be observed with **AB(D)** (see Figure 4.1, $k_{\mathbf{AB}}/k_{\mathbf{AB(D)}} = 1$). Assuming that any H_B transfer in the RDS would cause some kind of DKIE $\neq 1$, a DKIE of 1 is expected to indicate that the double H transfer is stepwise and the H_B transfer being fast occurring before or after the RDS.[9]

For the reaction of **1a** with **A(D)B**, a normal DKIE of 1.55 was obtained, indicating the participation of the breakage of the N-H bond in the RDS. For BD_3ND_3 (**A(D)B(D)**), the DKIE value was 1.61. This further addresses the fact that the H_N transfer is rate determining regardless of H_B or D_B in the neighborhood.

Since the reaction of a 1:1 molar mixture of **AB** and **1a** in THF was very fast at room temperature, a NMR sample with **1a** in excess (**AB** to **1a** 1:3) was prepared at low temperature in THF-D_8 and kept at -40 ^oC. A set of new signals appeared in the NMR (Figure 4.2, spectrum c), which apparently belong to a reaction intermediate (**3a**), since they disappeared with increasing temperature and prolonged reaction times.

Based on ^1H, ^{13}C NMR and DEPT (THF-D_8, -40 ^oC), the intermediate **3a** is a hydrogenation product formed *via* 1,2-addition of a B-H bond across the olefinic double bond, while the boron substituent went to the cyano substituted side; the C_{CN} atom is thus characterized by a very broad signal at ^{13}C NMR due to the quadrapolar broadening influence of the ^{11}B nucleus (Figure 4.2). The newly formed $-BH_2NH_3$ unit with a 4-coordinate boron showing a broad triplet at -14 ppm in the ^{11}B NMR

(different from cyclotriborazane which should be a sharp triplet at -11 ppm in the ^{11}B NMR). A new broad signal also developed at 5.15 ppm in the ^{1}H NMR, having no ^{11}B correlation, no (or invisible) NOE nor long range correlations to other ^{1}H or ^{13}C NMR signals indicating that this signal belongs to the H_N nuclei of **3a**. Given enough time at low temperature, the intensities of the signals for **3a** will increase until the signal of **AB** had completely disappeared from the ^{11}B NMR spectrum, while the signals of **2a** also started to grown in. The same experiment was also carried out in acetonitrile leading to similar observations but at lower rate.

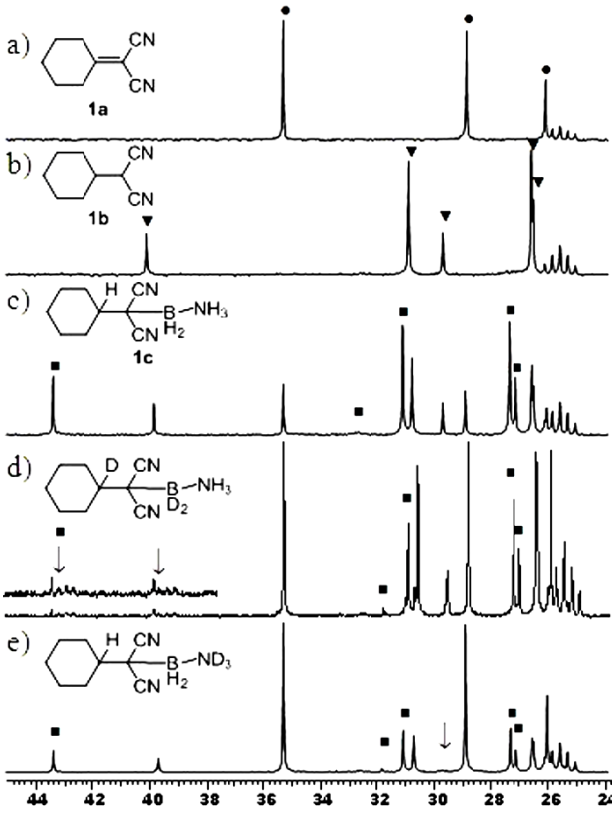

Figure 4.2 Selected ^{13}C NMR spectra (range of 24 to 45 ppm) in THF-D_8: a) pure **1a**, labeled with circles ●; b) pure **2a**, labeled with triangles ▼; c) *in situ* spectrum for the reaction of **1a** with **AB** (2/1 molar ratio) at -40 °C: five new reasonances from **3a** appeared (labeled with squares ■) - including a broad signal; d) *in situ* spectrum for the reaction of **1a** with **AB(D)** at -40 °C: two triplets belonging to C_D ($^{1}J_{DC}$ = 20 Hz) appeared as labeled with arrows ↓, and the broad resonance became sharper; e) *in situ* spectrum for the reaction of **1a** with **A(D)B** at -40 °C: only one triplet of **2a** appeared.

From the related reactions of **1a** with **AB(D)** and **A(D)B** at -40 °C, ^{1}H, ^{13}C and

^{11}B NMR spectra were taken. Comparing the ^{13}C NMR spectra with that of the reaction of **1a** with **AB**, it can clearly be seen that the H_B (or D_B) atom was in the intermediate already transferred, while the H_N (or D_N) atom was not, since a triplet due to C-D coupling ($^1J_{DC}$ = 20 Hz) was exclusively observed for the intermediate only when **AB(D)** was used (Figure 4.2, spectrum d).

Based on all these mechanistic facts, a two-step hydrogen transfer mechanism is proposed with fast initial hydroboration forming intermediate **3** (Scheme 4.2).[10] There are two possible routes to **3**, the ionic pathway A and the concerted pathway B. Considering the solvent effect and compare THF with acetonitrile, the ionic pathway A is expected to work better in the more polar solvent acetonitrile, while the concerted route B seems to be in operation in less polar solvents THF. Since the reaction proceeds much faster in THF than in acetonitrile, route B seems more reasonable. The RDS is the transfer of the H_N atom of **AB**, which could be transferred *via* an intra-molecular mode as shown in **4** of Scheme 4.2, followed by the elimination of the very reactive [BH_2NH_2], which will be rapidly further dehydrogenated to **BZ** presumably in a similar manner as the reaction of **1** with **AB**.

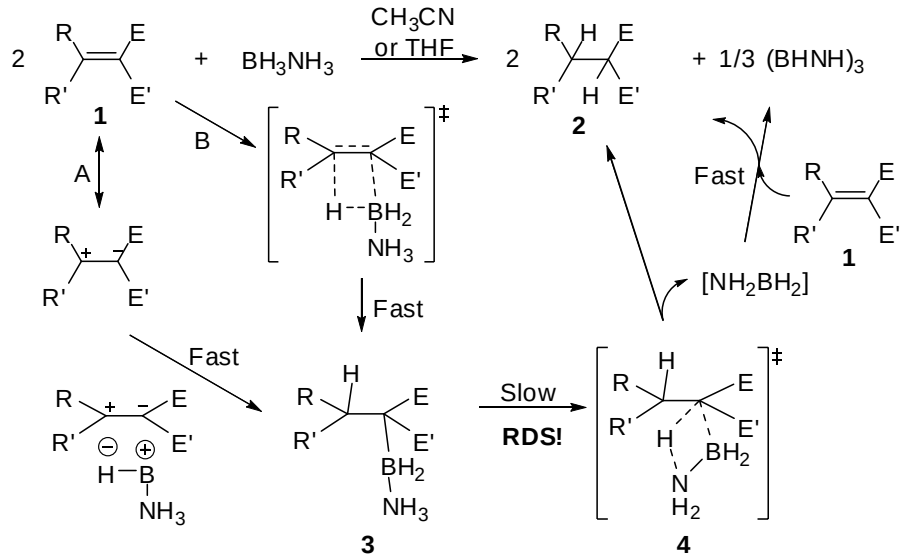

Scheme 4.2 Proposed reaction mechamism

4.3 Conclusions

In summary, we have demonstrated a very efficient metal free transfer hydrogenation of polarized olefins substituted with EWD groups on one side of the double bond with **AB** at room temperature. Deuterium labelling studies confirmed the regiospecificity in the H transfer processes. The DKIE demonstrated that only the H_N transfers get involved in the RDS, and the structure of the hydroboration intermediate clearly indicated that H_B transfer occurs before the H_N transfer. Thus, this double-H transfer can be defined as stepwise and in a polar terminology with hydride before proton transfer.

We gratefully thank the Swiss National Science Foundation and the University of Zurich for financial support.

4.4 References

[1] D. Klomp, U. Hanefeld and J. A. Peeters, in *Handbook of Homogeneous Hydrogenation,* Ed. J. G. De Vries and C. J. Elsevier, Wiley-VCH, Weinheim, Germany, 2007; S. Gladiali and E. Alberico, *Chem. Soc. Rev*. **2006**, *35*, 226-236; J. S. M. Samec, J.-E. Bäkvall, P. G. Andersson and P. Brandt, *Chem. Soc. Rev*. **2006**, *35*, 237-248.

[2] H. Berke, *ChemPhysChem*, **2010**, *11*, 1837-1849; A. Comas-Vives, G. Ujaque and A. Lledós, *J. Mol. Struc.: THEOCHEM*. **2009**, *903*, 123-132.

[3] M. Trincado, H. Grutzmacher, F. Vizza, C. Bianchini, *Chem. Eur. J*., **2010**, *16*, 2751-2757; Z. Shen, Y. Zhang, F. Jin, X. Zhou, A. Kishita and K. Tohji, *Ind. Eng. Chem. Res*. **2010**, *49*, 6255-6259; Z. S. Liu and G. L. Rempel, *Chem. Engin. J*. **2009**, *147*, 366-372.

[4] H. Meerwein and R. Schmidt, *Justus Liebigs Ann. Chem.* **1925**, *444*, 221-228; W. Ponndorf, *Angew. Chem.* **1926**, *39*, 138-143; Verley, *Bull. Soc. Chim. Fr.* **1925**, *37*, 871-874.

[5] R. Noyori, T. Okhuma, M. Kitamura, H. Takaya, N. Sayo, H. Kumobayashi and S. Akuragawa, *J. Am. Chem. Soc.* **1987**, *109*, 5856-5858; R. Noyori, in *Asymmetric Catalysis In Organic Synthesis*. Wiley-Interscience. John Wiley & Sons, New York, 1994, pp. 16-94; Y. Blum, D. Czarkie, Y. Rahamim and Y. Shvo, *Organometallics* **1985**, *4*, 1459-1461; Y. Shvo, D. Czarkie, Y. Rahamim and D. F. Chodosh, *J. Am. Chem. Soc.* **1986**, *108*, 7400-7402 and references cited therein.

[6] A review on uncatalyzed transfer hydrogenation reactions: C. Rüchardt, M. Gerst and J. Ebenhoch, *Angew. Chem., Int. Ed.* **1997**, *36*, 1406-1430.

[7] X. Yang, L. Zhao, T. Fox, Z.-X. Wang and H. Berke, *Angew. Chem., Int. Ed.* **2010**, *49*, 2058-2062.

[8] For reactions on amine-borane adducts see: A. Staubitz, A. P. M. Robertson and I. Manners, *Chem. Rev.* **2010**, *110*, 4079-4124; A. Staubitz, A. P. M. Robertson, M. E. Sloan and I. Manners, *Chem. Rev.* **2010**, *110*, 4023-4078.

[9] J. H. Espenson, in *Chemical kinetics and reaction mechanisms*, *2nd edn*. McGRAW-HILL, Inc. 1995, pp. 214-228; H. H. Limbach, In *Hydrogen Transfer Reactions*. Ed. J. T. Hynes, J. Klinman, H. H. Limbach and R. L. Schowen, Wiley-VCH: Weinheim, Germany, 2007; Vols. 1 & 2, Chapter 6.

[10] P. M. Zimmerman, A. Paul, Z. Zhang, C. B. Musgrave, Angew. *Chem. Int. Ed.,* **2009**, *48*, 2201-2205; W. J. Shaw, J. C. Linehan, N. K. Szymczak, D. J. Heldebrant, C. Yonker, D. M. Camaioni, R. T. Baker and T. Autrey, *Angew. Chem. Int. Ed.* **2008**, *47*, 7493-7496; X. Yang, M. B. Hall, *J. Am. Chem. Soc.,* **2008**, *130*, 1798-1799; V. Pons, R. T. Baker, N. K. Szymczak, D. J. Heldebrant, J. C. Linehan, M. H. Matus, D. J. Grant, D. A. Dixon, *Chem. Commun.* **2008**, 6597- 6599.

4.5 Supplementary material

S1 General procedure: All the manipulations were carried out under a nitrogen atmosphere using Schlenk techniques or in a drybox (Model MB-150B-G). Reagent grade benzene, toluene, hexane, diethyl ether, and tetrahydrofuran were dried and distilled from sodium benzophenone ketyl prior to use. Acetonitrile was distilled from CaH_2, and chloroform was dried by P_2O_5. NMR spectra were measured on a Varian Mercury spectrometer at 200 MHz for ^1H and 50.3 MHz for $^{13}C\{^1H\}$, Varian Gemini-2000 spectrometer at 300.1 MHz for ^1H, 64.2 MHz for $^{11}B\{^1H\}$ and 75.4 MHz for $^{13}C\{^1H\}$ and on a Bruker-DRX-500 spectrometer at 500.2 MHz for ^1H, 107 MHz for $^{11}B\{^1H\}$ and 125.8 MHz for $^{13}C\{^1H\}$. Chemical shifts for ^1H and ^{13}C are given in ppm relative to TMS and those for ^{11}B relative to $Et_2O{\cdot}BF_3$.

S2 Synthesis of starting materials.

a) Ammonia borane (AB) and deuterated AB's:[1]

BD_3NH_3: $NaBD_4$ (126.6 mg), $(NH_4)_2CO_3$ (325.8 mg) and dry THF (5 mL) were added to a Young-Schlenk tube. The mixture was then heated with stirring at 40 °C for 24 h. The resulting mixture was diluted with additional THF and filtered. The filtrate was evaporated and the prepared crude BD_3NH_3 was sublimed at 60 °C under vacuum for purification. **AB** can be prepared from $NaBH_4$ in the same way. BH_3ND_3 was prepared by dissolving **AB** in D_2O and stripping off the D_2O under vacuum at room temperature, this procedure was repeated three times. BD_3ND_3 was prepared from BD_3NH_3 using this method. Formation of deuterated **AB** adducts were confirmed by IR, ^1H, ^2H and ^{11}B NMR spectra.

BD_3NH_3: δ_H (ppm; 300 MHz; THF-D_8) 3.84 (t, J = 48.5 Hz, NH_3); δ_D (ppm; THF) 1.29 (br, B-D_3); δ_B (ppm; 64.2 MHz; THF-D_8) -22.5 (s, BD_3) ; **IR** (ATR): υ = 3307 (N-H), 2340 (B-H residue), 1741, 1657, 1376, 1292, 1095.

BH_3ND_3: δ_H (ppm; 300 MHz; THF-D_8) 1.48 (q, J = 93Hz, BH_3); δ_D (ppm; THF) 3.90 (s, N-D_3); δ_B (ppm; 64.2 MHz; THF-D_8) -22.5 (q, J = 95.1 Hz, BH_3); **IR** (ATR): υ = 3298 (N-H residue), 2474, 2304 (B-H), 2271, 2151, 1154, 1064.

BD_3ND_3: δ_D (ppm; THF) 1.29 (br, B-D_3), 3.89 (s, N-D_3); δ_B (ppm; 64.2 MHz; THF-D_8) -22.5 (s, BD_3); **IR** (ATR): υ = 3289 (NH-residue), 2473, 2340 (BH-residue), 1714, 1165, 1064.

b) Preparation of polarized olefins:

All the polarized olefins were prepared with readily available materials.

Procedure A:[2] A ketone (0.1 mol), malononitrile (0.2 mol), ammonium acetate (1.5 g), acetic acid (4.8 g) and benzene (30 mL) are refluxed with a Dean-Stark trap over night or until water production ceases (> 6 h). The mixture was then washed with water (3 x 30 mL) and half saturated aqueous sodium chloride (1 x 30 mL) and then dried with magnesium sulfate. Then benzene was removed and the remaining liquid distilled under reduced pressure (for solid recrystallization). Olefins **1a-1f** were obtained with 50-70% yield use this method.

2-Cyclohexylidenemalononitrile (**1a**), colorless liquid: δ_H (ppm; 300 MHz; THF-D_8) 1.63-1.74 (m, 2 H, -CH_2-), 1.74-1.87 (m, 4 H, -CH_2-), 2.62-2.75 (m, 4 H, -CH_2-); δ_C (ppm; 75.4 MHz; THF-D_8) 24.83, 27.52, 34.14, 82.61 (1 C, -C=), 112.03 (2 C, -CN), 183.89(1 C, -C=).

Methyl 2-cyano-2-cyclohexylideneacetate (**1b**), colorless liquid: δ_H (ppm; 300 MHz; CD_3CN) 1.57-1.83 (m, 6 H, -CH_2-), 2.59-2.65 (m, 2 H, -CH_2-), 2.91-2.97 (m, 2 H, -CH_2-), 3.76 (s, 3H, -Me); δ_C (ppm; 75.4 MHz; CD_3CN) 26.20, 28.98, 29.30, 32.22, 37.51, 53.13, 102.15 (1 C, -C=), 116.53 (1 C, -CN), 163.41 (1 C, -C=O), 181.63 (1 C, -C=).

2-Cyclopentylidenemalononitrile (**1c**), colorless liquid: δ_H (ppm; 300 MHz; THF-D_8) 1.86-1.95 (m, 4 H, -CH_2-), 2.75-2.87 (m, 4 H, -CH_2-); δ_C (ppm; 75.4 MHz; C_6D_6) 25.61, 35.44, 81.25 (1 C, -C=), 112.21 (2 C, -CN), 191.71 (1 C, -C=).

2-(Propan-2-ylidene)malononitrile (**1d**), colorless liquid: δ_H (ppm; 300 MHz; THF-D_8) 2.30 (s, 6H, -Me); δ_C (ppm; 75.4 MHz; C_6D_6) 23.34, 86.09 (1 C, -C=), 112.22 (2 C, -CN), 178.01 (1 C, -C=).

2-(3,3-Dimethylbutan-2-ylidene)malononitrile (**1e**), colorless liquid: δ_H (ppm; 300 MHz; CD_3CN) 1.33 (s, 9 H, -Me), 2.29 (s, 3 H, Me); δ_C (ppm; 75.4 MHz; CD_3CN) 23.27, 28.88, 40.14, 84.80 (1 C, -C=), 114.51 (1 C, -CN), 114.74 (1 C, -CN), 191.59

(1 C, -C=).

2-(1-Phenylpropylidene)malononitrile (**1f**), white solid: δ_H (ppm; 300 MHz; CD_3CN) 1.01 (t, *J* = 7 Hz, 3 H, -Me), 2.96 (q, *J* = 7 Hz, 2 H, $-CH_2-$), 7.47-7.48 (m, 5 H, -CH=); δ_C (ppm; 75.4 MHz; CD_3CN) 12.65, 31.95, 85.26 (1 C, -C=), 113.65 (1 C, -CN), 114.12 (1 C, -CN), 128.53, 129.92, 132.60, 136.03, 183.11 (1 C, -C=).

Procedure B:[3] To a stirred solution of 0.01 mol of aldehyde in 0.01 mol of malononitrile (or methylcyanoacetate) was added 3 g of alumina Merck 90. The reaction was exothermic. After 5 min, the product was extracted with dichloromethane (2 x 20 ml). The solvent was then removed, leaving a product of a good purity. Generally, the purification was not necessary. Olefin **1i** and **1j** were prepared by this method with nearly 100% yield.

2-Benzylidenemalononitrile (**1i**), slightly pink solid: δ_H (ppm; 300 MHz; CD_3CN) 7.53-7.67 (m, 3 H, -CH=), 7.90 (m, 2 H, -CH=), 8.05 (s, 1 H, -CH=); δ_C (ppm; 75.4 MHz; CD_3CN) 83.34 (1 C, -C=), 113.95 (1 C, -CN), 115.01 (1 C, -CN), 130.47, 131.47, 132.27, 135.28, 161.89 (1 C, -C=).

(E)-Methyl 2-cyano-3-phenylacrylate (**1j**), white solid: δ_H (ppm; 300 MHz; C_6D_6) 3.29 (s, 3 H, -Me), 6.85-6.93 (m, 3 H, -CH=), 7.58-7.61 (m, 2 H, -CH=), 7.94 (s, 1 H, -CH=); δ_C (ppm; 75.4 MHz; C_6D_6) 52.65, 103.20 (1 C, -C=), 115.59 (1 C, -CN), 129.10, 131.07, 131.77, 132.91, 154.56 (1 C, -C=O), 162.75 (1 C, -C=).

Other olefins were prepared using various other methods, respectively.

2-(Diphenylmethylene)malononitrile (**1g**):[4] A 1 : 1 mixture of molononitrile and diphenyl-methanimine was stirred without solvent at room temperature for 5 minutes giving the target product with nearly 100% yield. White solid: δ_H (ppm; 300 MHz; THF-D_8) 7.49-7.63 (m); δ_C (ppm; 300 MHz; THF-D_8) 114.67 (2 C, -CN), 129.58, 131.30, 133.11, 137.57, 174.59.

2-(9H-Fluoren-9-ylidene)malononitrile (**1h**)[5] was prepared by melting and stirring of a 1:1 mixture of molononitrile and 9-flouronone without solvent for 5 min, nearly 100% yield was obtained. Orange-red solid: δ_H (ppm; 300 MHz; THF-D_8) 7.36-7.42 (m, 2 H, -CH=), 7.53-7.59 (m, 2 H, -CH=), 7.70-7.75 (m, 2 H, -CH=), 8.35-8.39 (m, 2 H, -CH=); δ_C (ppm; 300 MHz; THF-D_8) 114.24 (2 C, -CN), 121.85, 127.30, 127.40,

130.03, 135.50, 143.32, 161.38.

Dimethyl 2-benzylidenemalonate (**1k**):[6] A solution of benzaldehyde (1.01 mL, 10 mmol) in dry DMSO (5 mL) with 10% of proline (345 mg) was stirred for 5 min. Then dimethylmalonate (1.14 mL, 10 mmol) was added and the mixture was stirred at room temperature overnight. The reaction was diluted with AcOEt (30 mL) and washed twice with water (30 mL). The organic layer was dried over Na_2SO_4 and the solvent was removed *in vacuo* to afford the targeted product as colorless liquid with 52% yield. Colorless liquid: δ_H (ppm; 300 MHz; CD_3CN) 3.79 (s, 3 H, -Me), 3.80 (s, 3 H, -Me), 7.44 (s, 5 H, -CH=), 7.75 (s, 1 H, -CH=); δ_C (ppm; 75.4 MHz; CD_3CN) 53.29, 53.33, 126.79, 130.00, 130.25, 131.80, 133.66, 143.08, 165.18 (1 C, -C=O), 167.79 (1 C, -C=O).

S3 Typical transfer hydrogenation procedure.

In a glove-box, a 0.5 mm Young NMR tube was charged with olefin (0.1 mmol, for Pseudo-first order conditions 0.5 mmol), **AB** (0.1 mmol) and dry THF-D_8 or CD_3CN (0.6 mL). The tube was sealed with the screw cap and then lay at room temperature after shaking. The reaction was monitored by ^1H NMR every several minutes (depends on the reaction rate). The typical resonance of the starting materials decreased, and a new signal of the saturated products gradually appeared. The disappearance of starting material indicating that the transformation was completed and ^{13}C and ^{11}B NMR spectra were then recorded. Finally the reaction mixture was diluted for analysis on GC-MS. Samples for low temperature NMR were prepared at room temperature using chilled solvents, and immediately put into low temperature fridges until taken for NMR. All the reactions were carried out at least twice and similar results as reported were obtained.

For isolation of the products: 1 mmol olefin was added to a stirred solution of 1 mmol **AB** in 5 ml THF in a 20 ml glass vial. After the required time the mixture was filtered over a small column with celite (usually a pipette stopped with cotton or a small piece of tissue can be used for the NMR reactions) and then the solvent was removed *in vacuo* (polyborazylene was filtered and borazine evaporated), the residue

was further extracted with a unpolar solvent like hexane and the solvent was removed again (**AB** insoluble in hexane). The remaining residue was the pure hydrogenated product to the limit of NMR.

S4 Typical kinetic ^{11}B NMR spectra

For reaction of **1a** with **AB** (5 : 1 molar ratio) in acetonitrile at room temperature with 2 minutes intervals.

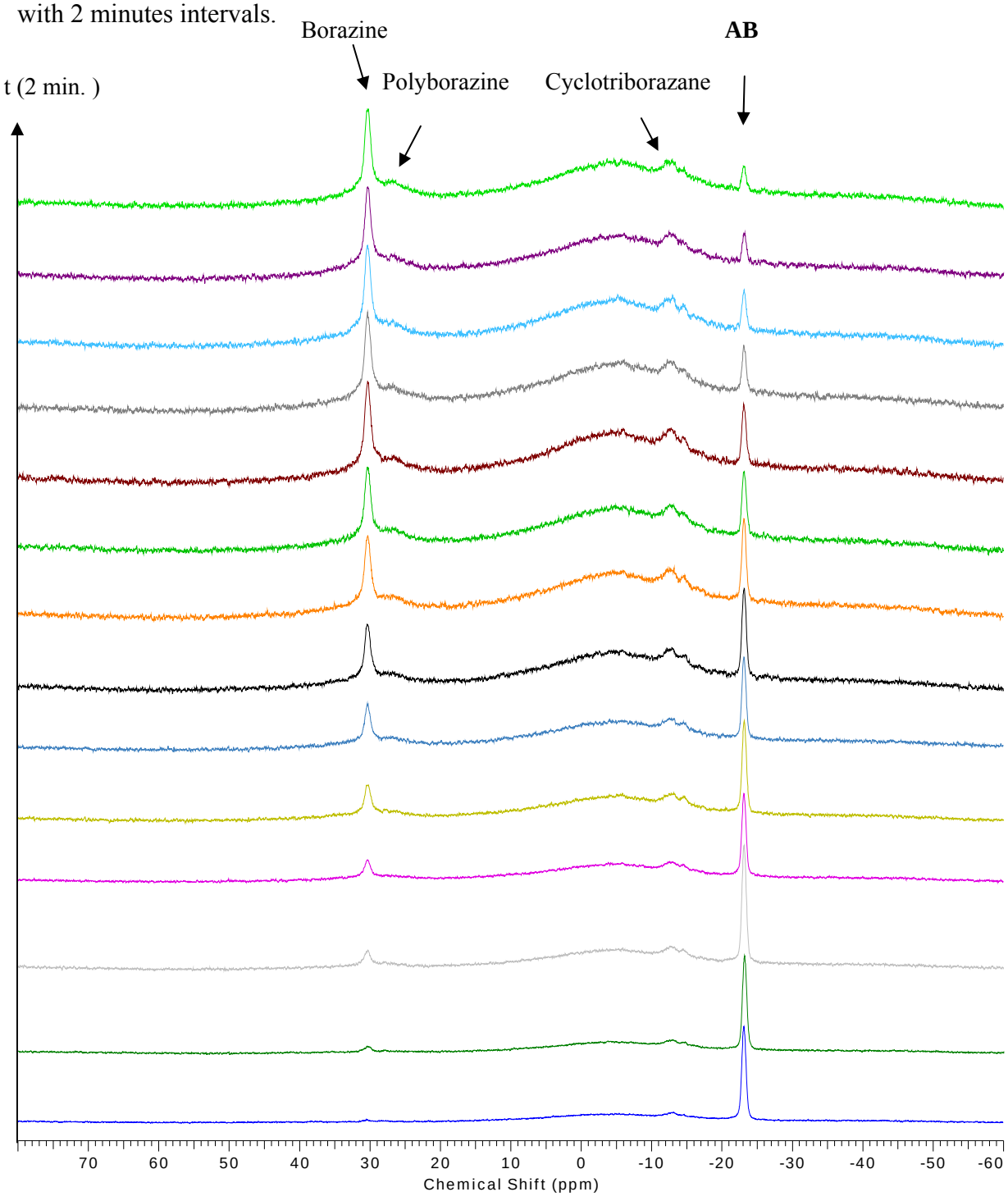

S5 *In situ* spectra for determination of the intermediate

(Reactions of **1a** with **AB** with 3 : 1 molar ratio at -40 °C).

^{1}H NMR in CD_3CN @ 500 MHz:

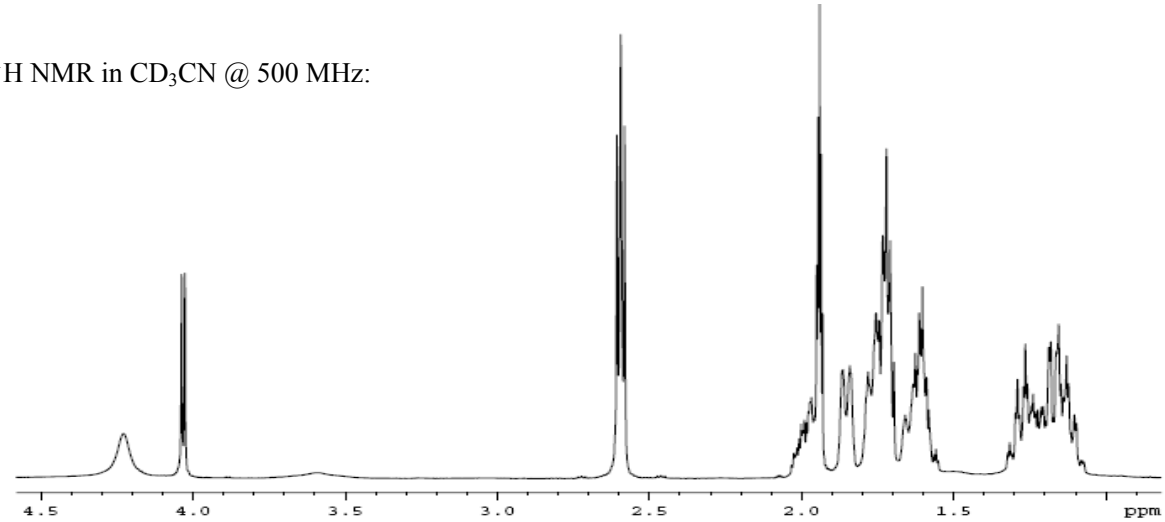

^{13}C NMR in CD_3CN @ 500 MHz:

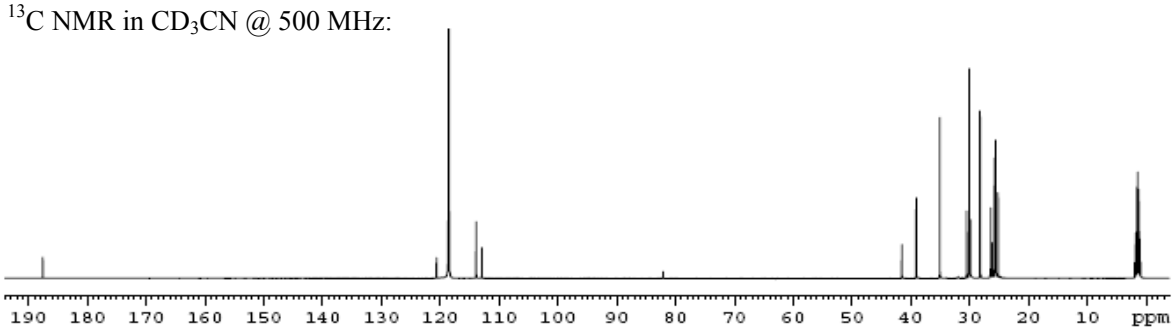

^{13}C NMR in CD_3CN @ 500 MHz: enlarged scale

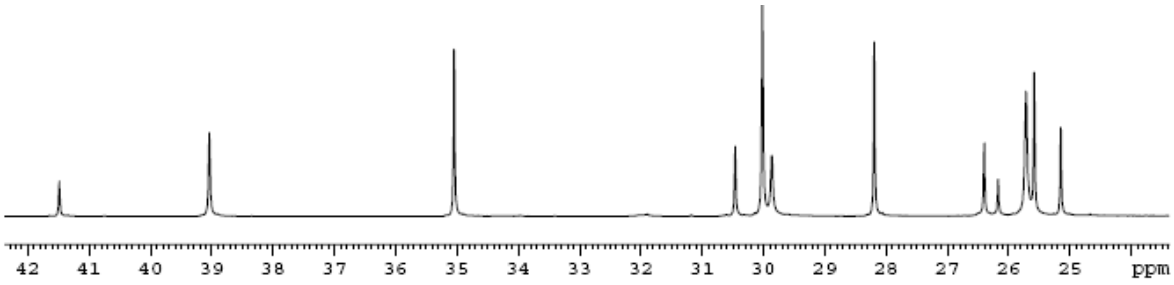

CH, CH3 up; CH2 down; C(q) zero

DEPT @ 500 MHz:

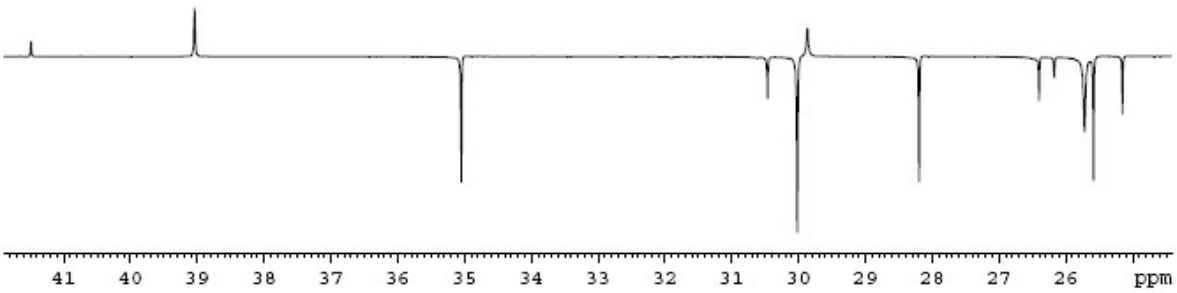

C, H-Correlation in THF-D_8 @ 500 MHz:

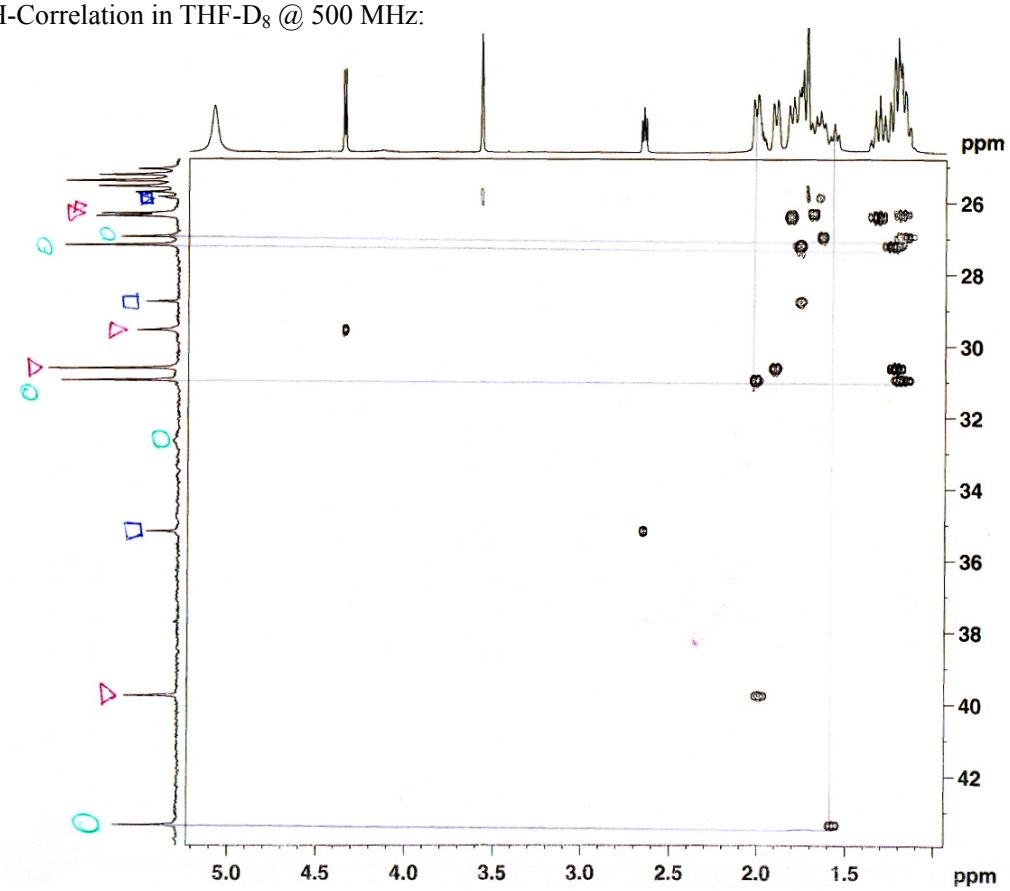

B, H-Correlation in THF-D_8 @ 500 MHz: ↓

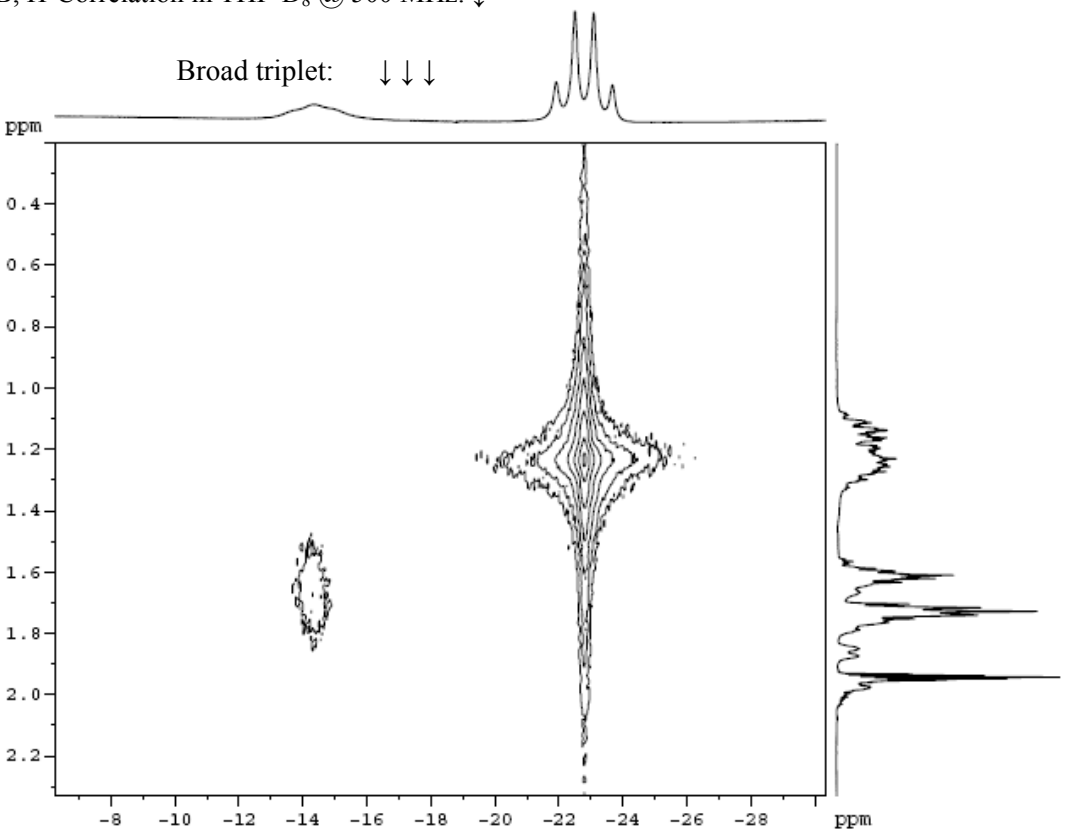

Long range C, H-Correlation in THF-D_8 @ 500 MHz:

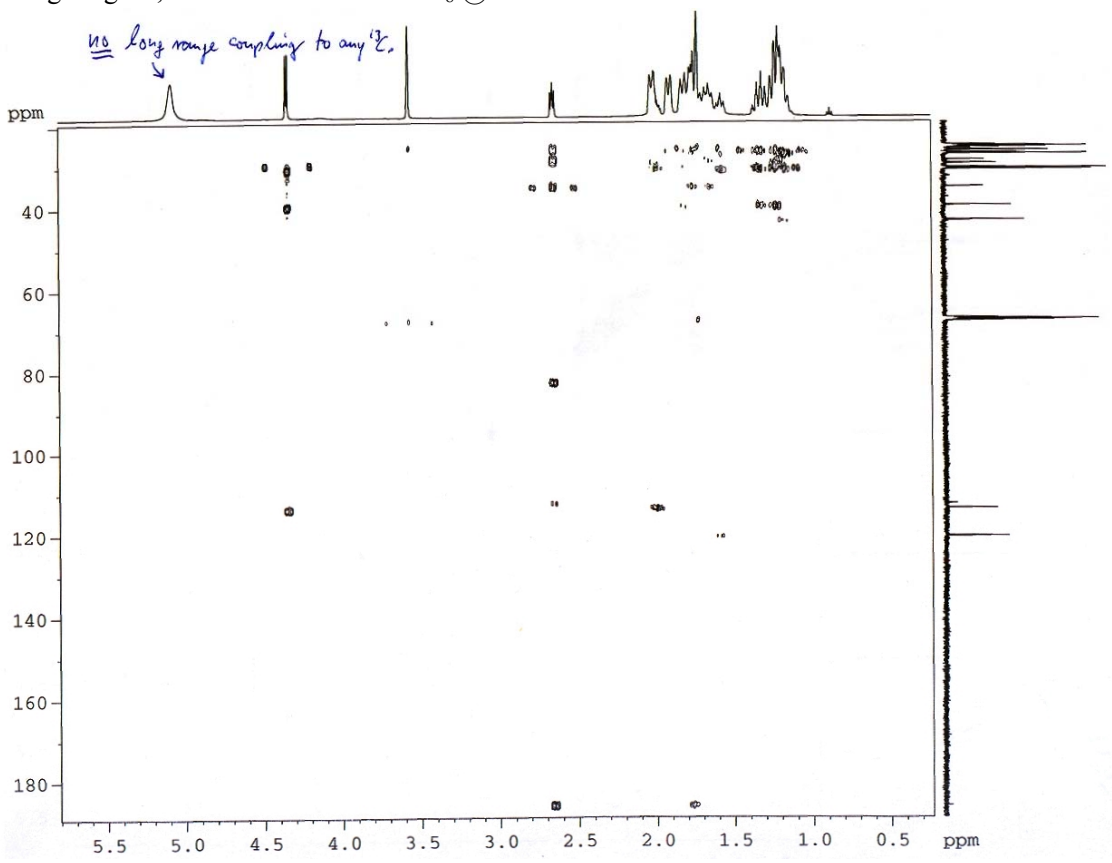

2D-ROSEY in THF-D_8 @ 500 MHz:

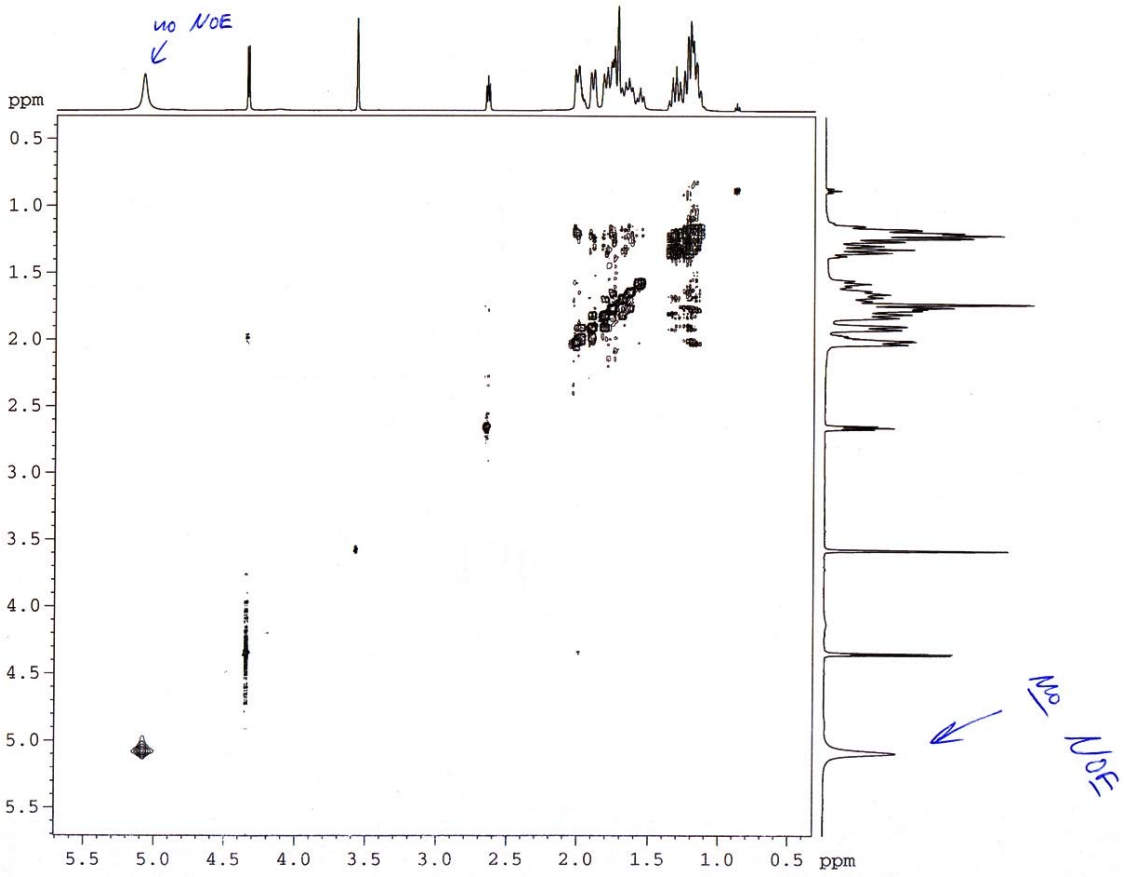

S6 NMR data of all the hydrogenated products.

All the hydrogenated products are described in literature, and the obtained NMR data match literature values.

2-Cyclohexylmalononitrile (**2a**),[7-8] colorless liquid, δ_H (ppm; 300 MHz; THF-D_8) 1.15-1.44 (m, 5 H, -CH-), 1.69-2.06 (m, 6 H, -CH-), 4.25 (d, *J* = 5 Hz, 1 H, -CH-); δ_C (ppm; 300 MHz; THF-D_8) 26.34, 26.41, 29.57, 30.76, 40.06, 113.64 (2 C, -CN).

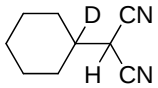

: δ_H (ppm; 300 MHz; THF-D_8) 1.15-1.42 (m, 5 H), 1.69-1.96 (m, 5 H), 4.21 (s, 1 H); δ_D (ppm; THF) 1.95 (s, C-D); δ_C (ppm; 75.4 MHz; THF-D_8) 26.35, 26.40, 29.52, 30.67, 39.61 (t, *J* = 20 Hz, C-D), 40.07 (C-H residue), 113.65.

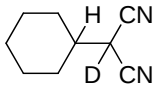

: δ_H (ppm; 300 MHz; THF-D_8) 1.14-1.43 (m, 5 H), 1.69-2.02 (m, 6 H); δ_D (ppm; THF) 4.20 (s, C-D); δ_C (ppm; 75.4 MHz; THF-D_8) 26.35, 26.41, 29.44 (t, *J* = 22 Hz, C-D), 30.74, 39.98 , 113.65.

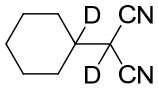

:δ_H (ppm; 300 MHz; THF-D_8) 1.15-1.43 (m, 5 H), 1.69-1.95 (m, 5 H); δ_D (ppm; THF) 1.95 (s, C-D), 4.20 (s, C-D); δ_C (ppm; 75.4 MHz; THF-D_8) 26.35, 26.39, 29.37 (t, *J* = 22 Hz, C-D), 30.63, 39.52 (t, *J* = 20 Hz, C-D), 39.97 (B-H residue), 113.65.

Methyl 2-cyano-2-cyclohexylacetate (**2b**),[9] colorless liquid: δ_H (ppm; 300 MHz; CD_3CN) 1.08-1.35 (m, 5 H, -CH-), 1.63-1.82 (m, 5 H, -CH-), 1.94-2.07 (m, 1 H, -CH-), 3.64 (d, *J* = 5 Hz, 1 H, -CH-), 3.74 (s, 3 H, -Me); δ_C (ppm; 75.4 MHz; CD_3CN) 26.27, 26.34, 26.51, 30.00, 31.62, 39.43, 45.11, 53.83, 117.10 (-CN), 167.60 (-C=O).

2-Cyclopentylmalononitrile (**2c**),[7] yellow liquid, δ_H (ppm; 300 MHz; THF-D_8) 1.44-1.56 (m, 2 H, -CH_2-), 1.61-1.82 (m, 4 H, -CH_2-), 1.95-2.05 (m, 2 H, -CH_2-), 2.44-2.60 (m, 1 H, -CH-), 4.34-4.36 (d, *J* = 7 Hz, 1 H, -CH-); δ_C (ppm; 75.4 MHz; THF-D_8) 26.06, 27.66, 31.05, 41.71, 114.20 (-CN).

2-Isopropylmalononitrile (**2d**),[7] yellow liquid, δ_H (ppm; 300 MHz; THF-D_8) 1.19 (d, *J* = 7 Hz, 6 H, -Me), 2.28-2.41 (m, 1 H, -CH-), 4.26 (d, *J* = 6 Hz, 1 H, -CH-); δ_C (ppm; 75.4 MHz; THF-D_8) 19.58, 30.50, 31.74, 113.70 (-CN).

2-(3,3-Dimethylbutan-2-yl)malononitrile (**2e**),[8] colorless liquid: δ_H (ppm; 300 MHz; CD_3CN) 0.98 (s, 9 H, -Me), 0.99 (s, 3 H, -Me), 1.23-1.27 (m, 1 H, -CH-), 4.22-4.25 (m, 1 H, -CH-); ^{13}C-NMR (CD_3CN): δ (ppm) 13.00, 26.56, 27.47, 34.36, 45.54, 115.72 (-CN).

2-(1-Phenylpropyl)malononitrile (**2f**),[10] white solid: δ_H (ppm; 300 MHz; CD_3CN) 0.81 (t, *J* = 7 Hz, 3 H, -Me), 1.89-1.99 (m, 2 H, -CH_2-), 3.20-3.27 (m, 1 H, -CH-), 4.36 (d, *J* = 7 Hz, 1 H, -CH-), 7.35-7.54 (m, 5 H, -CH=); ^{13}C-NMR (CD_3CN): δ (ppm) 11.85, 26.24, 30.63, 48.09, 114.04 (-CN), 129.13, 129.37, 129.86, 138.54.

2-Benzhydrylmalononitrile (**2g**),[11] white solid, δ_H (ppm; 300 MHz; THF-D_8) 4.81 (d, *J* = 9 Hz, 1 H, -CH-), 5.29 (d, *J* = 9 Hz, 1 H, -CH-), 7.23-7.44 (m, 10 H, -CH=); δ_C (ppm; 75.4 MHz; THF-D_8) 28.98, 52.14, 113.87 (-CN), 128.89, 128.96, 129.80, 139.70.

2-(9H-fluoren-9-yl)malononitrile (**2h**),[12] white solid, δ_H (ppm; 300 MHz; THF-D_8) 4.59 (d, *J* = 3.5 Hz, 1 H, -CH-), 5.18 (d, *J* = 4.5 Hz, 1 H, -CH-), 7.34-7.51 (m, 4 H, -CH=), 7.79-7.88 (m, 4 H, -CH=); δ_C (ppm; 75.4 MHz; THF-D_8) 27.78, 46.95, 113.41 (-CN-), 121.41, 125.63, 128.67, 130.07, 142.00, 142.64.

2-benzylmalononitrile (**2i**),[7,13] slightly yellow solid: δ_H (ppm; 300 MHz; THF-D_8) 3.31 (d, *J* = 7 Hz, 2 H, -CH_2-), 4.59 (t, *J* = 7 Hz, 1 H, -CH-), 7.32-7.38 (m, 5 H, -CH=); δ_C (ppm; 75.4 MHz; THF-D_8) 25.25, 36.91, 114.19 (-CN), 128.90, 129.61, 130.19, 135.65.

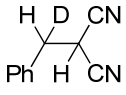

: δ_H (ppm; 300 MHz; THF-D_8) 3.28-3.32 (m, 1 H), 4.58 (d, *J* = 7 Hz, 1 H), 7.29-7.41 (m, 5 H); δ_D (ppm; THF) 3.29; δ_C (ppm; 75.4 MHz; THF-D_8) 25.18, 36.62 (t, *J* = 21 Hz, H-C-D), 114.19, 128.90, 129.61, 130.18, 135.60.

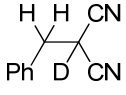

: δ_H (ppm; 300 MHz; THF-D_8) 3.30 (s, 2 H), 7.22-7.41 (m, 5 H); δ_D (ppm; THF) 4.54; δ_C (ppm; 75.4 MHz; THF-D_8) 25.26 (t, *J* = 10 Hz, C-D), 36.83, 114.18, 128.89, 129.61, 130.18, 135.635.

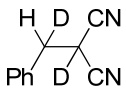

: δ_H (ppm; 300 MHz; THF-D_8) 3.30 (m, 1 H), 7.26-7.43 (m, 5 H); δ_D (ppm;

THF) 3.29, 4.52; δ_C (ppm; 75.4 MHz; THF-D_8) 25.05 (t, *J* = 19 Hz, C-D), 36.52 (t, *J* = 21 Hz, D-C-D), 114.17, 128.90, 129.61, 130.17, 135.58.

Methyl 2-cyano-3-phenylpropanoate (**2j**),[9] white solid: δ_H (ppm; 300 MHz; CD_3CN) 3.10-3.32 (m, 2 H, -CH_2-), 3.74 (s, 3 H, -Me), 4.01-4.13 (m, 1 H, -CH-), 7.25-7.41 (m, 5 H, -CH=); δ_C (ppm; 75.4 MHz; CD_3CN) 35.47, 39.80, 53.53, 117.07 (-CN), 127.96, 129.11, 129.59, 136.55, 166.89 (-C=O).

Dimethyl 2-benzylmalonate (**2k**),[14] colorless liquid: δ_H (ppm; 300 MHz; CD_3CN) 3.13-3.17 (d, *J* = 8 Hz, 2 H, -CH_2-), 3.63 (s, 6 H, -Me), 3.71 (t, *J* = 8 Hz, 1 H, -CH-), 7.09-7.36 (m, 5 H, -CH=); δ_C (ppm; 75.4 MHz; CD_3CN) 35.30, 53.04, 54.35, 127.70, 129.46, 129.76, 139.03, 170.12 (-C=O).

References:

[1] a) M. G. Hu, J. M. Van Paasschen and R. A. Geanangel, *J. Inorg. Nucl. Chem.* **1977**, *39*, 2147; b) G. H. Penner, Y. C. Phillis Chang and J. Hutzal, *Inorg. Chem.* **1999,** *38,* 2868.

[2] J. Mirek, M. Adamczyk and M. Mokrosz, *Synthesis*, **1980**, 296.

[3] F. Texier-Boullet and A. Foucaud, *Tetrahedron Lett.* **1982**, *23*, 4927.

[4] G. Charles, *Bull. Soc. Chimi. Fr.,* **1963**, *8-9*, 1559.

[5] G.-W. Wang and B. Cheng, *ARKIVOC*, **2004**, 4.

[6] G. Cardillo, S. Fabbroni, L. Gentilucci, M. Gianotti and A. Tolomelli, *Synthetic Commun.*, **2003**, *33*, 1587.

[7] J. C. Dunham, A. D. Richardson and R. E. Sammelson, *Synthesis*, **2006**, 680-686.

[8] R. E. Sammelson and M. J. Allen, *Synthesis* **2005**, 543-546.

[9] D. B. Ramachary, M. Kishor and Y. V. Reddy, *Eur. J. Org. Chem.* **2008**, 975-993.

[10] Z. Tu, C. Lin, Y. Jang, Y.-J. Jang, S. Ko, H. Fang, J.-T. Liu and C.-F. Yao, *Tetrahedron Lett.* **2006**, *47*, 6133-6137.

[11] C.-R. Liu, M.-B. Li, C.-F. Yang and S.-K. Tian, *Chem. Eur. J.*, **2009**, *15*, 793-797.

[12] X.-Q. Fang, H.-J. Xu, H. Jiang, Y.-C. Liu, Y. Fu and Y.-D. Wu, , *Tetrahedron Lett.* **2009**, *50*, 312-315.

[13] B. C. Ranu, J. Dutta and S. K. Guchhait, *Org. Lett.* **2001**, *3*, 2603.

[14] Q. Xu, B. Cheng, X. Ye and H. Zhai, *Org. Lett.*, **2009**, *11* , 4136-4138

Synthetic and Mechanistic Studies of Metal-Free Transfer Hydrogenations Applying Polarized Olefins as Hydrogen Acceptors and Amine Borane Adducts as Hydrogen Donors

5.1 Introduction

Transfer hydrogenations are hydrogenation reactions that involve a double H transfer from hydrogen donors to hydrogen acceptors containing unsaturated bonds, such as C=C, C=O and C=N bonds,[1] which can principally be carried out in a metal-free fashion (Scheme 5.1), but can also be catalyzed by transition metal complexes. The metal mediated reactions play an important role in modern organic synthesis and industrial processes.[2] Given suitable hydrogen donor and acceptor molecules, transfer hydrogenations offer in the metal-free form an eco-friendly alternative to present hydrogenation methods.[3] They are expected to be operable on a metal-free base especially when polar hydrogen donors and acceptors are applied.[1]

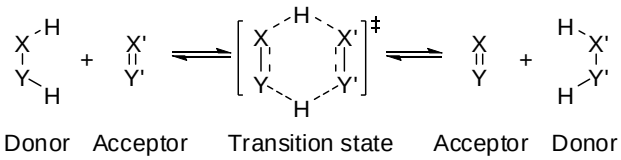

Scheme 5.1 Metal-free double H transfer as a concerted elementary process. X, Y, X' and Y': main group element fragments.

A great deal of hydrogen-rich molecules have been applied as hydrogen donors in hydrogen transfer reactions, such as hydrazine, dihydronaphthalene, dihydroanthracene, formic acid,[4] alcohols, esters,[2] and also ammonia borane (**AB**) and related amine boranes.[5] In recent years, amine borane adducts have attracted additional attention for their very high volumetric and gravimetric hydrogen storage density as potentially safe and stable hydrogen storage materials.[6] Intensive studies were carried out on the dehydrogenation and the hydrogenation (regeneration) of these compounds, which remains as a practically

unsolved problem.[7] Therefore, we became also interested in the use of such compounds as *in situ* hydrogen sources for the transfer hydrogenation of unsaturated compounds exploring new reaction pathways in the hope to create more reversible dehydrogenation processes of **AB**.

The catalytic reaction of **AB** in the presence of cyclohexene was reported to result in a hydroboration reaction with formation of Cy_2BNH_2 when using a rhodium[8] or platinum[9] catalysts. On the other hand, olefins including cyclohexene were seen to be transfer hydrogenated by **AB** or dimethylamine borane (**DMAB**) using Rh colloid[5a, b] or nitrosyl Re(I)[5c, d] complexes. Since the reaction course was found to be quite sensitive to the type of the catalyst, it might change completely if the substrate, solvent or other conditions are adjusted. Considering the strongly polarized hydridic H_B and protic H_N atoms in the amine borane molecules, the pathway might be switched from stepwise transfers to concerted double-H transfers as depicted in Scheme 5.1.

We have previously reported that aromatic imines, bearing a polarized C=N double bond, can be directly hydrogenated by **AB** via a 'polarity matched' concerted double-H transfer process.[10] Ketones and aldehydes can also be transfer hydrogenated by **AB**, but a protic solvent such as methanol was required, since otherwise in an aprotic solvent, like THF, hydroboration would take place.[11] Furthermore, a step-by-step H_B before H_N transfer from **AB** to polarized olefins was found to proceed under mild conditions in THF or acetonitrile.[11] In this paper, we report a detailed study of the metal-free transfer hydrogenation and its mechanism of polar olefins with amine borane adducts.

5.2 Results and discussions

5.2.1 Solvent dependence and scope of amine borane adducts.

2-Cyclohexylidenemalononitrile (**1a**) was selected as the model olefin and **AB** as a model amine borane adduct to test the general propensity of such compounds for

Table 5.1 Reactions of 2-cyclohexylidenemalononitrile (**1a**) with various amine borane adducts in different solvents. [a]

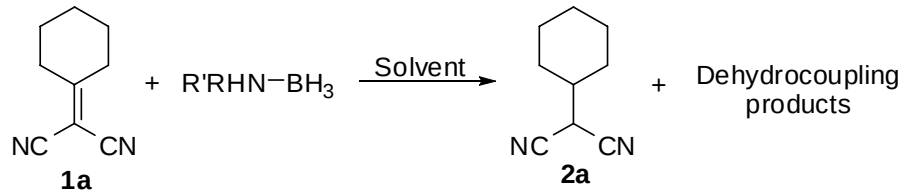

Entry	R, R'	Solvent	Temp.	Time [b]	Dehydrocoupling compounds [c]
1	R = R' = H	THF-D_8	r.t. 10 °C	< 10 min 1 h	30.71 (d, *J* = 133 Hz), $(BHNH)_3$
2	R = R' = H	CD_3CN	r.t.	1 h	$(BHNH)_3$
3 [d]	R = R' = H	Tol-D_8	r.t.	16 h	$(BHNH)_3$
4 [d]	R = R' = H	C_6D_6	r.t.	20 h	$(BHNH)_3$
5 [d]	R = R' = H	$CDCl_3$	r.t.	5 d	$(BHNH)_3$
6 [e]	R = R' = H	C_2D_6SO	r.t.	> 5 d	$(BHNH)_3$
7	R = R' = H	no solvent	r.t.	< 10 min	$(BHNH)_3$
8	R = R' = H	CD_3OD	r.t.	< 10 min	12.26 (s), $B(OCD_3)_3$
9	R = H, R' = Me	CD_3CN	r.t.	15 h	33.42 (d, *J* = 154 Hz), $(BHNMe)_3$
10	R = H, R' = ^{t}Bu	CD_3CN	r.t. 60 °C	3 d 5 h	28.78 (d, *J* = 124 Hz), $(BHN^tBu)_3$
11 [f]	R = R' = Me	CD_3CN	r.t. 60 °C	5 d 20 h	8.23 (t, *J* = 112 Hz), $(BH_2NMe_2)_2$ + 31.15 (d, *J* = 131 Hz), $BH(NMe_2)_2$

[a]The reactions were carried out in a NMR tube and monitored by *in situ* ^{1}H and ^{11}B NMR (1 : 1 molar ratio of **1a** to **AB** or 1 : 2 molar ratio of **1a** to the other amine boranes); [b]Required reaction times for full conversion of **1a** to **2a**. [c]The structure of the dehydrocoupling products of the amine boranes were determined by comparison of the resonances (in ppm) in ^{11}B NMR to literature values; a small amount of polymerized imino borane product was observed as an insoluble white precipitate; [d]The solubility of **AB** in either benzene or chloroform is very low; [e]Less than 10 % of the olefin was hydrogenated after 5 days at room temperature; [f]The ratio of the two dehydrocoupling compounds is 9 : 1 by integrations in the ^{11}B NMR spectra.

hydrogen transfer reactions in a variety of solvents (Table 5.1). The reaction in THF was completed within 10 min at room temperature (entry 1). When the condition was adjusted either by changing of the solvent to higher polarity, like acetonitrile or by

decreasing the temperature to 10 ^{o}C, 1 h was required to bring the hydrogen transfer to completion (entries 1 and 2). Other aprotic solvents were also tried. In toluene, benzene, chloroform and DMSO the reactions were slow, partially due to also poor solubility of **AB** in these solvents (reasonable solubility in DMSO). The reaction rates in less polar solvents, toluene and benzene (entries 3-4), were obviously higher than in the more polar solvents like chloroform and DMSO (entries 5-6). Such a preference for apolar solvent supports the idea of a non-polar transition state.[12] In all these reactions, borazine ($(BHNH)_3$, **BZ**) was the major dehydrocoupling product.

Compound **1a** is a liquid at room temperature and was found to dissolve **AB** and to induce solvent-free transfer hydrogenation forming **2a** and **BZ** at room temperature nearly instantaneously (Table 5.1, entry 7).

When the protic solvent methanol was applied as the reaction media, transfer hydrogenation of **1a** occurred also very fast. However, a completely different reaction took place in this case, only trimethyl borate was observed as the alcoholysis product of **AB** (Table 5.1, entry 8). The reaction proceeded along a hydroboration process, related to the reactions of **AB** with carbonyl compounds in methanol.

Amine-borane adducts other than **AB**, such as *N*-methyl amine borane (**MAB**), *N*-*tert*-butyl amine borane (**tBAB**) and *N,N*-dimethyl amine borane (**DMAB**), were then employed to react with **1a** in acetonitrile at room temperature. A transfer hydrogenation reaction similar to those with **AB** took place, but at much lower rates. Among these substituted amine boranes, **MAB** displayed superior reactivity towards **1a** with formation of the borazine analog $(BHNMe)_3$ as the dehydrocoupling product (Table 5.1, entry 9). The more sterically hindered mono-substituted amine borane adduct **tBAB** required much longer time to complete the hydrogen transfer (entry 10), while the di-substituted **DMAB** turned out to react slowest, with the four-membered ring $(BH_2NMe_2)_2$ as the main dehydrocoupling product together with about 10% of $BH(NMe_2)_2$[13] (entry 11). Naturally, an increase of the temperature to 60 ^{o}C accelerated the reaction rates significantly (entries 10 and 11).

5.2.2 Range of the applied polar olefins.

Based on the suitability of polar solvents in the transfer hydrogenations, CH_3CN was selected as the preferred solvent to test the substrate dependence of the double H transfer reaction with **AB** as the model amine borane adduct. A series of activated olefins was employed to test the range of the substituent tolerence (Table 5.2).

Most of the olefins with geminal electron-withdrawing (EWD) groups on one side of the CC double bond and H, alkyl or aromatic substituents on the other side could be successfully transfer hydrogenated by **AB** (Table 5.2, entries 1-7). In case there are two strongly polarized vinyl groups attached to a methylene group, deprotonation of the alkylic H took place yielding a stable anion (**2h**, entry 8). Otherwise, transfer hydrogenation of diolefinic substrates tended to occur primarily at the more strongly polarized double bond (**2i** and **2j**, entries 9-10). A completely different type of reaction takes place when the olefin is stabilized by a π push-pull interaction, such as in **1k**, or depolarized by two geminal strong EWD groups on the other side of the double bond as in **1l**, a complex mixture of compounds other than those originating from hydrogenation resulted (entries 11-12). Olefins with only one EWD group on the double bond became more reluctant to undergo transfer hydrogenation, even when heated to 60 ^{o}C for a prolonged reaction time (entries 13-14). The dehydrogenated Hantzsch Ester could not be directly hydrogenated by **AB** neither (**1o**, entry 15).

5.2.3 Regio-specificity of the H transfer and deuterium kinetic isotope effects.

The regio-specificity and deuterium kinetic isotope effect (DKIE) were exemplarily investigated via the reactions of **1a** with **AB** using the selectively deuterated **AB** derivatives (NH_3BD_3 (**AB(D)**), ND_3BH_3 (**A(D)B**) and BD_3ND_3 (**A(D)B(D)**)). Tracing the regioselectivity of the deuterium addition, it was found that the protic $(H/D)_N$ and the hydridic $(H/D)_B$ end up at the C_{CN} atom of the double bond and the cyclohexylidene C atom, respectively.[11]

Table 5.2 Transfer hydrogenation of various polarized olefins with **AB** (1:1 molar ratio) in CD_3CN.

Entry	Olefin		Temp.	Time	Yield (%) [a]
1	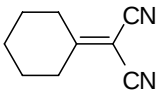	**1a**	r.t.	1 h	99
2	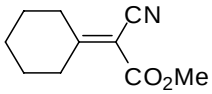	**1b**	r.t.	2 h	99
3	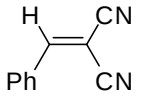	**1c**	r.t.	10 min	99
4	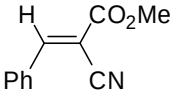	**1d**	r.t.	30 min	99
5	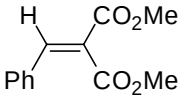	**1e**	r.t.	3 d	98
6	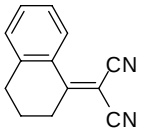	**1f**	r.t.	10 h	99
7	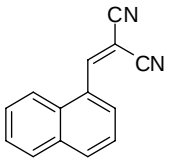	**1g**	r.t.	30 min	99
8 [b]	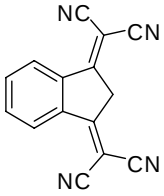	**1h**	r.t.	1 d	99
9 [c]	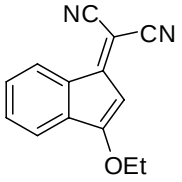	**1i**	60 °C	1 d	86
10 [c]	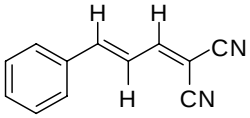	**1j**	r.t. 60 °C	2 d 1.5 h	85 82
11 [d]	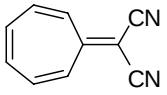	**1k**	r.t. 60 °C	5 d 1 d	Complex mixture

12 [d]	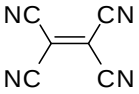	**1l**	r.t.	10 min	Complex mixture
13 [e]	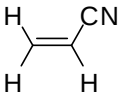	**1m**	r.t. 60 °C	2 d 2 d	Trace 50 [d]
14	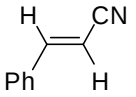	**1n**	r.t. 60 °C	5 d 5 d	n.r. Trace
15	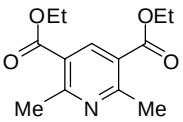	**1o**	60 °C	5 d	n.r.

[a]The reaction courses were monitored by *in situ* ^{1}H NMR spectroscopy and the yields of the hydrogenated products were determined by integrations of the GC peaks within the GC-MS analyses; [b]No hydrogenation took place rather deprotonation, yielding exclusively the anionic product dicyano(1-(dicyanomethylene)-1H-inden-3-yl) methanide. [c]Hydrogenation reactions occurred mainly with the double bond substituted by two -CN groups, the percentages adding up to 100% were attributed to products with both double bonds hydrogenated; [d]Hydrogenation reaction did not take place; [e]Besides the hydrogenation product, there were some amount of compounds, which could not be identified due to a quite rough base line in the NMR spectra.

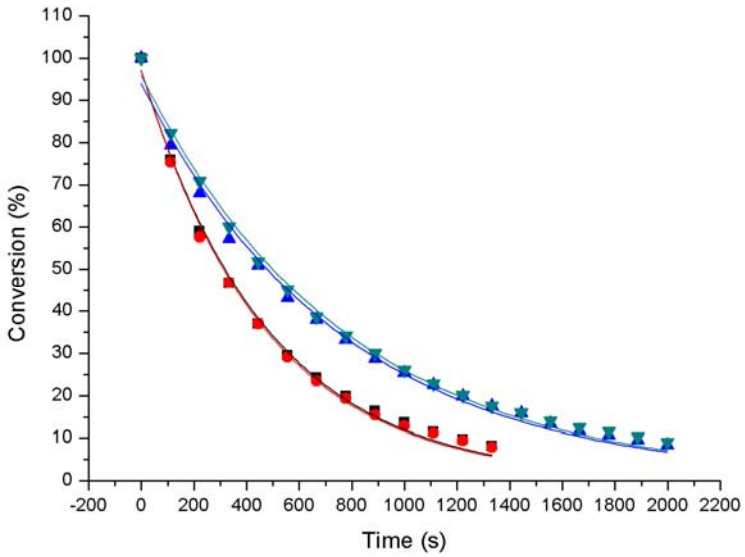

Fig. 5.1 Kinetic conversion chart of the reactions of 0.5 mmol **1a** with 0.1 mmol **AB**, **AB(D)**, **A(D)B** or **A(D)B(D)** pursued by *in situ* ^{11}B NMR in acetonitrile at room temperatures with 2 min intervals. Concentrations were taken from the intensities of **AB** of the ^{11}B NMR spectra and filled to the first order reactions. The ■ stands for reactions with **AB**, ● for **AB(D)**, ▲ for **A(D)B** and ▼ for **A(D)B(D)**. Simulated deuterium kinetic isotope effects: $k_{\mathbf{AB}}/k_{\mathbf{AB(D)}} = 1.00$, $k_{\mathbf{A(D)B}}/k_{\mathbf{A(D)B(D)}} = 1.04$, $k_{\mathbf{AB}}/k_{\mathbf{A(D)B}} = 1.55$, $k_{\mathbf{AB(D)}}/k_{\mathbf{A(D)B(D)}} = 1.62$.

According to the kinetic conversion chart obtained by *in situ* ^{11}B NMR analyses for the reactions under pseudo-first order conditions (Fig. 5.1), the DKIE values were calculated from the simulated rate constants (k). Nearly no DKIE could be observed for deuterium labeling on the boron atoms (Fig. 5.1, $k_{AB}/k_{AB(D)} = 1$, $k_{A(D)B}/k_{A(D)B(D)} = 1.04$) and normal DKIEs were obtained with deuterium on the nitrogen atoms (Fig. 5.1, $k_{AB}/k_{A(D)B} = 1.55$, $k_{AB(D)}/k_{A(D)B(D)} = 1.62$). Assuming that the H_B transfer constitutes the rate determining step (RDS), this would render DKIE values ≠ 1. A DKIE of 1 is expected to indicate that the double H transfer is stepwise and the H_B transfer would be fast occurring before or after the rate determining step.[14]

5.2.4 *p*-Aryl substituent effects and Hammett correlations.

Electronic substitutent effects are usually studied by thr effect of *para*-substituted phenyl groups at the crucial C atoms of the substrate.[15] Since the reaction of **AB** with the phenyl substituted olefin **1c** in CD_3CN was too fast to be measured at ambient conditions and the reaction with **1e** was too slow, **1d** was chosen for a model study of substituent effects (Table 5.2, entries 3-5). Several *para*-substituted derivatives of **1d** were used to react with **AB** at room temperature in CD_3CN in a 1:1 molar ratio (Scheme 5.2).

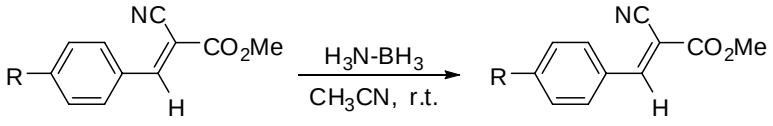

1 **2**

R = OMe	**1p**	3 h	99%
R = NMe_2	**1q**	2 d	90%
R = H	**1d**	0.5 h	99%
R = Cl	**1r**	20 min	99%
R = NO_2	**1s**	8 min	99%
R = CN	**1t**	5 min	99%

Substituent constants	
-OMe:	-0.268
-NMe_2:	-0.205
-H:	0
-Cl:	0.227
-NO_2:	0.778
-CN:	1.00

Scheme 5.2 Transfer hydrogenation of **AB** with **1d** derivatives with different substituents in the *para*-positions (1:1 molar ratio) carried out in acetonitrile at room temperature, the trend in reaction time is comparable to the sequence of the substituent constants.

A sequence of reaction rates **1t** > **1s** > **1r** > **1d** > **1p** > **1q** was derived (Scheme 5.2), closely correlating with the sequence of the substituents constants[16] –OMe > –NMe_2 > –H > –Cl > –NO_2 > –CN. The only exception was the –NMe_2 substituted **1q**, which is expected to cause faster rate than the –OMe substituted **1p**. But actually **1q** was found to react much slower, perhaps due to its extremely low solubility in acetonitrile or THF. However, the solubilities of the –NO_2 and –CN substituted olefins were also not high in acetonitrile, but did not show much influence on the reaction rates.

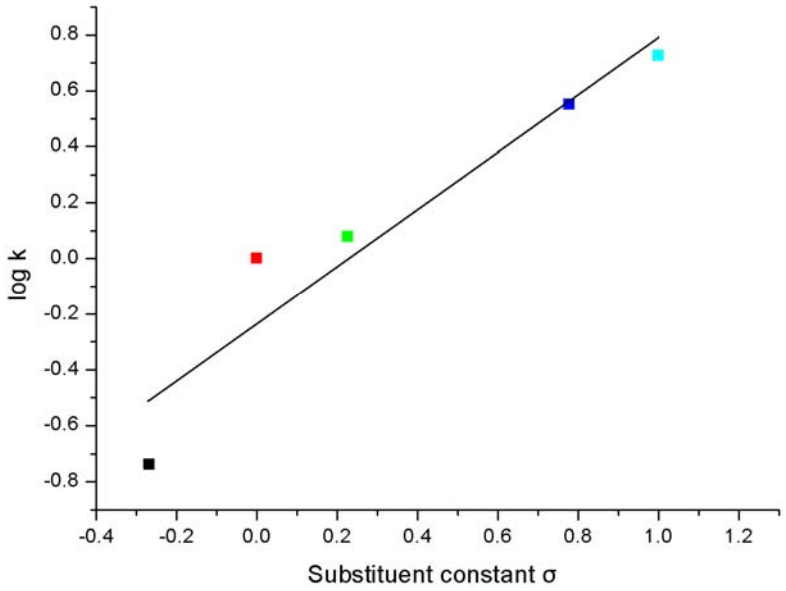

Fig. 5.2 Hammett correlation for the substituent effect in the transfer hydrogenation of polarized olefins with **AB**. The rate constants k were obtained from kinetic pursuits of the ^{11}B NMR spectra of the reactions of 0.1 mmol **AB** with 0.5 mmol of the *p*-substituted **1d** derivatives in acetonirtile. The values of the substituent constant σ were taken from literature. From left to right (or bottom to top), ■ represents the –OMe, –H, –Cl, –NO_2 and –CN group, respectively. The slope of the kinetic curve was $\rho = 1.02$.

$$\log (k/k_0) = \log k - \log k_0 \quad = \rho^*\sigma \qquad (1)$$

$$\log k = \rho^*\sigma + \log k_0 \qquad (2)$$

While: k and k_0 are the rate constants of the reactions with substituted and unsubstituted substrates, respectively; σ is the substitutent constant and ρ is the reaction constant.

Due to the Hammett equation (Eq. 1),[16b] the reaction constant ρ was obtained as the slope of the σ vs. log k plot (Eq. 2). The Hammett correlation was plotted with **1d**，**1p**，**1r**，**1s** and **1t** (Fig. 5.2, **1q** was excluded based on the arguments given in the earlier context) and a ρ = 1.02 was obtained. The positive ρ value indicated increased electron density in the aromatic ring[17] suggesting that negative charge is generated in the transition state. Since the transfer of the protic H_N is participating in the RDS of these reactions and the attack of a H^+ ion would generate positive charge, it seemed reasonable to assueme that the reaction passes over a concerted transition state.

5.2.5 The dehydrocoupling pathway of AB.

In an attempt to trap boron bared intermediates, cyclohexene was added into the reaction mixture of **1a** with **AB** in THF. Cy_2BNH_2 was observed at a much faster rate than the direct reaction of cyclohexene with **AB** (Scheme 5.3). As reported in the literature, such an observation indicated the intermediacy of $[NH_2{=}BH_2]$ along the reaction path. [8]

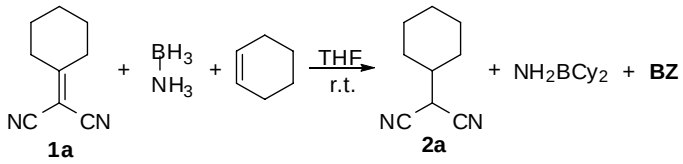

Scheme 5.3 Transfer hydrogenation of **1a** with **AB** in the presence of excess cyclohexene in THF at room temperature.

To determine whether the final dehydrocoupling product **BZ** was formed via dehydrogenation of cyclotriborazane (**CTB**), a reaction of **1a** with **CTB** (1:2 molar ratio) was carried out in THF. After 2 days at room temperature **1a** was still not completely hydrogenated (Scheme 5.4).

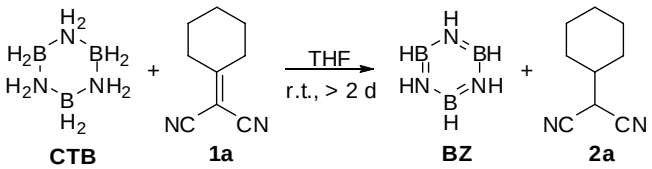

Scheme 5.4 Hydrogenation of **1a** with cyclotriborazane (**CTB**) in a 1 : 1.5 molar ratio in THF at room temperature.

This reaction proceeded much slower than the reaction of **1a** with **AB** which was finished within 10 min in THF at room temperature (Table 5.1, entry 1). Since the formation of **BZ** via the dehydrogenation of **CTB** was so slow, we anticipated the existence of another pathway leading to **BZ** or **PBZ**, for instance the direct dehydrocoupling of $[NH_2{=}BH_2]$ or preferably a solvent-stabilized $[NH_2{=}BH_2]$-(solvent) (Scheme 5.5).

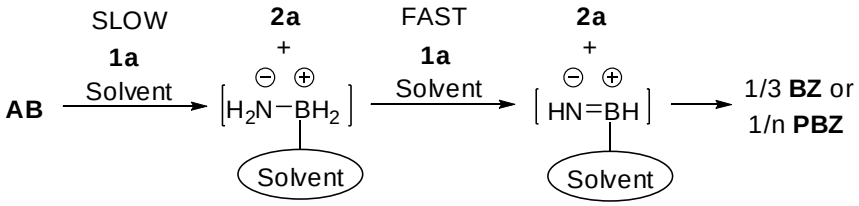

Scheme 5.5 Possible formation pathway of **BZ** (**PBZ**) from direct dehydrocoupling of a solvent-stabilized $[NH_2{=}BH_2]$-(solvent).

5.2.6 Reactivity of the hydroboration intermediate.

According to the ^{11}B NMR spectra, the intermediate **3a** was formed via hydroboration of **1a** by **AB** (Scheme 5.6). A triplet appeared for **3a** at around -14 ppm at temperatures below -40 ^{o}C in deuterated THF or acetonitrile.

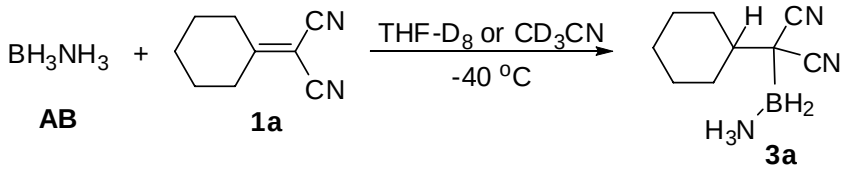

Scheme 5.6 Trapping of the hydroboration intermediate (**3a**) by *in situ* NMR of the reaction of **1a** with **AB** at low temperature.

In another reaction batch using **1a** in excess, **AB** was completely transformed into **3a** (together with a small amount of **BZ**) at -40 ^{o}C in THF-D_8 requiring 7 days. The subsequent reaction step of **3a** was then pursued at room temperature by *in situ* ^{11}B NMR. It was found that **3a** was rapidly converted to **BZ** and polyborazine (**PBZ**), with **CTB** to be initially detected in tiny amounts as a shoulder to the signal of **3a**. **CTB** finally remained as the only $–BH_2–$ species remaining till the end of the reaction (Fig. 5.3).

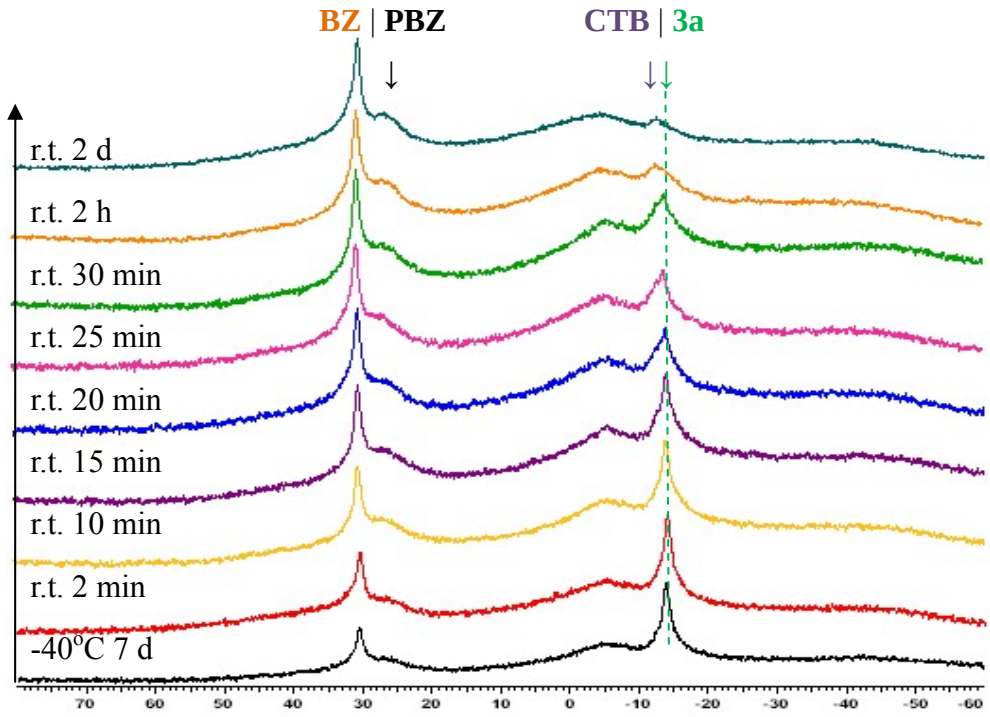

Fig. 5.3 *In situ* ^{11}B NMR spectra in THF-D_8 showing the decomposition of **3a** at room temperature. Initially **3a** was formed by keeping a NMR sample of **1a** with **AB** (3:1 molar ratio) at –40°C over a week; by that time **AB** was completely consumed with concomitant formation of a small amount of **BZ**.

This further substantiated that **CTB** reacts very slowly with **1a**. Nevertheless, if the reaction was carried out at low temperature with 1:2 molar ratio of **1a** to **AB** until the complete formation of **3a** (no free olefin detectable in the mixture) and then warmed up to room temperature, **CTB** would be the only dehydrocoupling product of **AB**. Since in the room temperature reactions of **1a** with **AB** only –BH– species from **BZ** and **PBZ** were observed, they are expected to have been formed directly from dehydrocoupling of $[NH_2{=}BH_2]$ after elimination from **3a**, rather than dehydrogenation of **CTB**.

5.2.7 Mechanism of the double H transfer reaction.

Based on the acquired mechanistic facts, a two–step hydrogen transfer mechanism is proposed for the reactions of polar olefins with **AB** (Scheme 5.7). The first step is the H_B transfer forming a hydroboration intermediate **3**, presumably via the concerted transition state **4**. Subsequently H_N transfer occurred as the RDS, which

might be transferred in an intra-molecular mode as shown in **5** of Scheme 5.7, releasing the reactive iminoborane species [NH_2=BH_2] presumably in the solvent stabilized form [NH_2=BH_2]-(solvent). [NH_2=BH_2] or [NH_2=BH_2]-(solvent) was dehydrogenated subsequently in a fast reaction by another equivalent of **1a** generating **BZ** and **PBZ** as the final dehydrocoupling products, presumably via simultaneous double H transfer as shown in **6** (Scheme 5.7). The cyclic trimer **CTB** can be formed by direct cyclization of [NH_2=BH_2], but only as a side reaction or when the dehydrogenation of [NH_2=BH_2] is slowed down applying low temperature and/or low concentrations of the olefin. Such a mechanistic scheme is anticipated to be applicable to other amine boranes.

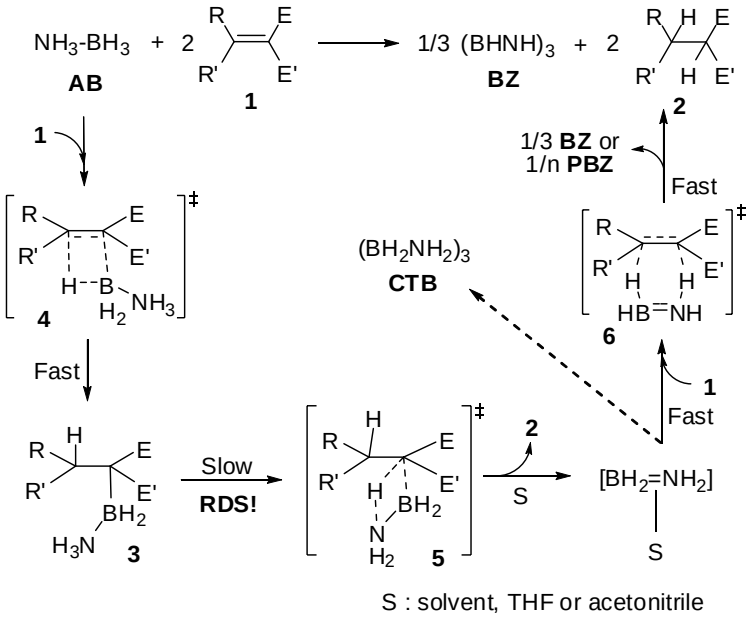

Scheme 5.7 Mechanistic scheme for the transfer hydrogenation of polarized olefins with ammonia borane.

5.3 Conclusions

In conclusion, the transfer hydrogenation of a series of activated olefins, equipped with geminal electron-withdrawing groups on one side of the double bond and H or organyl on the other side, with amine borane adducts as hydrogen donors could be accomplished metal-free under mild conditions. The reaction constant obtained from Hammett correlations indicated that negative charge is accumulated in the transition

state. Together with deuterium kinetic isotope studies and explorations on the hydroboration intermediate, the actual reaction course could be established: primary hydridic H_B transfer occurs rapidly from the borane part to the olefin before the RDS, then the transfer of the protic H_N occurs as the RDS, presumably via a concerted cyclic transition state. The routes to the dehydrocoupling products of ammonia borane were rationalized on the basis that the main product borazine was formed directly from dehydrocoupling of $[NH_2=BH_2]$ or of its solvent stabilized adduct $[NH_2=BH_2]$-(solvent), rather than by dehydrogenation of cyclotriborazane formed by trimerization of $[NH_2=BH_2]$.

We gratefully thank the Swiss National Science Foundation, the Swiss-German joint project 'Unconventional approaches to the activation of dihydrogen' and the University of Zurich for financial support.

5.4 Experimental

All of the hydrogen-transfer reactions were carried out at least twice with reported reproducible results.

All the manipulations were carried out under a nitrogen atmosphere using Schlenk techniques or a drybox (Model MB-150B-G). Reagent grade benzene, toluene, chloroform, diethyl ether, and tetrahydrofuran were dried and distilled from sodium benzophenone ketyl prior to use. Acetonitrile was distilled from CaH_2, and chloroform was dried by P_2O_5. All the amine borane adducts and olefins **1l-1o** are commercially available and purified prior to use. Olefins olefins **1a-1e** were synthesized as described in the other communication.[11] NMR spectra were measured on a Varian Mercury spectrometer at 200 MHz for ^1H, Varian Gemini-2000 spectrometer at 300.1 MHz for ^1H, 96.3 MHz for $^{11}B\{^1H\}$ and 75.5 MHz for $^{13}C\{^1H\}$ and on a Bruker-DRX-500 spectrometer at 500.2 MHz for ^1H, 107 MHz for $^{11}B\{^1H\}$ and 125.8 MHz for $^{13}C\{^1H\}$. Chemical shifts for ^1H and ^{13}C are given in ppm relative to TMS and those for ^{11}B relative to $Et_2O{\cdot}BF_3$. GC-MS was measured on a Varian 450

GC (Saturn 2000 GC/MS/MS).

Olefin **1f**, **1g**, **1j**and **1p-1t** were prepared via the following method with nearly 100% yield: To a stirred solution of 0.01 mol of aldehyde in 0.01 mol of malononitrile (or methylcyanoacetate) was added 3 g of alumina Merck 90. The reaction was exothermic. After the reaction was cooled down, the product was extracted with dichloromethane (2 x 20 ml).[18] The solvent was then removed, leaving a product of a good purity. Generally, the purification was not necessary.

2-(3,4-Dihydronaphthalen-1(2H)-ylidene)malononitrile (**1f**),[19] white solid: δ_H (ppm; 300 MHz; CD_3CN) 1.89-2.14 (m, 2H, -CH_2-), 2.85 (t, J = 6 Hz, 2H, -CH_2-), 2.98 (t, J = 6 Hz, 2H, -CH_2-), 7.33-7.38 (m, 2H), 7.50-7.55 (m, 1H), 8.12 (d, J = 8 Hz, 1H); δ_C (ppm; 75.4 MHz; CD_3CN) 22.64, 30.12, 33.68, 80.45 (=<u>*C*</u>-$(CN)_2$), 114.57 (=C-(<u>*C*</u>N)$_2$), 115.35 (=C-(<u>*C*</u>N)$_2$), 127.36, 128.63, 130.38, 131.10, 134.53, 143.80, 174.39 (<u>*C*</u>=C-$(CN)_2$).

2-(Naphthalen-1-ylmethylene)malononitrile (**1g**),[20] yellow solid: δ_H (ppm; 300 MHz; CD_3CN) 7.60-7.73 (m, 3H), 7.98-8.19 (m, 4H), 8.90 (s, 1H); δ_C (ppm; 75.4 MHz; CD_3CN) 86.58 (=<u>*C*</u>-$(CN)_2$), 113.96 (=C-(<u>*C*</u>N)$_2$), 114.85 (=C-(<u>*C*</u>N)$_2$), 124.24, 126.34, 128.23, 129.13, 129.16, 129.33, 130.04, 131.93, 134.45, 135.22, 160.36 (<u>*C*</u>=C-$(CN)_2$).

(E)-2-(3-Phenylallylidene)malononitrile (**1j**),[20] Yellow solid: δ_H (ppm; 300 MHz; CD_3CN) 7.18-7.23 (m, 1H), 7.25-7.31 (m, 1H), 7.39-7.49 (m, 3H), 7.65-7.70 (m, 2H), 7.81-7.87 (m, 1H); δ_C (ppm; 75.4 MHz; CD_3CN) 83.06 (=<u>*C*</u>-$(CN)_2$), 112.94 (=C-(<u>*C*</u>N)$_2$), 114.93 (=C-(<u>*C*</u>N)$_2$), 123.46, 130.04, 130.19, 132.75, 135.35, 151.53, 162.18 (<u>*C*</u>=C-$(CN)_2$).

(E)-Methyl 2-cyano-3-(4-methoxyphenyl)acrylate (**1p**),[21] white solid: δ_H (ppm; 300 MHz; C_6D_6) 3.84 (s, 3H, -Me), 3.87 (s, 3H, -Me), 7.06 (d, J = 9 Hz, 2H), 8.00 (d, J = 9 Hz, 2H), 8.19 (s, 1H, -C<u>*H*</u>=C(CN)(CO_2Me)); δ_C (ppm; 75.4 MHz; C_6D_6) 53.77 (-Me), 56.49 (-Me), 100.06 (=<u>*C*</u>(CN)(CO_2Me)), 115.78, 117.21 (-<u>*C*</u>N), 125.28, 134.49,

155.33 (-<u>*C*</u>H=C(CN)(CO_2Me)), 164.32, 164.88 (<u>*C*</u>O_2Me).

(E)-Methyl 2-cyano-3-(4-(dimethylamino)phenyl)acrylate (**1q**),[22] orange solid: δ_H (ppm; 300 MHz; $CDCl_3$) 3.12 (s, 6H, -NMe_2), 3.90 (s, 3H, -Me), 6.67-6.70 (m, 2H), 7.91-7.94 (m, 2H), 8.07 (s, 1H, -C<u>*H*</u>=C(CN)(CO_2Me)); δ_C (ppm; 75.4 MHz; $CDCl_3$) 40.01 (-NMe_2), 52.78 (-Me), 93.41 (=<u>*C*</u>(CN)(CO_2Me)), 111.45, 117.56 (-<u>*C*</u>N), 119.25, 134.07, 153.58 (-<u>*C*</u>H=C(CN)(CO_2Me)), 154.68, 164.73 (<u>*C*</u>O_2Me).

(E)-Methyl 3-(4-chlorophenyl)-2-cyanoacrylate (**1r**),[21] white solid: δ_H (ppm; 300 MHz; CD_3CN) 3.87 (s, 3H, -Me), 7.54 (d, J = 8 Hz, 2H), 7.96 (d, J = 8 Hz, 2H), 8.25 (s, 1H, -C<u>*H*</u>=C(CN)(CO_2Me)); δ_C (ppm; 75.4 MHz; CD_3CN) 54.11 (-Me), 104.54 (=<u>*C*</u>(CN)(CO_2Me)), 116.31 (-<u>*C*</u>N), 130.46, 131.34, 133.26, 139.66, 154.40 (-<u>*C*</u>H=C(CN)(CO_2Me)), 163.52 (<u>*C*</u>O_2Me).

(E)-Methyl 2-cyano-3-(4-nitrophenyl)acrylate (**1s**),[23] milk-yellow solid: δ_H (ppm; 300 MHz; $CDCl_3$) 3.99 (s, 3H, -Me), 8.12-8.15 (m, 2H), 8.32-8.37 (m, 3H); δ_C (ppm; 75.4 MHz; $CDCl_3$) 53.85 (-Me), 106.87 (=<u>*C*</u>(CN)(CO_2Me)), 114.44 (-<u>*C*</u>N), 124.29, 131.51, 136.75, 149.72, 151.95 (-<u>*C*</u>H=C(CN)(CO_2Me)), 161.86 (<u>*C*</u>O_2Me).

(E)-Methyl 2-cyano-3-(4-cyanophenyl)acrylate (**1t**),[23] white solid: δ_H (ppm; 300 MHz; $CDCl_3$) 3.98 (s, 3H, -Me), 7.78-7.81 (m, 2H), 8.05-8.08 (m, 2H), 8.26 (s, 1H); δ_C (ppm; 75.4 MHz; $CDCl_3$) 53.80 (-Me), 106.26 (=<u>*C*</u>(CN)(CO_2Me)), 114.54, 116.05 (-<u>*C*</u>N), 117.64 (-<u>*C*</u>N), 131.00, 132.82, 135.09, 152.47 (-<u>*C*</u>H=C(CN)(CO_2Me)), 161.97 (<u>*C*</u>O_2Me).

Olefin 2,2'-(1H-indene-1,3(2H)-diylidene)dimalononitrile (**1h**) was prepared via the following method:[24] A solution of indane-1,3-dione (0.48 g, 3.2 mmol), malononitrile (0.54 g, 8.2 mmol) and ammonium acetate (0.25 g, 3.2 mmol) dissolved in absolute ethanol (6 mL) was heated at reflux for 30 min. After cooling to room temperature, water (5 mL) was added and the solution acidified with concentrated hydrochloric acid. The brown precipitate was filtered off and washed with water. Recrystallisation from glacial acetic acid afforded compound **1h** (0.35 g, 45%) as a

brown yellow crystal. 2,2'-(1H-Indene-1,3(2H)-diylidene)dimalononitrile (**1h**):[24] δ_H (ppm; 300 MHz; CD_3CN) 4.31 (s, 2H, -C$\underline{H_2}$-), 7.93-9.96 (m, 2H), 8.53-8.56 (m, 2H); δ_C (ppm; 75.4 MHz; CD_3CN) 42.94 (-$\underline{C}H_2$-), 79.10 (=$\underline{C}(CN)_2$), 113.07 (-$\underline{C}$N), 113.29 (-$\underline{C}$N), 127.33, 137.03, 141.70, 167.92 (-$\underline{C}$H=C(CN)$_2$).

Olefin 2-(3-ethoxy-1H-inden-1-ylidene)malononitrile (**1i**) was prepared via the following method:[24] A solution of indane-l,3-dione (0.4 g, 2.74 mmol), malononitrile (0.45 g, 6.8 mmol) and ammonium acetate (60 mg, 0.78 mmol) dissolved in absolute ethanol (20 mL) was heated at reflux for 24 h. The solvent was removed in vacuo, leaving a purple solid from which a red product was extracted with boiling light petroleum (b.p. 40-60 ^oC). Recrystallisation of the red product in light petroleum afforded compound **1i** (10 mg, 10%) as a bright red powder. 2-(3-Ethoxy-1H-inden-1-ylidene)malononitrile (**1i**):[24] δ_H (ppm; 300 MHz; CD_3CN) 1.45 (t, *J* = 7 Hz, 3H, -Me), 4.34 (q, *J* = 7 Hz, 2H, -OC$\underline{H_2}$-), 5.75 (s, 1H), 7.28-7.31 (m, 1H), 7.37-7.46 (m, 2H), 7.98-8.00 (m, 1H); δ_C (ppm; 75.4 MHz; CD_3CN) 14.48 (-Me), 69.93 (-O$\underline{C}H_2$-), 70.08 (=$\underline{C}(CN)_2$), 97.75 (-$\underline{C}$H=C-OEt), 114.77 (-$\underline{C}$N), 121.00, 124.89, 131.32, 133.37, 138.65, 166.84 (-CH=$\underline{C}$-OEt), 173.46 (-$\underline{C}$H=C(CN)$_2$).

Olefin cyclohepta-2,4,6-trienylidene)malononitrile (**1k**) was prepared via the following method:[25] An oven-dried 50 mL three-necked round-bottomed flask, equipped with a nitrogen gas inlet, magnetic stirring bar, dropping funnel, thermometer, and condenser, under an inert nitrogen atmosphere, was placed in an ice bath and charged, while stirring, with 10 mL of pyridine and 0.9 g (5 mmol) of cycloheptatrienylium tetrafluoroborate at 0 °C. Bromomalononitrile (0.73 g, 5 mmol) is added drop by drop within a 10-min period, and the mixture is vigorously stirred at that temperature for 1 hr. The ice bath is replaced by a water bath, the temperature is gradually raised to 40°C, and the stirring mixture is kept at that temperature for 5 hr. The solution was acidified with 1 M HCl solution and the organic phase was extracted with chloroform. The final product **1k** was obtained as red powder by column chromatography eluted with hexane: ethyl ester = 1 : 5 (yield: 60%).δ_H (ppm; 300 MHz; THF-D_8) 6.96-7.11 (m, 4H), 7.32-7.37 (d*m, 2 H, *J* = 12

Hz); δ_C (ppm; 300 MHz; THF-D_8) 115.10 (-<u>C</u>N), 135.76, 138.47, 140.15, 164.47 (-<u>C</u>H=C(CN)$_2$).

Gerneral procedure for the transfer hydrogenation reactions: In a glove-box, a 0.5 mm Young NMR tube was charged with olefin (0.1 mmol), amine-borane adducts (0.1 mmol) and dry THF-D_8 or acetonitrile-D_3 (0.6 mL). The tube was sealed with the screw cap and then lay at room temperature or the required temperature after shaking. The reaction was monitored by ^{1}H NMR and ^{11}B NMR every several minutes (depends on the reaction rate). The typical resonance of the starting materials decreased, and a new signal of the saturated products gradually appeared. The disappearance of the starting olefin indicates that the transformation has completed, ^{13}C and ^{11}B NMR spectra were then recorded. Finally the reaction mixture was diluted for GC-MS analysis. Samples for low-temperature NMR were prepared at room temperature using chilled solvents, and immediately put into low-temerature fridges until taken for NMR.Samples for kinetic study were prepared with pseudo-first order conditions with the 0.1 mmol **AB** and the olefin in great excess (0.5 mmol).

All the hydrogenated products were described before, and the obtained NMR data match literature values.

2-Cyclohexylmalononitrile (**2a**),[26] colorless liquid, δ_H (ppm; 300 MHz; THF-D_8) 1.15-1.44 (m, 5 H, -CH-), 1.69-2.06 (m, 6 H, -CH-), 4.25 (d, J = 5 Hz, 1 H, -CH-); δ_C (ppm; 300 MHz; THF-D_8) 26.34, 26.41, 29.57, 30.76, 40.06, 113.64 (2 C, -CN); MS (m/z) = 149.

Methyl 2-cyano-2-cyclohexylacetate (**2b**),[27] colorless liquid: δ_H (ppm; 300 MHz; CD_3CN) 1.08-1.35 (m, 5 H, -CH-), 1.63-1.82 (m, 5 H, -CH-), 1.94-2.07 (m, 1 H, -CH-), 3.64 (d, J = 5 Hz, 1 H, -CH-), 3.74 (s, 3 H, -Me); δ_C (ppm; 75.4 MHz; CD_3CN) 26.27, 26.34, 26.51, 30.00, 31.62, 39.43, 45.11, 53.83, 117.10 (-CN), 167.60 (-C=O); MS (m/z) = 181.

2-benzylmalononitrile (**2c**),[19, 26-28] slightly yellow solid: δ_H (ppm; 300 MHz;

THF-D_8) 3.31 (d, J = 7 Hz, 2 H, -CH_2-), 4.59 (t, J = 7 Hz, 1 H, -CH-), 7.32-7.38 (m, 5 H, -CH=); δ_C (ppm; 75.4 MHz; THF-D_8) 25.25, 36.91, 114.19 (-CN), 128.90, 129.61, 130.19, 135.65; MS (m/z) = 156.

Methyl 2-cyano-3-phenylpropanoate (**2d**),[19, 27, 29] white solid: δ_H (ppm; 300 MHz; CD_3CN) 3.10-3.32 (m, 2 H, -CH_2-), 3.74 (s, 3 H, -Me), 4.01-4.13 (m, 1 H, -CH-), 7.25-7.41 (m, 5 H, -CH=); δ_C (ppm; 75.4 MHz; CD_3CN) 35.47, 39.80, 53.53, 117.07 (-CN), 127.96, 129.11, 129.59, 136.55, 166.89 (-C=O); MS (m/z) = 189.

Dimethyl 2-benzylmalonate (**2e**),[19, 30] colorless liquid: δ_H (ppm; 300 MHz; CD_3CN) 3.13-3.17 (d, J = 8 Hz, 2 H, -CH_2-), 3.63 (s, 6 H, -Me), 3.71 (t, J = 8 Hz, 1 H, -CH-), 7.09-7.36 (m, 5 H, -CH=); δ_C (ppm; 75.4 MHz; CD_3CN) 35.30, 53.04, 54.35, 127.70, 129.46, 129.76, 139.03, 170.12 (-C=O); MS (m/z) = 223.

2-(1,2,3,4-Tetrahydronaphthalen-1-yl)malononitrile (**2f**),[19, 31] white solid: δ_H (ppm; 300 MHz; CD_3CN) 1.67-1.81 (m, 1 H), 1.85-2.07 (m, 2H), 2.20-2.30 (m, 1H), 2.72-2.89 (m, 2H), 3.56-3.62 (m, 1H, -CH-), 4.63 (d, J = 5.5 hz, 1H, -$CH(CN)_2$), 7.16-7.30 (m, 4 H,=CH-); δ_C (ppm; 75.4 MHz; CD_3CN) 20.99, 27.74, 29.78, 30.44, 39.44, 114.10 (-CN), 114.30 (-CN), 127.21, 128.66, 128.74, 130.71, 133.73, 139.52; MS (m/z) = 196.

2-(Naphthalen-1-ylmethyl)malononitrile (**2g**),[32] white solid: δ_H (ppm; 300 MHz; CD_3CN) 3.81-3.84 (m, 2H, -CH_2-), 4.48-4.54 (m, 1H, -$CH(CN)_2$), 7.49-7.63 (m, 4H), 7.90-7.97 (m, 2H), 8.11-8.14 (m, 1H); δ_C (ppm; 75.4 MHz; CD_3CN) 24.60, 32.70, 113.91 (-CN), 123.68, 125.93, 126.69, 127.16, 128.81, 129.38, 129.46, 130.82, 131.74, 134.36; MS (m/z) = 206.

Dicyano(1-(dicyanomethylene)-1H-inden-3-yl)methanide (**2h**), purple solid: δ_H (ppm; 300 MHz; CD_3CN) 5.73 (s, 1 H, -C*H*=C($C(CN)_2^-$)-), 7.32-7.36 (m, 2H), 7.92-7.96 (m, 2H); δ_C (ppm; 75.4 MHz; CD_3CN) 104.19 (-*C*H=C($C(CN)_2^-$)-), 119.11 (-CN), 119.27 (-CN), 122.68, 124.93, 126.38, 130.65, 139.46, 159.75 (-*C*=$C(CN)_2$); (-)MS (m/z) = 241.

2-(3-Ethoxy-1H-inden-1-yl)malononitrile (**2i**), purple solid: δ_H (ppm; 300 MHz; CD_3CN) 1.67-1.81 (m, 1 H), 1.85-2.07 (m, 2H), 2.20-2.30 (m, 1H), 2.72-2.89 (m, 2H), 3.56-3.62 (m, 1H, -CH-), 4.63 (d, *J* = 5.5 hz, 1H, -$CH(CN)_2$), 7.16-7.30 (m, 4 H,=CH-); δ_C (ppm; 75.4 MHz; CD_3CN) 14.69, 27.58, 45.67, 66.81, 98.24, 119.66 (-CN), 124.39, 126.48, 128.10, 128.85, 129.66, 161.35; MS (m/z) = 224.

2-Cinnamylmalononitrile (**2j**),[26, 28] white solid: δ_H (ppm; 300 MHz; CD_3CN) 2.92-2.97 (m, 2H, -CH_2-), 4.28-4.32 (m, 1H, -$CH(CN)_2$), 6.24-6.35 (m, 1H, =CH-), 6.73-6.78 (m, 1H, =CH-), 7.26-7.51 (m, 5H); δ_C (ppm; 75.4 MHz; CD_3CN) 24.41, 34.41, 114.45 (-CN), 122.62, 127.39, 129.12, 129.31, 129.68, 136.65; MS (m/z) = 182.

Methyl 2-cyano-3-(4-methoxyphenyl)propanoate (**2p**),[19, 26, 29] white solid: δ_H (ppm; 300 MHz; CD_3CN) 3.14-3.28 (m, 2H, -CH_2-), 3.74 (s, 3H, -CH_3), 4.01-4.08 (m, 1H, -$CH(CN)_2$), 7.31-7.37 (m, 5H); δ_C (ppm; 75.4 MHz; CD_3CN) 35.99, 40.32, 54.07, 117.62 (-CN), 128.53, 129.67, 130.15, 137.11, 167.47; MS (m/z) = 219.

Methyl 2-cyano-3-(4-(dimethylamino)phenyl)propanoate (**2q**),[28] yellow solid: δ_H (ppm; 300 MHz; CD_3CN) 2.89 (s, 6H, -$N(CH_3)_2$), 3.01-3.16 (m, 2H, -CH_2-), 3.73 (s, 3H, -CH_3), 3.92-3.96 (m, 1H, -$CH(CN)_2$), 6.69-6.72 (m, 2H), 7.08-7.11 (m, 2H); δ_C (ppm; 75.4 MHz; CD_3CN) 35.38, 40.72, 40.81, 53.92, 113.47, 117.84, 124.13, 130.70, 151.21, 167.63; MS (m/z) = 232.

Methyl 3-(4-chlorophenyl)-2-cyanopropanoate (**2r**),[28-29] white solid: δ_H (ppm; 300 MHz; CD_3CN) 3.17-3.33 (m, 2H, -CH_2-), 3.79 (s, 3H, -CH_3), 4.06-4.11 (m, 1H, -$CH(CN)_2$), 7.29-7.44 (m, 4H); δ_C (ppm; 75.4 MHz; CD_3CN) 34.67, 39.56, 53.60, 116.90 (-CN), 129.08, 131.35, 133.35, 135.43, 166.69; MS (m/z) = 223.

Methyl 2-cyano-3-(4-nitrophenyl)propanoate (**2s**),[19, 28, 33] white solid: δ_H (ppm; 300 MHz; CD_3CN) 3.31-3.47 (m, 2H, -CH_2-), 3.80 (s, 3H, -CH_3), 4.16-4.21 (m, 1H, -$CH(CN)_2$), 7.56-7.59 (d, *J* = 10 Hz, 2H), 8.22-8.25 (d, *J* = 10 Hz, 2H); δ_C (ppm; 75.4 MHz; CD_3CN) 34.82, 39.00, 53.73, 116.69 (-CN), 124.11, 130.85, 144.20, 166.45;

MS (m/z) = 235.

Methyl 2-cyano-3-(4-cyanophenyl)propanoate (**2t**),[34] white solid: δ_H (ppm; 300 MHz; CD_3CN) 3.25-3.43 (m, 2H), 3.79 (s, 3H, $-CH_3$), 4.11-4.17 (m, 1H, $-CH(CN)_2$), 7.49-7.53 (m, 2H), 7.74-7.78 (m, 2H); δ_C (ppm; 75.4 MHz; CD_3CN) 35.15, 39.05, 53.70, 111.61, 116.71 (-CN), 118.96, 130.61, 132.92, 142.14, 166.48; MS (m/z) = 214.

5.5 References

[1] H. Berke, *ChemPhysChem* **2010**, *11*, 1837-1849.

[2] a) G. Brieger and T. J. Nestrick, *Chemical Reviews* **1974**, *74*, 567-580; b) R. A. W. Johnstone, A. H. Wilby and I. D. Entwistle, *Chemical Reviews* **1985**, *85*, 129-170; c) S. Gladiali and E. Alberico, *Chemical Society Reviews* **2006**, *35*, 226-236; d) J. S. M. Samec, J. E. Backvall, P. G. Andersson and P. Brandt, *Chemical Society Reviews* **2006**, *35*, 237-248.

[3] a) D. J. Miller, D. M. Smith, B. Chan and L. Radom, *Molecular Physics* **2006**, *104*, 777-794; b) C. Rüchardt, M. Gerst and J. Ebenhoch, *Angewandte Chemie International Edition in English* **1997**, *36*, 1406-1430.

[4] a) T. van Es and B. Staskun, *Org. Syn.* **1988**, *6*, 631; b) H. Wiener, J. Blum and Y. Sasson, *Journal of Organic Chemistry* **1991**, *56*, 4481-4486.

[5] a) C. A. Jaska and I. Manners, *J. Am. Chem. Soc.* **2004**, *126*, 2698-2699; b) T. J. Clark, K. Lee and I. Manners, *Chem. Eur. J.* **2006**, *12*, 8634-8648; c) Y. Jiang and H. Berke, *Chem. Commun.* **2007**, 3571; d) Y. Jiang, O. Blacque, T. Fox, C. M. Frech and H. Berke, *Organometallics* **2009**, *28*, 5493-5504.

[6] a) A. Staubitz, A. P. M. Robertson, M. E. Sloan and I. Manners, *Chem. Rev.* **2010**, *110*, 4023-4078; b) A. Staubitz, A. P. M. Robertson and I. Manners, *Chem. Rev.* **2010**, *110*, 4079-4124.

[7] a) N. C. Smythe and J. C. Gordon, *Eur. J. Inorg. Chem.* **2010**, 509-521; b) A. D. Sutton, A. K. Burrell, D. A. Dixon, E. B. Garner, J. C. Gordon, T. Nakagawa, K. C. Ott, J. P. Robinson and M. Vasiliu, *Science* **2011**, *331*, 1426-1429.

[8] V. Pons, R. T. Baker, N. K. Szymczak, D. J. Heldebrant, J. C. Linehan, M. H. Matus, D. J. Grant and D. A. Dixon, *Chemical Communications* **2008**, 6597-6599.

[9] R. P. Shrestha, H. V. K. Diyabalanage, T. A. Semelsberger, K. C. Ott and A. K. Burrell, *International Journal of Hydrogen Energy* **2009**, *34*, 2616-2621.

[10] X. H. Yang, L. L. Zhao, T. Fox, Z. X. Wang and H. Berke, *Angewandte Chemie-International Edition* **2010**, *49*, 2058-2062.

[11] X. H. Yang, T. Fox and H. Berke, *Chem. Commun.* **2011**, *47*, 2053-2055.

[12] C. Reichardt in *Solvents and Solvent Effects in Organic Chemistry*, *Vol.* WILEY-VCH Verlag GmbH & Co. KGaA, Weinheim, **2003**.

[13] M. E. Sloan, A. Staubitz, T. J. Clark, C. A. Russell, G. C. Lloyd-Jones and I. Manners, *J. Am. Chem. Soc.* **2010**, *132*, 3831-3841.

[14] a) C. P. Casey and J. B. Johnson, *J. Org. Chem.* **2003**, *68*, 1998-2001; b) T. Giagou and M. P. Meyer, *Chem. Eur. J.* **2010**, *16*, 10616-10628; c) C. P. Casey, S. W. Singer, D. R. Powell, R. K. Hayashi and M. Kavana, *J. Am. Chem. Soc.* **2001**, *123*, 1090-1100.

[15] a) S. R. Emamian, M. Aghaie, M. R. Zardoost, E. Zahedi and K. Zare, *Molecular Simulation* **2010**, *36*, 978-985; b) S. R. Reddy and P. Manikyamba, *Asian Journal of Chemistry* **2008**, *20*, 195-199; c) D. S. Bhuvaneshwari and K. P. Elango, *Zeitschrift Fur Naturforschung Section B-a Journal of Chemical Sciences* **2006**, *61*, 1254-1260.

[16] a) L. P. Hammett, *J. Am. Chem. Soc.* **1937**, *59*, 96-103; b) L. P. Hammett, *Chemical Reviews* **1935**, *17*, 125-136.

[17] A. C. Hopkinson, *Journal of the Chemical Society B: Physical Organic* **1969**, 203-205.

[18] F. Texier-Boullet and A. Foucaud, *Tetrahedron Letters* **1982**, *23*, 4927-4928.

[19] D. Xue, Y.-C. Chen, X. Cui, Q.-W. Wang, J. Zhu and J.-G. Deng, *J. Org. Chem.* **2005**, *70*, 3584-3591.

[20] D.-Z. Xu, Y. Liu, S. Shi and Y. Wang, *Green Chem.* **2010**, *12*, 514-517.

[21] S. Sorgel, N. Tokunaga, K. Sasaki, K. Okamoto and T. Hayashi, *Org. Lett.* **2008**, *10*, 589-592.

[22] M. A. Haidekker, T. P. Brady, S. H. Chalian, W. Akers, D. Lichlyter and E. A. Theodorakis, *Bioorg. Chem.* **2004**, *32*, 274-289.

[23] S. Wada and H. Suzuki, *Tetrahedron Lett.* **2003**, *44*, 399-401.

[24] A. S. Batsanov, M. R. Bryce, S. R. Davies, J. A. K. Howard, R. Whitehead and B. K. Tanner, *J. Chem. Soc., Perkin Trans. 2* **1993**, 313-319.

[25] H. Takeshita, A. Mori and K. Kibo, *Org. Synth.* **1998**, *75*, 210-214.

[26] J. Wang, G. Song, Y. Peng and Y. Zhu, *Tetrahedron Letters* **2008**, *49*, 6518-6520.

[27] D. B. Ramachary, M. Kishor and Y. V. Reddy, *European Journal of Organic Chemistry* **2008**, *2008*, 975-993.

[28] F. Tayyari, D. E. Wood, P. E. Fanwick and R. E. Sammelson, *Synthesis* **2008**, 279-285

[29] S. Nakamura, H. Sugimoto and T. Ohwada, *The Journal of Organic Chemistry* **2008**, *73*, 4219-4224.

[30] D. B. Ramachary, C. Venkaiah, Y. V. Reddy and M. Kishor, *Org. Biomol. Chem.* **2009**, *7*, 2053-2062

[31] Y.-C. Chen, T.-F. Wu, L. Jiang, J.-G. Deng, H. Liu, J. Zhu and Y.-Z. Jiang, *The Journal of Organic Chemistry* **2005**, *70*, 1006-1010.

[32] E. Campaigne, D. R. Maulding and W. L. Roelofs, *The Journal of Organic Chemistry* **1964**, *29*, 1543-1549.

[33] Z. Rappoport and B. Avramovitch, *The Journal of Organic Chemistry* **1982**, *47*, 1397-1408.

[34] Z. Zhang, J. Gao, J.-J. Xia and G.-W. Wang, *Organic & Biomolecular Chemistry* **2005**, *3*, 1617-1619.

Ammonia Borane as a Metal Free Reductant for Ketones and Aldehydes: A Mechanistic Study

6.1 Introduction

Ammonia borane (NH_3BH_3, **AB**) has attracted great attention as a potential hydrogen storage material with very high volumetric and gravimetric storage densities.[1] Chemical H_2 storage requires reactions for fueling and re-fueling of the storage compounds. In this context intensive studies were carried out on the dehydrogenations of **AB**,[2] either thermally,[3] catalytically[4] or by other methods.[5] Besides these dehydrogenation reactions, we became interested in its use as an *in situ* hydrogen source for direct reduction of polar unsaturated compounds, which constitutes an important fundamental reaction mode of organic synthesis.

We have previously reported that polarized olefins such as 2-cyclohexylidene-malononitrile can be hydrogenated by **AB** as a hydrogen donor without use of a catalyst.[6] A hydroboration intermediate **HBI** was detected in low temperature NMR studies indicating a two step mechanism with hydride before proton transfer (Scheme 6.1).[7]

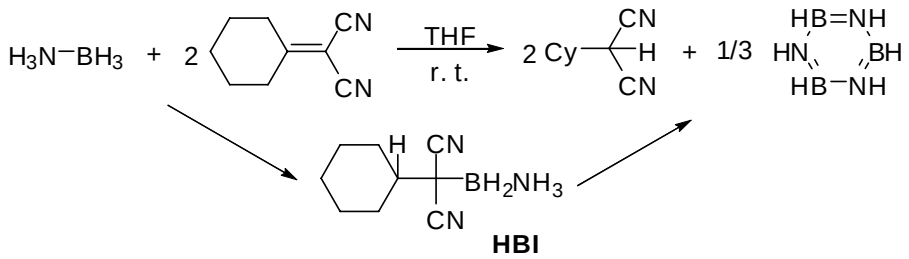

Scheme 6.1 Transfer hydrogenation of polarized olefin by **AB** *via* the hydroboration intermediate **HBI**.

Hydrogenation of aromatic imines bearing polar C=N double bonds could also be achieved applying **AB**.[6] Detailed mechanistic studies revealed a 'polarity matched' concerted pathway with a double-hydrogen transfer process.

Ketones and aldehydes, possessing a polarized C=O bond related to imines, were now subjected to reactions with **AB**. We presumed mechanistic analogies for all these H transfer processes.

6.2 Results and discussions

6.2.1 Reactions of ketones and aldehydes with AB in THF

Benzophenone (**1a**) indeed reacts with **AB** in THF at room temperature, but at a rather low rate, which could naturally be accelerated by heating (Table 6.1, entry 1). However, diphenylmethanol (**2a**) originating from transfers of the H_B and H_N atoms of **AB** could not be detected by *in situ* NMR investigations (Scheme 6.2). The ^{11}B NMR spectrum revealed that an alkyl borate was formed (signal at 19 ppm in ^{11}B NMR). ^{1}H and ^{13}C NMR studies confirmed that hydroboration of **1a** had taken place establishing the tribenzhydryl borate **3a** (Scheme 6.2). Related hydroboration reactions were also reported from the reactions of ketones with other B-H containing compounds.[9] Only H_B and not H_N of **AB** seemingly got involved in the reaction, since a broad signal appeared in the ^{1}H NMR spectra at 0.4 ppm belonging to free ammonia (NH_3).

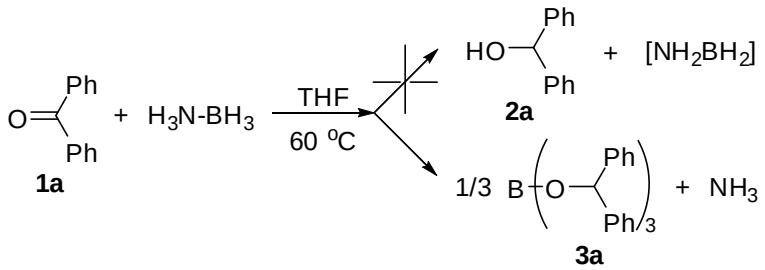

Scheme 6.2 Reaction of benzophenone (**1a**) with **AB** in THF at 60 °C producing **3a** via hydroboration.

Reactions of **AB** with various ketones were carried out to yield the corresponding hydroboration products (Table 6.1). In most of the ketone reactions temperatures of 60 °C were required and the reactions were completed within several hours (Table 6.1, entries 1-6). Cyclohexanone **1g** was the only exception among the tested ketones, which was converted by **AB** under milder conditions requiring only half an hour at

room temperature (Table 6.1, entry 7).

Table 6.1 Hydroboration of ketones with **AB**.

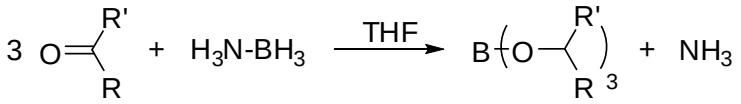

1 **3**

Entry	Substrate		Temperature	Time [a]
1	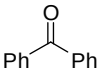	**1a**	r.t. 60 °C	1 d 2 h
2	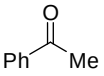	**1b**	60 °C	1.5 h
3	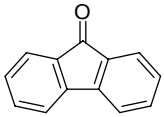	**1c**	60 °C	1.5 h
4	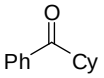	**1d**	60 °C	4 h
5 [b]	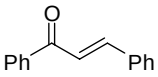	**1e**	60 °C	10 h
6		**1f**	60 °C	1 h
7	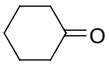	**1g**	r.t.	0.5 h

[a] Required reaction time for completely hydroboration of the ketones by **AB** with 2:1 molar ratio (**AB** in slightly excess); [b] The hydroboration reaction occurred mainly at the C=O bond.

The hydroboration reactions were found to be much faster with aldehydes than with ketones. Benzaldehyde (**1h**) was completely hydroborated at room temperature in less than half an hour (Table 6.2, entry 1). Beside the tribenzyl borate **3h**, acetal derived borate esters were additionally obtained even in presence of excess **AB**. The more reactive aldehyde **1h** seemed to undergo a follow-up process. NMR studies revealed the existence of new borate esters bearing $PhCH_2$-O-CH-O units like in **4h**, formed via a subsequent step or steps of **3h** with **1h** (Scheme 6.3).[10] The exact composition of **4h**, in particular whether n = 1 or 2 could not be determined due to the instability of the borate compound to GC, MS, column chromatography and severe signal overlaps in the ^{11}B NMR and ^{1}H NMR spectra.

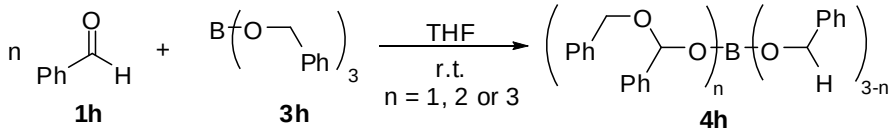

1h **3h** **4h**

Scheme 6.3 Insertion reactions of benzaldehyde (**1h**) into tribenzyl borate (**3h**) forming the borate esters **4h**.

Similar reactions were observed in the hydroborations of other aldehydes with **AB** varying however in the product ratios of type **3** and **4** compounds (Table 6.2, 'n' assumed to be 1).

Table 6.2 Hydroboration of aldehydes with **AB**.

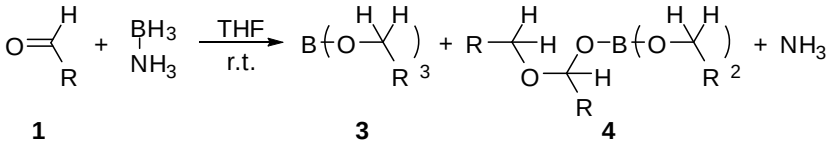

1 **3** **4**

Entry	Substrate		Time [a]	**3** / **4** [b]
1	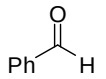	**1h**	0.5 h	0.6 / 0.4
2	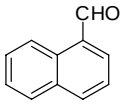	**1i**	< 0.5 h	0.8 / 0.2
3	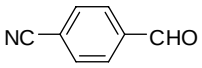	**1j**	< 5 min	0.7 / 0.3
4	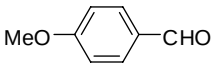	**1k**	1.5 h	0.7 / 0.3
5	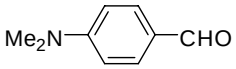	**1l**	> 2 d	0.8 / 0.2

[a] Required reaction time for completely hydroboration of the aldehydes by **AB** with 2:1 molar ratio of aldehydes to **AB**; [b] The molar ratio of the borate esters **3** to **4** were determined by integrations of the -O-C*H*-O- in compassion to that of the -CH_2-O- portion of the *in situ* ^{1}H NMR spectra.

It is worth mentioning that we tested the reaction of **AB** with phenylmethanol **2h** which was found to be very slow, only trace amounts of **3h** were observed in the ^{11}B NMR spectrum after several hours even at 60 ^{o}C. Since no alcohol **2h** was detected in the reaction mixture of **1h** with **AB** in THF, the formation of **3h** via the subsequent reaction of **2h** with **AB** was excluded to proceed.

6.2.2 Reactions of ketones and aldehydes with AB in methanol

Alcohol metathesis of the trialkyl borates in methanol was a convenient way to set the alcohols from the trialkyl borates.[9b] In this context it should be mentioned that the direct alcoholysis of **AB** always needs a transition metal catalyst.[11] In addition the methanolysis of the borate ester could accelerate the hydroboration process under certain kinetic circumstances. Therefore, **AB** was put in methanol together with **1h**. Compound **2h** and trimethyl borate were formed spontaneously at room temperature, while the acetal derivatives (alcoholysis products of **4h**) were nearly undetectable (Scheme 6.4). On total the formation of **2h** constitutes by hydrogenation of **1h** via consecutive transfer of hydride and proton.

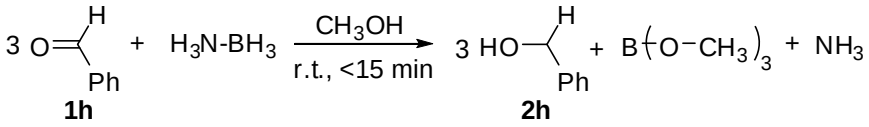

Scheme 6. 4 Metal free methanolysis of **AB** and hydrogenation of benzaldehyde **1h**.

This metal free methanolysis of **AB** was tested by NMR scale reactions with a broad range of ketones and aldehydes using deuterated methanol. In all cases the corresponding alcohol and trimethyl borate were obtained nearly quantitatively (Table 6.3), and the reactions became faster than the hydroborations in THF, only several minutes to several hours were required at room temperature.

The acceleration might come about via hydrogen bonding of methanol in crucial transition states of the hydroboration step, or via formation of a $MeOH{\cdot}BH_3$ complex from **AB** which undergoes double H transfer to the substrate with a complete switch in the mechanism.[12] Unfortunately these two mechanisms cannot easily be distinguished by the tool of isotopic substitution as applied to unravel the mechanisms for the hydroboration reactions in THF. The enormous acceleration is explained on the basis of the appearance of a new double H transfer transition state, apparently low-lying in energy (Scheme 6.5).

Table 6.3 Hydrogenation of ketones and aldehydes with **AB** in methanol-D_4.

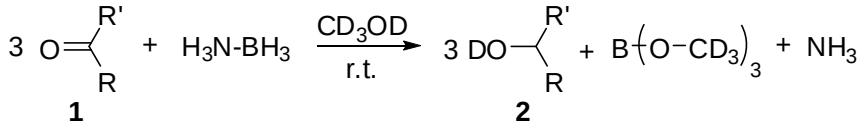

1 **2**

Entry	Substrate	Product	Time [a]
1	**1a**	**2a**	3 h
2	**1b**	**2b**	6 h
3	**1c**	**2c**	1 h
4	**1d**	**2d**	4 h
5	**1e**	**2e**	6 h
6	**1f**	**2f**	2 h
7	**1g**	**2g**	15 min
8[b]	**1h**	**2h**	10 min
9	**1i**	**2i**	10 min
10	**1j**	**2j**	< 5 min
11	**1k**	**2k**	1 h
12	**1l**	**2l**	1 d

[a] Required reaction time for completely hydrogenation of the unsaturated substrates **1** by **AB** with 2:1 molar ratio of **1** to **AB**; [b] The formation of the acetal derived alcohol was not obtained to the limit of NMR, neither for other aldehydes.

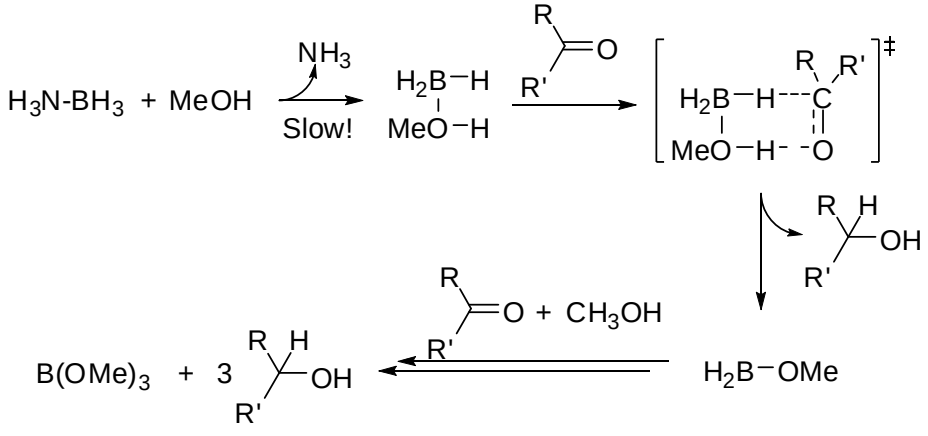

Scheme 6.5 Possible reaction route for transfer hydrogenation of carbonyl compounds by **AB** in methanol.

6.3 Mechanistic studies of the hydroboration process

6.3.1 Deuterium labeling and kinetic isotope effects

Further studies were envisaged to clarify the way of the H_B atoms transfer and potentially also the transfer of the H_N atoms of **AB** in THF. Benzophenone **1a** was exemplarily employed to react with deuterated **AB** derivatives BD_3NH_3 (**AB(D)**), BH_3ND_3 (**A(D)B**) and BD_3ND_3 (**A(D)B(D)**) in THF at 60 ^oC, respectively. The reactions were pursued by various NMR spectroscopies.

In the reaction of **1a** with **AB(D)**, a D_C signal was observed at 6.4 ppm in the ^2H NMR spectrum and a C_D triplet in the ^{13}C NMR spectrum, which corresponded to the -CD-O- fragment of the borate ester **3a**. From the reaction with **A(D)B**, only a D_N signal was observed at 0.4 ppm in the ^2H NMR spectrum, which was expected to belong to the ND_3 unit. In the sample reacted with **A(D)B(D)**, no signals other than the mentioned D_C and D_N resonances were observed. Such findings exclude the formation of diphenylmethanol **2a**, which would be expected as the product of a transfer hydrogenation process.

The deuterium kinetic isotope effects (DKIE) were then investigated using excess amounts of **1a** to react with deuterated **AB** derivatives in THF at 60 ^oC (Figure 6.1). Small primary DKIE values ($k_{AB}/k_{AB(D)}$ = 1.28 and $k_{A(D)B}/k_{A(D)B(D)}$ = 1.10) were determined with the ratios of the H_B/D_B transfer rates indicating that the cleavages of the B-H bonds were only to some minor extent involved in the rate determining step (RDS).[13] Since there are three B-H bonds broken during the reaction course, the small DKIE may in addition suggest that only one of the B-H bonds breakage had kinetic influence.

Normal DKIE values ($k_{AB}/k_{A(D)B}$ = 1.74 and $k_{AB(D)}/k_{A(D)B(D)}$ = 1.49) were observed in the reactions with the H_N/D_N derivative (Figure 6.1). Since D_N incorporation was not detected in the product, it is supposed that the dissociation of NH_3 from **AB** became involved in the RDS exerting a secondary kinetic isotope effect.

This would cope with related reports by H. C. Brown and Chandrasekharan.[14] For a secondary DKIE the given values were however large,[15] presumably due to relatively strong dihydrogen bonding in the respective transition state.[16]

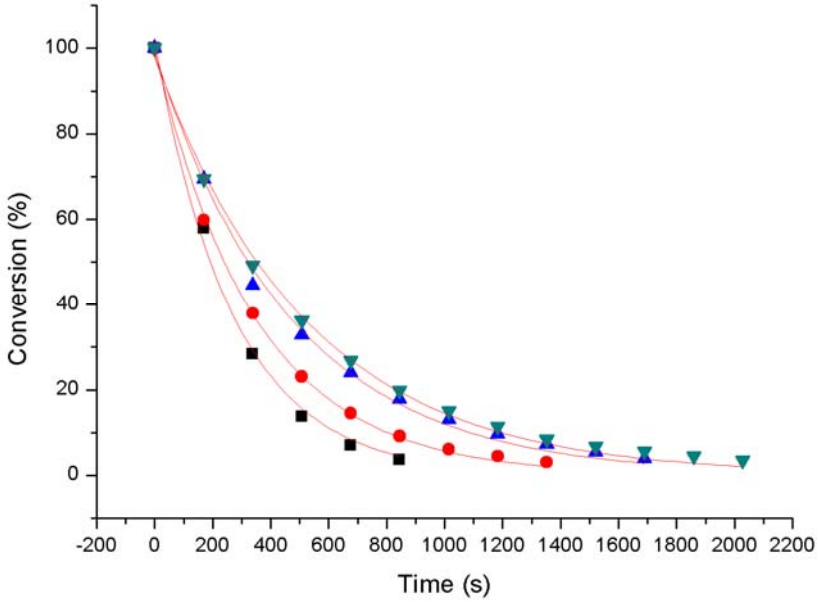

Figure 6.1 Conversion chart of the reactions of 0.5 mmol **1a** with 0.1 mmol **AB**, **AB(D)**, **A(D)B** or **A(D)B(D)** pursued by *in situ* ^{11}B NMR in THF at 60 ^{o}C determined by the intensities of the boron signals in the ^{11}B NMR spectra with 3 min intervals. The black squares stand for reactions with **AB**, red circles for **AB(D)**, blue triangles for **A(D)B** and green triangles for **A(D)B(D)**. Simulated DKIE values are: $k_{AB}/k_{AB(D)}$ = 1.28, $k_{AB}/k_{A(D)B}$ = 1.74, $k_{A(D)B}/k_{A(D)B(D)}$ = 1.10, and $k_{AB(D)}/k_{A(D)B(D)}$ = 1.49.

6.3.2 Transfer hydrogenation followed by alcoholysis?

In order to exclude the possibility of a primary transfer hydrogenation of the C=O bond followed by alcoholysis of **AB**, an NMR sample with a 4:1 molar ratio of **1a** with **AB** was prepared in THF-D_8 and pursued by ^{11}B NMR at low temperatures to acquire details of this reaction course. However, the expected dehydrocoupling products of **AB**, such as cyclotriborazane (**CTB**), B-(cyclodiborazanyl)amino-borohydride (**BCDB**) or borazine (**BZ**) were not found in the mixture, even at temperatures as low as -80 ^{o}C. This clearly excluded transfer hydrogenation with **AB** to take place before hydroboration.

Nevertheless, lowering of the temperature caused the signal for **3a** at around 19

ppm to decrease, while a broad signal gradually increased at around 2 ppm (Figure 6.2). These two signals seemed to be in equilibrium and changed in intensity on each other's expense with increasing or decreasing temperature. The signal at 19 ppm turned reversibly into the signal at 2 ppm with lowering of the temperature.

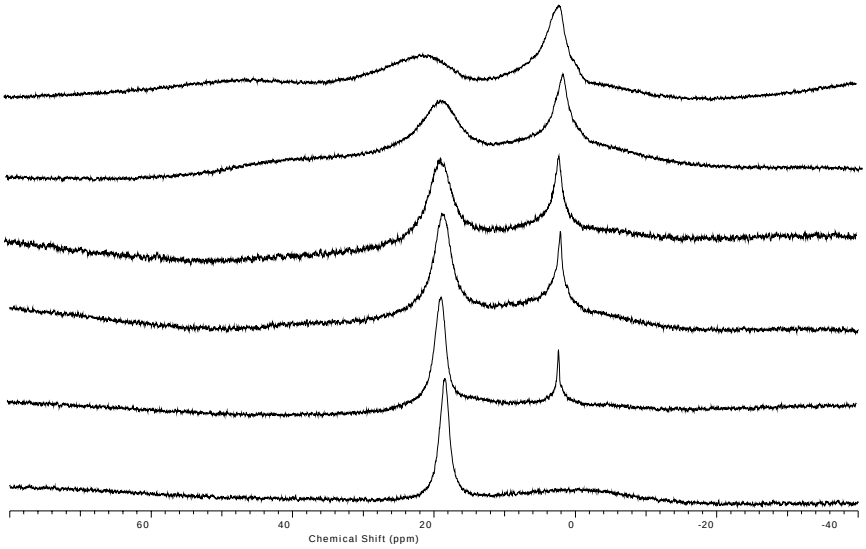

Figure 6.2 *In situ* ^{11}B NMR spectra at various temperatures for the completed reaction of **1a** and **AB** with 4:1 molar ratio in THF. Temperatures (in ^{o}C) from top to bottom: -80, -60, -40, -20, 0, 20. Besides a notable signal broadening with decreasing temperature, reversible exchanges between the two resonaces at 19 ppm and 2 ppm occurred.

On the other hand, no significant difference was observed in the ^{1}H and ^{13}C NMR spectra at different temperatures except for a small shift of the broad signal for the NH_3 unit at 0.4 ppm in the ^{1}H NMR spectrum. This could be explained in terms of fast and reversible coordination of NH_3 to a tricoordinate boron center. At room temperature, the ammonia dissociation became more prominent, recognizable in the ^{11}B NMR via a low field shift (19 ppm). At lower temperatures the ammonia equilibrium shifts to the associated side showing then preference for the four coordinated boron compound indicated by the signal at relatively high field at around 2 ppm. However, this assumption seems not fully valid. The ammonia attachment to boron could occur, but was not expected to be the dominating factor, since evacuation of the NMR tube and removal of all volatiles including the solvent furnished the same temperature dependent NMR behavior as described before.

Apparently the ammonia part of **AB** did not get involved in the hydroboration process. Therefore it seemed possible that other borane complexes, like BH_3·THF, would furnish the same or similar hydroboration results. Thus, BH_3·THF was reacted with **1a** at room temperature in THF. Formation of the dialkoxy borine derivative **5a** was observed at room temperature immediately after the sample was prepared, the same product as the reaction of diborane with ketones and aldehydes.[17] **5a** slowly reacted with another equivalent of the substrate at room temperature, forming the boron ester compound **3a** (Scheme 6.6). In absence of NH_3, the boron ester exhibited the same temperature dependent equilibrium as shown in the NMR of Figure 6.2.

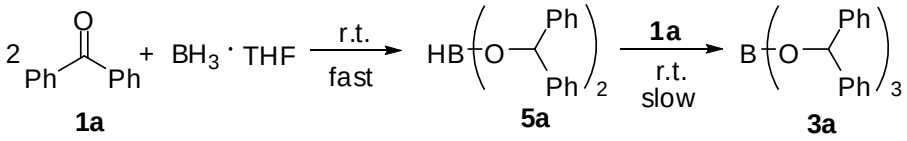

Scheme 6.6 Hydroboration of benzophenone with BH_3·THF.

Up to now, there are still two possible equilibria hidden by the signals of the temperature dependent NMR equilibrium of Figure 6.2: (a) a monomer-dimer equilibrium, which would lead to a four-coordinate borate dimer via two bridging oxygens prevailing at lower temperatures (Scheme 6.7, top); or (b) a complexation equilibrium of the borate ester with THF (Scheme 6.7, bottom).

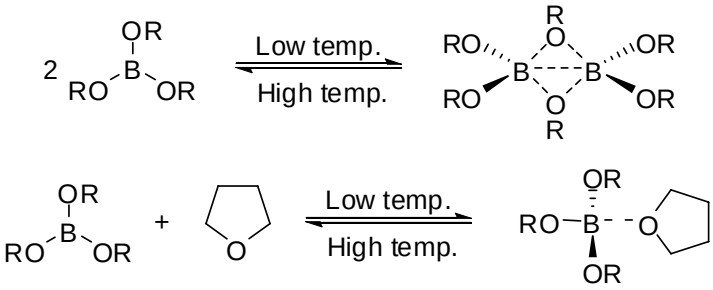

Scheme 6.7 Potential temperature dependent equilibria for borate esters in THF.

These two possibilities could be distinguished by substitution of the more donating solvent THF with less donating solvents such as toluene. Thus, **3a** was dissolved in toluene and ^{11}B NMR spectra were measured at low temperatures. The complete disappearance of the signal at 2 ppm clearly excluded dimer formation and stressed the importance of THF adducts.

6.3.3 Reaction course of the hydroboration in THF

Earlier reports on the mechanism of the hydroboration of carbonyl containing compounds involved a four-centered transition state, similar to that of compound **6**.[18,19] Our studies on ketone and aldehyde hydroborations support this hypothesis in the formation of alkyl borates (Scheme 6.8):

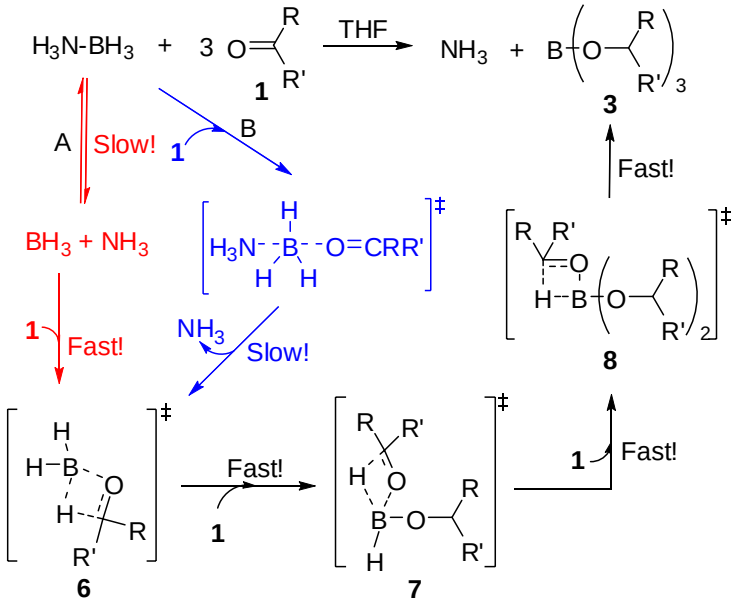

Scheme 6.8 Mechanism for the hydroboration of ketones and aldehydes with **AB**.

The first step and also the RDS could be the dissociation of NH_3 from **AB**. There are two possible pathways as shown in Scheme 6.8 (pathway A in red and B in blue). Along pathway A, dissociation of NH_3 from **AB** occurred first, then free BH_3 would coordinate the aldehyde or the ketone **1**, which insert into a B-H bond presumably via the four-membered ring structure **6** (SN_1 type). Along pathway B, release of NH_3 occurs by a SN_2 type replacement with **1** at **AB**, where steric pressure at the boron center would enforce NH_3 to leave and then to form **6**. Since no intermediate nor significant signal shifts were detected in the low temperature NMR studies, path A seems to be more reasonable. After this primary hydroboration step, another two substrate molecules would get to react with **6** via two related four-membered transition states **7** and **8** finally leading to the type **3** products.

With each consecutive hydroboration step it becomes more difficult for the

substrate to access to the boron center. In Table 6.1 mono- and diaryl ketones of various steric demands are shown to be subjected to the hydroboration reaction. Compared to **1a**, acetophenone (**1b**) and 9*H*-fluoren-9-one (**1c**) are less bulky, while cyclohexyl- (phenyl)-methanone (**1d**) and (E)-chalcone (**1e**) are quite sterically hindered. The elapsed reaction times mirror this steric order: **1b** and **1c** require shorter reaction time, while **1d** and **1e** longer ones. The least sterically hindered ketone **1g** can react fastest with **AB** at room temperature stressing further the importance of the steric influence on the reaction rates.

A concerted transition state as in **6** accumulates electron density at the $C_{C=O}$ atoms.[20] Thus, substituents that help to decrease the electron density at this center would support the hydroboration process. Compounds **1j**, **1k** and **1l** are *para*-substituted benzaldehyde derivatives. The electron withdrawing (EWD) group -CN substituted aldehyde **1j** reacted with **AB** much faster than **1h**, while the electron donating groups -OMe and -NMe_2 substituted substrates **1k** and **1l** displayed slower reaction rates (Table 6.2, entries 1 and 3-5). As mentioned before, such observations are supportive of a concerted transition state.[19,20]

Three types of reactions might occur with **3** as shown in Scheme 6.9: If the reaction takes place in THF, reversible complexation of **3** with THF would form the 4-coordinate borate **9**, in particular when the temperature is decreased. Compounds of type **3** could be reacted with methanol (or other lower alcohols) via alcohol metathesis giving trimethyl borate and the corresponding alcohol **2**. For aldehydes, compounds of type **3** could be reacted further with **1** to end up in a mixture of **3** and **4**.

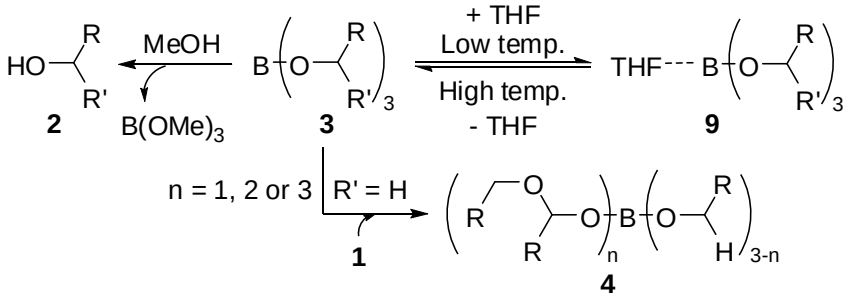

Scheme 6.9 Possible reactions concerning borate ester **3**.

6.4 Conclusions

In conclusion, as a class of unsaturated compounds containing polar C=O bonds, ketones and aldehydes can react with ammonia borane under mild conditions. In the reactions with THF as the solvent, borate esters as the only organic products are formed by hydroboration with H atoms transfer from the BH_3 part, much different from the reactions of ammonia borane with other polar unsaturated compounds, such as imines and polar olefins which are hydrogenated with the transfers of both H_B and H_N atoms from ammonia borane. The hydroboration of ketones is relatively slow but uniform, while for aldehydes, rapid hydroboration occurs followed by insertion of the starting aldehyde into at least one of the B-O bonds of the trialkyl borates. Mechanistic studies revealed that dissociation of ammonia from ammonia borane is rate determining. When methanol is used as the solvent, direct hydrogenation of the carbonyl compounds would occur from a initially formed $MeOH{\cdot}BH_3$, presumably via a single step double H transfer.

We gratefully thank the Swiss National Science Foundation and the University of Zurich for financial support.

6.5 Experimental section

6.5.1 General

All the manipulations were carried out under a nitrogen atmosphere using Schlenk techniques or in a drybox (Model MB-150B-G). Reagent grade benzene, toluene, hexane, diethyl ether, and THF were dried and distilled from sodium benzophenone ketyl prior to use. All the ketones and aldehydes were purchased from Aldrich or Fluka and used after being degased. Commercial methanol and CD_3OD were applied for reactions in methanol. NMR spectra were measured on a Varian Mercury spectrometer at 200 MHz for ^1H, Varian Gemini-2000 spectrometer at 300.1 MHz for ^1H, 96.3 MHz for $^{11}B\{^1H\}$ and 75.5 MHz for $^{13}C\{^1H\}$ and on a Bruker-DRX-500 spectrometer at 500.2 MHz for ^1H and 125.8 MHz for $^{13}C\{^1H\}$. Chemical shifts for ^1H and ^{13}C are given in ppm relative to TMS and those for ^{11}B relative to $Et_2O{\cdot}BF_3$.

All of these mentioned reactions were carried out at least twice to check for reproducibility.

6.5.2 Reactions of AB with ketones in THF

A 0.5 mm Young NMR tube was charged in the glove box with ketone (0.2 mmol, for kinetics 0.5 mmol), **AB** (0.1 mmol) and with dry THF-D_8 (0.6 ml) as the reaction media. The tube was sealed with a screw cap and then heated in an oil bath to 60 ^oC right after shaking. For dynamic NMR experiments, the samples were heated in the NMR machine. The reactions were monitored by ^1H and ^{11}B NMR every several minutes (depending on the reaction rates). The typical resonances of the starting materials gradually decreased (-22.4 ppm in ^{11}B NMR for **AB**) while new signals of the saturated products appeared (the -CH-O- in ^1H NMR and 19 ppm in ^{11}B NMR). The disappearance of the starting material indicated completion of the hydroboration, ^{13}C NMR spectra were then recorded. Only borate resonances were observed in the ^{11}B NMR (around 19 ppm) and the signals in the ^1H NMR spectra were slightly

broadened due to the quadrapole effect of ^{11}B. Finally the solvent and the released NH_3 were removed under reduced pressure, the residue in the NMR tube was pure borate ester to the limit of NMR with nearly 100% yield. The methanolysis of borate esters were carried out by addition of excess methanol, forming the corresponding alcohols and trimethyl borate, while trimethyl borate and the excess methanol can be removed by high vaccum.[9b].

Tribenzhydryl borate (**3a**),[21] white solid: δ_H (ppm; 300 MHz; THF-D_8) 6.18 (s, 0.5 H, -C*H*-O), 6.41 (s, 3 H, -C*H*-O), 7.21-7.24 (m, 35 H, -C_6H_5); δ_C (ppm; 75.5 MHz; THF-D_8) 77.41 (-*C*H-O), 78.22 (-*C*H-O), 127.20, 127.26, 127.59, 127.73, 128.86, 128.96, 144.95, 145.57; δ_B (ppm; 96.3 MHz; THF-D_8) 18.79. Diphenylmethanol (**2a**) was obtained exclusively after methanolysis of **3a**.

Tris(1-phenylethyl) borate (**3b**),[22] colorless gel: δ_H (ppm; 300 MHz; THF-D_8) 1.33 (d, *J* = 6 Hz, 3 H, -C*H*$_3$), 1.43 (d, *J* = 6 Hz, 3 H, -CH_3), 1.47 (d, *J* = 6 Hz, 3 H, -C*H*$_3$), 5.35-5.45 (m, 3 H), 7.04-7.42 (m, 15 H); δ_C (ppm; 75.5 MHz; THF-D_8) 25.77, 25.88, 25.95, 71.97 (-*C*H-O), 125.98, 126.10, 126.19, 127.35, 127.54, 127.66, 128.80, 128.87, 128.92, 146.51; δ_B (ppm; 96.3 MHz; THF-D_8) 18.00. 1-Phenylethanol (**2b**) was obtained exclusively after methanolysis of **3b**.

Tri(9*H*-fluoren-9-yl) borate (**3c**), white solid: [Found: C, 84.31; H, 5.19%. $C_{39}H_{27}BO_3$ requires C, 84.48; H, 4.91%]; δ_H (ppm; 300 MHz; THF-D_8) 6.30 (s, 3 H), 7.25-7.38 (m, 8 H), 7.66-7.72 (m, 8H); δ_C (ppm; 75.5 MHz; THF-D_8) 76.59 (-*C*H-O), 120.72, 126.18, 128.37, 129.71, 141.49, 145.83; δ_B (ppm; 96.3 MHz; THF-D_8) 19.89. 9*H*-fluoren-9-ol (**2c**) was obtained exclusively after methanlysis of **3c**.

Tris(cyclohexyl(phenyl)methyl) borate (**3d**), colorless gel: δ_H (ppm; 300 MHz; THF-D_8) 0.65-1.83 (m, 33 H), 4.90 (d, *J* = 6 Hz, 1 H, -C*H*-O), 4.95 (d, *J* = 6 Hz, 2 H, -C*H*-O), 6.71-7.32 (m, 15 H); δ_C (ppm; 75.5 MHz; THF-D_8) 27.09, 27.16, 27.23, 27.28, 27.48, 27.60, 28.63, 29.03, 29.19, 30.20, 30.40, 30.49, 46.01, 46.11, 80.39 (-*C*H-O), 80.44 (-*C*H-O), 127.13, 127.28, 127.37, 127.40, 127.55, 128.38, 128.48,

128.57, 144.16, 144.29, 144.40; δ_B (ppm; 96.3 MHz; THF-D_8) 18.36. Cyclohexyl-(phenyl)-methanol (**2d**) was obtained exclusively after methanolysis of **3d**.

Tris((E)-1,3-diphenylallyl) borate (**3e**), colorless gel: δ_H (ppm; 300 MHz; THF-D_8) 6.06 (d, *J* = 6 Hz, 3 H, -C*H*-O-B), 6.31-6.57 (m, 3 H, -C*H*=C), 6.65-6.83 (m, 3H), 7.19-7.53 (m, 30 H); δ_C (ppm; 75.5 MHz; THF-D_8) 76.93 (-*C*H-O), 127.13, 127.23, 127.32, 127.48, 128.01, 128.09, 128.24, 129.19, 130.49, 130.65, 130.73, 132.21, 137.90, 143.70; δ_B (ppm; 96.3 MHz; THF-D_8) 19.53. (*E*)-1,3-diphenylprop-2-en-1-ol (**2e**) was obtained exclusively after methanolysis of **3e**.

Tripentan-3-yl borate (**3f**),[23] colorless gel: δ_H (ppm; 300 MHz; THF-D_8) 0.91 (t, *J* = 7.4 Hz, 18 H, -CH_3), 1.36-1.55 (m, 12 H), 4.00-4.08 (m, 3H, -C*H*-O); δ_C (ppm; 75.5 MHz; THF-D_8) 10.45, 29.90, 75.34 (-*C*H-O); δ_B (ppm; 96.3 MHz; THF-D_8) 18.07. Pentan-3-ol (**2f**) was obtained exclusively after methanolysis of **3f**.

Tricyclohexyl borate (**3g**),[23,24] colorless gel: δ_H (ppm; 300 MHz; THF-D_8) 1.24-1.93 (m, 30 H), 3.99-4.15 (m, 3H, -C*H*-O); δ_C (ppm; 75.5 MHz; THF-D_8) 24.68, 26.78, 35.17, 70.92 (-*C*H-O); δ_B (ppm; 96.3 MHz; THF-D_8) 17.70. Cyclohexanol (**2g**) was obtained exclusively after methanolysis of **3g**.

6.5.3 Reactions of AB with aldehydes in THF

In the glove-box, a 0.5 mm Young NMR tube was charged with the aldehyde (0.2 mmol), **AB** (0.1 mmol) and dry THF-D_8 (0.6 ml). The tube was sealed with a screw cap and shaken to mix well. The reaction started immediately in the tube and was monitored by ^{1}H and ^{11}B NMR every several minutes (depending on the reaction rate). The typical resonance of the aldehyde rapidly decreased (the –HC=O on around 10 ppm in the ^{1}H NMR, -22.4 ppm in the ^{11}B NMR for **AB**) and new signals of the saturated products appeared. The total disappearance of the starting material indicated that the transformation completed, ^{13}C NMR spectra were then recorded. Since the product is a mixture of compounds, 2D NMR[10] was applied to unravel the spectra of the product species for the reaction of 0.3 mmol of benzaldehyde (**1h**) with 0.1 mmol

of **AB**. Reactions of the aldehydes with BH_3·THF were carried out to separate the resonances of the trialkyl borates from the spectra for the mixture products.

Tribenzyl borate (**3h**),[25] colorless gel: δ_H (ppm; 300 MHz; THF-D_8) 4.99 (s, 6 H, -C$\underline{H}_2$-O), 7.23-7.38 (m, 15 H, -$C_6\underline{H}_5$); δ_C (ppm; 75.5 MHz; THF-D_8) 66.26 (-$\underline{C}H_2$-O), 127.46, 127.88, 128.98, 141.07; δ_B (ppm; 96.3 MHz; THF-D_8) 18.64.

Tris(naphthalen-1-ylmethyl) borate (**3i**), light yellow gel: δ_H (ppm; 300 MHz; THF-D_8) 5.48-5.52 (m, 6 H, -C$\underline{H}_2$-O), 7.35-7.55 (m, 12 H), 7.78-7.89 (m, 6 H,), 8.09-8.14 (m, 3 H); δ_C (ppm; 75.5 MHz; THF-D_8) 64.88 (-$\underline{C}$H-O), 66.53, 124.45, 124.65, 125.90, 126.09, 126.18, 126.39, 126.49, 126.81, 126.89, 128.94, 129.08, 129.33, 129.38, 132.44, 134.88, 136.28; δ_B (ppm; 96.3 MHz; THF-D_8) 18.64.

Tris(4-cyanobenzyl) borate (**3j**), white powder: δ_H (ppm; 300 MHz; THF-D_8) 5.11 (s, 6 H, -C$\underline{H}_2$-O-), 7.51-7.53 (m, 6 H), 7.70-7.72 (m, 6 H,); δ_C (ppm; 75.5 MHz; THF-D_8) 65.73 (-$\underline{C}H_2$-O-), 112.41, 119.24 (-$\underline{C}$N), 127.86, 133.01, 146.02; δ_B (ppm; 96.3 MHz; THF-D_8) 18.48.

Tris(4-methoxybenzyl) borate (**3k**),[26] colorless gel: δ_H (ppm; 300 MHz; THF-D_8) 3.76 (s, 9 H, O-Me), 4.86 (s, 6 H, -C$\underline{H}_2$-O), 6.84-6.88 (m, 6 H), 7.23-7.32 (m, 6 H); δ_C (ppm; 75.5 MHz; THF-D_8) 55.41 (O-$\underline{C}H_3$), 65.96 (-$\underline{C}H_2$-O), 114.35, 129.16, 133.11, 160.17; δ_B (ppm; 96.3 MHz; THF-D_8) 18.49.

Tris(4-(dimethylamino)benzyl) borate (**3l**), yellow gel: δ_H (ppm; 300 MHz; THF-D_8) 2.90 (s, 18 H, -N(C$\underline{H}_3$)$_2$), 4.80 (s, 6 H, -C$\underline{H}_2$-O-), 6.66-6.69 (m, 6 H), 7.15-7.19 (m, 6H); δ_C (ppm; 75.5 MHz; THF-D_8) 40.96 (-N($\underline{C}H_3$)$_2$), 66.18 (-$\underline{C}H_2$-O-), 113.16, 129.62, 130.29, 150.77; δ_B (ppm; 96.3 MHz; THF-D_8) 18.71.

6.5.4 Reactions of ketones and aldehydes with AB in methanol

A 0.5 mm NMR tube was charged with ketone or aldehyde (0.2 mmol), **AB** (0.1 mmol) and deuterated methanol. The tube was covered with a plastic cap and inserted into the NMR machine after shaking. The reaction courses were monitored by ^1H and

^{11}B NMR every several minutes (depending on the reaction rates). The typical resonances of the starting materials gradually decreased while new signals of the saturated products appeared. After the ketone or aldehyde disappeared completely in the ^{1}H NMR spectrum, ^{13}C NMR spectrum was recorded. For a large scale reaction in normal methanol, the solvent and all volatile compounds (trimethyl borate and ammonia) were removed by high vacuum after the reaction, and the remaining alcohol was pure to the limit of the NMR with nearly 100% yield.

Diphenylmethanol (**2a**),[27,28] white solid, δ_H (ppm; 300 MHz; CD_3OD) 5.51 (s, 1 H, -C*H*-OD), 7.26-7.38 (m, 4 H), 7.58-7.68 (m, 4 H); δ_C (ppm; 75.5 MHz; CD_3OD) 75.44, 120.78, 126.05, 128.59, 129.77, 141.34, 147.35.

1-Phenylethanol (**2b**),[27,29] colorless liquid, δ_H (ppm; 300 MHz; CD_3OD) 1.43 (d, J = 6.5 Hz, 3 H, -C*H*$_3$), 4.82 (q, J = 6.5 Hz, 1 H, -C*H*-OD), 7.18-7.40 (m, 5 H); δ_C (ppm; 75.5 MHz; CD_3OD) 25.75 (-*C*H$_3$), 70.85 (-*C*H-OD), 126.47, 128.08, 129.27, 147.55.

9*H*-fluoren-9-ol (**2c**),[29,30] white solid, δ_H (ppm; 300 MHz; CD_3OD) 5.51 (s, 1 H, -C*H*-OD), 7.26-7.38 (m, 4 H), 7.58-7.68 (m, 4 H); δ_C (ppm; 75.5 MHz; CD_3OD) 75.44, 120.78, 126.05, 128.59, 129.77, 141.34, 147.35.

Cyclohexyl-(phenyl)methanol (**2d**),[28,31] colorless liquid, δ_H (ppm; 300 MHz; CD_3OD) 0.93-1.41 (m, 5 H),1.54-1.80 (m, 5 H), 1.92-1.99 (m, 1 H), 4.33 (d, J = 7 Hz, 1 H, -C*H*-OD), 7.26-7.42 (m, 5 H, -C$_6$*H*$_5$); δ_C (ppm; 75.5 MHz; CD_3OD) 26.87, 26.94, 27.32, 29.44, 30.27, 46.06, 78.91 (-*C*H-OH), 127.55, 127.76, 128.78, 145.53.

(*E*)-1,3-diphenylprop-2-en-1-ol (**2e**),[27,32,33] white solid, δ_H (ppm; 300 MHz; CD_3OD) 5.37 (d, J = 6 Hz, 1 H, -C*H*-OH), 6.45 (dd, J = 6, 16 Hz, 1 H, -CH(OH)-C*H*=CH-), 6.74 (d, J = 16 Hz, 1 H, -CH(OH)-CH=C*H*-); δ_C (ppm; 75.5 MHz; CD_3OD) 74.98 (-*C*H-OH), 118.30 (-*C*H=CH-Ph), 127.23, 127.36, 128.22, 128.53, 129.35, 129.59, 130.15, 133.67 (-CH=*C*H-Ph), 137.88, 144.84.

Pentan-3-ol (**2f**),[34] colorless liquid, δ_H (ppm; 300 MHz; CD_3OD) 0.92 (td, J = 7.5 Hz, 6 H, -C$\underline{H}_3$), 1.31-1.56 (m, 4 H, -CH_2), 3.27-3.40 (m, 2 H, -C$\underline{H}$-OD); δ_C (ppm; 75.5 MHz; CD_3OD) 10.39 (-$\underline{C}H_3$), 30.510 (-$\underline{C}H_2$), 75.32(-$\underline{C}$H-OD).

Cyclohexanol (**2g**),[27,34] colorless liquid, δ_H (ppm; 300 MHz; CD_3OD) 0.92 (td, J = 7.5 Hz, 6 H, -C$\underline{H}_3$), 1.31-1.56 (m, 4 H, -CH_2), 3.27-3.40 (m, 2 H, -C$\underline{H}$-OD); δ_C (ppm; 75.5 MHz; CD_3OD) 10.39 (-$\underline{C}H_3$), 30.510 (-$\underline{C}H_2$), 75.32(-$\underline{C}$H-OD).

Phenylmethanol (**2h**),[27,35,36] colorless liquid, δ_H (ppm; 300 MHz; CD_3OD) 4.59 (s, 2 H, -C$\underline{H}_2$), 7.15-7.50 (m, 4 H); δ_C (ppm; 75.5 MHz; CD_3OD) 65.23 (-$\underline{C}H_2$), 127.97, 128.23, 129.32, 142.67.

Naphthalen-1-ylmethanol (**2i**),[27,32,36] colorless liquid, δ_H (ppm; 300 MHz; CD_3CN) 3.28 (br, 1 H, -CH_2-O$\underline{H}$), 5.10 (s, 2 H, C$\underline{H}_2$-OH), 7.48-7.60 (m, 4 H), 7.85-7.96 (m, 2 H), 8.13-8.18 (m, 1 H); δ_C (ppm; 75.5 MHz; CD_3CN) 62.98, 124.71, 125.62, 126.45, 126.66, 126.90, 128.63, 129.34, 132.06, 134.60, 137.16.

4-(Hydroxymethyl)benzonitrile (**2j**),[27] white solid, δ_H (ppm; 300 MHz; CD_3CN) 4.93 (s, 2 H, -C$\underline{H}_2$-O-), 7.50-7.53 (m, 2 H), 7.66-7.69 (m, 2 H,); δ_C (ppm; 75.5 MHz; CD_3CN) 63.85 (-$\underline{C}H_2$-O-), 111.18, 119.84 (-$\underline{C}$N), 127.87, 130.08, 148.74.

(4-Methoxyphenyl)methanol (**2k**),[32] δ_H (ppm; 300 MHz; CD_3OD) 3.75 (s, 3 H, -C$\underline{H}_3$), 4.51 (s, 2 H, -CH_2), 6.87 (d, J = 9 Hz, 2 H), 7.26 (d, J = 9 Hz, 2 H); δ_C (ppm; 75.5 MHz; CD_3OD) 55.68 (-$\underline{C}H_3$), 64.93 (-$\underline{C}H_2$-OD), 114.72, 129.61, 134.69, 160.47.

(4-(Dimethylamino)phenyl)methanol (**2l**),[36] white solid, δ_H (ppm; 300 MHz; CD_3CN) 2.94 (s, 6 H, -N(C$\underline{H}_3$)$_2$), 3.65 (s, 1 H, -CH_2-O$\underline{H}$), 4.48 (s, 2 H, -C$\underline{H}_2$-OH), 6.74-6.78 (m, 2 H), 7.18-7.23 (m, 2H); δ_C (ppm; 75.5 MHz; CD_3CN) 40.95 (-N($\underline{C}H_3$)$_2$), 64.75 (-$\underline{C}H_2$-O-), 113.38, 129.15, 129.95, 150.92.

6.6 References

1. a) Stephens, F. H.; Pons, V.; Baker, R. T. *Dalton Trans.* **2007**, 2613-2626; b) Umegaki, T.; Yan, J. M.; Zhang, X. B.; Shioyama, H.; Kuriyama, N.; Xu, Q. *Int. J. Hydrogen Energ.* **2009**, *34*, 2303-2311; c) Hamilton, C. W.; Baker, R. T.; Staubitz, A.; Manners, I.; *Chem. Soc. Rev.* **2009**, *38*, 279-293; d) Alcaraz, G.; Vendier, L.; Clot, E.; Sabo-Etienne, S. *Angew. Chem. Int. Ed.* **2010**, *49*, 918-920; e) Tang, C. Y.; Thompson, A. L.; Aldridge, S. *Angew. Chem. Int. Ed.* **2010**, *49*, 921-925; f) Sutton, A. D.; Burrell, A. K.; Dixon, D. A.; Garner, E. B.; Gordon, J. C.; Nakagawa, T.; Ott, K. C.; Robinson, J. P.; Vasiliu, M. *Science*, **2011**, *331*, 1426-1429; g) Crabtree, R. H. *Organometallics*, **2011**, *30*, 17-19.
2. a) Staubitz, A.; Robertson, A. P. M.; Manners, I. *Chem. Rev.* **2010**, *110*, 4079-4124; b) Smythe, N. C.; Gordon, J. C. *Eur. J. Inorg. Chem.* **2010**, 509-521 and references cited therein.
3. a) Grochala, W.; Edwards, P. P. *Chem. Rev.* **2004**, *104*, 1283-1315; b) Bowden, M.; Autrey, T.; Brown, I.; Ryan, M. *Current Appl. Phys.* **2008**, *8*, 498-500; c) Shaw, W. J.; Linehan, J. C.; Szymczak, N. K.; Heldebrant, D. J.; Yonker, C.; Camaioni, D. M.; Baker, R. T.; Autrey, T. *Angew. Chem. Int. Ed.* **2008**, *47*, 7493-7496; d) Rassat, S. D.; Aardahl, C. L.; Autrey, T.; Smith, R. S. *Energ. Fuel.* **2010**, *24*, 2596-2606; e) Demirci, U. B.; Bernard, S.; Chiriac, R.; Toche, F.; Miele, P. *J. Power Sources*, **2011**, *196*, 279-286.
4. a) Chaplin, A. B.; Weller, A. S. *Inorg. Chem.* **2010**, *49*, 1111-1121; b) Conley, B. L.; Williams, T. J. *Chem. Commun.* **2010**, *46*, 4815-4817; c) Kim, S. K.; Han, W. S.; Kim, T. J.; Kim, T. Y.; Nam, S. W.; Mitoraj, M.; Piekos, L.; Michalak, A.; Hwang, S. J.; Kang, S. O. *J. Am. Chem. Soc.* **2010**, *132*, 9954-9955; d) Miller, A. J. M.; Bercaw, J. E. *Chem. Commun.* **2010**, *46*, 1709-1711; e) Sloan, M. E.; Staubitz, A.; Clark, T. J.; Russell, C. A.; Lloyd-Jones, G. C.; Manners, I. *J. Am. Chem. Soc.* **2010**, *132*, 3831-3841; f) Tong, D. G.; Zeng, X. L.; Chu, W.; Wang, D.; Wu, P. *J. Mater. Sci.* **2010**, *45*, 2862-2867; g) Kakizawa, T.; Kawano, Y.; Naganeyama, K.; Shimoi, M. *Chem. Lett.*, **2011**, *40*, 171-173; h) Cowley, H. J.; Holt, M. S.; Melen, R. L.; Rawson, J. M.; Wright, D. S., *Chem. Commun.*, **2011**, *47*, 2682-2684; i) Vogt, M.; de Bruin, B.; Berke, H.; Trincado, M.; Grutzmacher, H. *Chem. Sci.*, **2011**, *2*, 723-727; j) Wright, W. R. H.; Berkeley, E. R.; Alden, L. R.; Baker, R. T.; Sneddon, L. G. *Chem. Commun.*, **2011**, *47*, 3177-3179.
5. References on hydrolysis, hydrothermolysis and dehydrogenation of **AB** in ionic liquid or on surfaces: a) Bluhm, M. E.; Bradley, M. G.; Butterick, III, R.; Kusari, U.; Sneddon, L. G. *J. Am. Chem. Soc.* **2006**, *128*, 7748-7749; b)

Himmelberger, D. W.; Alden, L. R.; Bluhm, M. E.; Sneddon, L. G. *Inorg. Chem.* **2009**, *48*, 9883-9889; c) Brockman, A.; Zheng, Y. A.; Gore, J. *Int. J. Hydrogen Energ.* **2010**, *35*, 7350-7356; d) Ciganda, R.; Garralda, M. A.; Ibarlucea, L.; Pinilla, E.; Torres, M. R. *Dalton Trans.* **2010**, *39*, 7226-7229; e) Liu, C.; Li, F.; Ma, L. P.; Cheng, H. M. *Adv. Mater*. **2010**, *22*, E28-E62; f) Demirci, U. B.; Miele, P. *J. Power Sources* **2010**, *195*, 4030-4035; g) K. Eom, K. Cho, H. Kwon, *Int. J. Hydrogen Energ.* **2010**, *35*, 181-186; h) Diwan, M.; Hwang, H. T.; Al-Kukhun, A.; Varma, A. *Aiche J.* **2011**, *57*, 259-264; i) Yang, X. J.; Cheng, F. Y.; Tao, Z. L.; Chen, J. *J. Power Sources*, **2011**, *196*, 2785-2789; j) Basu, S.; Zheng, Y.; Gore, J. P. *J. Power Sources*, **2011**, *196*, 734-740; k) Metin, O.; Ozkar, S. *Int. J. Hydrogen Energ.*, **2011**, *36*, 1424-1432.

6. Yang, X.; Fox, T.; Berke, H. *Chem. Commun.* **2011**, *47*, 2053-2055.
7. Berke, H. *ChemPhysChem*, **2010**, *11*, 1837-1849.
8. Yang, X.; Zhao, L.; Fox, T.; Wang, Z.-X. Berke, H. *Angew. Chem. Int. Ed.* **2010**, *49*, 2058-2062.
9. a) Brown, H. C.; Mead, E. J. *J. Am. Chem. Soc.*, **1953**, *75*, 6263-6265; b) Brown, H. C. U.S. Patent 2,709,704, 1959; c) Klein, J.; Dunkelblum, E. *Tetrahedron*, **1968**, *24*, 5701-5710; d) Koren-Selfridge, L.; Londino, H. N.; Vellucci, J. K.; Simmons, B. J.; Casey, C. P.; Clark, T. B. *Organometallics*, **2009**, *28*, 2085-2090; e) Huettenhain, S. H.; Schmidt, M. U.; Schoepke, F. R.; Rueping, M. *Tetrahedron*, **2006**, *62*, 12420-12423.
10. Multiple NMR spectra and the structure of the adduct was discussed in detail in the supporting information.
11. a) Couturier, M.; Andresen, B. M.; Tucker, J. L.; Dube, P.; Brenek, S. J.; Negri, J. T. *Tetrahedron Lett.*, **2001**, *42*, 2763-2766; b) Ramachandran, P. V.; Gagare, P. D. *Inorg. Chem.*, **2007**, *46*, 7810-7817; c) Erdogan, H.; Metin, O.; Ozkar, S. *Phys. Chem. Chem. Phys.* **2009**, *11*, 10519-10525; d) Kalidindi, S. B.; Vernekar, A. A.; Jagirdar, B. R. *Phys. Chem. Chem. Phys.* **2009**, *11*, 770-775; e) Caliskan, S.; Zahmakiran, M.; Ozkar, S. *Appl. Cata. B-Environ.*, **2010**, *93*, 387-394; f) Dai, H. B.; Kang, X. D.; Wang, P. *Int. J. Hydrogen Energ.*, **2010**, *35*, 10317-10323.
12. Dong, H.; Berke, H. *J. Organomet. Chem.* **2011**, *696*, 1803-1808.
13. a) Espenson, J. H. in *Chemical kinetics and reaction mechanisms*, *2nd ed*. McGRAW-HILL, Inc. New York, **1995**, pp. 214-220, 225-228; b) Giagou, T.; Meyer, M. P. *Chem. Eur. J.*. **2010**, *16*, 10616-10628.
14. Brown, H. C.; Chandrasekharan, J. *Organometallics.* **1983**, *2*, 1261-1263.
15. Limbach, H. H. Single and multiple hydrogen/deuterium transfer reactions in liquids and solids. In *Hydrogen Transfer Reactions*. Hynes, J. T.; Klinman, J.;

Limbach, H. H.; Schowen, R. L. Eds.; Wiley-VCH: Weinheim, Germany, 2007; Vols. 1 & 2, Chapter 6, pp. 135-221, and references cited therein.

16. a) Popelier, P. L. A. *J. Phys. Chem. A*, **1998**, *102*, 1873-1878; b) Kulkarni, S. A. *J. Phys. Chem. A.* **1999**, *103*, 9330-9335; c) Custelcean, R.; Dreger, Z. A. *J. Phys. Chem. B*, **2003**, *107*, 9231-9235.
17. Brown, H. C.; Schlesinger, H. I.; Burg, A. B. *J. Am. Chem. Soc.*, **1939**, *61*, 673-680.
18. Brown, H. C.; Wang, K, K.; Chandrasekharan, J. *J. Am. Chem. Soc.* **1983**, *105*, 2343-2350.
19. Kudo, T.; Higashide, T. Ikedate, S. Yamataka, H. *J. Org. Chem.* **2005**, *70*, 5157-5163.
20. Hammett, L. P. *J. Am. Chem. Soc.* **1937**, *59*, 96-103.
21. Ogata, Y.; Kosugi, Y. *Tetrahedron*, **1970**, *26*, 2321-2327.
22. Gerrard, W.; Lappert, M. F. *J. Chem. Soc.*, **1951**, 1020-1024.
23. Brown, C. A.; Krishnamurthy, S. *J. Org. Chem.*, **1978**, *43*, 2731-2732.
24. Cook, H. G.; Ilett, J. D.; Saunders, B. C.; Stacey, G. J. *J. Chem. Soc.*, **1950**, 3125-3128.
25. Cole, T. E.; Quintanilla, R.; Rodewald, S. *Syn. React. Inorg. Metal-Org. Nano-Metal Chem.*, **1990**, *20*, 55-63.
26. Ditrich, K. *Science Synth.* **2007**, *25*, 563-574.
27. Cho, B. T.; Kang, S. K.; Kim, M. S.; Ryu, S. R.; An, D. K. *Tetrahedron*, **2006**, *62*, 8164-8168.
28. Kuriyama, M; Shimazawa, R; Shirai, *J. Org. Chem.* **2008**, *73*, 1597-1600.
29. a) Meddour, A.; Berdague, P.; Courtieu, H. J.; Lesot, P. *J. Am. Chem. Soc.*, **1997**, *119*, 4502-4508; b) Wang, C. H.; Kingsbury, C. A. *J. Org. Chem.*, **1972**, *37*, 2489-2494.
30. Chan, Audrey; Scheidt, Karl A. *J. Am. Chem. Soc.* **2006**, *128*, 4558-4559.
31. Ueda, M.; Miyaura, N. *J. Org. Chem*. **2000**, *65*, 4450-4452.
32. Trindade, A. F.; Andre, V.; Duarte, M. T.; Veiros, L. F.; Gois, P. M. P.; Afonso, C. A. M. *Tetrahedron*, **2010**, *66*, 8494-8502.
33. Kumari, P.; Poonam; Chauhan, S. M. S. *Chem. Commun.* **2009**, *42*, 6397-6399.
34. Kawamorita, S.; Hamasaka, G.; Ohmiya, H.; Hara, K.; Fukuoka, A.; Sawamura, M. *Org. Lett.*, **2008**, *10*, 4697-4700.
35. Jagdale, A. R.; Paraskar, A. S.; Sudalai, A. *Synthesis*, **2009**, 660-664.
36. Ragnarsson, U.; Grehn, L.; Monteiro, L. S.; Maia, H. L. S. *Synlett*, **2003**, 2386-2388.

Theoretical Study and Metal-Free Transfer Hydrogenation and Dehydrogenation Reactions Applying Polarized Olefins

As mentioned in Chapter 2, the goal of this thesis is '*to carry out metal-free transfer hydrogenations with amine borane complexes (especially ammonia borane (**AB**)) as hydrogen sources, aim at finding certain organic molecules which can first uptake hydrogen from **AB** and in the end be able to release hydrogen again.*' In Chapters 3-6, metal-free transfer hydrogenations of polar unsaturated compounds including imines, polarized olefins and carbonyl compounds were successfully carried out with amine borane complexes as hydrogen donors, fulfilling the major part of our goal. In this Chapter, we attempted to complete our goal by trying to find organic molecules which can be used for dehydrogenation of **AB**, or be firstly transfer-hydrogenated by **AB** and finally release hydrogen.

7.1 DFT calculations of hydrogenation/dehydrogenation energies

Since a broad variety of polar unsaturated compounds were tested in the metal-free transfer hydrogenation processes and some of them could not be easily dehydrogenated such as amines and alcohols, only the hydrogenation products of the polarized olefins were considered for dehydrogenation. An easy and eco-friendly way to judge the dehydrogenation reactivity is to theoretically calculate the energies between the substrate and its dehydrogenated form as a measure of the involved thermodynamics. Therefore, the total energies of the applied compounds before and after hydrogenation were calculated using Gaussian 03[1] program at the B3LYP/6-31+G* level in the gas phase at 298 K. The energies for hydrogenations ($\triangle E_H$) were obtained according to Eq. (1) and the results were listed in Table 7.1.

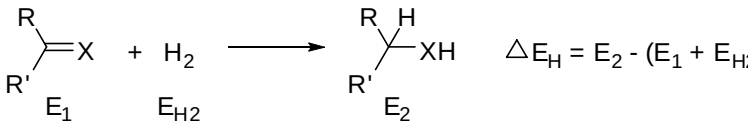

$$\triangle E_H = E_2 - (E_1 + E_{H2}) \quad (1)$$

Table 7.1 Calculated energies for hydrogenation reactions.

Entry	Unsaturated form	Saturated form	$\triangle E_H$ (kcal/mol)
1	$NH_2=BH_2$	NH_3-BH_3	1.5
2	$CH_2=CH_2$	CH_3-CH_3	-40.7
3			-34.3
4	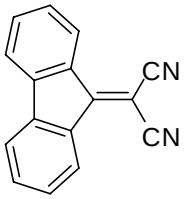	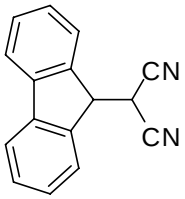	-19.0
5	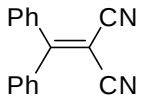	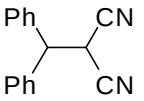	-19.9
6	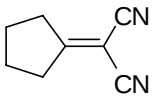	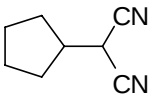	-20.2
7	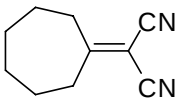	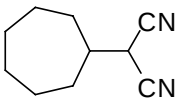	-22.4
8	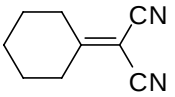	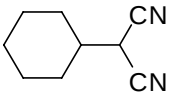	-23.3
9	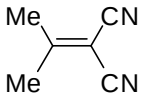	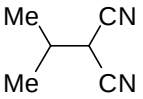	-24.3
10	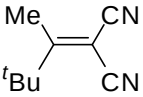	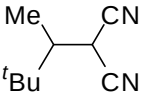	-23.3
11	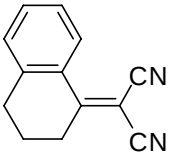	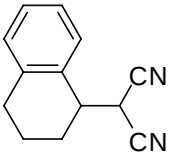	-19.3
12	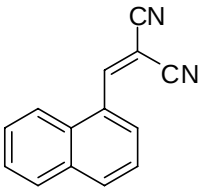	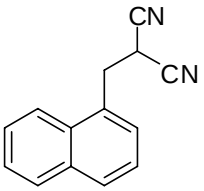	-26.5
13	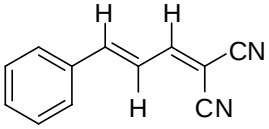	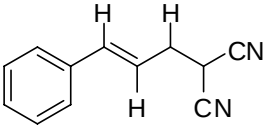	-19.2

14	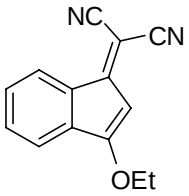	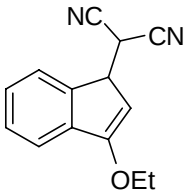	-17.2
15	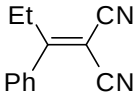	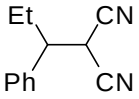	-24.3
16	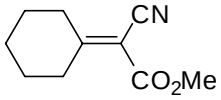	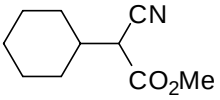	-26.1
17	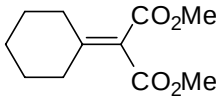	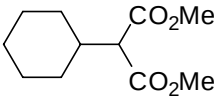	-30.9
18	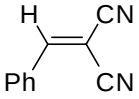	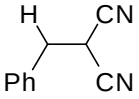	-24.9
19	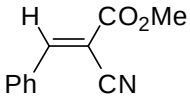	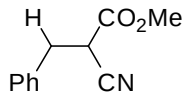	-25.4
20	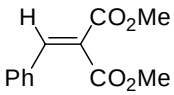	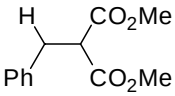	-31.8
21	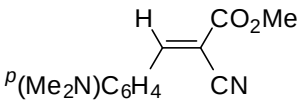	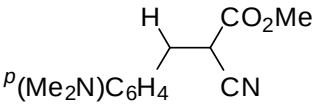	-21.0
22	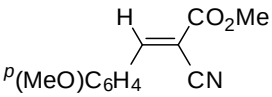	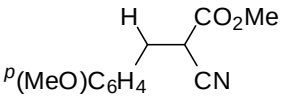	-23.1
23	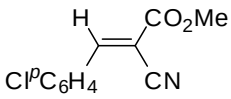	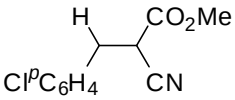	-25.5
24	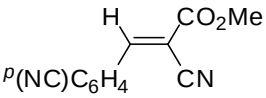	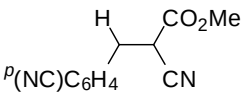	-26.9
25	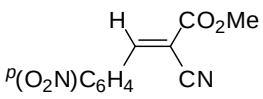	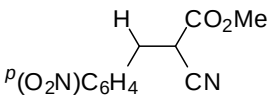	-27.5
26	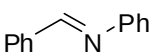	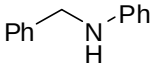	-21.9
27	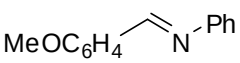	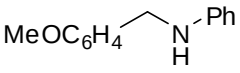	-20.9
28	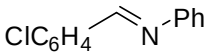	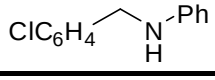	-21.8

29	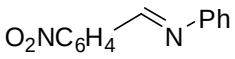	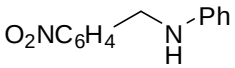	-22.3
30	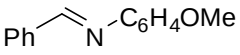	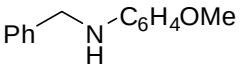	-20.1
31	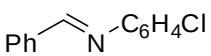	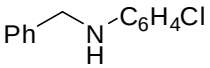	-21.9
32	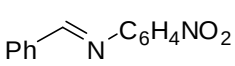	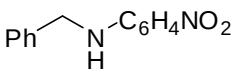	-24.8
33	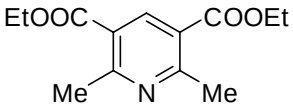	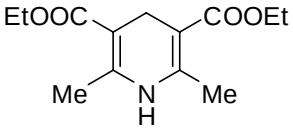	-9.1
34	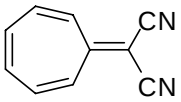	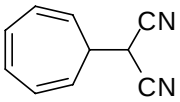	-9.3
35	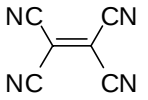	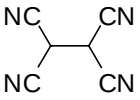	-26.9
36	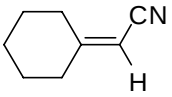	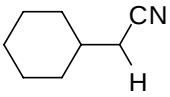	-28.7
37	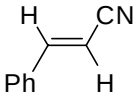	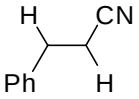	-31.6
38	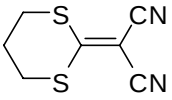	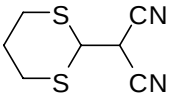	-20.0
39	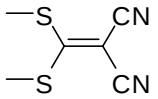	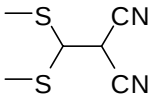	-21.4
40	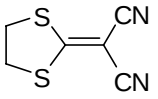	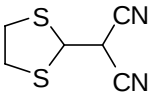	-16.7
41	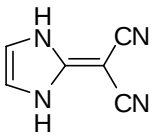	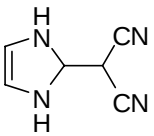	6.9
42	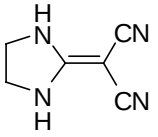	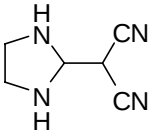	0.1

43	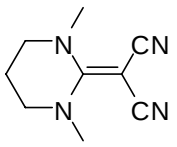	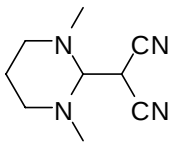	-2.0
44	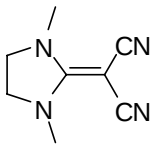	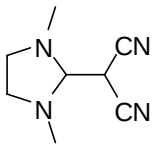	-3.3
45	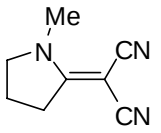	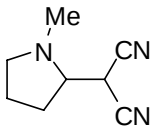	-10.6

Although the Gibbs free energies were not calculated, it still can be estimated from the ΔE_H that **AB** has a great thermodynamic tendency to lose hydrogen, since a positive ΔE_H was obtained (Table 7.1, entry 1). Very negative ΔE_H values were obtained with apolar olefins like ethylene and cyclohexene (entries 2-3). It's worth noting that all of the polarized olefins and imines, which had experimentally proved to react with **AB**, have moderate ΔE_H between -17 to -30 kcal/mol (entries 4-32). Interestingly, clues for the *para*-substituent effects were provided by comparison the ΔE_H with the corresponding substituent constants σ and the reaction rates (discussed in former chapters): the bigger the absolute ΔE_H, the larger the substituent constants σ and the faster the reaction rates (entries 19-25 for *para*-substituted polarized olefins and entries 26-32 for imines), which indicates that thermodynamics and kinetics of the hydrogenations maybe related by a Free-Energy Relationship.[2]

The dehydrogenated Hanztsch ester has a relatively small ΔE_H of -9.1 kcal/mol (entry 33). Considering that it could not be directly hydrogenated by **AB** as discussed in Chapter 5, such a ΔE_H might imply that the dehydrogenated form is more preferred than the hydrogenated form. A similar ΔE_H was obtained with cyclohepta-2,4,6-trienylidenemalononitrile (entry 34), which is on a absolute scale more stable in the dehydrogenated form due to a strong electronic push-pull effect. Large ΔE_H values were obtained with olefins in entries 35-37, however, they experimentally proved unreactive to **AB**, most probably due to lack of polarities

hindering kinetics in a special but not yet identified way.

Olefins bearing heterocycles opposite to the geminal –CN groups were also calculated and their reactivity patterns were predicted: For the olefins with sulfur containing rings (entries 38-40), the calculated ΔE_H fall into the moderate range of thermicity like the other polarized olefins, indicating that they might react with **AB** in one way or another. For those species bearing nitrogen heterocycles (entries 41-45), very small ΔE_H values were obtained. As discussed for the olefins in entries 33 and 34, such small ΔE_H value might suggest that no reaction with **AB** can occur because the olefins are in a too stable form and there is presumably too little gain in free energy in the transfer hydrogenation.

7.2 Attempts of metal-free dehydrocoupling of AB using push-pull olefins

A push-pull olefin is the type of olefin characterized by electron-withdrawing groups (EWG) on one side of the double bond and electron-donating groups (EDG) on the other side, which makes it a so-called bifunctional molecule. Typical EWGs includes -CN, -COOR or NO_2 groups, while -OR, -SR, -NHR or -NR_2 are typical EDGs. Olefins calculated in entries 38-45 of Table 7.1 are typical push-pull olefins. According to the calculations, some of these olefins were applied to react with **AB** in the hope of finding a metal-free catalyst for the dehydrocoupling of **AB**.

Firstly, the $(RS)_2C=C(CN)_2$ type olefins (**1a-1d**) were reacted stoichiometrically with **AB** in THF at room temperature. On the one hand, dehydrogenation of **AB** did occur, yet showing a reaction pattern different from dehydrocoupling, since new signals appeared in the ^{11}B NMR at around 45 ppm probably presenting B-C bonds. On the other hand, hydrogenation products of the olefins were not formed, since decomposition of the olefin took place along the reaction course, yielding 2-methylmalononitrile, H_2 and some undefined complex compounds in all cases (Scheme 7.1). When DMSO was used as the reaction media for a 1:1 reaction of **AB** with these olefins, cyclotriborazane (**CTB**) was observed in the ^{11}B NMR as the main

dehydrocoupling product of **AB**. However, the reaction itself was diverse leading to a complex mixture, as it was dirived from the ^{1}H and ^{13}C NMR spectra or GC/MS, even the formation of 2-methylmalononitrile could not be confirmed (Scheme 7.1).

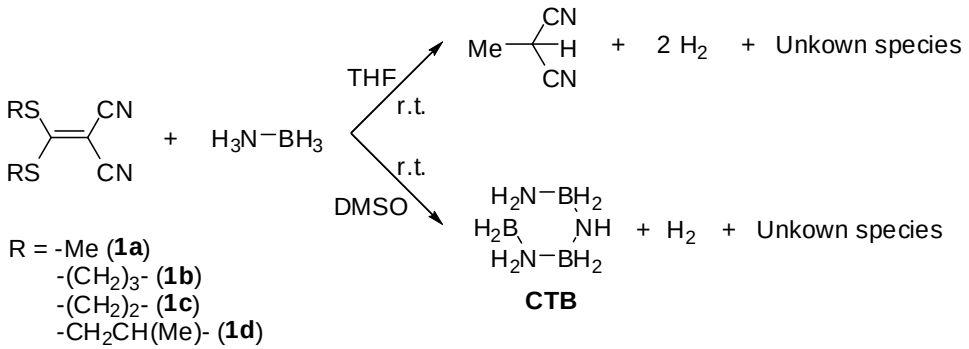

Scheme 7.1

The generation of H_2 via the 1:1 reactions of **AB** with the olefins **1a** and **1b** was confirmed by GC-TCD. When collected in a gas burette, about 0.8 eq. of H_2 was generated in a 1:1 reaction in DMSO and about 1.7 eq. of H_2 in THF (Figure 7.1).

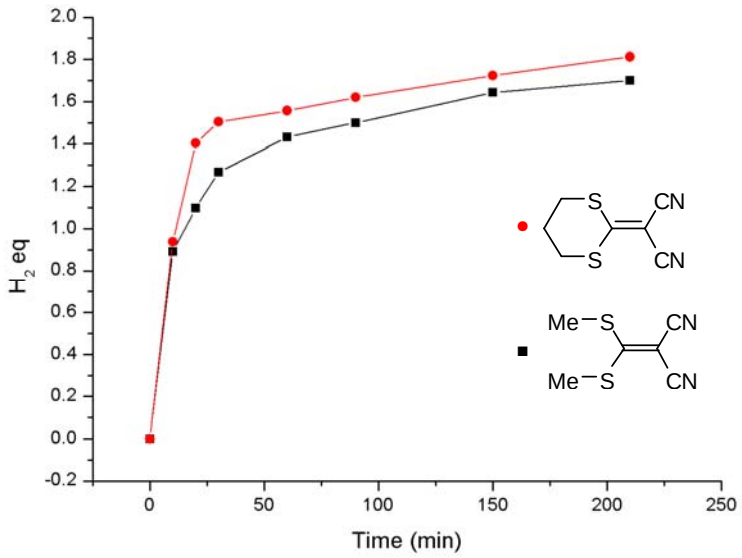

Figure 7.1 Generation of H_2 from a 1:1 mixture of **AB** with olefins **1a** and **1b** in THF at room temperature. The kinetic chart was plotted with eq. of H_2 vs. time.

Use of these olefins as catalysts failed to initiate the catalytic dehydrocoupling of **AB**, nor the catalytic transfer hydrogenation of the *N*-ethylcarbazole or the dehydrogenated Hanztsch ester using **AB** as the hydrogen donor (Scheme 7.2), probably due to a too high instability of the olefins at any of their reaction

intermediate decomposition.

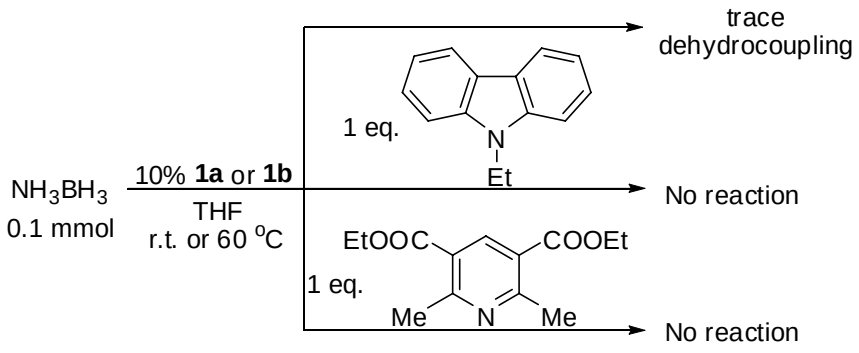

Scheme 7.2

Nevertheless, the transfer hydrogenation of imines with **AB** can be promoted by catalytic amounts of these olefins, as shown in Table 7.2.

Table 7.2 Transfer hydrogenation of imines with **AB** catalyzed by push-pull olefins.

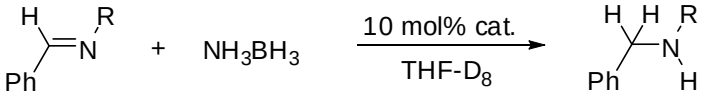

0.1 mmol 0.1 mmol

entry	R	catalyst	temperature	time	result*
1	Ph	none	r.t.	9 d.	67%
2	Ph	**1a**	r.t.	9 d.	80%
3	Ph	none	45 °C	3 d.	> 99%
4	Ph	**1a**	45 °C	1.5 d.	> 99%
5	Ph	**1b**	45 °C	14 h	> 99%
6	^{t}Bu	none	65 °C	6 d	95%
7	^{t}Bu	**1b**	65 °C	12 h	> 99%

*Conversions were determined by integrations of the *in situ* ^{1}H NMR spectra.

Another push-pull olefin containing a diamine ring (**1e**) was also reacted with **AB** in THF or DMSO to initiate transfer hydrogenations. However, as predicted by the calculations (Table 7.1, entry 42), no reaction could be observed even when heating the reaction mixture to 60 °C for a prolonged period of time (Scheme 7.3).

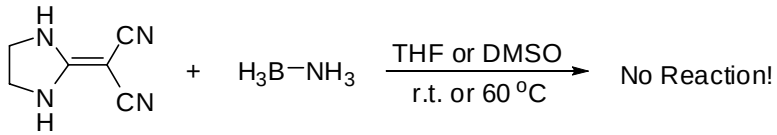

Scheme 7.3

7.3 Metal-free transfer-hydrogenations using hydrogenated olefins as hydrogen donors

Based on the DFT calculations of Table 7.1, energies for transfer hydrogenations (ΔE_{TH}) between different unsaturated/saturated pairs can be obtained according to Eq. (2). Representative polarized olefins with geminal –CN groups **1f**, **1g** and **1i**, the imine *N*-benzylideneaniline (**1h**) and its most reactive –NO_2 substituted derivative (**1j**) were selected for the calculation (Table 7.3).

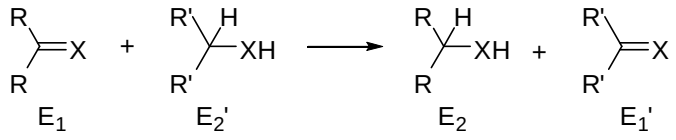

$$\Delta E_{TH} = E_2 + E_1' - (E_1 + E_2') = [E_2 - (E_1 + E_{H2})] - [E_2' - (E_1' + E_{H2})] = \Delta E_H - \Delta E_H' \qquad (2)$$

Firstly, ΔE_{TH} values were calculated for the experimentally successful transfer hydrogenations of compounds **1f**–**1j** with **AB** as the hydrogen donor and were found to be very close to the calculated ΔE_H values (Table 7.3, entries 1-5). Among all these experimentally tested polar unsaturated compounds, 2-(9H-fluoren-9-ylidene)-malononitrile (**1f**) demonstrated a relatively small ΔE_H value of -19.0 kcal/mol (Table 7.1, entry 4) with respect to other olefins. Subsequently, ΔE_{TH} values were calculated for the transfer hydrogenations of compounds **1g**–**1j** with 2-(9H-fluoren-9-yl)-malononitrile (**2f**) as the hydrogen donor. Negative ΔE_{TH} values were obtained in all cases, indicating that the desired hydrogen transfers would be thermodynamically feasible (Table 7.3, entries 6-9). Similar calculations were also carried out for transfer hydrogenation of the compounds in entries 10-17 of Table 7.3, applying 2-benzhydrylmalononitrile (**2g**) and 2-cyclohexylmalononitrile (**2i**) as hydrogen donors, for which positive to small negative ΔE_{TH} values were obtained.

Table 7.3 Calculated energies for transfer hydrogenation reactions.

Entry	Hydrogen donor		Hydrogen acceptor		ΔE_{TH} (kcal/mol)
1	NH_3-BH_3	**AB**	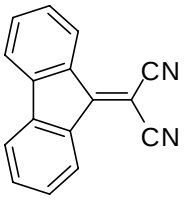	**1f**	-20.4
2	NH_3-BH_3	**AB**	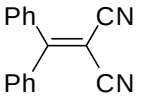	**1g**	-21.3
3	NH_3-BH_3	**AB**	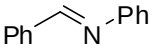	**1h**	-23.3
4	NH_3-BH_3	**AB**	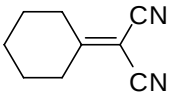	**1i**	-24.8
5	NH_3-BH_3	**AB**	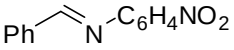	**1j**	-26.3
6	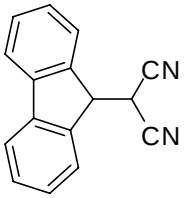	**2f**	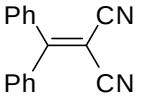	**1g**	-0.9
7	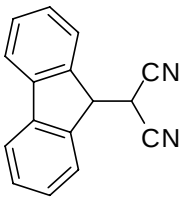	**2f**	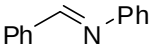	**1h**	-2.9
8	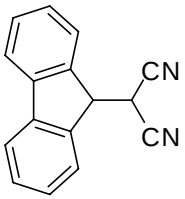	**2f**	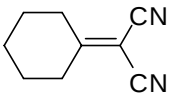	**1i**	-4.3
9	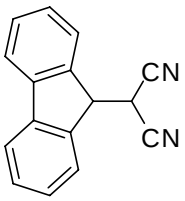	**2f**	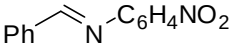	**1j**	-5.9
10	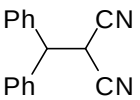	**2g**	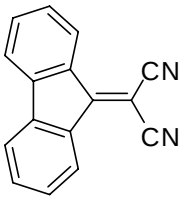	**1f**	0.9

11	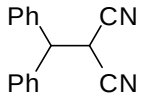	**2g**	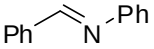	**1h**	-2.0
12	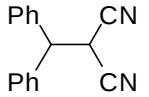	**2g**	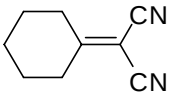	**1i**	-3.5
13	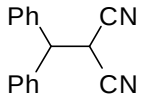	**2g**	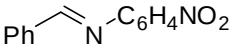	**1j**	-5.0
14	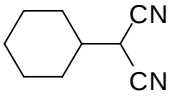	**2i**	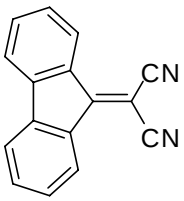	**1f**	4.3
15	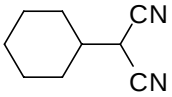	**2i**	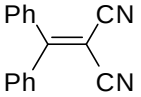	**1g**	3.4
16	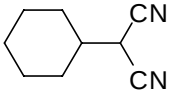	**2i**	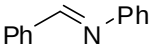	**1h**	1.4
17	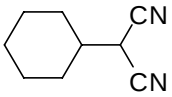	**2i**	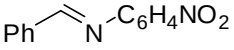	**1j**	-1.5

As can be seen from Table 7.3, compounds **2f** and **2g** are very close in transfer hydrogenation energies. Since **1f** is an orange crystal of very poor solubility in most organic solvents and **2f** is a white powder which has very good solubility, the generation of **1f** as precipitation would naturally provide driving force for the dehydrogenation of **2f**. Thus, the saturated/unsaturated pair of **2f**/**1f** is supposed to be better transfer hydrogenated than the **2g/1g** pair, which are both well soluble in most organic solvents. Therefore, only **2f** was used as hydrogen donors for the transfer hydrogenation experiments as shown in Scheme 7.4. However, no transfer hydrogenation occurred under thermal conditions. The thermal dehydrogenation of **2f** was also carried out either in solutions or in solid state, but no decomposition of **2f** nor hydrogen generation was observed at temperatures up to 200 ^{o}C.

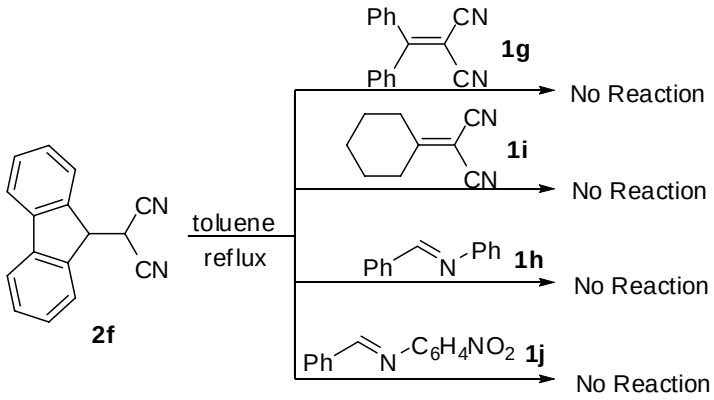

Scheme 7.4

Surprisingly, in a reaction of **1i** with **2f** in refluxing toluene using freshly prepared **2f** by transfer hydrogenation of **1f** with **AB** in THF followed by removal of the volatiles (THF and borazine) in high vacuum without further purification (with small amount of polyborazine as impurities), the targeted transfer hydrogenation reaction was indeed observed in refluxing toluene (Scheme 7.5). Because the hydrogen transfer could not occur using purified **2f** as shown in Scheme 7.4, it suggests that the thermodynamically favored process of the hydrogen transfer from **2f** to **1i** is achievable, but higher temperatures than 110 ^{o}C or a special catalyst is required.

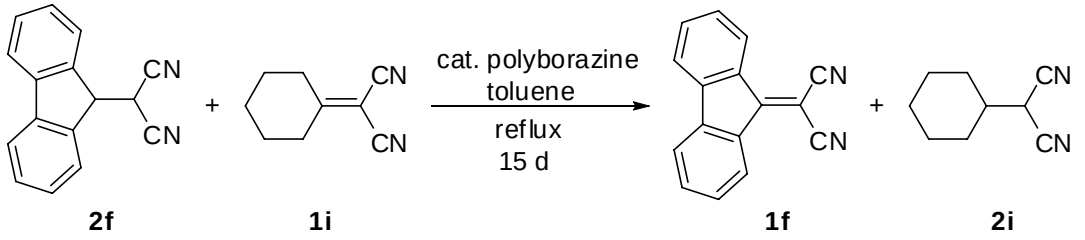

Scheme 7.5

7.4 Outlook

Although the uncatalyzed transfer hydrogenation using **2f** as the hydrogen donor was not accomplished, the accidently success due to the presence of some impurities implied that it is an achievable experiment. Out of the field of 'metal-free' chemistry, lots of metal-catalysts of very good activities toward transfer hydrogenation need to

be tested. Beside the transfer hydrogenation properties, the difference in hydrogen numbers between **1f** ($C_{16}H_8N_2$) and its completely hydrogenated form ($C_{16}H_{30}N_2$) is 22 H atoms, which add up to 8.8 wt% of the molecule weight and is higher than in the explored *N*-ethylcarbozole derivatives (5.8 wt%). Thus, the potential utility of the 2-(9H-fluoren-9-ylidene)malononitrile derivatives as hydrogen storage material is worthy of exploring.

7.5 Experimental

All the manipulations were carried out under a nitrogen atmosphere using Schlenk techniques or in a drybox (Model MB-150B-G). Reagent grade benzene, toluene, hexane, diethyl ether, and tetrahydrofuran were dried and distilled from sodium benzophenone ketyl prior to use. Acetonitrile was distilled from CaH_2, and chloroform was dried by P_2O_5. NMR spectra were measured on a Varian Mercury spectrometer at 200 MHz for ^1H and 50.3 MHz for $^{13}C\{^1H\}$, Varian Gemini-2000 spectrometer at 300.1 MHz for ^1H, 64.2 MHz for $^{11}B\{^1H\}$ and 75.4 MHz for $^{13}C\{^1H\}$ and on a Bruker-DRX-500 spectrometer at 500.2 MHz for ^1H, 107 MHz for $^{11}B\{^1H\}$ and 125.8 MHz for $^{13}C\{^1H\}$. Chemical shifts for ^1H and ^{13}C are given in ppm relative to TMS and those for ^{11}B relative to $Et_2O{\cdot}BF_3$.

Push-pull olefins **1a-1d** were prepared as follows:[3] To a solution of malononitrile (0.66 g, 10 mmol) in DMF (5 mL) was added an excess of anhydrous K_2CO_3 (1 g) and, after 10 min, CS_2 in small amount (0.72 mL, 12 mmol). After 10 min was added a catalytic amount of tetrabutylammonium bromide and methyl iodide (1.37 mL, 22 mmol) or the corresponding bromide (12 mmol) in small portions, and the mixture was stirred at room temperature for 30 min, heated at 50 °C for 2 h, and finally stirred at room temperature overnight. The residue was washed with water, and the solid formed was collected by filtration and washed with cold water.

2-(Bis(methylthio)methylene)malononitrile (**1a**)[3] was recrystallized from ethanol- water as orange needles (38%): δ_H (ppm; 300 MHz; $CDCl_3$) 2.76 (s, 6H, 2

-SCH_3); δ_C (ppm; 75.4 MHz; $CDCl_3$) 19.43 (-SCH_3), 76.26, 112.88 (-CN), 184.04.

2-(1,3-Dithian-2-ylidene)malononitrile (**1b**)[3] was recrystallized from ethanol-water as a yellow to pink solid (43%): δ_H (ppm; 300 MHz; $CDCl_3$) 2.37 (p, 2H, C-CH_2-C), 3.18 (t, 4H, 2 S-CH_2-); δ_C (ppm; 75.4 MHz; $CDCl_3$) 22.45 (-CH_2-), 29.82 (S-CH_2-), 112.14 (-CN).

2-(1,3-Dithiolan-2-ylidene)malononitrile (**1c**),[3] light yellow solid (46%):δ_H (ppm; 300 MHz; THF-D_8) 3.88 (s); δ_C (ppm; 75.4 MHz; THF-D_8) (ppm) 42.33.

2-(4-Methyl-1,3-dithiolan-2-ylidene)malononitrile (**1d**),[3] light yellow solid (35%):δ_H (ppm; 300 MHz; THF-D_8) 1.54-1.57 (d, J = 6 Hz, 3H), 3.61-3.71 (d*d, J_3 = 6 Hz, J_2 = -12 Hz, 1H), 3.93-4.02 (d*d, J_3 = 6 Hz, J_2 = -12 Hz, 1H), 4.43-4.59 (m, 1H); δ_C (ppm; 75.4 MHz; THF-D_8) 19.19, 48.34, 54.86, 113.89, 189.34.

2-(Imidazolidin-2-ylidene)malononitrile (**1e**) was prepared by reaction of **1a** with ethane-1,2-diamine in THF and precipitated as a orange solid:[4] δ_H (ppm; 300 MHz; DMSO-D_6) 3.55 (s, N-CH_2-CH_2-N); δ_C (ppm; 75.4 MHz; DMSO-D_6) 44.03 (-CH_2-), 118.10 (-CN), 166.81 (N-C=).

2-(9H-Fluoren-9-ylidene)malononitrile (**1f**) was prepared by melting and stirring of a 1:1 mixture of molononitrile and 9-flouronone without solvent for 5 min, nearly 100% yield was obtained.[5] Orange-red solid: δ_H (ppm; 300 MHz; THF-D_8) 7.36-7.42 (m, 2 H, -CH=), 7.53-7.59 (m, 2 H, -CH=), 7.70-7.75 (m, 2 H, -CH=), 8.35-8.39 (m, 2 H, -CH=); δ_C (ppm; 75.4 MHz; THF-D_8) 114.24 (2 C, -CN), 121.85, 127.30, 127.40, 130.03, 135.50, 143.32, 161.38.

2-(9H-fluoren-9-yl)malononitrile (**2f**),[6] white solid, δ_H (ppm; 300 MHz; THF-D_8) 4.59 (d, J = 3.5 Hz, 1 H, -CH-), 5.18 (d, J = 4.5 Hz, 1 H, -CH-), 7.34-7.51 (m, 4 H, -CH=), 7.79-7.88 (m, 4 H, -CH=); δ_C (ppm; 75.4 MHz; THF-D_8) 27.78, 46.95, 113.41 (-CN-), 121.41, 125.63, 128.67, 130.07, 142.00, 142.64.

2-(Diphenylmethylene)malononitrile (**1g**): A 1 : 1 mixture of molononitrile and

diphenyl-methanimine was stirred without solvent at room temperature for 5 minutes giving the target product with nearly 100% yield.[7] White solid: δ_H (ppm; 300 MHz; THF-D_8) 7.49-7.63 (m); δ_C (ppm; 300 MHz; THF-D_8) 114.67 (2 C, -CN), 129.58, 131.30, 133.11, 137.57, 174.59.

2-Benzhydrylmalononitrile (**2g**),[8] white solid, δ_H (ppm; 300 MHz; THF-D_8) 4.81 (d, J = 9 Hz, 1 H, -CH-), 5.29 (d, J = 9 Hz, 1 H, -CH-), 7.23-7.44 (m, 10 H, -CH=); δ_C (ppm; 75.4 MHz; THF-D_8) 28.98, 52.14, 113.87 (-CN), 128.89, 128.96, 129.80, 139.70.

N-benzylaniline (**2h**): δ_H (ppm; 300 MHz; THF-D_8)[9-12] 4.27-4.30 (d, J = 6 Hz, 2H), 5.32 (br, N-H), 6.50-6.59 (m, 3H), 6.99-7.38 (m, 7H); δ_C (ppm; 300 MHz; THF-D_8) 48.63, 113.36, 117.21, 127.58, 128.09, 129.18, 129.67, 141.45, 150.02.

2-Cyclohexylidenemalononitrile (**1i**), colorless liquid: A ketone (0.1 mol), malononitrile (0.2 mol), ammonium acetate (1.5 g), acetic acid (4.8 g) and benzene (30 mL) are refluxed with a Dean-Stark trap over night or until water production ceases (> 6 h). The mixture was then washed with water (3 x 30 mL) and half saturated aqueous sodium chloride (1 x 30 mL) and then dried with magnesium sulfate. Then benzene was removed and the remaining liquid distilled under reduced pressure (for solid recrystallization).[14] δ_H (ppm; 300 MHz; THF-D_8) 1.63-1.74 (m, 2 H, -CH_2-), 1.74-1.87 (m, 4 H, -CH_2-), 2.62-2.75 (m, 4 H, -CH_2-); δ_C (ppm; 75.4 MHz; THF-D_8) 24.83, 27.52, 34.14, 82.61 (1 C, -C=), 112.03 (2 C, -CN), 183.89(1 C, -C=).

2-Cyclohexylmalononitrile (**2i**),[15] colorless liquid, δ_H (ppm; 300 MHz; THF-D_8) 1.15-1.44 (m, 5 H, -CH-), 1.69-2.06 (m, 6 H, -CH-), 4.25 (d, J = 5 Hz, 1 H, -CH-); δ_C (ppm; 300 MHz; THF-D_8) 26.34, 26.41, 29.57, 30.76, 40.06, 113.64 (2 C, -CN).

N-benzyl-4-nitroaniline (**2j**):[9] δ_H (ppm; 300 MHz; THF-D_8) 4.41-4.43 (d, J = 6 Hz, 2H), 6.61-6.65 (m, 2H), 6.75 (br, N-H), 7.20-7.34 (m, 5H), 7.97-8.02 (m, 2H); δ_C (ppm; 300 MHz; THF-D_8) 46.83, 110.82, 125.65, 127.19, 128.38, 137.49, 138.50, 154.02.

7.6 References

[1] Gaussian 03, Revision D.01, M. J. Frisch, G. W. Trucks, H. B. Schlegel, G. E. Scuseria, M. A. Robb, J. R. Cheeseman, J. A. Montgomery, Jr., T. Vreven, K. N. Kudin, J. C. Burant, J. M. Millam, S. S. Iyengar, J. Tomasi, V. Barone, B. Mennucci, M. Cossi, G. Scalmani, N. Rega, G. A. Petersson, H. Nakatsuji, M. Hada, M. Ehara, K. Toyota,R. Fukuda, J. Hasegawa, M. Ishida, T.Nakajima, Y. Honda, O. Kitao, H. Nakai, M. Klene, X. Li, J. E. Knox, H. P. Hratchian, J. B. Cross, V. Bakken, C. Adamo, J. Jaramillo, R. Gomperts, R. E. Stratmann, O. Yazyev, A. J. Austin, R. Cammi, C. Pomelli, J. W. Ochterski, P. Y. Ayala, K. Morokuma, G. A. Voth, P. Salvador, J. J. Dannenberg, V. G. Zakrzewski, S. Dapprich, A. D. Daniels, M. C. Strain, O. Farkas, D. K. Malick, A. D. Rabuck, K. Raghavachari, J. B. Foresman, J. V. Ortiz, Q. Cui, A. G. Baboul, S. Clifford, J. Cioslowski, B. B. Stefanov, G. Liu, A. Liashenko, P. Piskorz, I. Komaromi, R. L. Martin, D. J. Fox, T. Keith, M. A. Al-Laham, C. Y. Peng, A. Nanayakkara, M. Challacombe, P. M. W. Gill, B. Johnson, W. Chen, M. W. Wong, C. Gonzalez, and J. A. Pople, Gaussian, Inc., Wallingford CT, 2004.

[2] C. Hansch, J. E. Quinlan and G. L. Lawrence, *J. Org. Chem.*, **1968**, *33*, 347-350.

[3] P. G. Baraldi, F. Fruttarolo, M. A. Tabrizi, D. Preti, R. Romagnoli, H. El-Kashef, A. Moorman, K. Varani, S. Gessi, S. Merighi and P. A. Borea, *Journal of Medicinal Chemistry* **2003**, *46*, 1229-1241.

[4] S. Sasho, T. Seishi, M. Kawamura, R. Hirose, S. Toki and J. Shimada, *Bioorganic & Medicinal Chemistry Letters*, **2008**, *18*, 2288-2291

[5] G.-W. Wang and B. Cheng, *ARKIVOC*, **2004**, 4.

[6] X.-Q. Fang, H.-J. Xu, H. Jiang, Y.-C. Liu, Y. Fu and Y.-D. Wu, *Tetrahedron Lett.* **2009**, *50*, 312-315.

[7] G. Charles, *Bull. Soc. Chimi. Fr.,* **1963**, *8-9*, 1559.

[8] C.-R. Liu, M.-B. Li, C.-F. Yang and S.-K. Tian, *Chem. Eur. J.*, **2009**, *15*, 793-797.

[9] M. Tajbakhsh, M. M. Lakouraj, M. S. Mahalli, *Synth. Commun.* **2008**, *38*, 1976-1983.

[10] K.-i. Fujita, Y. Enoki, R. Yamaguchi, *Tetrahedron* **2008**, *64*, 1943-1954.

[11] R. Apodaca, W. Xiao, *Org. Lett.* **2001**, *3*, 1745-1748.

[12] Y. Kayaki, H. Ikeda, J. Tsurumaki, I. Shimizu, A. Yamamoto, *Bull. Chem. Soc. Jpn*. **2008**, *81*, 1053–1061.

[13] E. J. Roskamp, S. F. T. Pedersen, *J. Am. Chem. Soc.* **1987**, *109*, 6551-6553.

[14] J. Mirek, M. Adamczyk and M. Mokrosz, *Synthesis*, **1980**, 296.

[15] a) R. E. Sammelson and M. J. Allen, *Synthesis* **2005**, 543-546; b) J. C. Dunham, A. D. Richardson and R. E. Sammelson, *Synthesis*, **2006**, 680-686.

Summary

Hydrogen may play a future role as an energy carrier and bridge the era of fossil energy and the future of renewable energies or nuclear energy. It has become an important part of energy strategies and technology competition. In conjunction with this, hydrogen storage technology is to be developed. Thus, amine borane adducts, especially ammonia borane (NH_3BH_3, **AB**), attract much research attention as feasible materials with high hydrogen capacities. Great effort was focused on the release/uptake of H_2 from these compounds through metallocatalysis, either via dehydrocoupling or solvolysis. Our approach to the dehydrogenation of such complexes was to use a metal-free transfer hydrogenation process.

In this thesis, amine borane adducts were successfully applied as polar hydrogen donors for metal-free reductions of three types of polar double bond containing compounds: imines (C=N), polarized olefins (C=C) and carbonyl compounds (C=O). Although they are all seemingly 'polarity matched' metal-free transfer hydrogenations, mechanistic studies revealed that different reaction mechanisms were involved for different substrates and/or in different solvents (Scheme 8.1).

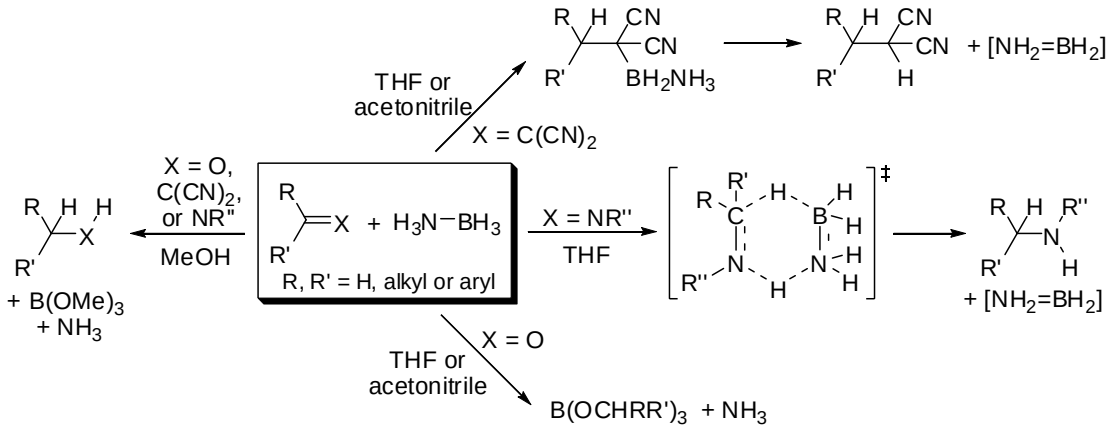

Scheme 8.1 Overall scheme for the transfer hydrogenation reactions of **AB** with various substrates under different conditions.

In Chapter 3, a metal-free regio-selective transfer hydrogenation of imines with amine borane compounds was achieved in THF at 60 °C (Table 8.1).[1] For the imine,

hydrogenation reaction happened exclusively with the corresponding amine as the only product. But the dehydrocoupling of **AB** seems much more complex: four boron compounds were detected by the *in situ* ^{11}B NMR, including cyclotriborazane (**CTB**), B-(cyclodiborazanyl) aminoborohydride (**BCDB**), borazine (**BZ**) and poly(borazylene) (**PBZ**) (Scheme 8.2). Moreover, the exact pathway from **AB** to **BZ** and/or **PBZ**, either through **CTB** or **BCDB**, was not clear yet. Deuterium labeling experiment using selectively deuterated **AB** derivatives, NH_3BD_3 (**AB(D)**), ND_3BH_3 (**A(D)B**) and ND_3BD_3 (**A(D)B(D)**), confirmed the regio-selectivity that H_B went to the C terminal and H_N went to the N terminal of the C=N double bond, respectively. Studies of deuterium kinetic isotope effects (DKIE) were also carried out, where inverse DKIEs ($k_{AB}/k_{AB(D)}$ = 0.87, $k_{A(D)B}/k_{A(D)B(D)}$ = 0.72) were obtained with the deuterium label on the borane side (D_B) and normal DKIEs ($k_{AB}/k_{A(D)B}$ = 1.93, $k_{AB(D)}/k_{A(D)B(D)}$ = 1.61) were obtained with D_N. Similar DKIE values were obtained by DFT calculations (0.82 for D_B and 1.84 for D_N), revealing the involvement of both H_B and H_N in the rate-determining step (RDS). Positive reaction constant ρ values obtained from Hammett correlations further proved that negative charge was generated during the RDS. Therefore, a simultaneous double hydrogen transfer from **AB** to imines via a concerted six-membered ring transition state was proposed. DFT calculations confirmed that such a concerted pathway would undergo much lower energy barriers ($\triangle H$ = 14.6 kcal/mol and $\triangle G$ = 28 kcal/mol) comparing to possible stepwise pathways ($\triangle H$ = 45.2 kcal/mol and $\triangle G$ = 44.9 kcal/mol as the lowest values).

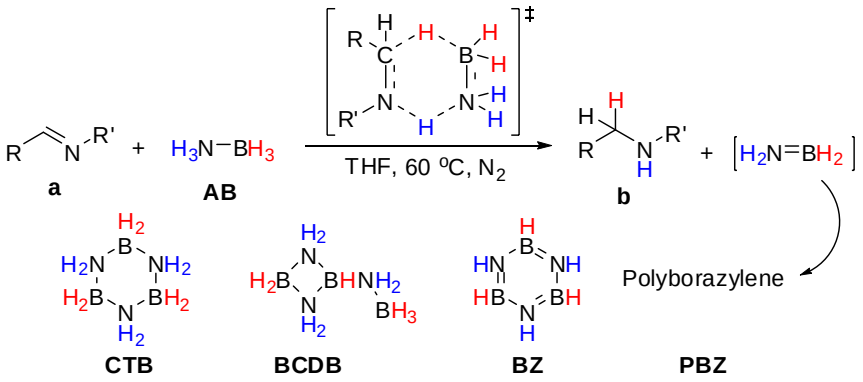

Scheme 8.2 Metal-free transfer hydrogenation of imines with **AB**.[1]

Table 8.1 Chapter 3: Metal-free transfer hydrogenation of imines with **AB**.[1]

	List of imines		List of amines
1a	Ph−CH=N−Ph	**1b**	Ph−CH_2−NH−Ph
2a	Ph−CH=N−Bn	**2b**	Ph−CH_2−NH−Bn
3a	Ph−CH=N−^{t}Bu	**3b**	Ph−CH_2−NH−^{t}Bu
4a	Cy−CH=N−^{t}Bu	**4b**	Cy−CH_2−NH−^{t}Bu
5a	Ph−CH=N−$CHPh_2$	**5b**	Ph−CH_2−NH−$CHPh_2$
6a	Ph_2−C=NH	**6b**	Ph_2−CH−NH_2
7a	*p*-$MeOC_6H_4$−CH=N−Ph	**7b**	*p*-$MeOC_6H_4$−CH_2−NH−Ph
8a	*p*-ClC_6H_4−CH=N−Ph	**8b**	*p*-ClC_6H_4−CH_2−NH−Ph
9a	*p*-$O_2NC_6H_4$−CH=N−Ph	**9b**	*p*-$O_2NC_6H_4$−CH_2−NH−Ph
10a	Ph−CH=N−C_6H_4(*p*-OMe)	**10b**	Ph−CH_2−NH−C_6H_4(*p*-OMe)
11a	Ph−CH=N−C_6H_4(*p*-Cl)	**11b**	Ph−CH_2−NH−C_6H_4(*p*-Cl)
12a	Ph−CH=N−C_6H_4(*p*-NO_2)	**12b**	Ph−CH_2−NH−C_6H_4(*p*-NO_2)
13a	*p*-ClC_6H_4−CH=N−C_6H_4(*p*-OMe)	**13b**	*p*-ClC_6H_4−CH_2−NH−C_6H_4(*p*-OMe)
14a	*p*-ClC_6H_4−CH=N−C_6H_4(*p*-Cl)	**14b**	*p*-ClC_6H_4−CH_2−NH−C_6H_4(*p*-Cl)
15a	*p*-$MeOC_6H_4$−CH=N−C_6H_4(*p*-Cl)	**15b**	*p*-$MeOC_6H_4$−CH_2−NH−C_6H_4(*p*-Cl)
16a	*p*-$MeOC_6H_4$−CH=N−C_6H_4(*p*-OMe)	**16b**	*p*-$MeOC_6H_4$−CH_2−NH−C_6H_4(*p*-OMe)

In Chapter 4, olefins with two electron-withdrawing groups (EWGs) (−CN or $-CO_2Me$) on one of the termini of the C=C double bond and alkyl groups on the other one were reacted with **AB** in THF or acetonitrile, where metal-free transfer hydrogenation of the olefins proceeded rapidly at room temperature. Again, only the hydrogenation products of the olefins were observed with nearly 100% conversions. The dehydrocoupling reaction of **AB** was also rather selective: **BZ** was obtained as the main product together with a small amount of **PBZ** (Table 8.2). To trace the reaction mechanism, deuterium labeling studies were carried out, which demonstrated a similar regio-selectivity as for imines that the H_N atoms added to the EWG terminus of the C=C double bond and the H_B atoms added to the other C terminus. However, the results of DKIEs were quite different with respect to those of the imines: DKIE values nearly equal to 1 were obtained with D_B ($k_{\mathbf{AB}}/k_{\mathbf{AB(D)}}$ = 1.00, $k_{\mathbf{A(D)B}}/k_{\mathbf{A(D)B(D)}}$ = 1.04), indicating that there is no kinetic isotope effect with deuterium on boron, while normal DKIEs were obtained with D_N ($k_{\mathbf{AB}}/k_{\mathbf{A(D)B}}$ = 1.55, $k_{\mathbf{AB(D)}}/k_{\mathbf{A(D)B(D)}}$ = 1.62), manifesting that only $H(D)_N$ was involved in the RDS. Furthermore, a hydroboration

intermediate **HBI** (Scheme 8.3) was trapped under low temperature by *in situ* NMR measurements, clearly stating that the transfer of H_B happened before the RDS and the transfer of H_N occurred in the RDS.

Table 8.2 Chapter 4: Transfer hydrogenation of polarized olefins with **AB**.[2]

	List of polar olefins		List of hydrogenated products
1a	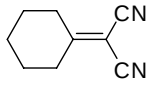	**2a**	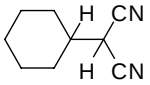
1b	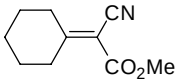	**2b**	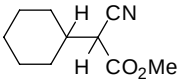
1c	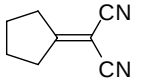	**2c**	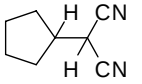
1d	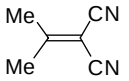	**2d**	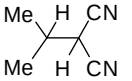
1e	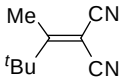	**2e**	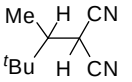
1f	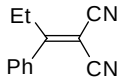	**2f**	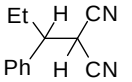
1g	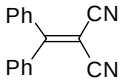	**2g**	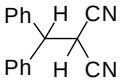
1h	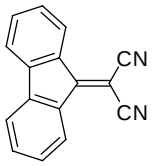	**2h**	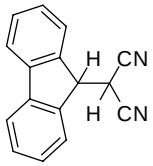
1i	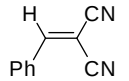	**2i**	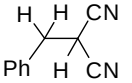
1j	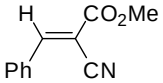	**2j**	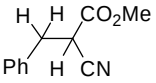
1k	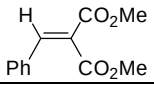	**2k**	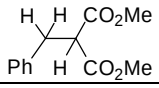

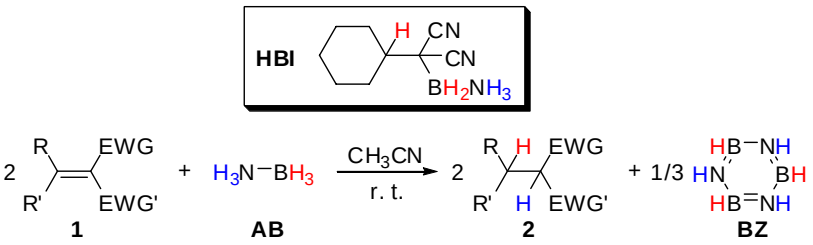

Scheme 8.3 Transfer hydrogenation of polarized olefins with **AB** at room temperature via a hydroboration intermediate (**HBI**).[2]

In chapter 5, transfer hydrogenation reactions were carried out with more activated olefins and amine borane adducts in a variety of solvents.[3] It was found

that only strongly polarized olefins with two geminal EWGs on one terminus of the CC bond and alkyl and/or aromatic groups on the other C terminus could be easily hydrogenated at room temperature (Table 8.3). Special cases were: a) When two strongly polarized vinyl groups were attached to a methylene group (**1h**), deprotonation of the alkylic H would take place yielding a stable anion; b) When the typical push-pull olefin **1k** or pull-pull olefin **1l**, a complex mixture was obtained; c) Olefins bearing only one EWG (**1n**), or the dehydrogenated Hanztsch ester (**1o**), could not be hydrogenated by **AB** (Scheme 8.4). Besides **AB**, some alkylated amine borane adducts such as $MeNH_2BH_3$, Me_2NHBH_3 and $^tBuNH_2BH_3$ were also attempted to react with **1a** and similar transfer hydrogenation reaction occurred, but **AB** displayed by far the best activity compared to the other amine boranes. The dehydrocoupling pathway of **AB** was then studied in details: the dehydrocoupling intermediate [NH_2=BH_2] was trapped by addition of cyclohexene into the reaction mixture, **BZ** and **PBZ** were proved to be formed via dehydrocoupling of BH_2 species such as possibly solvent stabilized [NH_2=BH_2] rather than dehydrogenation of **CTB**.[3]

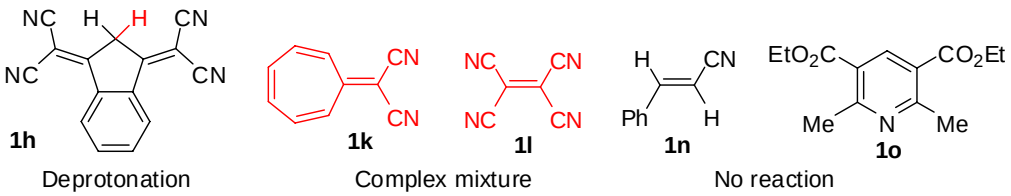

Scheme 8.4 Olefins that could not be hydrogenated by amine borane adducts.

It was also found that the hydrogen transfer proceeded faster in apolar solvents (THF, toluene or benzene) than in polar aprotic solvents (acetonitrile, chloroform or DMSO). While a protic solvent like methanol was used, the olefin could be transfer hydrogenated rapidly at room temperature, however, solvolysis of the amine borane took place instead of dehydrocoupling (Scheme 8.5).[3]

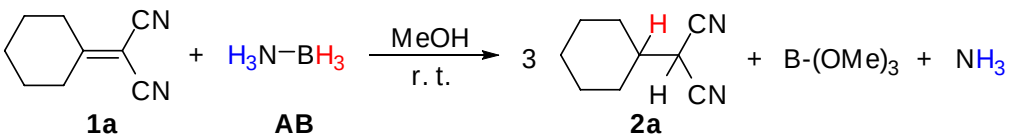

Scheme 8.5 Transfer hydrogenation of 2-cyclohexylidenemalononitrile and solvolysis of **AB** in methanol.

Table 8.3 Chapter 5: Transfer hydrogenation of activated olefins with amine borane adducts.[3]

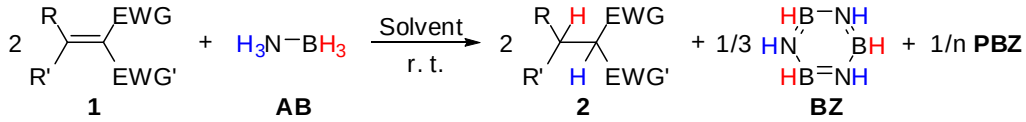

Solvents: THF, CH_3CN, $CHCl_3$, C_6H_6, DMSO, etc.

List of activated olefins		List of hydrogenated products	
1a	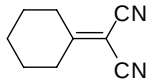	**2a**	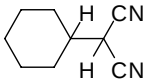
1b	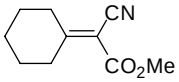	**2b**	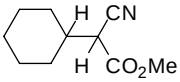
1c	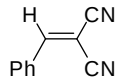	**2c**	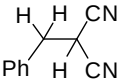
1d	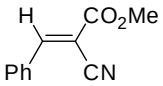	**2d**	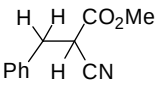
1e	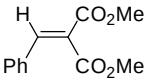	**2e**	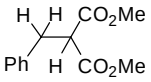
1f	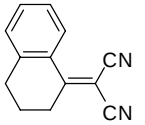	**2f**	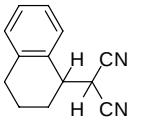
1g	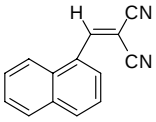	**2g**	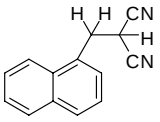
1i	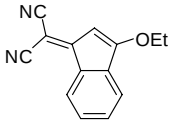	**2i**	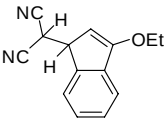
1j	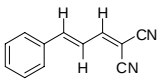	**2j**	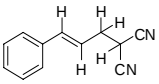
1p	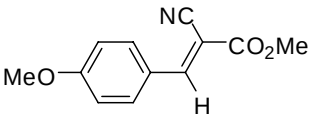	**2p**	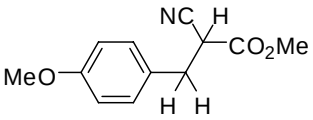
1q	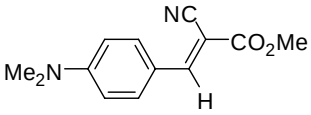	**2q**	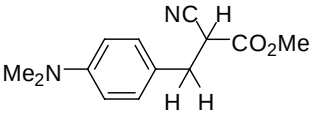
1r	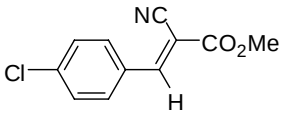	**2r**	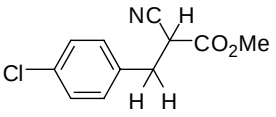
1s	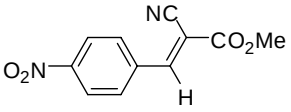	**2s**	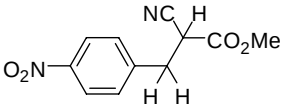
1t	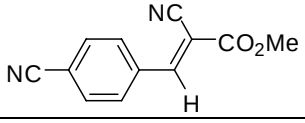	**2t**	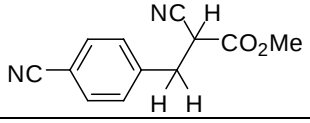

In Chapter 6, C=O group containing compounds (ketones and aldehydes) were reacted with **AB** in THF without a catalyst. Unlike the double-H transfer reactions of amine boranes with imines or polar olefins, hydroboration products trialkyl borates were obtained exclusively in the reactions with carbonyl compounds (Table 8.4).

Table 8.4 Chapter 6: Reduction of carbonyl compounds with **AB**.[4]

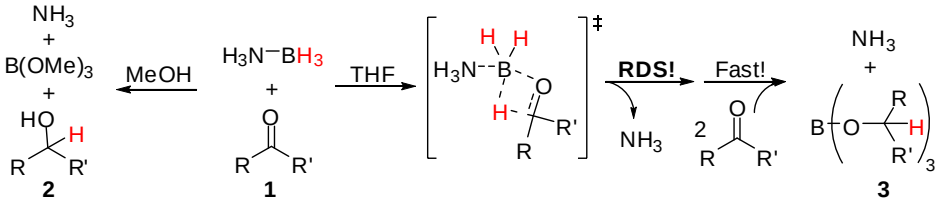

List of hydrogenation products		List of hydroboration products	
2a	Ph_2CH-OH	**3a**	$(Ph_2CH-O-)_3B$
2b	PhMeCH−OH	**3b**	$(PhMeCH-O-)_3B$
2c	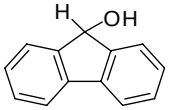	**3c**	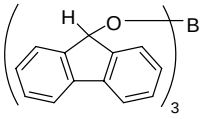
2d	PhCyCH−OH	**3d**	$(PhCyCH-O-)_3B$
2e	(*E*)PhCH=CH−CH(Ph)−OH	**3e**	((*E*)PhH=CH−CH(Ph)−O−)$_3$B
2f	Et_2CH-OH	**3f**	$(Et_2CH-O-)_3B$
2g	Cy−OH	**3g**	$(Cy-O-)_3B$
2h	$Ph-CH_2-OH$	**3h**	$(Ph-CH_2-O-)_3B$
2i	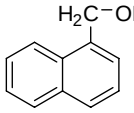	**3i**	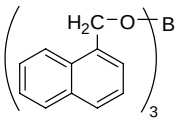
2j	*p*-CN−C_6H_4−CH_2−OH	**3j**	(*p*-CN−C_6H_4−CH_2−O−)$_3$B
2k	*p*-MeO−C_6H_4−CH_2−OH	**3k**	(*p*-MeO−C_6H_4−CH_2−O−)$_3$B
2l	*p*-Me_2N−C_6H_4−CH_2−OH	**3l**	(*p*-Me_2N−C_6H_4−CH_2−O−)$_3$B

To find out whether transfer hydrogenation was involved in this hydroboration process, mechanistic studies were carried out. In the low temperature *in situ* ^{11}B NMR experiment, no dehydrocoupling product of **AB** such as **CTB**, **BZ** or **PBZ** was detected, but an interesting temperature-dependent equilibrium between $B(OR)_3$ and its THF complex THF·$B(OR)_3$ was observed. Deuterium labeling studies revealed that H_B was transfered to the alkyl borates, while H_N appeared in the form of free NH_3. Even though, normal DKIE values were obtained with both D_B and D_N ($k_{AB}/k_{AB(D)}$ = 1.28, $k_{AB}/k_{A(D)B}$ = 1.74, $k_{A(D)B}/k_{A(D)B(D)}$ = 1.10, and $k_{AB(D)}/k_{A(D)B(D)}$ = 1.49). Since

$H(D)_N$ was not transferred to the hydroboration product and no dehydrocoupling products of **AB** was observed even at low temperatures, it was assumed that the dissociation of ammonia from **AB** occurred as the RDS before the hydroboration step. When a protic solvent (methanol) was used, metal-free methanolysis of **AB** took place with the carbonyl compounds being directly hydrogenated (Table 8.4).[4]

Unpublished results on dehydrogenation and transfer hydrogenation reactions were discussed in Chapter 7. Firstly, the total energies of a broad scope of polar unsaturated compounds and their saturated products were calculated using the Gaussian 03 program at the B3LYP/6-31+G* level in the gas phase at 298 K. The energies for hydrogenations (ΔE_H) were obtained according to Eq. (1) and the results were listed in Table 8.5.

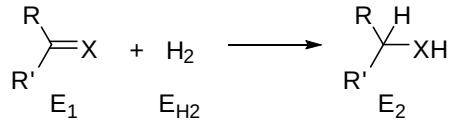

$$\triangle E_H = E_2 - (E_1 + E_{H2}) \quad (1)$$

Table 8.5 Calculated hydrogenation energies for polar unsaturated compounds.

unsaturated compounds	ΔE_H (kcal/mol)	unsaturated compounds	ΔE_H (kcal/mol)
NH_2=BH_2	1.5	CH_2=CH_2	-40.7
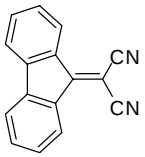	-19.0	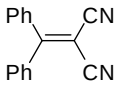	-19.9
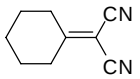	-23.3	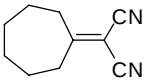	-22.4
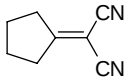	-20.2	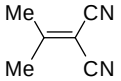	-24.3
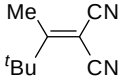	-23.3	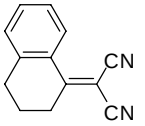	-19.3
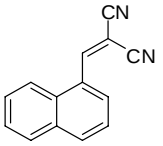	-26.5	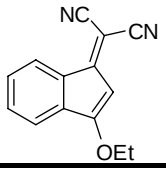	-17.2

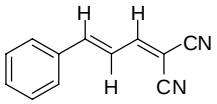	-19.2	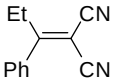	-24.3
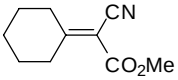	-26.1	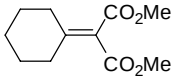	-30.9
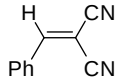	-24.9	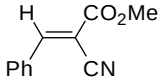	-25.4
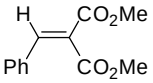	-31.8	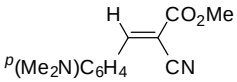	-21.0
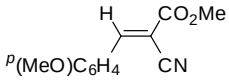	-23.1	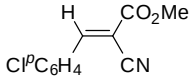	-25.5
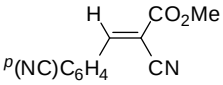	-26.9	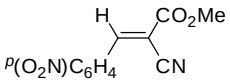	-27.5
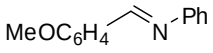	-20.9	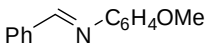	-20.1
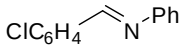	-21.8	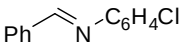	-21.9
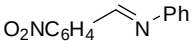	-22.3	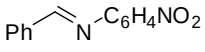	-24.8
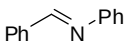	-21.9	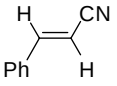	-31.6
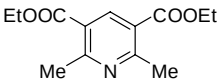	-9.1	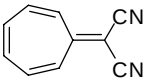	-9.3
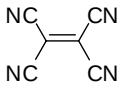	-26.9	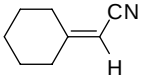	-28.7
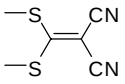	-21.4	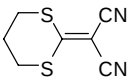	-20.0
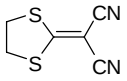	-16.7	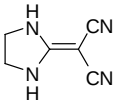	0.1
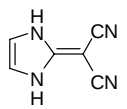	6.9	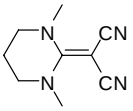	-2.0
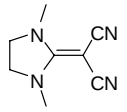	-3.3	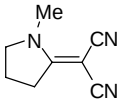	-10.6

By comparing the ΔE_H values with the transfer hydrogenation reactivity of the tested compounds with **AB** as the hydrogen donor, it was found that compounds of good reactivity all possess moderated ΔE_H in the range of -19 to -30 kcal/mol, and ΔE_H values out of this range were obtained with those compounds that have no reaction or complex reactions with **AB**. The ΔE_H of several push-pull olefins were

also calculated and their reactivity patterns were predicted (last 4 rows of Table 8.5): Moderate ΔE_H values of around -20 kcal/mol were obtained with the sulfur-heterocycle containing olefins – similar to the tested polarized olefins, indicating that they might react with **AB** in one way or another. For those push-pull olefins bearing nitrogen-heterocycles, very small ΔE_H values of around 0 were obtained, suggesting that no reaction or complex reaction would occur with **AB**.

Subsequently, 1:1 reactions of **AB** with these push-pull olefins **1a-1e** were carried out. Generation of H_2 was detected when the sulfur-heterocycle containing olefins (**1a-1d**) were used, but the reaction courses were very complex and could not be fuuly elucidated (Scheme 8.6). They were then proved unable to catalyze the dehydrogenation of **AB**. However, the transfer hydrogenations of imines with **AB** can indeed be accelerated by using 10 mol% of these olefins. When a nitrogen-heterocycle containing olefin 2-(imidazolidin-2-ylidene)malononitrile (**1e**) was used, no reaction occured – right as what was predicted by its ΔE_H value (0.1 kcal/mol) of close to 0.

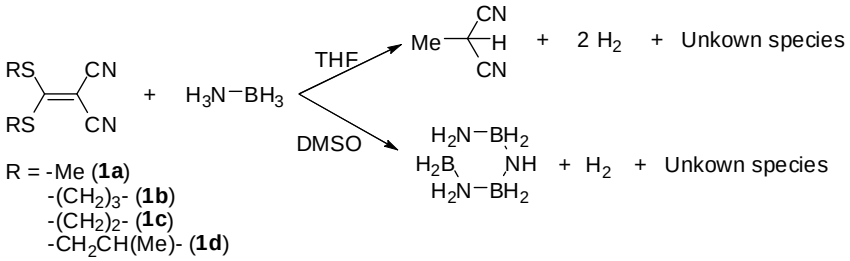

Scheme 8.6

Finally, energies for transfer hydrogenations (ΔE_{TH}) were calculated, applying the saturated products of selected polar olefins as hydrogen donors and other polar olefins as hydrogen acceptors (Table 8.6). However, even the hydrogen transfer is thermodynamically favored ($\Delta E_{TH} < 0$), no transfer hydrogenation occurred under non-catalytic conditions in refluxing toluene. Nevertheless, in case there is small amount of polyborazine in the reaction with **2f** as the hydrogen donor and **1i** as the hydrogen accptor, the transfer hydrogenation would occur in refluxing toluene (Scheme 8.7).

Table 8.6 Calculated energies for transfer hydrogenation reactions.

Hydrogen donor	Hydrogen acceptor	ΔE_{TH} (kcal/mol)
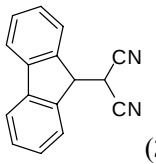 (**2f**)	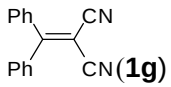 (**1g**)	-0.9
2f	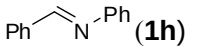 (**1h**)	-2.9
2f	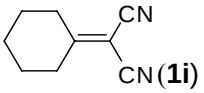 (**1i**)	-4.3
2f	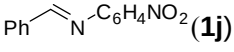 (**1j**)	-5.9
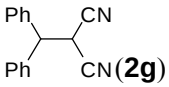 (**2g**)	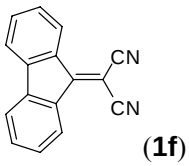 (**1f**)	0.9
2g	**1h**	-2.0
2g	**1i**	-3.5
2g	**1j**	-5.0
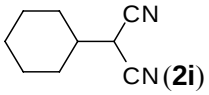 (**2i**)	**1f**	4.3
2i	**1g**	3.4
2i	**1h**	1.4
2i	**1j**	-1.5

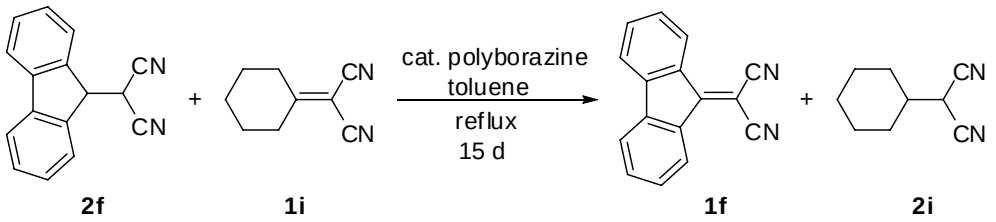

2f **1i** **1f** **2i**

Scheme 8.7

Summarizing, transfer hydrogenation of three types of polar double bond containing compounds were achieved using amine borane adducts as the hydrogen donors under mild conditions in the absence of a catalyst, which added greatly to the rarely explored field of uncatalyzed transfer hydrogenation. Moreover, the hydrogenated compounds especially products of the activated olefins, which contain two differently polarized hydrogen atoms originating from hydridic H_B and protic H_N

of amine boranes, might open up possibilities for thermal dehydrogenations, hydrogen transfers, or even be employed as catalysts in organocatalytic hydrogen transfer reactions.

References

[1] **Chapter 3:** Yang, Xianghua; Zhao, Lili; Fox, Thomas; Wang, Zhi-Xiang; Berke, Heinz.* Transfer hydrogenation of imines with ammonia-borane: a concerted double-hydrogen transfer reaction. *Angew. Chem. Int. Ed.* **2010**, *49(11)*, 2058-2062.

[2] **Chapter 4:** Yang, Xianghua; Fox, Thomas; Berke, Heinz.* Facile metal free regioselective transfer hydrogenation of polarized olefins with ammonia borane. *Chem. Commun.* **2011**, *47(7)*, 2053-2055.

[3] **Chapter 5:** Yang, Xianghua; Fox, Thomas; Berke, Heinz.* Synthetic and Mechanistic Studies of Metal-Free Transfer Hydrogenations Applying Polarized Olefins as Hydrogen Acceptors and Amine Borane Adducts as Hydrogen Donors. *Org. Biomol. Chem.* DOI: 10.1039/C1OB06381B.

[4] **Chapter 6:** Yang, Xianghua; Fox, Thomas; Berke, Heinz.* Ammonia borane as a metal free reductant for ketones and aldehydes: A mechanistic study. *Tetrahedron.* **2011**, 7121-7127.

Zusammenfassung

Wasserstoff wird als potentieller Energieträger diskutiert, der das Zeitalter der fossilen Energieträger und die Zukunft der erneuerbaren Energien miteinander verbinden könnte. Wasserstofftechnologie stellt einen wichtigen Bestandteil von Energiestrategien im Technologiewettbewerb dar. In diesem Zusammenhang haben Amin-Boranaddukte grosse Bedeutung in der Forschung als mögliche Materialien für die chemische Wasserstoffspeicherung. Viele Ansätze konzentrierten sich bisher auf die Wasserstofffreisetzung aus Amin-Boranaddukten mittels Metallkatalyse, entweder über Dehydrokupplungen oder Solvolyse. Die Grundidee zur Dehydrierung solcher Addukte bestand aus einem metallfreien Transferhydrierungsprozess, in welchem ungesättigte Verbindungen mit polarisierten Doppelbindungen, wie Imine, Carbonylverbindungen und aktivierte Olefine eingesetzt werden sollten. In der Tat konnten Amin-Boranaddukte erfolgreich als Wasserstoffdonoren in der Reduktion polarer ungesättigter Verbindungen unter milden Bedingungen und in Abwesenheit eines Katalysators angewandt werden. DFT-Rechnumgen bestätigen, dass derartige metallfreie Transferhydrierungen thermodynamisch begünstigt sind und die wasserstofffreisetzung aus den erhaltenen Produkten möglich ist.

Curriculum Vitae

- **Surname:** YANG
- **First name:** Xianghua
- **Date of birth:** 20, Jan. 1983
- **Nationality:** China
- **Education:**

09/1997-07/2000: No. 1 Senior Middle School of Xinhua, Hu'nan, China

09/2000-07/2004: Dalian Jiaotong University, Liaoning, China

09/2004-07/2007: Tsinghua University, Beijing, China
Master Project: Transition metal promoted C-H activation of aniline derivatives.
Supervisor: Prof. Dr. Chanjuan Xi

10/2007-present: University of Zurich, Zurich, Switzerland
PhD student in the Institute of Inorganic Chemistry
Supervisor: Prof. Dr. Heinz Berke

- **Honors:**

- SCNAT/SCS Chemistry Travel Award (2011).
- Chinese government award for outstanding self-financed students abroad (2010).
- First prize of the Dong-Gang scholarship, Tsinghua University (2006).
- Best Photographer of the graduates' news agency, Tsinghua University (2005)
- Outstanding graduate of Dalian city & Excellent dissertation of the university (2004).
- Chinese government scholarship for undergraduates (2002).
- First prize of Outstanding student scholarship (2001-2004)
- First prize of the Scholarship for freshmen, Dalian Jiaotong University (2000).

- **Publications:**

1. Synthetic and mechanistic studies of metal-free transfer hydrogenations applying polarized olefins as hydrogen acceptors and amine borane adducts as hydrogen donors.

   Yang, Xianghua; Fox, Thomas; Berke, Heinz.* *Org. Biomol. Chem.* DOI: 10.1039/C1OB06381B.
2. Ammonia borane as a metal free reductant for ketones and aldehydes: A mechanistic study.

   Yang, Xianghua; Fox, Thomas; Berke, Heinz.* *Tetrahedron.* **2011**, 7121-7127.
3. Facile metal free regioselective transfer hydrogenation of polarized olefins with ammonia borane. (ChemComm 'Hydrogen' web-based themed issue)

Yang, Xianghua; Fox, Thomas; Berke, Heinz.* *Chem. Commun.* **2011**, *47(7)*, 2053-2055.

4. Transfer hydrogenation of imines with ammonia borane: a concerted double-hydrogen transfer reaction.

   Yang, Xianghua; Zhao, Lili; Fox, Thomas; Wang, Zhi-Xiang; Berke, Heinz.* *Angew. Chem. Int. Ed.* **2010**, *49(11)*, 2058-2062.

   Yang, Xianghua; Zhao, Lili; Fox, Thomas; Wang, Zhi-Xiang; Berke, Heinz.* *Angew. Chem.* **2010**, *122(11)*, 2102-2106.

   Also appeared as *Swiss Science Concentrate Highlight* in: *Chimia*, **2010**, *64(6)*, 425.

5. Cerium salt promoted homocoupling reaction of dialkylanilines in water.

   Yang, Xianghua; Lu, Wenchao; Liao, Qian; Xi, Chan-juan.* *Chem. Res. Chinese U.*, **2008**, *24(2)*, 226-230.

6. An Efficient Nitration of *N*,*N*-dialkylanilines in water using $NaNO_2$ and $Ce(SO_4)_2$.

   Yang, Xianghua; Xi, Chanjuan.* *Synthetic Commun.* **2007**, *37*(19), 3381-3392.

7. $CuCl_2$-catalyzed one-pot formation of tetrahydroquinolines from *N*-methyl-*N*-alkylanilines and vinyl ethers in the presence of *t*-butylhydroperoxide.

   Yang, Xianghua; Xi, Chanjuan;* Jiang, Yanfeng. *Molecules* **2006**, *11*(12), 978-987

8. Oxidative coupling reaction of *N*,*N*-dialkylanilines with cerium(IV) ammonium nitrate in the solid state.

   Yang, Xianghua; Xi, Chanjuan;* Jiang, Yanfeng. *Synthetic Commun.* **2006**, *36*(17), 2413-2419.

9. Regioselective nitration of *N*,*N*-dialkylanilines using cerium(IV) ammonium nitrate in acetonitrile.

   Yang, Xianghua; Xi, Chanjuan;* Jiang, Yanfeng. *Tetrahedron Lett.* **2005**, *46*(50), 8781-8783.

10. Synthesis and crystal structure of (1-naphthyl){[3-(2,6-dibromo-4-methylphenylimino)methyl]-5-chloro-2-hydroxy-benzaldehyde}(triphenylphosphine) Nickel(II)Triphenylphosphine.

    Jiang, Yanfeng; Xi, Chanjuan;* Yang, Xianghua. *Chinese J. Struc. Chem.* **2006**, *25*, 73-77.

11. $CuBr/H_2O_2$-mediated oxidative coupling of *N*,*N*-dialkylarylamines in water. A practical synthesis of benzidine derivatives.

    Jiang, Yanfeng; Xi, Chanjuan;* Yang, Xianghua. *Synlett*, **2005**, (9), 1381-1384.

12. Remarkably efficient oxidative coupling of *N*,*N*-dialkylarylamines in water mediated by cerium(IV) ammonium nitrate.

    Xi, Chanjuan;* Jiang, Yanfeng; Yang, Xianghua**.** *Tetrahedron Lett.* **2005**, *46*(22), 3909-3911.

13. Studies on selenium content of laying hens rich in selenium.

    Wu, Dunhu;* Yang, Xianghua; Tian, Ying; Liu, Jun; Li, Haiyan. *Studies of Trace Elements and Health* (Chinese journal), **2005**, *22*(1), 29-30.